CURCUMIN-RELATED HYBRID COMPOUNDS AS POTENTIAL ANTIMALARIAL AGENTS:

DESIGN, SYNTHESIS, MECHANISTIC INVESTIGATIONS, BIOLOGICAL EVALUATION AND PHARMACOKINETIC STUDIES

Eric Guantai

Supervisors:

Prof. Kelly Chibale, Dept. of Chemistry, UCT

Assoc. Prof. Peter Smith, Division of Pharmacology, UCT

Thesis submitted in fulfillment of the requirements for the degree of

Doctor of Philosophy

December, 2010

UNIVERSITY OF CAPE TOWN
IYUNIVESITHI YASEKAPA • UNIVERSITEIT VAN KAAPSTAD

DECLARATION

I, Eric Muriithi Guantai, hereby:

- declare that this thesis is based on my original work (except where acknowledgements indicate otherwise) and that neither the substance nor any part of the thesis has been submitted in the past, or is being, or is to be submitted for a degree at this University or any other University;
- grant the University of Cape Town free license to reproduce the thesis, in whole or in part, for the purpose of research.

Signed: _____

Date: _____

DEDICATION

This work is dedicated to my late elder brother, Benjamin Kimenyi Guantai, whose warmth, friendship and companionship I still cherish to this day.

ACKNOWLEDGEMENTS

I would like to humbly acknowledge the boundless love, inspiration, protection and guidance of the Almighty God, for which I am eternally grateful.

I would also like to extend my heartfelt gratitude and appreciation to my two supervisors. Professor Kelly Chibale, for taking a chance with me, for his support, guidance and motivation, as well as for showing an almost limitless confidence in my abilities throughout the last five years; Associate Professor Peter J. Smith, for his confidence in me, and for allowing me free reign in his pharmacology labs, and access to all I required.

My sincere appreciation also goes out to my immediate family for bearing with my extended absences from home, and for their unconditional love, caring, motivation and support for as long as I can remember: my parents Mr. and Prof. Guantai, my sisters Edna and Christine Guantai, and my brother Christopher Guantai, a family like no other.

I would also like to gratefully acknowledge the technical assistance received from Noel Hendricks and Peter Roberts (^{1}H- and ^{13}C-NMR analysis), and Piero Benincassa and Alicia Evans (microanalysis and LRMS analysis). I would also like to thank Dr. Tracy Kellerman and Dr. Lubbe Wiessner for their invaluable contribution to the pharmacokinetic studies reported herein, as well as Dale Taylor for his assistance with the *in vivo* antimalarial efficacy studies.

I sincerely acknowledge all our collaborators and collaborating laboratories for their vital contributions to this study, and for the results that they provided: Prof. Collen Masimirembwa (African Institute of Biomedical Science and Technology, AiBST); Prof. Philip J. Rosenthal (University of California, San Francisco, UCSF); Prof Timothy Egan (Department of Chemistry, UCT); Dr. Karen White and Prof. Susan Charman (Centre for Drug Candidate Optimization, CDCO, Monash University).

It gives me great pleasure to acknowledge the friendship and camaraderie of all my colleagues and fellow research group members, past and present, both in the Dept. of Chemistry and at the Division of Pharmacology. The assistance of all members of the academic and administrative staff of the Dept. of Chemistry, UCT, is also duly acknowledged.

Finally, I would like to sincerely thank the South African National Research Foundation (NRF) and the Dept. of Chemistry for their financial assistance, without which my stay in Cape Town would not have been possible.

ABSTRACT

Malaria remains one of the most devastating tropical diseases, with staggering infection and mortality statistics. Over 200 million clinical cases of malaria (resulting in 1 - 3 million deaths) are reported annually. Africa bears the greatest burden of this disease, with the vast majority of malaria cases (>85%), and malaria-related deaths (>90%), being reported in sub-Saharan Africa. The main challenge to malaria control has been the development of clinically significant resistance of the parasite to most known antimalarial drugs. This suggests that the development of new, highly efficacious drugs and/or treatment regimens for the management of malaria remains a key priority.

This study applied molecular hybridization as a strategy in the development of novel potential antimalarial agents. The aim was to try and identify novel hybrid compounds containing scaffolds that are structurally related to the natural product curcumin, and which exhibit *in vitro* and *in vivo* antimalarial activity. Part of the study involved investigations into the pharmacokinetics and possible antimalarial mechanisms of action of selected target compounds.

This work was carried out in three phases:

A:

Series of hybrid compounds containing chalcones and dienones (curcumin-related scaffolds) linked to either 3'-azido-2',3'-dideoxythymidine (AZT, an azide-bearing, relatively hydrophilic nucleoside analog with intrinsic anti-HIV activity) or 7-chloroquinoline (a known antimalarial pharmacophore present in several clinically available antimalarials) were designed and synthesized as novel hybrid antimalarial compounds. Hybridization was effected by application of the experimentally simple and robust Cu(I) catalyzed 1,3-dipolar cycloaddition reaction of azides and terminal alkynes (click chemistry).

In vitro testing revealed that the acetylenic chalcone and dienone intermediates, as well as the chalcone-AZT, dienone-chloroquinoline and dienone-AZT hybrid compounds, showed moderate antiplasmodial activity, exhibiting lower micromolar IC_{50} values against three different strains of *P. falciparum*. However, the chalcone-chloroquinoline hybrid compounds **3.15b**, **3.15c** and **3.17b** showed notably high *in vitro* antimalarial activity, all three exhibiting submicromolar IC_{50} values. Compound **3.15b** was the most active, with IC_{50} values of 0.04 μM, 0.07 μM and 0.09 μM against the D10, Dd2 and W2 strains of *P. falciparum*, respectively. The presence of the chloroquinoline moiety on the three more active compounds was most likely responsible for the improved activity that these compounds exhibited, though this significant improvement in activity was not universal.

A limited mechanistic investigation carried out on the chalcone-chloroquinoline hybrid compounds suggested that inhibition of hemozoin formation was likely to be a primary mechanism of antimalarial activity, particularly for the hybrid compounds **3.15b**, **3.15c** and **3.15e**, which were all comparably or more potent than chloroquine in inhibiting β-hematin formation. The moderate inhibition of Falcipain 2 suggested that this mechanism could also contribute to the overall observed antimalarial activities of these compounds, albeit to a limited extent. Inhibition of parasite-induced new permeability pathways (NPPs) did not appear to be a notable mechanism of action for these compounds.

B:

The next phase was to identify analogs of **3.15b** (and intermediate **3.19**) with improved predicted physicochemical and pharmacokinetic parameters, factors which could potentially translate into improved oral bioavailability. To this end, three software packages with varying but complementary capabilities were applied for use in the *in silico* prediction of various physicochemical and ADME parameters. By the rational replacement of the triazole linkers in **3.15b** and **3.19**, several analogs were proposed that had improved predicted solubilities relative to their parent compounds, particularly at lower pH. The analogs also maintained acceptably high predicted Caco2 permeability. The main alert was their possible metabolic instability, primarily due to N-dealkylation of their nitrogen-containing linkers. The *in silico* solubility and metabolism predictions were supported by experimental solubility determinations and *in vitro* metabolism studies.

All the target analogs exhibited notable antimalarial activity, with IC_{50} values in the lower micromolar to mid-nanomolar range, though none were as active as **3.15b**. The related analogs **5.13** and **5.15**, both of which were analogs of **3.15b** that bore piperazinyl linkers, were the most active of the analogs. These compounds had IC_{50} values between 0.3 – 0.6 nM against three strains of *P. falciparum*. The analogs were also very potent inhibitors of β-hematin formation, more potent than chloroquine. Compounds **5.11** and **5.15** were extremely potent, with the lowest IC_{50} values of 0.2 equivalents. This suggested that inhibition of hemozoin formation could contribute substantially to the antimalarial action of these compounds. The analogs showed moderate to poor inhibition of Falcipain 2, and were poor inhibitors of parasite-induced new permeability pathways.

C:

Compounds **3.15b** and **5.13** were selected for preliminary PK profiling and *in vivo* antimalarial testing in mice, and were administered in different formulations and at varying doses. The DMSO-water formulation afforded notably higher oral bioavailability for both **3.15b** and **5.13** relative to the other formulations used for the PK studies. Compound **3.15b** exhibited a bi-phasic PK profile after oral administration as a DMSO-water formulation, which was most likely due to staggered absorption in separate sections of the GI tract. Also, significantly higher exposure and circulating concentrations were observed for **3.15b** compared to **5.13** after oral administration. The rapid decline in the circulating concentrations of both compounds after IV administration indicated an extremely efficient clearance of the compounds, possibly a combination of both hepatic (metabolic) and renal clearance. The two compounds did not exhibit significant *in vivo* antimalarial activity, showing only marginal improvement to the untreated controls in terms of suppression of parasitemia, decline in average mouse weights and overall mouse survival. This activity was significantly inferior to that observed for chloroquine. Compound **3.15b** showed slightly better efficacy that **5.13**, with a notably slower rise in parasitemia in the middle and later stages of the study as well as more mice surviving for longer (relative to their respective untreated controls).

LIST OF ABBREVIATIONS

ACT	Artemisinin-based Combination Therapy
ADME(T)	Absorption, Distribution, Metabolism, Excretion (and Toxicity)
AZT	3'-azido-2',3'-dideoxythymidine (Zidovudine®)
BTIQ	Benzyltetrahydroisoquinoline
^{13}C-NMR	Carbon-13 Nuclear Magnetic Resonance
Cmax	Maximum concentration
CQR	Chloroquine resistant
CQS	Chloroquine sensitive
d	Doublet
DCM	Dichloromethane
dd	Doublet of doublets
DFO	Desferrioxamine
DHA	Dihydroartemisinin
DHFR	Dihydrofolate reductase
DHODH	Dihydroorotate dehydrogenase
DHTS	Dihydropteroate synthase
DIAD	Di-isopropyl azodicarboxylate
DEG	Di-ethylene glycol
DMF	*N,N*-Dimethylformamide
DMSO	Dimethylsulphoxide
EtOAc	Ethyl acetate
G.I.	Gastro-intestinal
^{1}H-NMR	Proton Nuclear Magnetic Resonance
HAP	Histo-aspartic protease
HPLC	High Performance Liquid Chromatography
HTS	High-throughput screening
Hz	Hertz
IC_{50}	Concentration inhibiting 50% of parasite survival
IR	Infra-Red
ITN	Insecticide-treated net
LC-MS	Liquid chromatography – Mass spectrometry
LRMS	Low Resolution Mass Spectroscopy
m	Multiplet

M	_____	Molar
MEM	_____	Methoxyethoxymethyl
MeOH	_____	Methanol
MHz	_____	Megahertz
MOM	_____	Methoxymethyl
MS	_____	Mass Spectroscopy
m/z	_____	Mass to Charge ratio
NADPH	_____	Nicotinamide Adenine Dinucleotide Phosphate
NMP	_____	*N*-Methyl pyrrolidinone
NO	_____	Nitric oxide
NPP	_____	New permeability pathways
NRTI	_____	Nucleoside reverse transcriptase inhibitor
NSAID	_____	Non-steroidal anti-inflammatory drug
o/w	_____	Oil-in-water
PABA	_____	*Para*-aminobenzoic acid
PfCRT	_____	*Plasmodium falciparum* chloroquine resistance transporter
PfMDR	_____	*Plasmodium falciparum* multi-drug resistance (gene)
PGH1	_____	P-glycoprotein homologue 1
PK	_____	Pharmacokinetic
PPh3	_____	Triphenylphosphine
ppm	_____	Parts per million
s	_____	Singlet
SERCA	_____	Sarco/endoplasmic reticulum Ca2+-ATPase
SMEDDS	_____	Self-micro emulsifying drug delivery system
t	_____	Triplet
THP	_____	Tetrahydropyran
TLC	_____	Thin Layer Chromatography
TNF	_____	Tumor Necrosis Factor
UCT	_____	University of Cape Town
UDPGA	_____	Glucuronic acid (UDP-activated)
v/v	_____	Volume by Volume

TABLE OF CONTENTS

LIST OF FIGURES

LIST OF TABLES

PUBLICATIONS, CONFERENCES AND TRAINING COURSES

Publications So Far Arising from This Thesis

Renate H. Hans, Eric M. Guantai, Carmen Lategan, Peter J. Smith, Baojie Wan, Scott G. Franzblau, Jiri Gut, Philip J. Rosenthal, Kelly Chibale. Synthesis, antimalarial and antitubercular activity of acetylenic chalcones. *Bioorganic & Medicinal Chemistry Letters* 2010, 20, 942–944.

Eric M. Guantai, Kanyile Ncokazi, Timothy J. Egan, Jiri Gut, Philip J. Rosenthal, Peter J. Smith, Kelly Chibale. Design, synthesis and in vitro antimalarial evaluation of triazole-linked chalcone and dienone hybrid compounds. *Bioorganic & Medicinal Chemistry* 2010, 18, 8243–8256.

Eric M. Guantai, Kanyile Ncokazi, Timothy J. Egan, Jiri Gut, Philip J. Rosenthal, Ravi Bhampidipati, Anitha Kopinathan, Peter J. Smith, Kelly Chibale. Enone- and Chalcone-Chloroquinoline Hybrid Analogs: In Silico-Guided Design, Synthesis, Antiplasmodial Activity, in Vitro Metabolism, and Mechanistic Studies. *Journal of Medicinal Chemistry* 2011 (In press).

Reviews and miscellaneous articles

Eric Guantai and Kelly Chibale. Chloroquine Resistance: Proposed Mechanisms and Countermeasures. *Current Drug Delivery*, 2010, 7, 312-323.

Eric Guantai and Kelly Chibale. How can natural products serve as a viable source of lead compounds for the development of new/novel antimalarials? *Malaria Journal.* 2011, 10 (Suppl 1):S2

Eric M. Guantai, Collen Masimirembwa and Kelly Chibale. Extracting Molecular Information from African Natural Products to Facilitate Unique African-led Medicinal Chemistry Efforts. *Future Medicinal Chemistry.* 2011, 3(3), 257–261

Conferences and Training Courses attended

GIBEX/UCT training course: Preserving and Evaluating Biodiversity through Screens-To-Nature (STN) technology. University of Cape Town, South Africa (2008).

Bi-National Organic Chemistry Conference (2008). Berg-en-Dal, Kruger National Park, South Africa (Poster presentation)

Keystone Symposia Conference (2009) Drug Discovery for Protozoan Parasites. Beaver Run Resort, Breckenridge, Colorado, USA (Poster presentation)

AiBST/UCT Industrial DMPK Course on ADMET for Medicinal Chemistry. University of Cape Town, South Africa (2009)

IRTG 1522 workshop: From Bioinformatics to rational drug design. University of Wurzburg (2009).

CHAPTER ONE

INTRODUCTION

1.1 Preamble

This chapter introduces malaria: the aetiology, geographical distribution, impact and presentation of the disease. It then goes on to highlight some of the measures available to control the disease, focusing on available antimalarial drugs and the main challenges associated with their use.

1.2 Malaria

Malaria refers to the clinical disease caused by infection of humans by protozoa of the *Plasmodium* genus. Four species of *Plasmodium* are known to infect humans: *Plasmodium falciparum*, *P. vivax*, *P. ovale* and *P. malariae*. Other species of *Plasmodium* are primarily parasites of monkeys, birds and apes, affecting man only rarely and not seriously [1.2].

1.3 Geographical Distribution of the *Plasmodium* Species

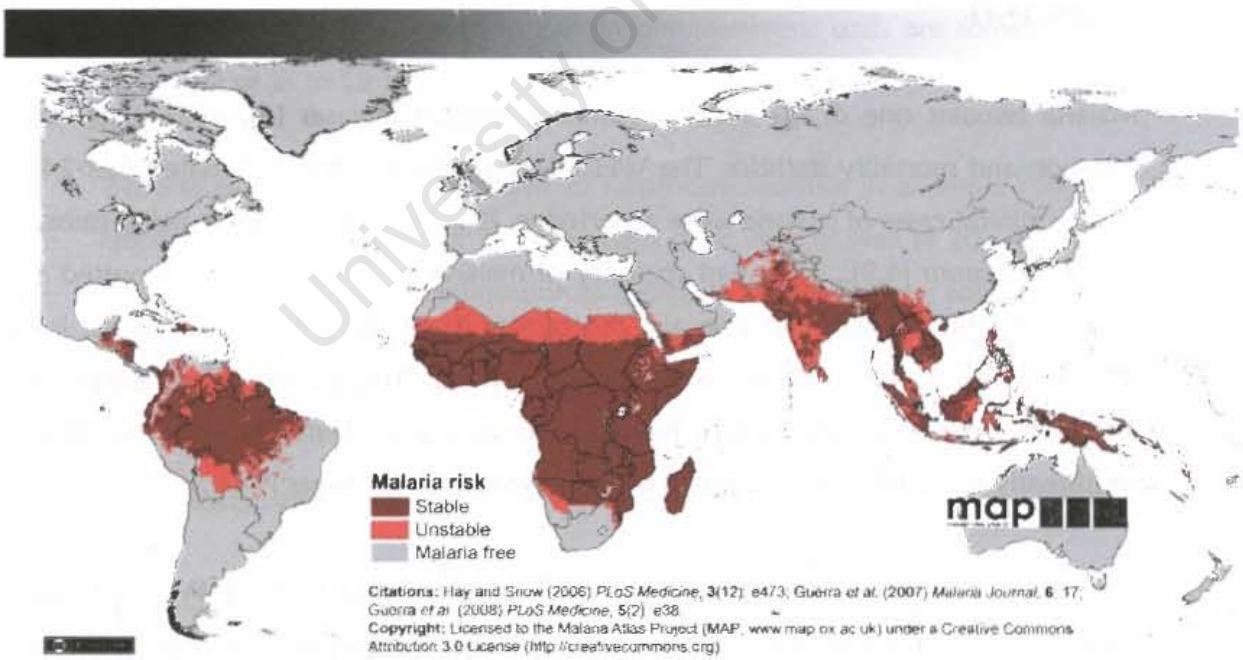

Figure 1.1: Map showing the global distribution of malaria [3]

As can be deduced from the map above (**Figure 1.1**), malaria is predominantly a tropical disease, being highly endemic in sub-Saharan Africa, Central and South

America, and Asia. However, parts of the Middle East and the Western Pacific also bear some of the global burden of malaria, albeit to a much lesser degree [2,4].

P. falciparum is the predominant species in Africa though *P. vivax* and *P. ovale* also occur. *P. ovale* seems to be restricted to western Africa [2]. *P. vivax* is thought to be responsible for approximately 1–20% of malaria infections in tropical Africa, and also for 50% of the global non-African malaria burden [5]. 50–70% of malaria infections in south Asia, the western Pacific, and South America, rising to 80–100% in the subtropical and more temperate regions of Central America, the eastern Mediterranean, the Middle East, and south-central Asia, are also attributed to *P. vivax* [6]. Both *P. vivax* and *P. falciparum* are found in South America, other parts of Asia and the western Pacific. *P. malariae* is made out to be in only a few pockets around the world, but is probably more wide spread than has been hitherto anticipated [2].

1.4 Impact of Malaria

Approximately 2 - 3 billion people, representing a significant proportion of the world's population, are at risk of infection in over 109 malarious countries and territories, and it is estimated that, at any one time, 1 billion of these people are carrying the malaria parasite [4,7].

Malaria remains one of the most devastating tropical diseases [8], with staggering infection and mortality statistics. The WHO Malaria Report 2008 estimated that 247 million clinical cases of malaria were reported in 2006, 80-90% of these being caused by *P. falciparum* [4,9]. The vast majority of malaria cases (86%) were reported in sub-Saharan Africa, with East Asia and the eastern Mediterranean accounting for just 9% and 3% of the reported cases, respectively [4]. This pattern of geographical distribution of the disease, which has Africa bearing the greatest burden, has been consistently replicated in other global health reports over the years [9-11].

P. falciparum is responsible for practically all mortality and most of the morbidity associated with malaria [2], and, with the bulk of *P. falciparum* infections being reported in sub-Saharan Africa [5], it comes as no surprise that by far the majority of malaria deaths (in excess of 90%) occur in tropical Africa [4,10]. However, the proportion of malaria burden is somewhat lower in the southern Africa sub-region than in the high transmission regions [12] of the central, eastern and western sub-regions of Africa [10].

In the year 2000, the WHO Expert Committee on Malaria reported an annual death rate from malaria of between 1.1 and 2.7 million people [9]; these figures have since been reviewed downwards, and current reports put the tally at between 0.6 – 1.2 million deaths a year, with 85% of these deaths being children below the age of 5 years in sub-Saharan Africa [4]. Occurring mainly in rural areas [12], this corresponds to about 18 – 25% of the total mortality of children under the age of 5 years in this region, with death resulting mainly from cerebral malaria and anaemia [9,10,12]. Fatalities of 10 - 30% have been reported among children referred to hospital with severe malaria, especially in rural areas where patients have restricted access to adequate healthcare [9]. Even more worrying are the reports indicating that as low as one in five malaria deaths are actually reported [4].

Though the malaria toll in terms of human life is rather obvious from these statistics, the attendant economic burden resulting from treatment and prevention initiatives, though less obvious, is also equally staggering. Annually, it is estimated that affected African countries spend in excess of USD 12 million in malaria treatment and prevention programs [5]. Studies in several sub-Saharan African countries have reported that as much as 28% of household incomes in less-privileged populations may be spent on malaria treatment, with costs ranging from $4 to as high as $60 per patient for in-patient treatment; out-patient treatment costs are somewhat lower, in the range of $1 to $3 per patient [13].

Malaria also poses a great burden to healthcare facilities in endemic countries, being responsible for 20 - 35% of all out-patient clinic visits as well as 20 - 45% of hospital admissions. It is a major contributor to in-patient deaths in these countries, mainly due to late presentation, inadequate clinical management and the unavailability or stock-outs of effective antimalarial drugs [10].

1.5 Transmission and Life Cycle

Knowledge of the life-cycle of the malaria parasite, particularly the human phase of the cycle, is necessary for the understanding of, among other things, the clinical presentation of the disease (Section 1.6), the microbiological diagnosis of the disease, as well as certain aspects of *in vitro* antimalarial testing (Chapter Four).

The malaria parasite is spread by the female *Anopheles* mosquito [2,14]. Sixty species of this mosquito have been identified as vectors of human malaria, and their distribution varies from country to country [2].

The life cycle of all *Plasmodium* species is complex (**Figure 1.2**), involving both sexual and asexual replication. Infection in humans begins with the bite of an infected female *Anopheles* mosquito. As the mosquito bites to get a blood meal to nourish her eggs, she injects sporozoites in her saliva into the bloodstream of her victim. Sporozoites represent the terminal stage of the parasite's life cycle in the mosquito [15,16].

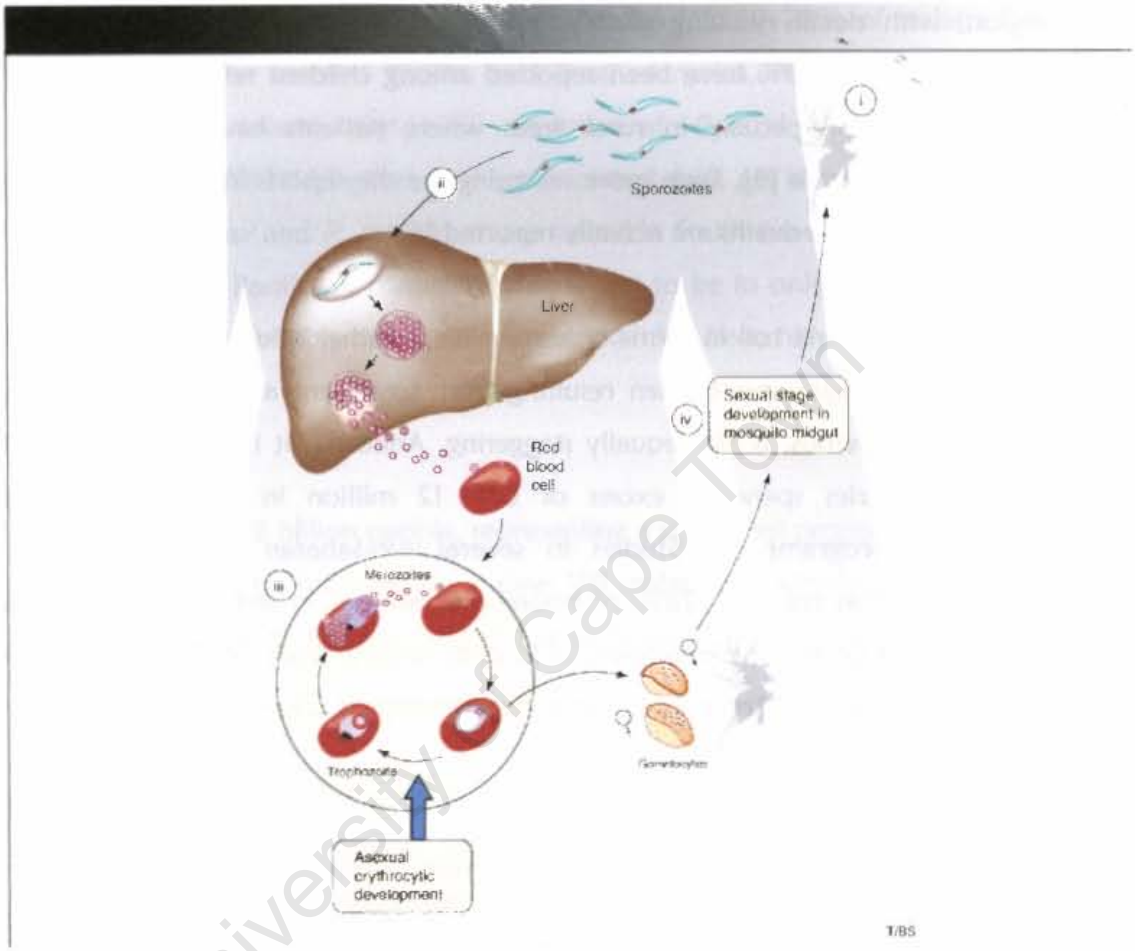

Figure 1.2: Schematic diagram outlining the asexual life cycle of the *Plasmodium* parasite [17]

The injected sporozoites quickly invade liver cells (hepatocytes), and have been reported to disappear from peripheral circulation within 30 minutes to 1 hour after the mosquito bite. This liver-stage, also called tissue phase or pre-patent period, lasts for different periods depending on the infecting species: 8 – 25 days for *P. falciparum* and 8 – 27 days for *P. vivax* [2]. During this phase the parasites differentiate and undergo asexual multiplication resulting in tens of thousands of merozoites. The invaded hepatocytes, now filled with merozoites and referred to as hepatic schizonts, lyse to release the merozoites into circulation [2,15]. In the case of *P. vivax* and *P. ovale*, some sporozoites may go into hibernation within hepatocytes, and in this state are referred to as hypnozoites. This latent phase is sometimes termed the cryptobiotic phase, and

the hypnozoites can lie dormant for months or years, and on reactivation can cause clinical relapse [2].

Upon release from the hepatocytes, individual merozoites attach onto the red blood cell (erythrocyte) membranes and, by a process of invagination, invade them. Here, asexual multiplication continues, and each merozoite replicates producing 12 – 16 progeny merozoites. Parasitic development within the erythrocytes can be microscopically characterized as proceeding through the stages of rings, trophozoites, early schizonts and mature schizonts (**Figure 1.3**); each mature schizont contains tens of erythrocytic merozoites [2,15].

Mature erythrocytic schizonts then lyse to release these merozoites into the bloodstream. These merozoites immediately invade other uninfected red cells, and the erythrocytic cycle of invasion – multiplication – release – invasion begins again. The length of this intra-erythrocytic cycle depends again on the infecting species: about 48 hours in *P. vivax*, *P. ovale* and *P. falciparum* infections and 72 hours in case of *P. malariae* infection. It occurs synchronously and the merozoites are released at approximately the same time of the day. The contents of the infected cells that are released upon their lysis stimulate the release of Tumour Necrosis Factor (TNF) and other cytokines, which result in the characteristic clinical manifestations of the disease – fever and chills [2,15].

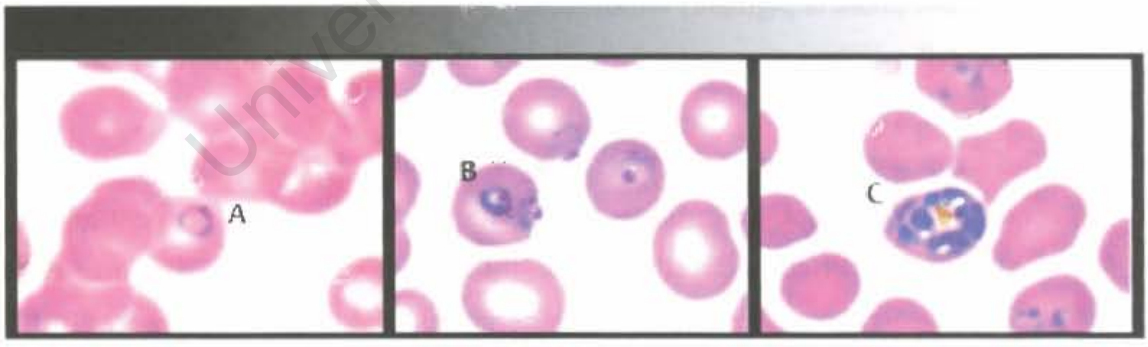

Figure 1.3: Thin blood smear micrographs showing intra-erythrocytic development of *P. falciparum* through the ring (A), trophozoite (B) and schizont (C)stages [16].

It should be noted, however, that not all of the merozoites divide into schizonts. Some differentiate into the sexual forms of the parasite, i.e. male and female gametocytes. Mature gametocytes appear in the peripheral blood after a variable period (8 - 11 days for *P. falciparum*), and it is these gametocytes that are taken up by a female *Anopheles* mosquito during a blood meal, whereupon the parasite commences the sexual part of its life cycle. Gametocytes may persist in circulation for several weeks [2,15].

Within the mosquito mid-gut, the male gametocyte undergoes a rapid nuclear division, each producing eight flagellated microgametes. These then fertilize the female macrogamete resulting in an ookinete that traverses the mosquito gut wall and encysts on the exterior of the gut wall as an oocyst. Sporozoites rapidly develop asexually within the oocyst, which soon ruptures, releasing hundreds of sporozoites into the mosquito body cavity. These sporozoites eventually migrate to the mosquito salivary gland, and during the mosquito's next blood meal, get injected into the victim's bloodstream along with mosquito saliva [2,15].

1.6 The Clinical Disease

The initial phase of infection, during which sporozoites invade and develop within hepatocytes, is accompanied by few symptoms, if any. Rarely, vague aches and pains, headache and nausea may be present. Such symptoms are usually atypical, and may resemble any febrile illness; this is termed the primary attack [2].

Clinical features of malaria occur during the subsequent erythrocytic phase of the infection, and are more profound and severe in the case of *P. falciparum* malaria. Upon invasion of the erythrocytes, the parasite rapidly and efficiently degrades and consumes intracellular components, principally hemoglobin. Hemoglobin degradation is an important source of free amino acids for the parasite, useful in the synthesis of parasitic proteins (section 1.7) [18,19]. This metabolic process results in the formation of hemozoin (malaria pigment) which, coupled to parasite-induced alterations of the red-blood cell membranes, eventually leads to the lysis of the erythrocytes [2,20].

This rupture of erythrocytes releases certain factors and toxins such as phospholipoproteins, erythrocyte membrane products, malaria pigment and malarial toxins, which in turn directly induce the release of cytokines such as TNF and interleukin-1 from macrophages, resulting in chills and high grade fever. This is why malaria is essentially a febrile illness characterised by fever and related symptoms [2].

Due to the relatively synchronised lysis of erythrocytic schizonts and the subsequent release of pyrogenic substances, the febrile symptoms of malaria follow a similarly regular pattern, recurring and escalating in intervals of 48 – 72 hours (depending on the infecting species). In malaria due to *P. vivax* and *P. ovale*, this typical pattern of fever recurs once every 48 hours (Benign Tertian malaria). However, in *P. falciparum* infection (malignant tertian malaria), this pattern may often not be seen and the febrile

episodes tend to be more frequent. In *P. malariae* infection, the relapses occur once every 72 hours (quartan malaria) [2].

The typical "text book" presentation of malaria would involve the above described febrile episodes, which would ideally be characterised by three phases [2]:

- Cold phase, characterized by shaking chills usually at around mid-day and lasting for 15 minutes to 1 hour;
- Hot phase, evidenced by a high grade fever which lasts 2 to 6 hours;
- Sweating phase, characterised by profuse sweating and the gradual subsiding of the fever over 2 - 4 hours.

These febrile episodes are usually accompanied by head aches, vomiting, delirium, anxiety and restlessness, which are, as a rule, transient and disappear with normalization of body temperature [2].

However, this classical presentation is rarely observed as described, and malaria is also known to present with a myriad of atypical symptoms such as atypical fever, headache, body aches, back ache and joint pains, vertigo, altered behaviour, acute psychosis, altered sensorium, convulsions, coma, cough, breathlessness, chest pain, acute abdomen, weakness, vomiting and diarrhoea, jaundice, pallor, puffiness of eyelids, hepato-splenomegaly and combinations of the above. This picture is usually further complicated by the common presence of secondary infections as well as symptoms of adverse drug reactions to administered antimalarials [2].

1.7 Hemoglobin Degradation

Of special interest among the parasite's many metabolic pathways is the process of hemoglobin degradation, by which the erythrocytic parasite breaks down the host cell hemoglobin and utilises the resulting amino acids and iron for its own metabolic processes. Interest in this process stems from the fact that it is essential for the parasite's survival [18,20,21].

Though the malaria parasite has the ability to synthesize asparagine, glutamine, glycine, proline, aspartate and glutamate [22], hemoglobin degradation appears to be a critical source of amino acids for parasite utilisation in protein synthesis and energy metabolism [18]. Hemoglobin is also an important source of parasitic iron, which it utilises in the synthesis of iron-dependent proteins such as the enzymes ribonucleotide reductase, superoxide dismutase and cytochromes [20,21].

However, hemoglobin is a poor source of the amino acids methionine, cysteine and glutamine and contains no isoleucine at all – these have to be taken up by the parasite from the host cell cytosol. The entry of these amino acids into infected erythrocytes is facilitated by the presence of parasite induced transport channels, dubbed new permeability pathways (NPPs), on the erythrocyte membrane [23]. Upon entering the infected erythrocyte, uptake of isoleucine by the parasite has two components: one component involves the influx of isoleucine *via* a saturable, ATP-independent transporter capable of exchanging intracellular leucine for isoleucine; the second component involves the glucose/ATP-dependent active accumulation of the amino acid within the parasite [24]

Hemoglobin uptake is primarily by trophozoites and early schizonts, and has been shown to involve the process of micropinocytosis. Host cell (erythrocyte) cytoplasm is taken up by the invagination of the parasitophorous vacoular membrane and the parasite plasma membrane resulting in the formation of large, double-membraned cytostomes. Smaller, double-membraned vesicles then form by budding from the cytostomes, and these migrate and fuse with the acidic food vacuole of the parasite. These digestive vacuoles have an internal pH of 5.18±0.05 [25], and are the definitive site of hemoglobin degradation [20,21].

The process of hemoglobin dissociation and metabolism within the parasite has been demonstrated to be a semi-ordered, enzymatic process involving distinct classes of enzymes (Figure 1.4) [21,26]. Initial cleavage of hemoglobin into its heme and globulin components has been demonstrated to be effected by aspartic proteases, specifically the four highly homologous Plasmepsins I, II, III (more commonly referred to as histo-aspartic protease [HAP]) and IV. Cysteine proteases may also play an albeit unclear role in this initial cleavage, either directly in a so far undefined role, or indirectly *via* participating in the processing of aspartic proteases [20,21,26-30].

The subsequent breakdown of the globulin component into smaller globin fragments is known to involve the activity of cysteine proteases, principally Falcipain 2 and Falcipain 3 [27,29,31]. This process proceeds quite rapidly, with the Falcipains cleaving the polypeptide at multiple sites [32]. Aspartic proteases have also been demonstrated to play a role at this stage as well, with HAP being the most efficient of them [28].

The smaller globin fragments are then substrates for the metalloprotease Falcilysin, which breaks them down to even smaller peptides, usually containing 6 – 8 amino acid residues [33]. These are then substrates of dipeptidyl aminopeptidase 1 (DPAP1), a

plasmodial orthologue of Cathepsin C, which further reduces these small peptides to dipeptides [34], small enough to exit the parasite's food vacuole. In the cytoplasm, these dipeptides are substrates for neutral aminopeptidases such as M1 alanyl aminopeptidase (PfM1AAP) and M17 leucine aminopeptidase (PfM17LAP). These are zinc metalloenzymes that conclude the globulin catabolism, releasing free amino acids available for parasite utilization [17].

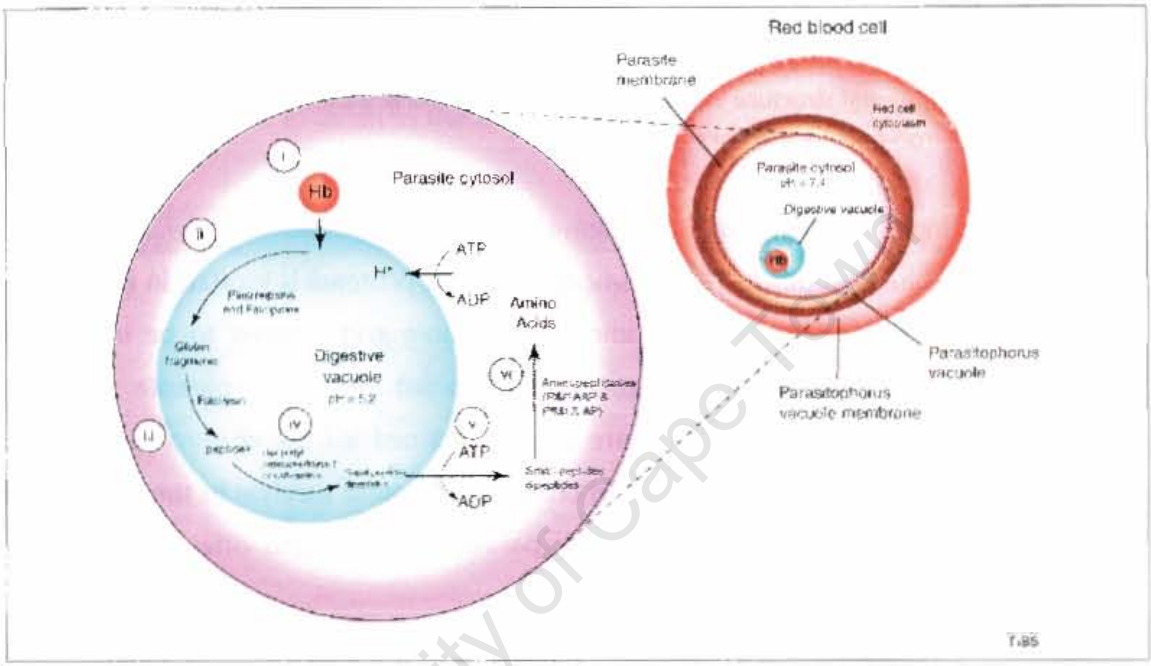

Figure 1.4: Hemoglobin degradation pathway in *Plasmodium* food vacuole [17]

Heme is toxic to the malaria parasite, and is efficiently detoxified by conversion into the crystalline hemozoin, an almost inert form of heme. The course of detoxification to hemozoin has been reported to be a two-step process involving histidine-rich proteins and lipids [35]. This hemozoin consists of chains of dimeric heme units formed by iron-carboxylate bonds involving the central ferric iron of one heme unit and the propionate side chain of the adjacent heme unit (Figure 1.5). These dimeric heme units then interact *via* hydrogen bonding to form the chains that constitute crystalline hemozoin [35-39].

In view of the above description, it can be seen that the hemoglobin degradation process offers a plethora of potential antimalarial drug targets. Established antimalarial drugs (e.g. the quinoline-based antimalarials chloroquine and amodiaquine) act by interfering with hemozoin formation (Section 1.9.1.4). The myriad of enzymes involved offer alternative antimalarial targets, and Plasmepsin inhibitors [40], Falcipain

inhibitors [31] and even inhibitors of plasmodial neutral aminopeptidases [17] have all been studied as potential antimalarial agents.

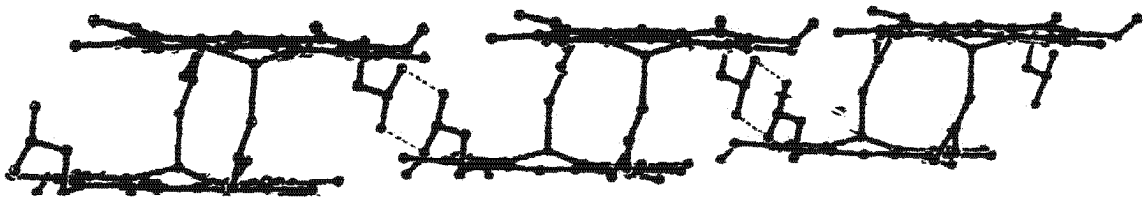

Figure 1.5: Partial structure of a β-hemeatin chain, clearly showing the dimeric heme units linked by ferric iron-propionate linkages [38]

Interestingly, another aspartic protease, Plasmepsin V, does not seem to be involved in hemoglobin catabolism. This plasmodial aspartic protease is located in the endoplasmic reticulum rather than in the acidic food vacuole and appears to be involved in the processing of the over 300 proteins exported from the parasite into the host cell/erythrocyte. These proteins are usually destined for the erythrocyte membrane or cytoskeleton, where they play roles crucial for parasite survival in the host cell [41,42]. This enzyme is therefore essential for parasite survival, and offers yet another novel target for therapeutic intervention.

1.8 Strategies for the control of malaria

The control of malaria can be considered on two levels, i.e. pre-infection (before the infected mosquito bites and infects the human host) or post-infection (after the infectious bite by the vector).

The main strategies towards pre-infection control involve preventing access of the vector to human hosts. These include:

- Indoor residual spraying: this is the application of insecticides to the inner surfaces of dwellings, where mosquitoes are likely to rest after taking a blood meal [4].
- Use of insecticide-treated nets (ITNs): there is strong evidence that the widespread use of ITNs can significantly reduce the incidence and effects of malaria in endemic areas [43].
- Use of insect repellents: certain chemicals, when applied on the human skin, strongly discourage the approach by mosquitoes and other arthropods. Such chemicals are therefore useful in preventing mosquito bites, and examples include

diethyl toluamide (DEET), which has been used for a long time and is considered safe and reliable [44].

After an infectious bite of a human by the vector (i.e. post-infection), the only recourse is the use of antimalarial drugs. The drugs may be applied to:

- Prevent the clinical establishment of the infection, referred to as chemoprophylaxis;
- Eradicate the parasite and manage the disease after the establishment of clinical manifestations, referred to as chemotherapy.
- Prevent maturation of the parasite and onward infection of the vector – prevention of transmission.

These are elaborated in detail in the following section.

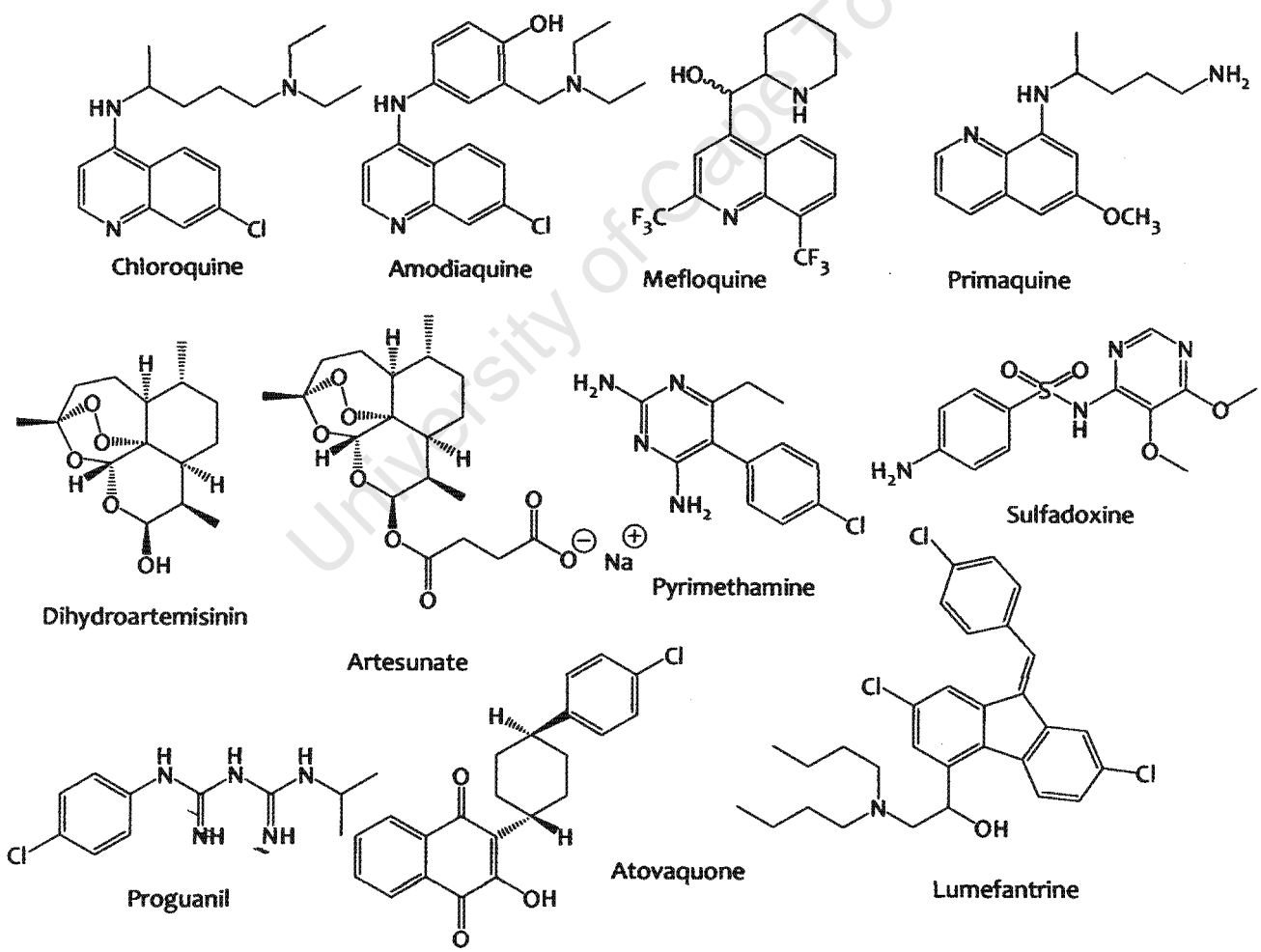

Figure 1.6: Examples of drugs that are currently in use as antimalarials

1.9 Current Therapy

1.9.1 Classification of available antimalarial agents

Antimalarials may be classed based on their:

- Chemical structures;
- Stage of the parasite life-cycle upon which they act;
- Clinical application;
- Mechanism of antimalarial action.

1.9.1.1 Classification based on chemical structure

Table 1.1: The various classes of available antimalarial drugs (based on chemical structure) [2,45,46]

Class	Examples
4-aminoquinolines	Chloroquine, amodiaquine
8-aminoquinolines	Primaquine
Aryl amino alcohols	Quinine, mefloquine,
Phenanthrene methanols	Halofantrine, lumefantrine
Diaminopyrimidines	Pyrimethamine
Sulfones	Dapsone
Sulfonamides	Sulfadoxine, sulfadiazine, sulfalene
Biguanides	Proguanil, chloroproguanil
Peroxides/sesquiterpene lactones	Artemisinin (Qinghaosu) derivatives and analogues - artemether, artesunate
Naphthoquinones	Atovaquone
Miscellaneous	*Antibiotics* (tetracycline, doxycycline); *Iron chelating agents* (desferrioxamine)

1.9.1.2 Classification based on the stage of the parasite life-cycle upon which they act

The various stages of the asexual (human) phase of the malaria parasite life cycle are distinct from each other not only by way of their morphology and metabolism, but also in their drug sensitivity [47], and this has been used as a basis for the classification of antimalarials.

prevention (suppression) of acute clinical symptoms. The slow onset, longer acting blood schizonticides pyrimethamine, atovaquone, sulfonamides, and sulfones are useful for malaria cases presenting with less severe symptoms, or for combination therapy with the rapid-onset blood schizonticides [2,48,49].

Anti-relapse antimalarial drugs are essentially those that have hypnozoiticidal activity/activity against the exo-erythrocytic phase of *P. vivax*, and *P. malariae* infections in the liver. Primaquine is useful for this purpose, usually being administered after the treatment of the primary attack in order to effect radical cure by eradicating the hypnozoites of *P. vivax* and *P. ovale*, which are responsible for relapsing infections [2,47,49].

1.9.1.4 Classification based on mechanism of antimalarial action

Inhibitors of nucleic acid synthesis – folate antagonists

The folate pathway is involved in the generation of tetrahydrofolate, a necessary co-factor for the biosynthesis of purine nucleotides, thymidylate and certain amino acids. Antimalarial drugs that inhibit this pathway therefore cause a decrease in purine (and hence DNA), serine and methionine synthesis by the parasite. Traditionally, antifolates are classified into two classes based on their target enzyme: dihydrofolate reductase (DHFR) inhibitors and dihydropteroate synthase (DHTS) inhibitors. These two enzymes are essential components of the folate pathway.

The sulfonamides (sulfadoxine, sulfadiazine, sulfalene) and the sulfones (dapsone) mimic *para*-aminobenzoic acid (PABA), thereby competitively inhibiting DHTS and interfering with the conversion of dihydropteroate from hydroxymethyldihydropterin. Pyrimethamine and the biguanides (proguanil, chloproguanil) inhibit DHFR, thus preventing the NADPH-dependent reduction of dihydrofolate to tetrahydrofolate [50,51].

Inhibitors of mitochondrial respiration

Atovaquone, a hydroxynaphthoquinone, has been shown to act on the mitochondrial electron transfer chain, where it interferes with the functions of the parasite's mitochondrial cytochrome *bc1* complex by mimicking the natural substrate ubiquinone (co-enzyme Q) [52-54].

There is evidence that artemisinins could also possibly exert their antimalarial activity by interfering with mitochondrial function. Based on experiments carried out in yeasts, it has been proposed that the mitochondrial electron transport chain activates the artemisinins, causing the local generation of free radicals/reactive oxygen species that subsequently damage the mitochondria and cause its depolarization [55]. This proposal is further supported by the fact that artemisinin has been shown to inhibit the mitochondrial respiratory chain of both sexual and asexual stages of *P. falciparum* [56].

Inhibitors of hemozoin (β-hematin) formation

As mentioned previously, heme is a by-product of hemoglobin metabolism by the malaria parasite, and is efficiently detoxified by conversion into the crystalline hemozoin, an almost inert form of heme [35]. Hemozoin formation is a validated target for most of the well-known antimalarial drugs, including the 4-aminoquinoline, quinoline methanol and phenanthrene methanol antimalarials (chloroquine, amodiaquine, quinine, mefloquine, halofantrine, and primaquine) [57-59]. π–π interactions between the quinoline (or the equivalent polycyclic) nucleus and the electronic system of heme monomers or dimers appears to be the basis for this inhibition, resulting in the inhibition of hemozoin formation either directly by inhibiting heme aggregation or indirectly by enzymatic inhibition of a protein that catalyses hemozoin crystallization. The resulting adducts and/or the accumulating free heme are lethal to the parasites, inducing oxidative stress and leading to the oxidative damage of vital intracellular components [37,60,61].

Inhibitors of *P. falciparum* ATPase (PfATP6) activity

Artemisinins have been shown to inhibit PfATP6, a plasmodial sarco/endoplasmic reticulum Ca^{2+}-ATPase (SERCA). This observation was made possible by transfection studies, where the PfATP6 was expressed in *Xenopus laevis* oocytes. Thapsigargin, a sesquiterpene lactone and a known highly specific SERCA inhibitor, has also been shown to competitively antagonize the parasiticidal activity of artemisinin. This inhibition of SERCA by artemisinins was proposed to occur after the activation of the artemisinins by iron when it was shown that chelation of iron by desferrioxamine diminishes the antiparasitic activity of artemisinins and correspondingly attenuates their inhibition of PfATP6 [62]. Some controversy still surrounds this proposed mechanism of action, largely because many aspects of this hypothesis still need to be examined [63] and the fact that results are often dependent on the methodologies used to study this inhibition [64].

1.9.2 Resistance to currently available antimalarial drugs

Current therapy of malaria faces major challenges such as poor toxicity profiles and, particularly, the development of clinically significant resistance of the parasite to most known antimalarial drugs. *P. falciparum* has been observed to have developed resistance to all the major classes of drugs (amodiaquine, chloroquine, mefloquine, quinine and sulfadoxine-pyrimethamine) [65,66]. There have been disturbing reports of possible artemisinin-resistant malaria in Southeast Asia; a recent study in western Cambodia reported reduced *in vivo* susceptibility of *P. falciparum* to artesunate that could not be explained by pharmacokinetic or other host factors [67,68], with the most likely explanation being a degree of resistance of the parasite to artesunate arising from the prolonged and inappropriate use of artemisinin mono-therapies in the country [69].

Chloroquine, which was the mainstay of antimalarial therapy for nearly half a century, has been rendered ineffective in vast zones of malaria endemic areas due to the development of resistance; this has led to health bodies recommending alternative therapies, which are commonly more expensive and less safe than chloroquine [65,66]. Reports of the emergence of chloroquine resistant malaria began in South America in the 1950s [70] and in the late 1970s in Africa [71], with the levels of resistance rising so rapidly that within the next 10 years chloroquine began to be replaced as the first-line treatment for malaria in African countries. Malawi was the first African country to do this in 1993 [72]. Unfortunately, the emergence of chloroquine resistance has been global, and it is estimated that in excess of 50% of malaria infections globally are resistant to chloroquine [73]. This situation has led to the intense and concerted efforts to understand the molecular mechanisms of chloroquine resistance, as well as to discover and/or develop new drug entities devoid of this shortcoming.

Chloroquine resistance has been associated with reduced lysosomal accumulation of chloroquine [71,74-76]. There also appears to be evidence of chloroquine efflux from the acidic food vacuole, accompanied by a H^+ 'leak' (acidic food vacuole alkalinization), that seems to be enhanced in chloroquine-resistant (CQR) strains [77]. Strong association has been shown between chloroquine resistance and mutations on the *pfcrt* gene. This gene codes for the protein PfCRT (*P. falciparum* Chloroquine Resistance Transporter), a 424 amino acid, 48.6kDa protein that localizes on the membrane of the parasite acidic food vacuole. *Pfcrt* mutations that code for the replacement of lysine residue 76 in the first transmembrane domain of PfCRT [78] by

either threonine (K76T) [78-80] or, to a lesser extent, isoleucine (K76I) and asparagine (K76N), have been associated with the CQR phenotype [81]. An association has also been demonstrated between chloroquine resistance and mutations of the *P. falciparum* gene *pfmdr1*, which codes for the glycoprotein PGH1 (P-glycoprotein homologue 1), also a lysosomal membrane protein [82]. Studies have shown that *pfcrt* polymorphisms are more strongly associated with chloroquine resistance than *pfmdr1* polymorphisms [82,83], though combinations of the two may result in higher levels of chloroquine resistance [82,84,85]. Chloroquine resistance reversal shall be discussed in Chapter Two as one of the approaches to antimalarial drug discovery.

Resistance to sulfadoxine-pyrimethamine was first noted on the Thai-Cambodian border in the mid-1960s, and is now commonplace in Asia and South America [86]. *P. vivax* has developed resistance rapidly to sulfadoxine-pyrimethamine, though it still remains sensitive to chloroquine in south-east Asia, the Indian sub-continent and the Korean peninsula [66]. The sulfadoxine-pyrimethamine combination replaced chloroquine as the first-line treatment for malaria in most African countries, though sensitivity started declining in the late 1980s and rapidly gained ground on this continent, more so in the east than in the west [65,86,87]. The molecular basis of resistance to DHFR and DHPS inhibitors (such as sulfadoxine-pyrimethamine) is single mutations on the genes encoding for the respective enzymes, resulting in amino acid substitutions on the enzymes themselves. Mutations at codons 108, 51, 59, 164, and also occasionally 50, 140, and the ``Bolivian repeat'' of the DHFR gene, and codons 436, 437, 540, 581, and 613 of the DHPS gene, have been shown to be associated with reduced susceptibility to antimalarial folate antagonists [50,86,88,89].

Mefloquine resistance was also first observed near the Thai-Cambodian border in the late 1980s, and is now common in Thailand and neighboring countries such as Cambodia, Bangladesh and India. Though reported, the degree and scope of mefloquine resistance in South America are still far below that of Southeast Asia. Clinical mefloquine resistance is rare in Africa [86]. Gene mutation and over-expression of the *pfmdr1* gene may be associated with the mechanism of mefloquine resistance [82,90].

Reports of clinical resistance to quinine, especially from the Thai-Cambodian border, began to accumulate during the mid-1960s. This situation was further compounded by the widespread use of quinine in Thailand in the early 1980s as an interim therapy due to the declining efficacy of sulfadoxine-pyrimethamine. *Pfmdr1* mutations similar to

those associated with chloroquine resistance may also account for reduced susceptibility to quinine [86].

With the number of reports of resistant malaria strains emerging from Southeast Asia, it is unsurprising that multidrug resistance of *P. falciparum*, which is defined as resistance to more than two operational antimalarial compounds of different chemical classes, is well established in this region, particularly around the border regions of Thailand [86].

Despite its possible novel mode of action, resistance occurs readily with atovaquone monotherapy. For this reason, it is recommended that atovaquone be used as a fixed-ratio combination with the antifolate drug proguanil (Malarone®) [50,91]. Atovaquone resistance may be the result of mutations in the plasmodial genes coding for the putative cytochrome *b* product, resulting in changes in the amino acid sequence such as V284T, M133I and L144S [53].

Studies that have tried to shed light on the molecular basis of diminished artemisinin susceptibility [86,92] have not yielded convincing results so far. No mutations of the candidate genes suggested by earlier studies have been found to confer artemisinin resistance.

1.10 Summary

The high levels of morbidity and mortality associated with malaria and the shortcomings associated with currently available antimalarial drugs suggest that the development of new, highly efficacious drugs and/or treatment regimens for the management of malaria remains a key priority [93].

This project therefore seeks to contribute to this aspect, and is an attempt to design and develop new (and cost effective) antimalarial agents. Chapter Two provides a discussion of some of the possible approaches for antimalarial drug discovery.

References

1. Malaria Fact Sheet. *Institute of One World Health* (2007)

2. Malaria Site: Comprehensive Malaria Website. http://www.malariasite.com (2009)

3. C A Guerra, P W Gikandi, A J Tatem, A M Noor, and D L Smith. The limits and intensity of Plasmodium falciparum transmission: implications for malaria control and elimination worldwide. *PLoS Med.* (2008) 5 (2) e38.

4. WHO. World Malaria Report 2008. (2008)

5. P Olumese. Epidemiology and Surveillance: Changing the global picture of malaria-myth or reality. *Acta Trop.* (2005) 95 265-269.

6. K Mendis, B J Sina, P Marchesini, and R Carter. The neglected burden of *Plasmodium vivax* malaria. *Am. J. Trop. Med. Hyg.* (2001) 64 ((1,2)S) 97-106.

7. P J Guerin, P Olliaro, F Nosten, P Druilhe, R Laxminarayan, F Binka, W L Kilama, N Ford, and N J White. Malaria: current status of control, diagnosis, treatment, and a proposed agenda for research and development. *Lancet Infect. Dis.* (2002) 2 564-573.

8. R Wurthwein, A Gbangou, R Sauerborn, and C M Schmidt. Measuring the local burden of disease: A study of years lost in sub-Saharan Africa. *Int. J. Epidemiol.* (2001) 30 501-508.

9. WHO Expert Committee on Malaria. *WHO Technical Report Series* (2000) Twentieth Report

10. Roll Back Malaria, WHO, and UNICEF. World Malaria Report 2005. (2005)

11. WHO. World Health Report 2005. (2005)

12. A K Rowe, S Y Rowe, R W Snow, E L Korenromp, J A Schellenberg, C Stein, B L Nahlen, J Bryce, R E Black, and R W Steketee. The burden of malaria mortality among African children in the year 2000. *Int. J. Epidemiol.* (2006) 35 (3) 691-704.

13. R I Chima, C A Goodman, and A Mills. The economic impact of malaria in Africa: a critical review of the evidence. *Health Policy* (2003) 63 17-36.

14. R Paul, M Diallo, and P T Brey. Mosquitoes and transmission of malaria parasites - not just vectors. *Malaria J.* (2004) 3 (39) doi:10.1186/1475-2875-3-39.

15. T Hayden. Making inroads on malaria. *Anal.Chem.* (2006) 78 (15) 5252-5260.

16. CDC Division of parasitic control website. http://www.dpd.cdc.gov/DPDx (2007)

17. T S Skinner-Adams, C M Stack, K R Trenholme, C L Brown, J Grembecka, J Lowther, A Mucha, M Drag, P Kafarski, S McGowan, J C Whisstock, D L Gardiner, and J P Dalton. *Plasmodium falciparum* neutral aminopeptidases: new targets for anti-malarials. *Trends Biochem. Sci.* (2009) 35 (1) 53-61.

18. J Liu, E S Istvan, I Y Gluzman, J Gross, and D E Goldberg. *Plasmodium falciparum* ensures its amino acid supply with multiple acquisition pathways and redundant proteolytic enzyme systems. *Proc. Natl. Acad. Sci. USA.* (2006) 103 (23) 8840-8845.

19. M Krugliak, J Zhang, and H Ginsburg. Intraerythrocytic *Plasmodium falciparum* utilizes only a fraction of the amino acids derived from the digestion of host cell cytosol for the biosynthesis of its proteins. *Mol. Biochem. Parasitol.* (2002) 119 249-256.

20. S E Francis, D J Sullivan, and D E Goldberg. Hemoglobin metabolism in the malaria parasite *Plasmodium falciparum*. *Annu. Rev. Microbiol.* (1997) 51 97-123.

21. P J Rosenthal and S R Meshnick. Mini Review: Hemoglobin catabolism and iron utilisation by malaria parasites. *Mol. Biochem. Parasitol.* (1996) 83 131-139.

22. S H Payne and W F Loomis. Retention and Loss of Amino Acid Biosynthetic Pathways Based on Analysis of Whole-Genome Sequences. *Eukaryotic Cell* (2006) 5 (2) 7272-276.

23. S M Huber, C Lang, F Lang, and C Duranton. Organic osmolyte channels in malaria-infected erythrocytes. *Biochem. Biophys. Res. Com.* (2008) 376 514-518.

24. R E Martin and K Kirk. Transport of the essential nutrient isoleucine in human erythrocytes infected with the malaria parasite *Plasmodium falciparum*. *Blood* (2007) 109 (5) 2217-2224.

25. Y Kuhn, P Rohrbach, and M Lanzer. Quantitative pH measurements in *Plasmodium falciparum*-infected erythrocytes using pHluorin. *Cell. Microbiol.* (2007) 9 (4) 1004-1013.

26. I Y Gluzman, S E Francis, A Oksman, C E Smith, K L Duffin, and D E Goldberg. Order and specificity of the *Plasmodium falciparum* hemoglobin degradation pathway. *J. Clin. Invest.* (1994) 93 1602-1608.

27. R Bhaskar and P J Rosenthal. Reducing requirements for hemoglobin hydrolysis by *Plasmodium falciparum* cysteine proteases. *Mol. Biochem. Parasitol.* (2002) 122 99-104.

28. R Banerjee, J Liu, W Beatty, L Pelosof, M Klemba, and D E Goldberg. Four plasmepsins are active in the *Plasmodium falciparum* food vacuole, including a protease with an active-site histidine. *Proc. Natl. Acad. Sci. USA.* (2002) 99 990-995.

29. P J Rosenthal. Cysteine proteases of malaria parasites. *Int. J. Epidemiol.* (2004) 34 1489-1499.

30. M E Drew, R Banerjee, E W Uffman, S Gilbertson, P J Rosenthal, and D E Goldberg. *Plasmodium* Food Vacuole Plasmepsins Are Activated by Falcipains. *J. Biol. Chem.* (2008) 283 (19) 12870-12876.

31. R Ettari, F Bova, M Zappalà, S Grasso, and N Micale. Falcipain-2 Inhibitors. *Med. Res. Rev.* (2010) 30 (1) 136-167.

32. S Subramanian, M Hardt, Y Chloe, R K Niles, and E B Johansen. Hemoglobin Cleavage Site-Specificity of the *Plasmodium falciparum* Cysteine Proteases Falcipain-2 and Falcipain-3. *PLoS ONE* (2009) 4 (4) e5156.

33. C E Murata and D E Goldberg. *Plasmodium falciparum* falcilysin: an unprocessed food vacuole enzyme. *Mol. Biochem. Parasit.* (2003) 129 123-126.

34. M Klemba, I Gluzman, and D E Goldberg. A *Plasmodium falciparum* Dipeptidyl Aminopeptidase I Participates in Vacuolar Hemoglobin Degradation. *J. Biol. Chem.* (2004) 279 (41) 43000-43007.

35. A V Pandey, V K Babbarwal, J N Okoyeh, R M Joshi, S K Puri, R L Singh, and V S Chauhan. Hemozoin formation in malaria: a two-step process involving histidine-rich proteins and lipids. *Biochem. Bioph. Res. Co.* (2003) 308 736-743.

36. A F G Slater, W J Swiggard, B R.Orton, W D Flitter, D E Goldberg, A Cerami, and G B Henderson. An iron-caboxylate bond links heme units of malaria pigment. *Proc. Natl. Acad. Sci. USA.* (1991) 88 325-329.

37. S Pagola, P W Stephens, D S Bohle, A D Kosar, and S K Madsen. The structure of malaria pigment β-haematin. *Nature* (2000) 404 307-310.

38. D S Bohle, A D Kosar, and P W Stephens. Phase homogeneity and crystal morphology of the malaria pigment β-hematin. *Acta Crystallogr.* (2002) D58 1752-1756.

39. E Hempelmann. Hemozoin Biocrystallization in *Plasmodium falciparum* and the antimalarial activity of crystallization inhibitors. *Parasitol. Res.* (2007) 100 671-676.

40. D Gupta, R S Yedidi, S Varghese, L C Kovari, and P M Woster. Mechanism-Based Inhibitors of the Aspartyl Protease Plasmepsin II as Potential Antimalarial Agents. *J. Med. Chem.* (2010) 53 4234-4247.

41. J A Boddey, A N Hodder, S Günther, P R Gilson, H Patsiouras, E A Kapp, J A Pierce, T F de Koning-Ward, R J Simpson, B C Crabb, and A F Cowman. An aspartyl protease directs malaria effector proteins to the host cell. *Nature* (2010) 463 627-633.

42. I Russo, S Babbitt, V Muralidharan, T Butler, A Oksman, and D E Goldberg. Plasmepsin V licenses *Plasmodium* proteins for export into the host erythrocyte. *Nature* (2010) 463 632-636.

43. C Lengeler. Insecticide-treated bed nets and curtains for preventing malaria. *Chochrane Darabase Syst. Rev.* (2004) 2 (CD000363) DOI:10.1002/14651858.CD000363.pub2.

44. L H Chen, M E Wilson, and P Schlagenhauf. Prevention of Malaria in Long-term Travelers. *J. Am. Med. Assoc.* (2006) 296 (18) 2234-2244.

45. A Kumar, S B Katiyar, A Agarwal, and P M S Chauhan. Perspective in Antimalarial Chemotherapy. *Curr. Med. Chem.* (2003) 10 1137-1150.

46. P M S Chauhan and S K Srivastava. Present Trends and Future Strategy in Chemotherapy of Malaria. *Curr. Med. Chem.* (2001) 8 1535-1542.

47. T A Shapiro and D E Goldberg. Chemotherapy of protozoal infections. *In: Goodman and Gilman's The Pharmacological Basis of Therapeutics* (2006) 11th Edition. Edited by L L Brunton. McGraw-Hill: Medical Publishing Division. New York

48. M Frédérich, J M Dogné, L Angenot, and P de Mol. New Trends in Anti-Malarial Agents. *Curr. Med. Chem.* (2002) 9 1435-1456.

49. L J Bruce-Chwatt. Classification of Antimalarial Drugs in Relation to Different Stages in the Life-cycle of the Parasite: Commentary on a Diagram. *Bull. World Health Organ.* (1962) 27 (2) 287-290.

50. P Olliaro. Mode of action and mechanisms of resistance for antimalarial drugs. *Phamacol. Therap.* (2001) 89 207-219.

51. A Nzila. The past, present and future of antifolates in the treatment of *Plasmodium falciparum* infection. *J. Antimicrob. Chemother.* (2006) 57 1043-1054.

52. M W Mather, E Darrouzet, M Valkova-Valchanova, J W Cooley, M T McIntosh, F Daldal, and A B Vaidya. Uncovering the Molecular Mode of Action of the Antimalarial Drug Atovaquone Using a Bacterial System. *J. Biol. Chem.* (2005) 280 (29) 27458-27465.

53. D Syafruddin, J E Siregar, and S Marzuki. Mutations in the cytochrome b gene of *Plasmodium berghei* conferring resistance to atovaquone. *Mol. Biochem. Parasitol.* (1999) 104 185-194.

54. M Fry and M Pudney. Site of action of the antimalarial hydroxynaphthoquinone, 2-[trans-4-(4'-chlorophenyl) cyclohexyl]-3- hydroxy-1,4-naphthoquinone (566C80). *Biochem. Pharmacol.* (1992) 43 (7) 1545-1553.

55. W Li, W Mo, D Shen, L Sun, J Wang, S Lu, J M Gitschier, and B Zhou. Yeast Model Uncovers Dual Roles of Mitochondria in the Action of Artemisinin. *PLoS Gen.* (2005) 1 (3) e36.

56. J Krungkrai, D Burat, S Kudan, S Krungkrai, and P Prapunwattana. Mitochondrial oxygen consumption in asexual and sexual blood stages of the human malarial parasite, *Plasmodium falciparum*. *Southeast Asian J. Trop. Med. Public Health* (1999) 30 (4) 636-642.

57. M Mungthin, P G Bray, R G Ridley, and S A Ward. Central Role of Hemoglobin Degradation in Mechanisms of Action of 4-Aminoquinolines, Quinoline Methanols, and Phenanthrene Methanols. *Antimicrob. Agents Chemother.* (1998) 42 (11) 2973-2977.

58. K A de Villiers, H M Marques, and T J Egan. The crystal structure of halofantrine–ferriprotoporphyrin IX and the mechanism of action of arylmethanol antimalarials. *J. Inorg. Biochem.* (2008) 102 1660-1667.

59. T J Egan and K Ncokazi. Quinoline antimalarials decrease the rate of β-hematin formation. *J. Inorg. Biochem.* (2005) 99 1532-1539.

60. S Kumar, M Guha, V Choubey, P Maity, and U Bandyopadhay. Antimalarial drugs inhibiting hemozoin (β-hematin) formation: a mechanistic update. *Life Sci.* (2007) 80 813-828.

61. I Weissbuch and L Leiserowitz. Interplay Between Malaria, Crystalline Hemozoin Formation, and Antimalarial Drug Action and Design. *Chem. Rev.* (2008) 108 4899-4914.

62. U E Ludwig, R J Webb, L D A Goethem, J M East, A G Lee, M Kimura, P M O'Neill, P G Bray, S A Ward, and S Krishna. Artemisinins target the SERCA of *Plasmodium falciparum*. *Nature* (2003) 424 (21) 957-961.

63. S Krishna, A-C Uhlemann, and R K Haynes. Artemisinins: mechanisms of action and potential for resistance. *Drug Resist. Updates* (2004) 7 233-244.

64. S Krishna, S Pulcini, F Fatih, and H Staines. Artemisinins and the biological basis for the PfATP6/SERCA hypothesis. *Trends Parasitol.* (2010) 26 (11) 517-523.

65. R N Price and F Nosten. Drug resistant falciparum malaria: clinical consequences and strategies for prevention. *Drug Resist. Update* (2001) 4 187-196.

66. WHO. Guidelines for the treatment of malaria. *WHO* (2006)

67. H Noedl, Y Se, K Schaener, B L Smith, D Socheat, and M M Fukuda. Evidence of Artemisinin-Resistant Malaria in Western Cambodia. *New Engl. J. Med.* (2008) 359 (24) 2619-2620.

68. A M Dondorp, F Norsten, P Yi, D Das, A P Phyo, J Tarning, K M Lwin, F Ariey, W Hanpithithakpong, S J Lee, P Ringwald, K Silamut, M Imwong, K Chotivanich, P Lim, T Herdman, S S An, S Yeung, P Singhasivanon, N P J Day, N Lindegardh, D Socheat, and N J White. Artemisinin Resistance in *Plasmodium falciparum* Malaria. *N. Engl. J. Med.* (2009) 361 455-467.

69. R J Maude, C J Woodrow, and N J White. Artemisinin Antimalarials: Preserving the "Magic Bullet". *Drug Dev. Res.* (2010) 71 12-19.

70. D Payne. Spread of chloroquine resistance in *Plasmodium falciparum*. *Parasitol. Today* (1987) 3 241-246.

71. D Warhurst. New developments: Chloroquine-resistance in *Plasmodium falciparum*. *Drug Resist. Updates* (2001) 4 142-144.

72. L Mwai, E Ochong, A Abdirahman, S M Kiara, S Ward, G Kokwaro, P Sasi, K Marsh, S Borrmann, M Mackinnon, and A Nzila. Chloroquine resistance before and after its withdrawal in Kenya. *Malaria J.* (2009) 8 (1) 106.

73. B Gligorijevic, K Purdy, D A.Elliott, R A.Cooper, and P D.Roepe. Stage independent chloroquine resistance and chloroquine toxicity revealed via spinning disk confocal microscopy. *Mol. Biochem. Parasitol* (2008) 159 7-23.

74. M Cabrera, J Natarajan, M F.Paguio, C Wolf, J S.Urbach, and P D.Roepe. Chloroquine Transport in *Plasmodium falciparum*. 1. Influx and Efflux Kinetics for Live Trophozoite Parasites Using a Novel Fluorescent Chloroquine Probe. *Biochemistry.* (2009) 48 9471-9481.

75. R Hayward, K J Saliba, and K Kirk. The pH of the digestive vacuole of *Plasmodium falciparum* is not associated with chloroquine resistance. *J. Cell Sci.* (2006) 119 (6) 1016-1025.

76. K J Saliba, P I Folb, and P J Smith. Role for the *Plasmodium falciparum* Digestive Vacuole in Chloroquine Resistance. *Biochem. Pharmacol.* (1998) 56 313-320.

77. A M.Lehane, R Hayward, K J.Saliba, and K Kirk. A verapamil-sensitive chloroquine-associated H+ leak from the digestive vacuole in chloroquine-resistant malaria parasites. *J. Cell Sci.* (2008) 121 (10) 1624-1632.

78. D A Fidock, T Nomura, A K Talley, R A Cooper, S M Dzekunov, M T Ferdig, L M B Ursos, A B S Sidhu, B Naudé, K W Deitsch, X Su, J C Wootton, P D Roepe, and T E Wellems. Mutations in the *P. falciparum* Digestive Vacuole Transmembrane Protein PfCRT and Evidence for Their Role in Chloroquine Resistance. *Mol. Cell* (2000) 6 861-871.

79. R Durand, S Jafari, J Vauzelle, J-F Delabre, Z Jesic, and J Le Bras. Analysis of *pfcrt* point mutations and chloroquine susceptibility in isolates of *Plasmodium falciparum*. *Mol. Biochem. Parasitol* (2001) 114 95-102.

80. A B S Sidhu, D Verdier-Pinard, and D A.Fidock. Chloroquine Resistance in *Plasmodium falciparum* Malaria Parasites Conferred by Pfcrt Mutations. *Science* (2002) 298 210-213.

81. R A Cooper, M T Ferdig, X Su, L M B Ursos, J Mu, T Nomura, H Fujioka, D A Fidock, P D Roepe, and T E Wellems. Alternative Mutations at Position 76 of the Vacuolar Transmembrane Protein PfCRT Are Associated with Chloroquine Resistance and Unique Stereospecific Quinine and Quinidine Responses in *Plasmodium falciparum*. *Mol. Pharmacol.* (2002) 61 35-42.

82. M T Duraisingh and A F Cowman. Contribution of the pfmdr1 gene to antimalarial drug-resistance. *Acta Tropica* (2005) 94 181-190.

83. S Cojean, A Noël, D Garnier, V Hubert, J Le Bras, and R Durand. Lack of association between putative transporter gene polymorphisms in *Plasmodium falciparum* and chloroquine resistance in imported malaria isolates from Africa. *Malaria J.* (2006) 5 (1) 24.

84. M B Reed, K J Saliba, S R Caruana, K Kirk, and A F.Cowman. PGH1 modulates sensitivity and resistance to multiple antimalarials in *Plasmodium falciparum*. *Nature* (2000) 403 906-909.

85. H A Babiker, S J Pringle, A Abdel-Muhsin, M Mackinnon, P Hunt, and D Walliker. High-level chloroquine resistance in Sudanese isolates of *Plasmodium falciparum* is associated with mutations in the chloroquine resistance transporter *pfcrt* and the multi-drug resistance gene *pfmdr1*. *J. Infect. Dis.* (2001) 183 1535-1538.

86. C Wongsrichanalai, A M Lickard, W H Wernsdorfer, and S R Meshnick. Epidemiology of drug-resistant malaria. *Lancet Infect. Dis.* (2002) 2 209-218.

87. News. New strain of drug-resistant malaria in Africa. *Int. J. Epidemiol.* (2001) 30 1213-1215.

88. C V Plowe, J F Cortese, A Djimde, O C Nwanyanwu, W M Watkins, P A Winstanley, J G Estrada-Franco, R E Mollinedo, J C Avila, J L Cespedes, D Carter, and O K Doumbo. Mutations in *Plasmodium falciparum* Dihydrofolate Reductase and Dihydropteroate Synthase and Epidemiologic Patterns of Pyrimethamine-Sulfadoxine Use and Resistance. *J. Infect. Dis.* (1997) 176 1590-1596.

89. C V Plowe, J G Kublin, and O K Doumbo. *P. falciparum* dihydrofolate reductase and dihydropteroate synthase mutations: epidemiology and role in clinical resistance to antifolates. *Drug Resist. Update* (1998) 1 389-396.

90. Y Nishayama, Y Okuda, H-S Kim, T Huruta, M Kimura, and Y Wataya. Genetic analysis of mefloquine-resistant mechanism of *Plasmodium falciparum*. *Nucleic Acid Symp. Ser.* (2004) 48 163-164.

91. P D Radloff, J Phillips, M Nkeyi, D Hutchinson, and P G Kremsner. Atovaquone and proguanil for *Plasmodium falciparum* malaria. *Lancet* (1996) 347 1511-1514.

92. M Imwong, A M Dondorp, F Norsten, P Yi, M Mungthin, S Hanchana, D Das, A P Phyo, K M Lwin, S Pukrittayakamee, S J Lee, S Saisung, K Koecharoen, C Nguon, N P J Day, D Socheat, and N J White. Exploring the contribution of candidate genes to artemisinin resistance in *Plasmodium falciparum*. *Antimicrob. Agents Chemother.* (2010) 54 (7) 2886-2892.

93. R G Ridley. Medical need, scientific opportunity and the drive for antimalarial drugs. *Nature* (2002) 415 686-693.

CHAPTER TWO

APPROACHES TO ANTIMALARIAL DRUG DISCOVERY

2.1 Preamble

Having introduced malaria as a disease and the drugs available for its treatment in Chapter One, this chapter follows on to present some of the general strategies that have been, and continue to be, exploited for the discovery of antimalarial drugs. Representative examples are given for the various approaches, and the discussion is concluded by a brief account of some of the more modern techniques that can be applied to augment antimalarial drug discovery.
Some of the strategies that have been applied in this study are then highlighted.

2.2 Introduction

As has been alluded to in the previous Chapter, the development of new, highly efficacious drugs and/or treatment regimens for the management of malaria remains a key priority [1]. This must take into account specific concerns, in particular the requirement for affordable and simple to use new therapies [2]. Various strategies are available for this purpose, and include:

- Applying available drugs in new treatment regimens;
- Identification of antimalarial compounds arising from research on other diseases;
- Reversal of antimalarial drug resistance;
- Development of analogs of existing antimalarial chemotherapeutic agents;
- Discovery of uniquely novel antimalarial agents:
    - Identification and validation of novel antimalarial pharmacophores for further development;
    - *De novo* design of novel antimalarial compounds;
    - Application of high-throughput screening and virtual screening techniques;
    - Discovery and development of natural product-based therapeutic agents.

2.3 Applying available drugs in new treatment regimens

One of the strategies for evading the development of resistance to antimalarials is the use of combination therapies, which basically involves the co-administration of two or more antimalarial agents. The WHO defines antimalarial combination therapy as "the simultaneous use of two or more blood schizontocidal drugs with independent modes

It is for these reasons that ACTs generally combine the artemisinin-based antimalarials with longer-acting antimalarial agents. Examples of ACTs constituted in this way include artemether + lumefantrine (Co-Artem®), which was the first clinically available fixed combination of an artemisinin-based antimalarial and a longer-acting antimalarial. Other ACTs currently also recommended by WHO on the strength of clinical trials include artesunate + amodiaquine (Coarsucam®), artesunate + mefloquine (Artequin®), artesunate + sulfadoxine-pyrimethamine , and DHA + piperaquine (Duo-Cotecxin®). Sulfametopyrazine-pyrimethamine is considered an alternative to sulfadoxine-pyrimethamine [7]. Other antimalarial drugs that have been considered as partner drugs in ACTs include pyronaridine [4], chlorproguanil-dapsone and atovaquone-proguanil [3].

These ACTs take advantage of the rapid reduction in parasitemia afforded by the artemisinin antimalarial, with the additional agent(s) ensuring complete elimination of the parasite by essentially mopping up what's left of it. In this way rapid cure is achieved, with minimal risk of the survival of any strains of the parasite that may emerge as resistant to either of the administered agents. When given in combination with these slowly eliminated antimalarials, short courses of treatment (6 dose/3 day regimens) are effective. This is because a 3-day course of the artemisinin is required to eliminate at least 90% of the parasitemia; the partner medicine only has to clear the remaining 10% of the parasitemia, thus reducing the potential for development of resistance [3,7].

However, implementation of ACT has had its fair share of ethical and logistic considerations [11], and it has been argued that access to this form of therapy is still beyond the reach of the majority of the impoverished population that is heavily affected by malaria, the major barrier being cost [6].

2.3.2 Non-artemisinin based combination therapy (non-ACT)

These include combinations such as chloroquine + sulfadoxine-pyrimethamine and amodiaquine + sulfadoxine-pyrimethamine [3]. However, the prevailing high levels of resistance to these drugs as monotherapy have compromised their efficacy even in combinations. As a result of this, and the fact that these combinations are still less effective that ACTs, WHO no longer recommends non-ACTs for the treatment of uncomplicated malaria [7].

2.4 Antimalarial compounds arising from research on other diseases

Antimalarial drug discovery has benefited immensely from research aimed at discovering new therapies for other unrelated diseases.

For example, development of antifolates as therapeutic agents began with efforts to treat acute leukemias and other cancers, and which were based on the observed anti-proliferative effects of creating a folate deficient state. Antifolate anticancer agents such as methotrexate were the fruits of these efforts. Subsequent screens of antifolates against other rapidly dividing cells led to a demonstration of hitherto unknown antibacterial and antiparasitic activities, including antimalarial activity [12]. This led to the development of antifolate antimalarial agents, such as the dihydrofolate reductase (DHFR) inhibitors proguanil, chlorproguanil and pyrimethamine [12,13] as well as the dihydropteroate synthase (DHFS) inhibitors dapsone, sulfadoxine and sulfametopyrazine [12]. The combination of DHFR and DHPS inhibitors is markedly synergistic, and hence these agents are invariably used in combination in the treatment of malaria, e.g. as pyrimethamine + sulfadoxine (Fansidar®) and pyrimethamine + sulfametopyrazine (Metakelfin®) combinations. These drugs tend to have long elimination profiles with half-lives >80 hours, hence enabling effective single-dose therapy. Chlorproguanil-dapsone combination is also available [12], and novel antifolate drug combinations continue to be tested [14]. As mentioned previously, the pyrimethamine + sulfadoxine and pyrimethamine + sulfametopyrazine combinations have also been successfully incorporated into ACTs.

Atovaquone (Mepron®) was initially identified as a broad spectrum anti-infective [15], but its development was expedited by the discovery of its potential to treat *Pneumocystis carinii* pneumonia (PCP), one of the main opportunistic infections in HIV/AIDS patients [16]. Its antimalarial activity has been demonstrated [17], and its potential as an antimalarial has since been re-explored following the demonstration of its *in vitro* antimalarial synergy with proguanil [18,19] as well as its efficacy and safety when administered as the fixed dose antimalarial combination of atovaquone-proguanil (Malarone®) [20].

Iron chelators have been developed mainly for the treatment of iron overload particularly in patients suffering from blood disorders such as thalassemias, and who receive regular blood transfusions. These compounds sequester and allow for the elimination of iron, thereby preventing the complications (damage to the liver, heart and endocrine organs) that would arise from the inevitable accumulation of iron

resulting from the repeated transfusions. Classic examples of iron chelators used for this purpose are desferrioxamine (DFO) and deferiprone [21-23]. DFO is the most widely used iron chelator, and is a naturally occurring trihydroxamic acid derived from cultures of *Streptomyces pilosus* that has been used extensively for many years; it is remarkably safe and nontoxic [24]. Interestingly, these and other iron chelators have been shown to exhibit antimalarial activity *in vitro* [24,25]. This is possibly due to either their ability to withhold iron (thereby making it inaccessible for vital, iron-dependent metabolic pathways of the intra-erythrocytic parasite), or by the formation of complexes with iron that are toxic to the parasite. Following these observations *in vitro*, animal and human trials have subsequently been carried out on some of these agents. DFO has been shown to be effective as a single agent in reducing *P. falciparum* parasitemia in uncomplicated malaria in humans, and these findings suggest that iron chelation may be a potentially viable strategy for the chemotherapy of malaria [26].

2.5 Reversal of drug resistance

One of the main shortcomings of most of the currently available antimalarial drugs is the development of resistance by the malaria parasite; it therefore follows that the reversal of this resistance could potentially restore the efficacy of these agents [27].

This strategy has been actively pursued, with chloroquine resistance (CQR) reversal agents the subject of most of the reported studies of this nature. A range of structurally diverse compounds have been identified that act as CQR reversal agents, ranging from natural products and clinically available drugs to novel synthetic compounds.

2.5.1 Natural products as CQR reversal agents

In the mid-1980s, ethnobotanical studies in Madagascar revealed the application by traditional healers and local populations of extracts from various local plants as chloroquine adjuvants; these decoctions and infusions were co-administered with 1 - 2 tablets (100– 200 mg) of chloroquine with the aim of reinforcing the antimalarial effects of chloroquine [28]. Two of the plants used for this purpose, namely *Hernandia voyronii* (also known as *Hazomalania voyronii*) and *Strychnos myrtoides*, have had their possible chloroquine potentiating activities investigated further [28-30].

A series of dimeric, structurally-related, pavine-benzyltetrahydroisoquinoline (pavine-BTIQ) alkaloids have been isolated from *H. voyronii*, and are designated as Herveline A, B, C and D. Reticuline, the precursor of the BTIQ component of these alkaloids, has

resulting from the repeated transfusions. Classic examples of iron chelators used for this purpose are desferrioxamine (DFO) and deferiprone [21-23]. DFO is the most widely used iron chelator, and is a naturally occurring trihydroxamic acid derived from cultures of *Streptomyces pilosus* that has been used extensively for many years; it is remarkably safe and nontoxic [24]. Interestingly, these and other iron chelators have been shown to exhibit antimalarial activity *in vitro* [24,25]. This is possibly due to either their ability to withhold iron (thereby making it inaccessible for vital, iron-dependent metabolic pathways of the intra-erythrocytic parasite), or by the formation of complexes with iron that are toxic to the parasite. Following these observations *in vitro*, animal and human trials have subsequently been carried out on some of these agents. DFO has been shown to be effective as a single agent in reducing *P. falciparum* parasitemia in uncomplicated malaria in humans, and these findings suggest that iron chelation may be a potentially viable strategy for the chemotherapy of malaria [26].

2.5 Reversal of drug resistance

One of the main shortcomings of most of the currently available antimalarial drugs is the development of resistance by the malaria parasite; it therefore follows that the reversal of this resistance could potentially restore the efficacy of these agents [27].

This strategy has been actively pursued, with chloroquine resistance (CQR) reversal agents the subject of most of the reported studies of this nature. A range of structurally diverse compounds have been identified that act as CQR reversal agents, ranging from natural products and clinically available drugs to novel synthetic compounds.

2.5.1 Natural products as CQR reversal agents

In the mid-1980s, ethnobotanical studies in Madagascar revealed the application by traditional healers and local populations of extracts from various local plants as chloroquine adjuvants; these decoctions and infusions were co-administered with 1 - 2 tablets (100 – 200 mg) of chloroquine with the aim of reinforcing the antimalarial effects of chloroquine [28]. Two of the plants used for this purpose, namely *Hernandia voyronii* (also known as *Hazomalania voyronii*) and *Strychnos myrtoides*, have had their possible chloroquine potentiating activities investigated further [28-30].

A series of dimeric, structurally-related, pavine-benzyltetrahydroisoquinoline (pavine-BTIQ) alkaloids have been isolated from *H. voyronii*, and are designated as Herveline A, B, C and D. Reticuline, the precursor of the BTIQ component of these alkaloids, has

also been isolated, characterized and derivatized (by demethylation) to yield the semi-synthetic derivative laudanosine [30] (see Figure 2.1 for structures). These compounds showed moderate to weak *in vitro* antimalarial activity (IC_{50} values of 1 – 30 μM against the CQR *P. falciparum* FCM29 strain). Herveline B and C, and to a lesser extent laudanosine, showed significant chloroquine potentiating effects *in vitro* against the same CQR strain (FCM29); reticuline showed weak synergism with chloroquine. Herveline A showed only additive effects, while Herveline D showed mild antagonism with chloroquine [30].

A study of *S. myrtoides* showed that crude extracts from the plant lacked any intrinsic antimalarial activity *in vitro*, but reversed CQR in a dose-dependent manner against the CQR *P. falciparum* strain FCM29; they also potentiated the effects of chloroquine *in vivo* in mice infected with CQR *P. yoelii nigeriensis*. Bioassay guided fractionation yielded two indole alkaloids, malagashanine and strychnobrasiline (Fig. 2.1), which exhibited similar activities [29]. Malagashanine, the parent compound of a class of indole alkaloids, has also been reported to enhance the susceptibility of other CQR strains, such as W2 and K1, to chloroquine *in vitro* [31,32]. This chloroquine sensitization was not observed with the chloroquine sensitive (CQS) strain NS [31]. Malagashanine has also shown notable *in vitro* synergy with quinine and mefloquine, as well as the aminoacridines quinacrine and pyronaridine [30]. Icajine and isoretuline (Figure 2.1), two indole alkaloids also isolated from *Strychnos* species, have been shown to potentiate chloroquine *in vitro* against the CQR strains W-2 and PFB, though this activity is absent against the CQS FCA strain of *P. falciparum* [33].

Other plant species have also yielded compounds with chloroquine potentiating activity. Bisbenzylisoquinoline alkaloids, isolated from plants of the *Annonaceae* and *Menispermaceae* species, also exhibit moderate intrinsic antimalarial activity (IC_{50} values in the lower micromolar to high nanomolar range), and show *in vitro* synergy with chloroquine against the CQR strains FcB1 [34] and W2 [35]; the more potent of this class of alkaloids are fangchinoline [34] and cepharanthine [35] (Figure 2.1).

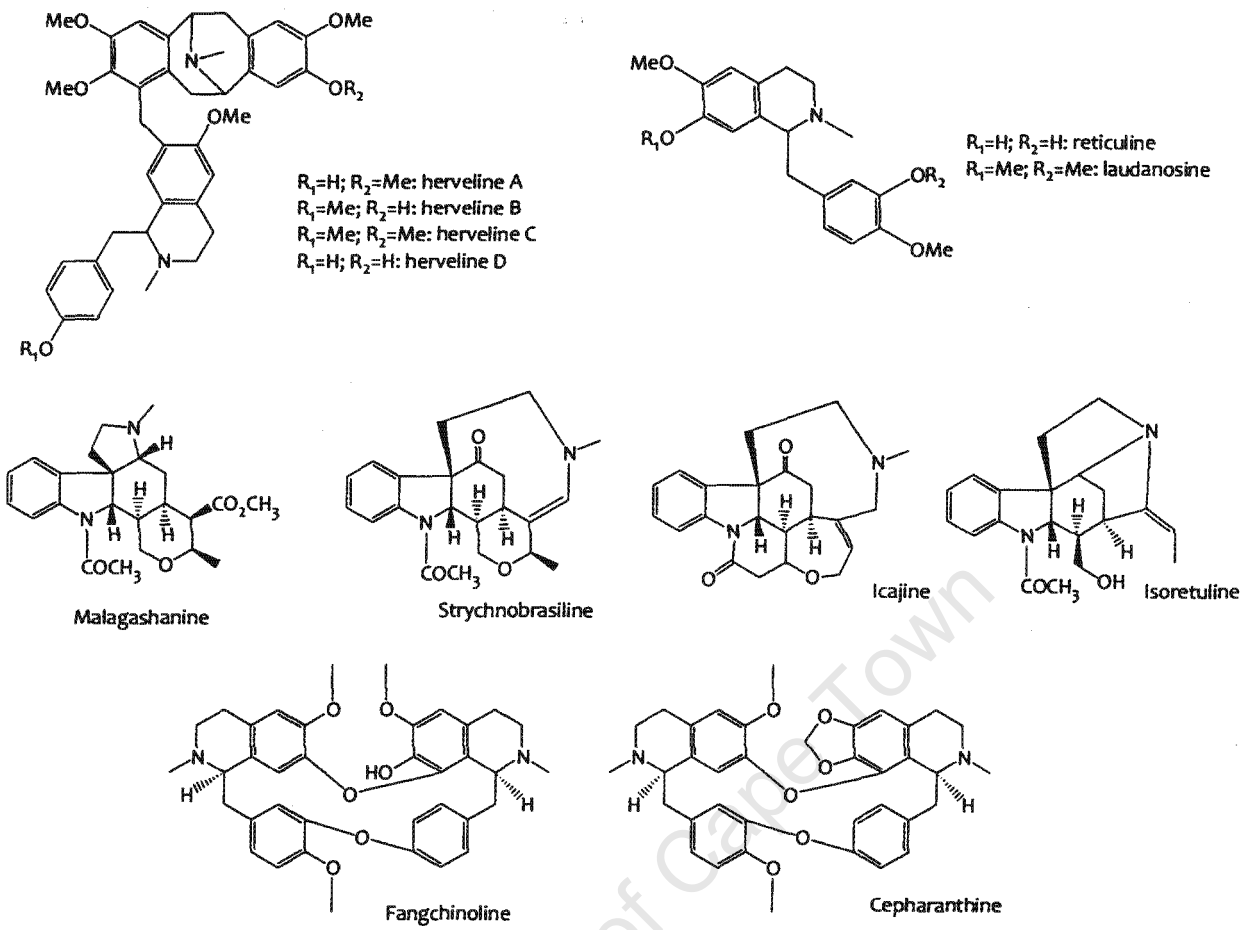

Figure 2.1: Chemical structures of some compounds of natural origin with CQ potentiating activity

2.5.2 Clinically available drugs as CQR reversal agents

A wide range of clinically available drugs have been experimentally shown to potentiate the antimalarial activity of chloroquine *in vitro* (Figure 2.2A). The clinically available Ca^{2+} channel blocker verapamil is probably the most widely known CQR reversal agent, and is regularly used as the reference compound in many CQR-reversal studies. It shows weak intrinsic antimalarial activity (IC_{50} of 2.5μM and 7.2μM against D10 (CQS) and Dd2 (CQR), respectively); at non-toxic concentrations, verapamil has been shown to enhance chloroquine susceptibility of CQR Dd2 but not CQS D10 *P. falciparum*, though it enhances chloroquine accumulation in both strains [36]. The actual mechanism of verapamil-mediated CQR reversal is yet to be established, but appears to be diminished *in vitro* in the presence of α1-glycoprotein, a plasma protein that interacts with basic compounds [37].

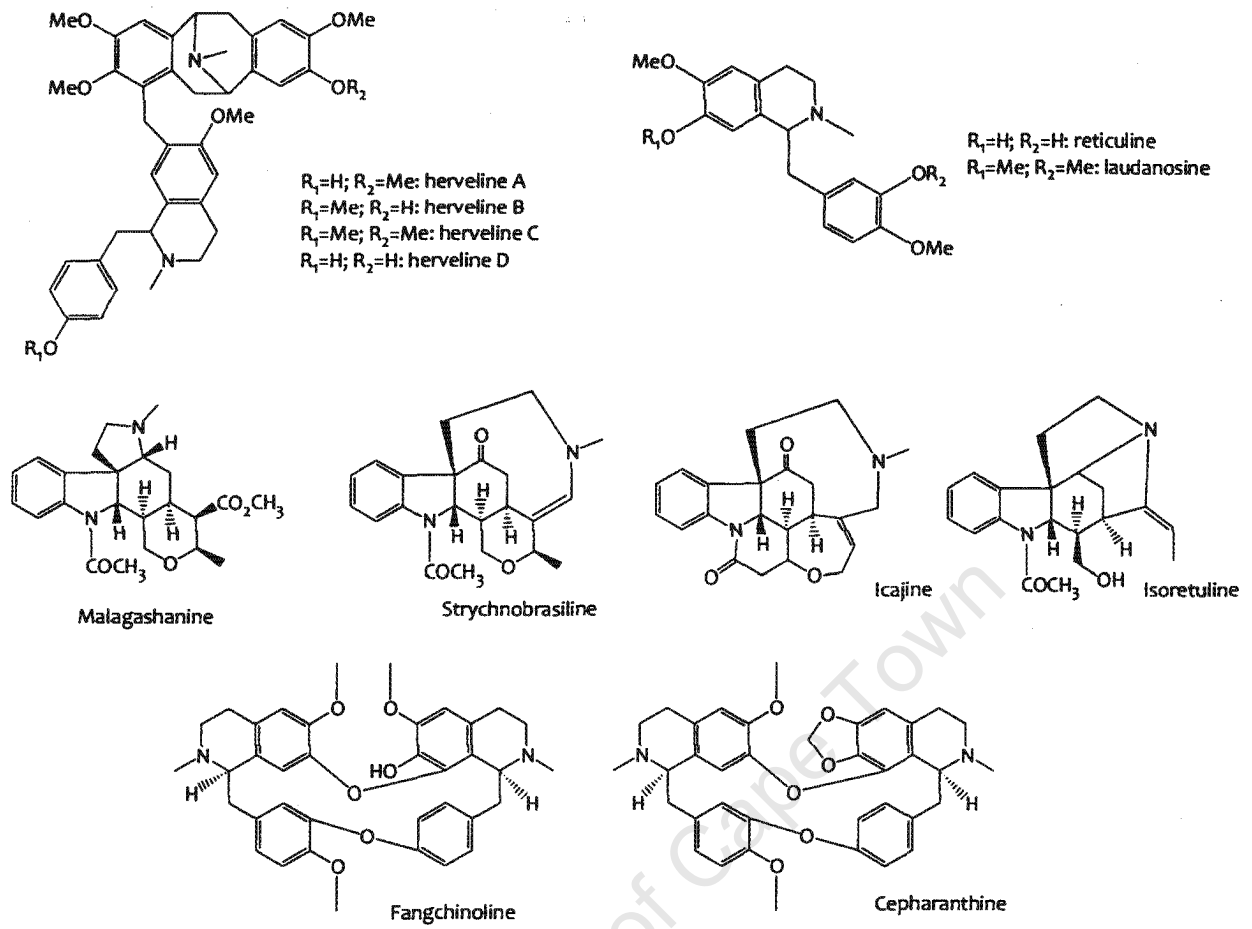

Figure 2.1: Chemical structures of some compounds of natural origin with CQ potentiating activity

2.5.2 Clinically available drugs as CQR reversal agents

A wide range of clinically available drugs have been experimentally shown to potentiate the antimalarial activity of chloroquine *in vitro* (Figure 2.2A). The clinically available Ca^{2+} channel blocker verapamil is probably the most widely known CQR reversal agent, and is regularly used as the reference compound in many CQR-reversal studies. It shows weak intrinsic antimalarial activity (IC_{50} of 2.5μM and 7.2μM against D10 (CQS) and Dd2 (CQR), respectively); at non-toxic concentrations, verapamil has been shown to enhance chloroquine susceptibility of CQR Dd2 but not CQS D10 *P. falciparum*, though it enhances chloroquine accumulation in both strains [36]. The actual mechanism of verapamil-mediated CQR reversal is yet to be established, but appears to be diminished *in vitro* in the presence of α1-glycoprotein, a plasma protein that interacts with basic compounds [37].

Other clinically available drugs with reported CQR-reversal activity include selected antihistamines [38-40], antiretroviral protease inhibitors [41], antidepressants [42,43] and antibiotics [44]. The use of combinations of chemosensitizers has also been suggested based on encouraging *in vitro* results; combinations of verapamil-trifluoperazine and verapamil-desipramine-trifluoperazine have been shown to lower the chloroquine IC_{50} of the CQR RSA11 strain to levels comparable with those of the CQS D10 strain [45].

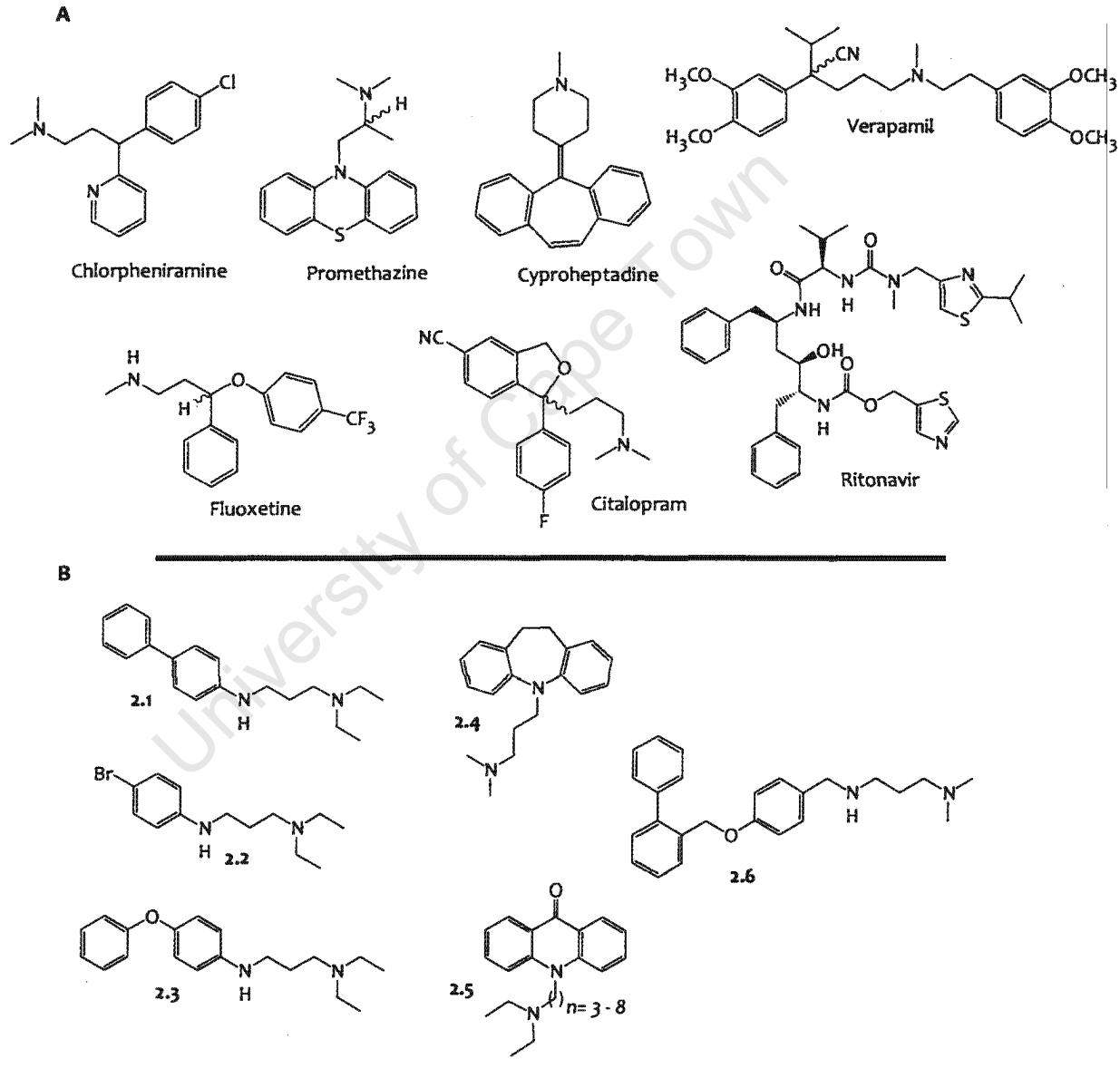

Figure 2.2: A: Chemical structures of selected clinically available drugs with CQ potentiating activity; B: structures of selected synthetic CQR reversal agents of various classes: biphenyl (2.1), arylbromide (2.2), biaryl-ether (2.3), diarylethane (2.4), acridone (2.5), and benzylamino (2.6) derivatives.

2.5.3 Synthetic CQR reversal agents and reversed chloroquines

The CQR reversal activity of a very diverse range of synthetic compounds has been reported. Some of these have been developed based on SAR analysis of known CQR reversal agents, as well as possible chloroquine chemosensitizing pharmacophores derived from such agents. Some examples of synthetic CQR reversal agents that have been identified are highlighted below.

A series of arylbromide, biphenyl and biaryl-ether compounds were designed as potential chemosensitizers, and were based on N-phenyl-1,3-diaminopropane, a possible chloroquine chemosensitizing pharmacophore derived from malagashanine and chlorpromazine. All compounds exhibited moderate (IC_{50} 1 - 5μM) to weak (IC_{50} >5μM) *in vitro* antimalarial activity against the CQR FCM29 strain of *P. falciparum*. Some of the compounds (such as compounds 2.1, 2.2 and 2.3, Figure 2.2B) also showed notable synergistic effects with chloroquine *in vitro* [46]. Another series of potential CQR reversal agents were designed exploiting an imipramine-based pharmacophore, namely a diarylmethane moiety linked by a 3-carbon chain to a secondary or tertiary nitrogen. These compounds were shown to possess notable *in vitro* CQR reversal activity, with some of them (such as compound 2.4, Figure 2.2B) rendering the CQR W2 strain fully sensitive to chloroquine [47].

Other classes of potential CQR-reversal agents include 9*H*-xanthenes [48], 10-N substituted acridones [49], dibenzosuberanylpiperazine derivatives [50] and benzylamine derivatives [51].

Reversed chloroquines are compounds in which chloroquine (or a chloroquine-like molecule) has been covalently linked to a proposed CQR reversal pharmacophore (usually derived from recognized CQR reversal agents). The rationale for this is that the presence of the additional pharmacophore may enable the chloroquine-like component evade the CQR mechanism(s) [52]. Such a molecule (compound 2.7, Figure 2.3) was designed and synthesized, with the CQR reversal pharmacophore derived from imipramine, a well studied CQR reversal agent. The compound was shown to be just as active as chloroquine against the CQS strain D6 (IC_{50} 2.9nM), but, more importantly, retained comparable activity against the CQR strain Dd2 (IC_{50} 5.3nM) [52].

Postulated reversed chloroquines have also been synthesized based on the 4-aryl-3,4-dihydropyrimidin-2(*1H*)-one (DHPM) scaffold. Selected for their easy synthetic

accessibility via the Biginelli multicomponent reaction, one of these compounds (compound 2.8, Figure 2.3), and its citrate salt, showed high activity against both the CQS 3D7 (IC_{50} 28nM) and CQR K1 (IC_{50} 4nM) strains of *P. falciparum* [53]. A similar approach has been used to design reversed acridone-based antimalarials; the most active compound (compound 2.9, Fig 2.3), though not as potent as chloroquine is against the CQS D6 strain, was equipotent across the CQR (Dd2) and CQS (D6) strains of *P. falciparum*, [54].

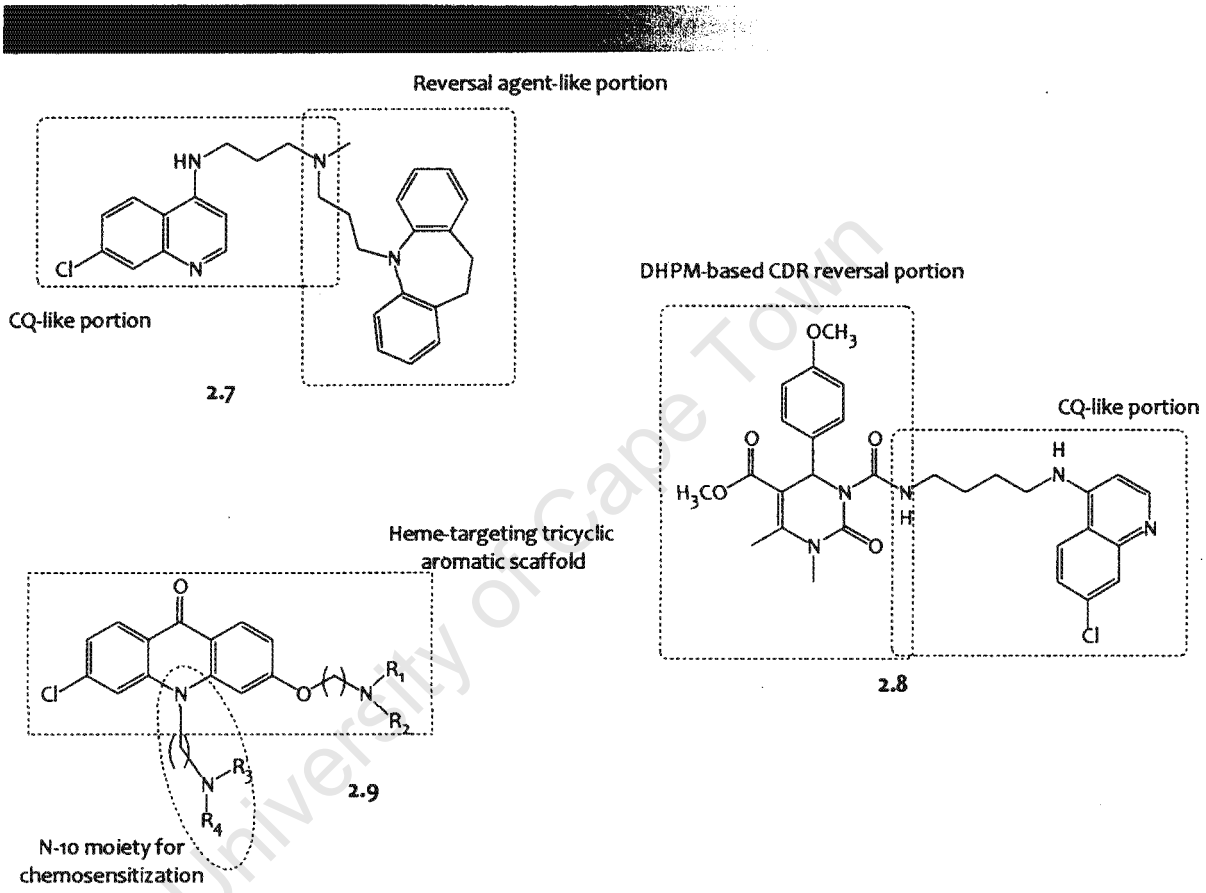

Figure 2.3: Figure showing a imipramine-based (2.7) and DHPM-based (2.8) reversed CQs, as well as the general structure of reversed acridone-based antimalarials (2.9)

2.6 Development of analogs of existing antimalarials

The late Sir James Black, joint winner of the 1988 Nobel Prize in Physiology and Medicine, has been quoted as saying that *"The most fruitful basis for the discovery of a new drug is to start with an old drug"* [55]. This has been underscored by an analysis of the origins of recently launched drugs, which revealed that most were derived by modification of the chemical structure of known drugs or lead structures derived from scientific literature [56].

Pharmacophores/substructural motifs that are thought to be largely responsible for the observed antimalarial activity of known antimalarial drugs can be derived from the structures of these compounds. Such scaffolds can then be used as templates for the rational design of various derivatives of the parent drugs which may then be synthesized and tested for antimalarial activity [2]. In this way, new, potent antimalarial agents that are analogs of the parent drug may be identified. Some examples of this are highlighted below.

The 7-chloro-4-aminoquinoline moiety, derived from chloroquine, is arguably the most widely used template for the design of new antimalarial compounds [2]. The generation of chloroquine analogs by derivatization of this central moiety has been driven by structure-activity relationship (SAR) studies focusing on the effects of modifications of the chloroquine side-chain and, to a lesser extent, replacement of the 7-chloro group. For example, a study of the antimalarial activities of several 4-aminoquinolines with shortened side chains found that the derivatives studied, such as **2.10**, **2.11** and **2.12** (**Figure 2.4**) retained significant antimalarial activity *in vitro*, with IC_{50} values in the lower nanomolar range. These compounds were somewhat less active against the CQR K1 strain of *P. falciparum* than against the CQS NF54 strain, suggesting that they retain a degree of cross-resistance with chloroquine [57]. It has also been demonstrated that replacement of the 7-chloro group with either the 7-bromo or the 7-iodo groups is associated with retention of antimalarial activity for a variety of aminoquinolines [58,59], mainly thought to be due to their moderately strong electron-withdrawing capacity and strong lipophilicity [59].

Additionally, the degree of resistance to 4-aminoquinolines was inversely correlated with the lipid solubility of the compounds [60] which is largely determined by the lipophilicity of their corresponding side-chains. This may suggest that an increase in the lipophilicity of quinoline and related antimalarials relative to chloroquine renders them less susceptible to the CQR mechanism [60,61]. This argument is further supported by the identification of chloroquine-like molecules that bear highly lipophilic side chains that not only retain chloroquine-like potency against CQS *P. falciparum* strains, but also completely lack any *in vitro* cross resistance with chloroquine against CQR strains. Ferroquine, ruthenoquine and (*ortho*)-phenylequine (**Figure 2.4**) are examples of such compounds, all of which show remarkable activity against *P. falciparum* strains, with IC_{50} of <30nM against both CQS D10 and CQR K1 strains [62-65].

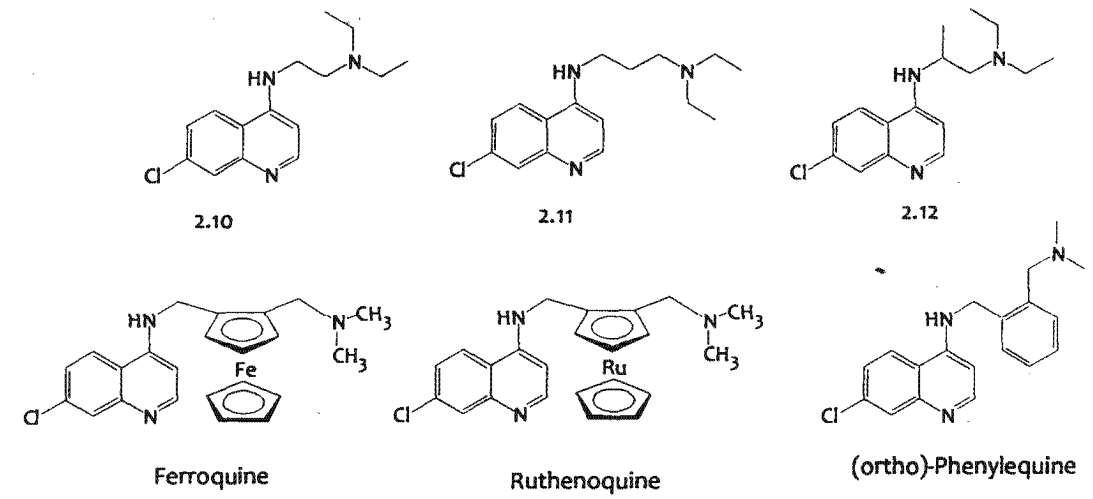

Figure 2.4: Figure showing selected chloroquine analogs, including the chloroquine analogs with lipophilic side chains (*o*)-phenylequine, ferroquine and ruthenoquine

Derivatization of the side-chains of other aminoquinoline antimalarials has also been attempted. A series of Mannich base derivatives of amodiaquine, for example, identified analogs that were more active than chloroquine *in vitro*. These analogs were also found to be more efficacious than amodiaquine *in vivo* against CQR *P. berghei*, irrespective of the route of administration (oral or intraperitoneal) [66].

2.7 Development of uniquely novel antimalarial chemotherapeutic agents

The identification of new chemical entities that possess antimalarial activity is an attractive strategy for the development of new antimalarial drugs. This may be by the identification and validation of new antimalarial pharmacophores for use as templates in the design of new antimalarial agents, the rational (*de novo*) design of compounds based on known molecular targets/mechanisms of action, high-throughput screening (HTS) of compound libraries, structure-based or ligand-based virtual screening of virtual compound libraries and/or the discovery of natural products with antimalarial activity. This approach to antimalarial drug discovery borrows heavily from more modern drug discovery strategies, particularly computational techniques.

2.7.1 Identification of new antimalarial pharmacophores/chemical scaffolds

One of the ways by which new antimalarial pharmacophores may be identified is by the targeting of chemical motifs that are structurally similar to known pharmacophores. For example, acridones and quinoxalines, both of which bear distinct structural similarities to the quinoline nucleus present in chloroquine and other quinoline-based

antimalarials, have been used as templates in the design of potential antimalarials. An acridone derivative coded T3.5 (Figure 2.5) was reportedly more active than chloroquine *in vitro* against the CQR Dd2, 7G8 and Tm90-C2B strains of *P. falciparum*, though it was less active against the CQR D6 strain [67]. Compound 2.13 (Figure 2.5), a bispyrrolo[1,2-*a*]quinoxaline, was extremely active, with IC_{50} values of 50 nM against the CQS Thai and the CQR K1 *P. falciparum* [68].

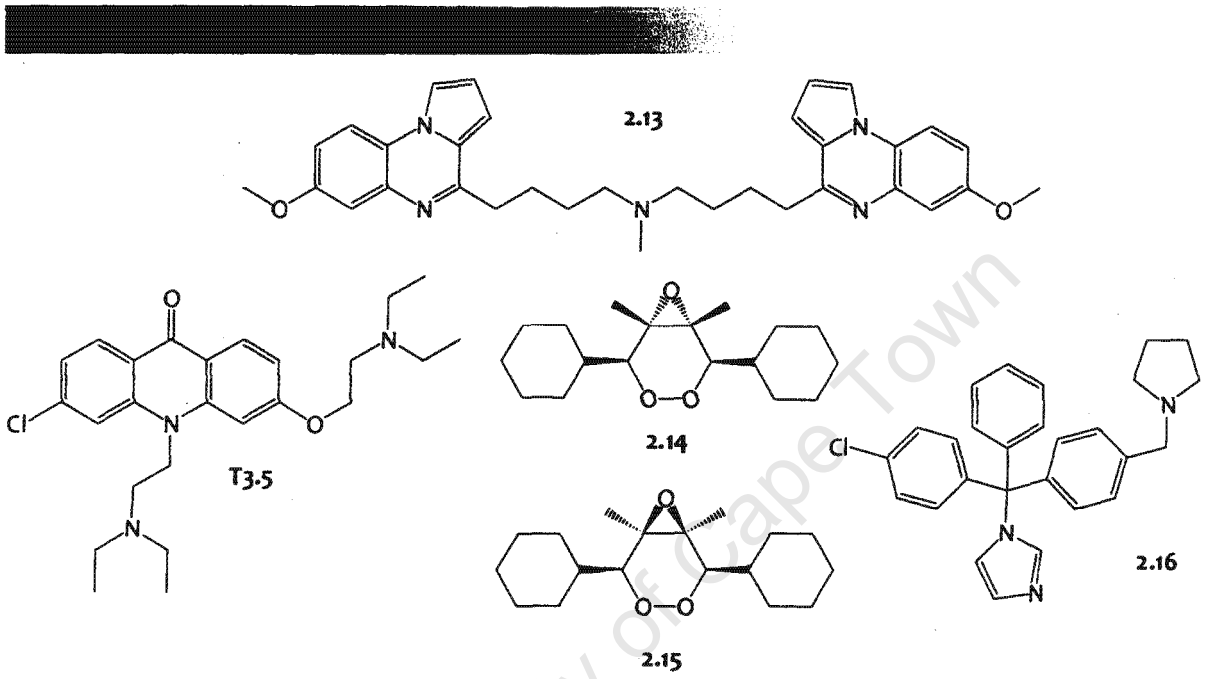

Figure 2.5: Examples of highly active antimalarial compounds based on novel chemical scaffolds

Similarly, the highly active artemisinin antimalarials have been used to inspire the design of related compounds as potential novel antimalarial compounds. For example, studies of epoxy-endoperoxides and bicyclic epoxy-endoperoxides identified several potent compounds that exhibited sub-micromolar IC_{50} values against both CQS and CQR *P. falciparum* [69,70]. The activities of bicyclic epoxy-endoperoxides such as 2.14 and 2.15 (Figure 2.5) were significantly better than those of similarly substituted monocyclic versions [70].

Novel antimalarial scaffolds unrelated to known antimalarials can be derived from miscellaneous compounds that have been shown to possess antimalarial activity. Clotrimazole is an antifungal azole has been shown to exhibit significant antimalarial activity *in vitro* (W2, IC_{50} 0.55 μM) [71,72]. This compound was used to derive a polycyclic antimalarial pharmacophore that was then applied in the design of potential antimalarial clotrimazole analogs. Compound 2.16 (Figure 2.5) was the most potent

compound identified from the series, and was more active than chloroquine or clotrimazole *in vitro*, with IC_{50} values <10 nM against 3D7 and K1 *P. falciparum* [73].

2.7.2 *De novo* design of novel antimalarial compounds

The potential of *de novo* design in the discovery of potential antimalarials is exemplified by the following examples.

Plasmepsin II (PII) is a malaria parasite aspartic protease involved in the hemoglobin degradation process that takes place in an acidic vacuole, and has been identified as a potential target for antimalarial therapy (section 1.7). A new class of non-peptidic PII inhibitors that display single-digit micromolar IC_{50} values and good selectivity towards (the mammalian aspartic protease) renin have been reportedly developed with the help of structure-based *de novo* design guided by molecular modeling of the active site of PII. Compound 2.17 (Figure 2.6) was the most active of the derivatives studied [74].

Dihydroorotate dehydrogenase (DHODH) is the fourth enzyme in the pyrimidine biosynthetic pathway, and catalyses the oxidation of dihydroorotate (DHO) to orotate in the presence of the co-factors flavin mononucleotide (FMN) and ubiquinone. The selective inhibition of *P. falciparum* DHODH (PfDHODH) offers itself as an attractive strategy for the development of novel antimalarial agents. In what was essentially a proof-of-principle study, the *de novo* design of potential PfDHODH inhibitors was attempted, guided by the molecular design program SPROUT. The designed inhibitors, which were simple and readily prepared amides of anthranilic acid, showed only modest enzyme affinities, but were considered as excellent starting points for further optimization [75].

2.7.3 High-throughput screening for the discovery of novel antimalarial compounds

High-throughput screening (HTS) involves the rapid, large scale, usually automated testing of physical libraries of compounds for activity against a particular microorganism or druggable target. The libraries of compounds used for this purpose may have been designed and synthesized based on the particular target of interest (e.g. by combinatorial chemistry), though for the most part these libraries have usually been previously synthesized during other non-related chemistry or drug discovery endeavors. In this way, compounds that may not have hitherto been known to possess certain biological activities may be identified. Growth inhibition assays [76], hematin

polymerization assays [77] and a variety of enzyme-based assays are examples of assays that have been adapted for the HTS of potential antimalarial compounds.

1039 compounds initially designed and synthesized as potential Cathepsin D inhibitors were screened against PII using a high-throughput fluorogenic peptide-substrate assay. 13 compounds showed greater than 50% inhibitory activity against PII. Of these, compounds 2.18 and 2.19 (Figure 2.6) were synthesized and evaluated for inhibition of PII, and were shown to exhibit sub-micromolar K*i* values against PII [78].

The *Plasmodium falciparum* dihydroorotate dehydrogenase (*Pf*DHODH) inhibitor DSM 1 (Figure 2.6) that is potent (*Ki* = 15nM) and species-selective (>5000-fold over the human enzyme) was also identified by high-throughput screening [79].

An efficient and robust high-throughput cell-based screen (1,536-well format) based on proliferation of *P. falciparum* in erythrocytes was applied in the screening of 1.7 million compounds. 17,000 compounds were identified that showed significant antimalarial activity. Most known antimalarials were identified in this screen, though many novel chemical scaffolds, which likely act through both known and novel pathways, were also identified. *In silico* compound activity profiling also revealed the cellular pathways and/or protein targets for a number of these compounds [80].

2.7.4 Virtual screening for the identification of novel antimalarial compounds

Virtual screening can be considered as a form of HTS which computationally screens virtual (rather than physical) chemical libraries for potential active agents. This technique may be structure-based (where the search is aimed at finding compounds that are structurally similar to, or share common 3-D molecular interaction fields with, known pharmacophores/active compounds) or ligand-based (where the search is aimed at identifying compounds with complementary 3-D molecular interaction fields to those described for the active site of a particular enzyme target, and which are therefore likely to interact with it).

In an attempt to identify novel non-peptide inhibitors of malarial cysteine proteases, the ChemBridge database consisting of approximately 241 000 compounds was screened against homology models of Falcipain-2 and Falcipain-3 in three consecutive stages of docking. Eighty four of the most promising compounds were procured and subjected to both enzymatic and cell-based biological evaluations. Of these compounds, twenty two were shown to experimentally inhibit the Falcipains, with

IC_{50} values ranging from 1 - 63 μM; twelve compounds showed dual activity. Compounds 2.20, 2.21 and 2.22 (Figure 2.6) exhibited single-digit micromolar IC_{50} values against both D6 and W2 *P. falciparum* [81]. A similar search was carried out on The Available Chemical Directory, which comprises nearly 355,000 compounds. One hundred compounds were subsequently selected for biological screening, from which twenty two cysteine protease inhibitors were identified, eighteen of which were found to be low micromolar inhibitors of Falcipain-2. Unfortunately, only one of these Falcipain-2 inhibitors also exhibited *in vitro* antiplasmodial activity (W2, IC_{50} 9.5 μM); the others did not show noticeable antiplasmodial activity at concentrations of up to 20 μM [82].

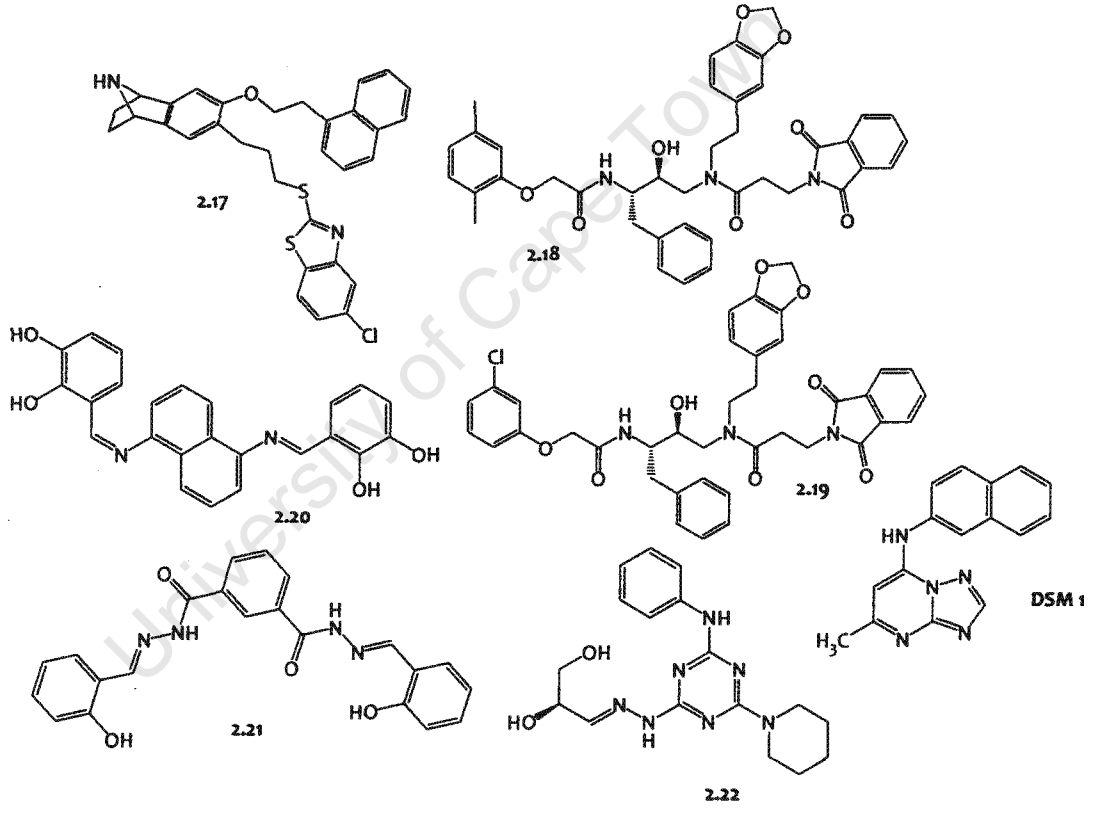

Figure 2.6: Examples of highly active antimalarial compounds derived by *de novo* design or from HTS and virtual screening efforts.

2.7.5 Natural products as a source of novel antimalarial compounds

Nature is, as ever, an extremely rich source of potential antimalarial agents [83,84], with the antimalarial drugs quinine and artemisinin being outstanding examples of therapeutic natural products. Following the serendipitous or rational discovery of a biologically active natural material, the conventional approach to natural product

development has been the bioassay-guided fractionation of extracts derived from such material, and the subsequent isolation and characterization of pure, active compounds. Identification of promising compounds in this way usually triggers medicinal chemistry efforts geared towards the total synthesis of the identified compounds and/or the generation of analogs, and which are aimed at providing a supplementary source of the product for further study, revealing structure-activity relationships, identifying more potent analogs and/or overcoming challenging physicochemical and biological properties.

A classic example of this approach is the discovery of artemisinin. Based on age-old reports in Chinese traditional medicine of the antipyretic effects of extracts of the Chinese herb *Qinghao* (*Artemisia annua* L.), scientific studies went on to demonstrate significant antimalarial activity of the ethanolic extracts of this plant against both chloroquine-sensitive (CQS) and chloroquine-resistant (CQR) strains of *P. falciparum* [85]. Further studies led to the isolation and characterization of a highly active sesquiterpene lactone, artemisinin, in 1971 [86,87]; artemisinin has since been derivatized to yield a very diverse range of semi-synthetic analogues [88]. Using comparable approaches, the continuing search for new antimalarial drugs from natural sources, and in particular from plant, marine and fresh-water sources, has led to the identification of an impressive range of structurally diverse compounds from a variety of chemical classes, some of which are highlighted in Figure 2.7 [87,89-91].

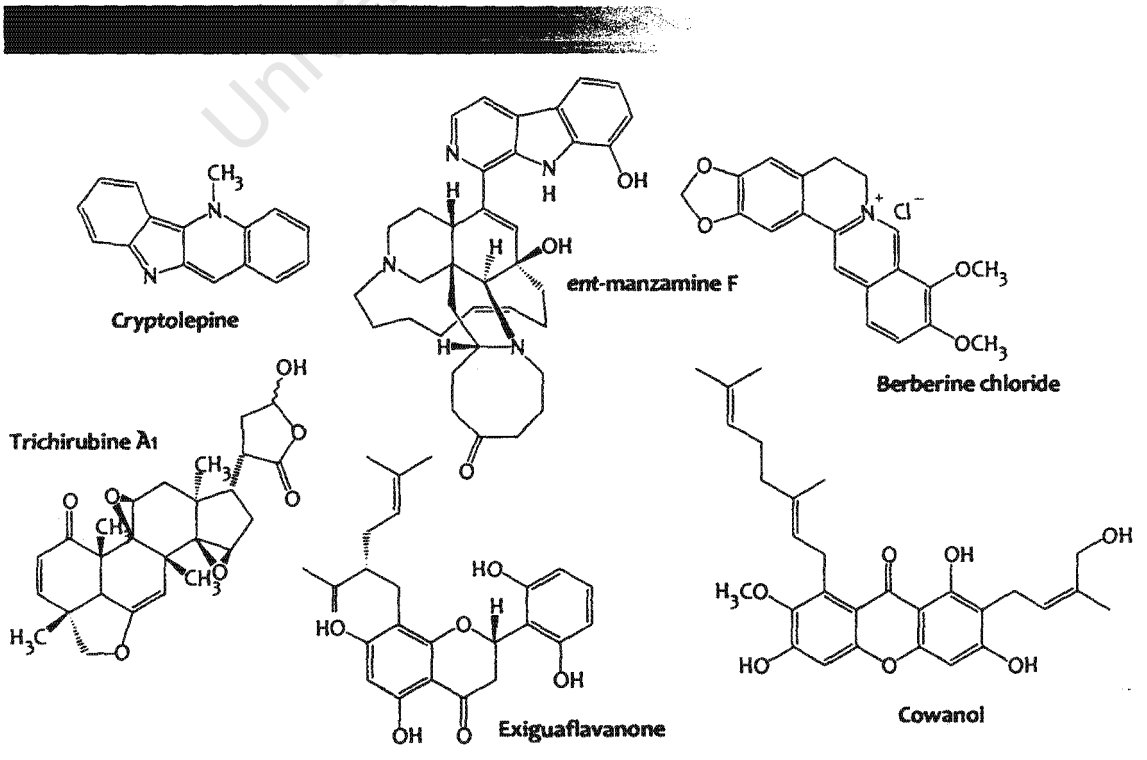

Figure 2.7: Chemical structures of some antimalarial natural products

Upon the elucidation of the structure of a novel antimalarial compound from natural sources, and possibly informed by preliminary SAR data, it may be possible to reduce this structure to its basic pharmacophoric unit(s). Pharmacophores derived in this way can be utilized in much the same way as pharmacophores derived from synthetic compounds (see above); they may be useful in the design of novel analogs, or be used as templates in the structure-based virtual screening of databases and libraries of known compounds (from both natural and synthetic sources) for structural analogs. These may then be acquired/synthesized and assayed alongside the primary compound and possibly even lead to the identification of additional active compounds.

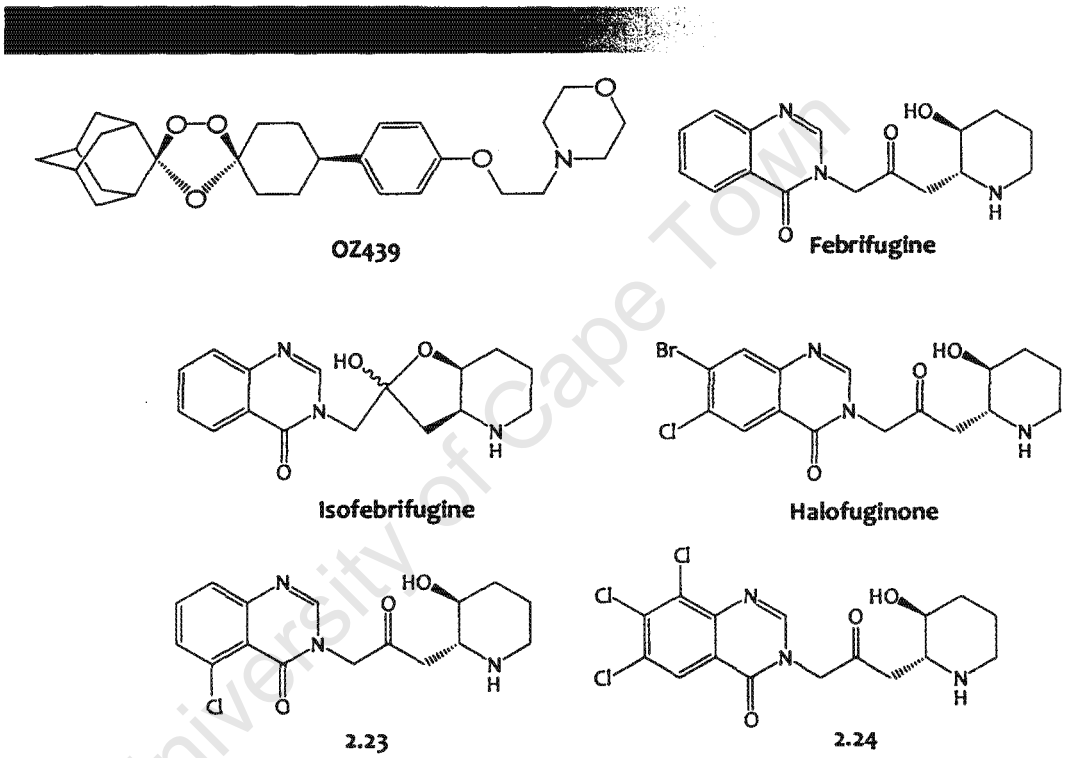

Figure 2.8: Chemical structures of OZ439 (a synthetic peroxide antimalarial drug candidate) as well as febrifugine and some of its highly active analogs

For example, artemisinin has inspired the design and synthesis of very promising, longer-acting analogs that are now in clinical development such as OZ439 (Figure 2.8), a promising synthetic peroxide antimalarial drug candidate [92,93]. Another example of this relates to febrifugine (Figure 2.8), a highly potent antimalarial alkaloid isolated from the roots, stem and leaves of the plant *Dichroa febrifuga* Lour., a Chinese herb locally referred to as *Chang Shan* [94]. The piperidinyl-(acetonyl)quinazoline moiety, a structural unit derived from febrifugine, was used as a template in the search for analogs in the Walter Reed Army Institute of Research (WRAIR) Chemical Information System (CIS) database. This yielded 133 analogs, of which 35 were selected for *in vitro* antimalarial assays. Some of these compounds had been previously reported in

literature (e.g. halofuginone); other potent analogs were also identified, though these were less active that febrifugine. These included the 5-chloro analog (2.23) and the 6,7,8-trichloro analog (2.24) of febrifugine (Figure 2.8), both of which had IC_{50} values of <5ng/mL against the D6 (CQS) and W2 (CQR) strains of *P. falciparum*, as well as significantly reduced *in vitro* cytotoxicity against a variety of mammalian cell lines [95].

An impressively large number of novel naturally-derived compounds have been isolated and characterized over the years. The volume and variety of these compounds looks set to increase particularly with the current conscious effort to expand the range of biodiversity sampled for this purpose by, for example, the exploration of extreme habitats not routinely considered [96]. The creation of virtual and/or physical repositories of these compounds helps to keep track of these compounds and simultaneously create a rich resource that can be tapped for drug discovery efforts. Examples of such databases already exist, such as the Dictionary of Natural Products [97] and a marine natural products database that reportedly holds approximately 6000 chemical compounds [98]. Such databases can be valuable for structure-based or ligand-based virtual screening, as well as for ligand docking studies on a variety of known protein targets; physical repositories of purified natural products can provide compound libraries for HTS.

As mentioned earlier, one of the strategies for evading the development of resistance to antimalarials is the use of combination therapies, which basically involves the co-administration of two or more antimalarial agents. Although the emphasis is currently on ACTs [4-6], the identification of new and efficacious combinations remains a priority, and the identification of new, active, naturally-derived compounds could provide additional possibilities. The potential of combinations of established antimalarial drugs with new bioactive compounds derived from natural sources has already been demonstrated experimentally. When a mixture of febrifugine and isofebrifugine, isolated from the leaves of *Hydrangea macrophylla* Seringe var. *Otsaka* Makino, was administered concurrently with chloroquine (20 mg/kg once a day orally for 2 days) in mice infected with *P. berghei* NK65, no parasites could be detected microscopically after the end of the treatment period, and all mice treated in this way survived. This was in contrast to the observations made for those *P. berghei* NK65 infected mice treated solely with either chloroquine or the alkaloid mixture, whereby recrudescence was observed after the treatment period, and was subsequently followed by the death of all the mice [99].

2.8 Application of conventional and modern techniques to augment antimalarial drug discovery

2.8.1 Development of dual drugs

Dual drugs, also known as hybrid compounds, refer to single chemical entities that consist of two drugs/active compounds/pharmacophoric units linked together covalently by a linker [100]. The selection of the two principles in the dual drug is usually based on their observed (or anticipated) synergistic or additive pharmacological activities, with their combination into one unit being aimed at taking advantage of this synergy and possibly enabling the identification of highly active novel chemical entities.

A typical example of this approach is exemplified by a study of chalcone-chloroquinoline hybrid compounds. The study of chalcones as potential antimalarials mainly stems from the identification of Licochalcone A (Figure 2.9A), a naturally occurring chalcone isolated from the Chinese licorice roots locally called *Gan Cao* that showed significant dose-dependent inhibition of parasite viability *in vitro* against *P. falciparum* 3D7 (CQS) and Dd2 (CQR) strains, with an IC_{50} of approximately 0.6 μg/mL for both strains [101,102]. The study of chalcone-chloroquinoline hybrid compounds identified several analogs (compounds 2.25 – 2.28, Figure 2.9A) that showed inhibition of β-hematin formation comparable with that exhibited by chloroquine. Unfortunately the study did not report the *in vitro* antimalarial activities of these compounds against *P. falciparum* [103].

2.8.2 Metabolism and metabolite identification studies

In silico (computational) and *in vitro* metabolism studies are primarily aimed at assessing the metabolic stability of promising hit and lead compounds, and are usually geared at providing useful information to guide and/or help in the interpretation of the results from subsequent pharmacokinetic studies and *in vivo* assays. In addition, such information also enables the drug discovery scientists to design and synthesize analogs of the primary compound(s) that are potentially more stable to metabolism and are likely to have improved bioavailability profiles – this is particularly so for compounds administered orally as metabolic stability is a key determinant of oral bioavailability [104].

However, and probably just as importantly, the generation and identification of primary metabolites of a compound can be an effective way of generating chemical

diversity and augmenting the efforts aimed at identifying novel active compounds based on an identified hit. This approach is well justified by the fact that, in a variety of cases, pharmacologically active metabolites have been found to contribute significantly to the overall observed *in vivo* antimalarial activity of a compound. A typical example of this is N-desethylchloroquine, the primary metabolite of chloroquine, which exhibits potent antimalarial activity comparable to that of chloroquine [105,106]. This concept of pharmacologically active metabolites is just as applicable to antimalarial hits derived from natural sources. For example, Y. Oshima and co-workers (2003) reported the isolation and structural elucidation of two primary metabolites of febrifugine after its incubation for 1 hour with mouse liver S9 (in the presence of cofactor for the NADPH-regenerating system) in phosphate buffer at 37°C. The two metabolites, designated feb-A and feb-B (Figure 2.9B), were then synthesized to afford enough material for antimalarial testing. Feb-A, as well as its synthetic isofebrifugine analog isofeb-A, showed extremely potent *in vitro* antimalarial activity against the FCR-3 strain of *P. falciparum*, with isofeb-A being even more potent than febrifugine (EC50 = 0.27 nM) and having a significantly higher selectivity index. Feb-A, however, was more potent than isofeb-A *in vivo* in mice infected with *P. berghei* [107]

In addition, metabolism studies may be useful in understanding the *in vivo* toxicity of a particular compound; this is because any toxic effects observed after the administration of a particular compound could very well be due to the generation of toxic metabolites. Such information derived from metabolism studies would then be crucial in the design of potent compounds devoid of the unwanted toxicity of the parent compound. S. Zhu and co-workers (2006, 2009) drew upon prior studies on the SAR, toxicity and metabolism of febrifugine to design a series of febrifugine analogs with the aim of identifying compounds with enhanced potency and/or attenuated toxicity relative to febrifugine. Their first study focused only on modifications of the quinazolinone ring of febrifugine that targeted the elimination of the tendency to form chemically reactive and toxic intermediates and metabolites such as the arene oxide 2.29. Compounds 2.30 (5,6-difluoro analog) and 2.31 (5-trifluoromethyl analog) (Figure 2.9B) showed antimalarial activity superior to that of febrifugine *in vitro*, with IC_{50} values of less than 1 nM against both the D6 (CQS) and W2 (CQR) strains of *P. falciparum*, and were over 100 times less toxic than febrifugine based on an *in vitro* cytotoxicity assay on rat hepatocytes. Introduction of an extra nitrogen at either position 5, 6, 7, or 8, or fluoro substitution at only position 5, did not enhance antimalarial potency, but yielded analogs with significantly reduced cytotoxicity (and hence improved therapeutic indices). The study therefore concluded that selected

substitutions at the 5- and 6- positions, as well as an increase in the oxidation potential of the quinazolinone ring (by the introduction of electron-withdrawing substituents or extra nitrogens) are associated with a reduction in cytotoxicity [108]. Their subsequent study considered similarly substituted/modified analogs of febrifugine, but in which the piperidine ring had now been replaced with a pyrrolidine ring like in compound 2.32 (Figure 2.9B); antimalarial activity was retained, with a similar activity/toxicity pattern observed between both sets of analogs [109].

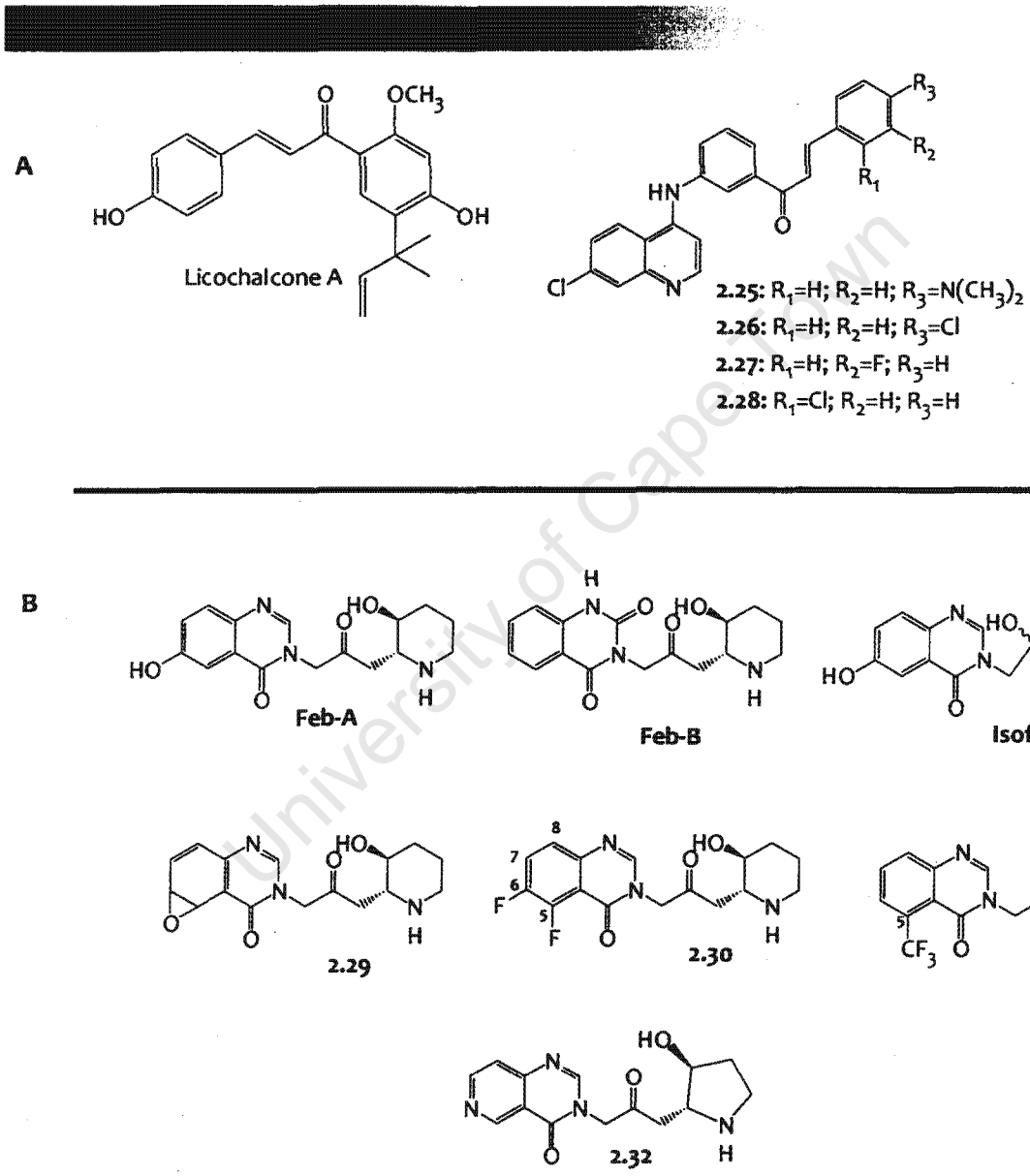

Figure 2.9: A: structure of Licochalcone A, and chalcone hybrid compounds with antimalarial activity; B: some metabolites of febrifugine, and examples of compounds designed to be more stable to metabolism.

2.8.3 Identification of novel targets and reverse pharmacology

The mechanisms of action of many antimalarial compounds are usually unknown at the time of their discovery, and generally tend to remain so for extended periods of their development as potential lead compounds. This is particularly so because most antimalarial compounds are usually assessed in whole-cell parasite cultures. The implication of this is that chemical derivatization and attendant SAR studies, which could benefit immensely from a clear understanding of how the particular compounds exert their antimalarial activity and (where possible) their actual molecular targets, are usually carried out without this knowledge.

However, it is acknowledged that the identification of the mechanisms of action of a novel antimalarial compound is indeed quite challenging considering the myriad of possible molecular targets (including unknown targets), the cost and complexities involved in actually testing compounds against a variety of targets, and the possibility of the overall observed antimalarial activity being the result of the action of the compound on multiple targets. However, where possible, it is well advised to try and identify the actual targets of the active compounds, including natural products and their derivatives.

Metabolic profiling offers an exciting approach to the identification of (oftentimes new) molecular targets of biologically active molecules, and involves the assessment of the metabolic response of an organism/cell/parasite following exposure to a bioactive molecule. The majority of biologically active molecules elicit their responses by interfering with protein function (e.g. by enzyme inhibition/over-activation or protein-protein interaction inhibition), and this typically leads to a perturbation in the normal metabolic activity of the parasite that may be detectable *via* post-exposure metabolic profiling. In this way, the pathway/function that the molecule interferes with may be revealed, along with its actual molecular target(s) [110]. Such an approach may be adapted for the high-throughput phenotypic screening of libraries of compounds [111], and bioactive natural products, by virtue of their chemical diversity, are particularly suited to act as probes for the identification of new molecular targets in this way [110,111]. The metabolic profiling of the malaria parasite has been reported [112,113], which would suggest the latent potential in this approach.

Activity-Based Protein Profiling (ABPP) is another useful approach for the identification of druggable targets. Synthetic or naturally-derived molecules (or privileged structures derived from them) that may have a high affinity for active sites of individual enzymes

and that are equipped with a tag either for the purpose of visualization/detection or enrichment, could be incubated with proteomes from, for example, two different stages of the malaria pathogen. These small probes would then bind in the target enzyme(s) and provide a practical means for their isolation and identification by techniques such as gel electrophoresis and fluorescence detection. Proteins/enzymes identified in this way can then be investigated further as potential therapeutic targets by both classical mechanism of action studies or reverse pharmacology (see below) [114]. The application of comparative ABPP has been successful in identifying irreversible inhibitors of a specific papain cysteine protease in the malaria parasite and used to demonstrate a role for the enzyme in the parasite invasion processes [115].

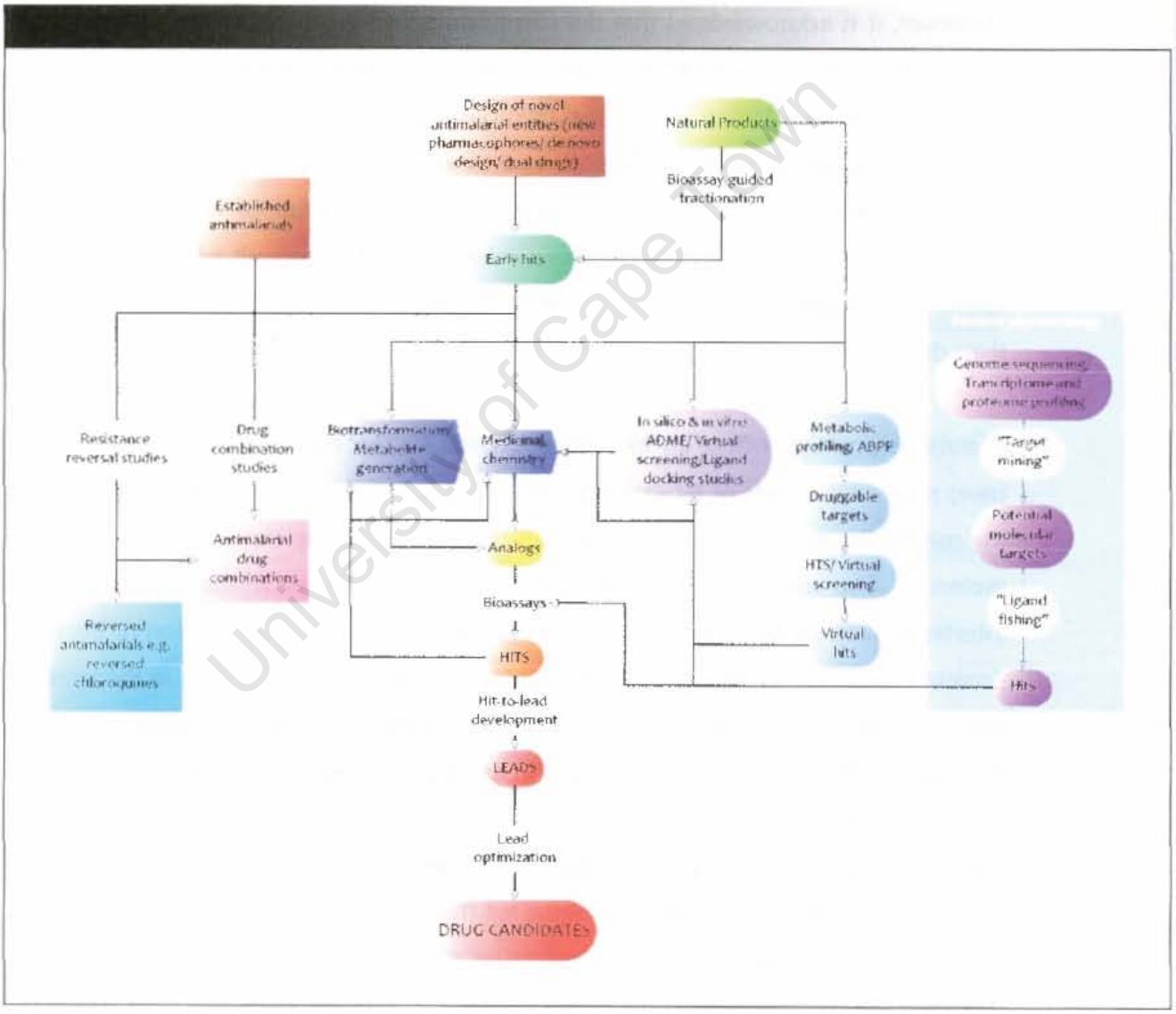

Figure 2.10: Schematic representation of the various approaches to antimalarial drug discovery, including some of the more modern approaches

vitro physicochemical and ADME prediction to guide in the design and selection of target compounds for synthesis.

The natural product basis of the study is introduced in section 2.9.1 below; the approach to molecular hybridization and the selection of the hybrid components will be introduced and discussed in Chapter Three; the use of *in silico* and *in vitro* physicochemical and ADME predictions to guide target compound design is elaborated in Chapter Five.

2.9.1 Curcumin and chalcones

2.9.1.1 Introduction

As mentioned above, nature continues to be a rich source of chemical diversity for drug discovery [83,84]. Curcumin [*diferuloylmethane; 1,7-bis(4-hydroxy-3-methoxyphenyl)-1,6-heptadiene-3,5-dione*] is one such example of a bioactive compound of natural origin. It is the major one of three phenolic diketone molecules isolated from turmeric, the rhizomes of *Curcuma longa* L. (Zingiberaceae), the other two being demethoxycurcumin and bis-demethoxycurcumin [122]. These three compounds (as well as other structurally related synthetic and semi-synthetic compounds) are usually collectively referred to as curcuminoids.

In solution, these compounds exist as equilibrium mixtures of the symmetrical keto (diene-dione) and unsymmetrical enol tautomers (Figure 2.11); the enol tautomer predominates due to the dual stabilization effects of the resultant extended conjugation and intra-molecular hydrogen-bonding [123]. Interestingly, curcumin could also exist as a quinone-methide radical – the product of photo-catalyzed auto-oxidation in basic aqueous media [124].

Curcuma longa has for centuries been cultivated in India and other parts of Asia, and its rhizome (turmeric) used to impart colour and flavour to food as well as for medicinal purposes in the treatment of diabetic wounds, hepatic disorders, jaundice, anorexia, coryza, cough, rheumatoid arthritis among numerous other maladies [125]. These medicinal properties of turmeric have since been attributed to the curcuminoids present in it [126], and subsequent extensive studies of curcumin, the principle curcuminoid, have demonstrated a very diverse range of biological activities, as discussed below.

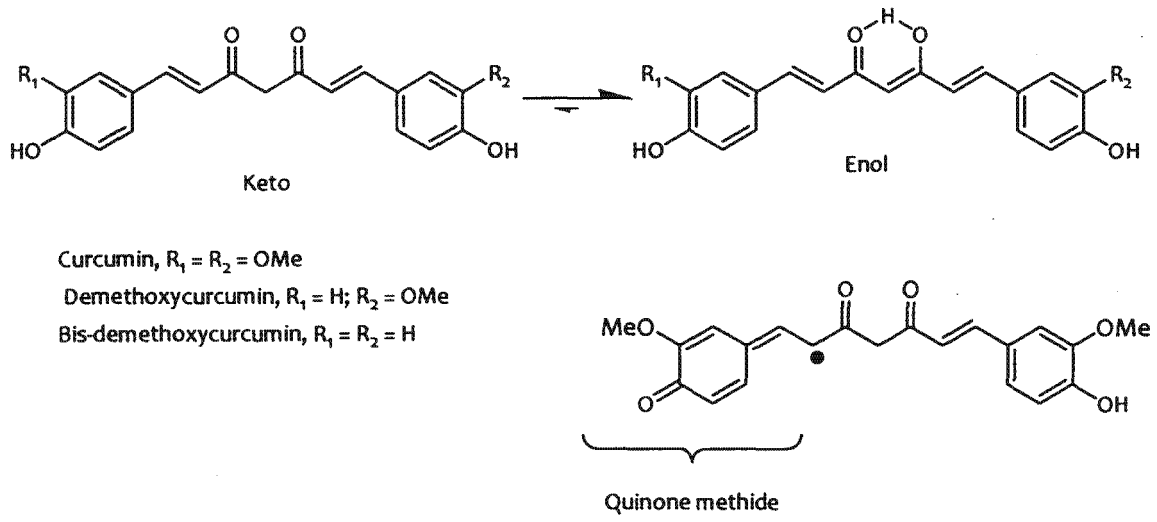

Figure 2.11: Structures of curcumin, demethoxycurcumin, and bis-demethoxycurcumin, showing their 'keto' and 'enol' forms [122,123] and the structure of the curcumin quinone-methide radical [124]

On the other hand, chalcones are 1,3-diarylprop-2-ene-1-ones, i.e. compounds containing two aromatic rings linked by an α,β-unsaturated carbonyl system in the form of a propenone chain, or compounds that contain this basic sub-structure [127]. The structural similarity of chalcones (and dienones) to curcumin is obvious (see Figure 2.12) both having two aryl rings linked by a chain that contains an α,β-unsaturated carbonyl system. It comes as no surprise, therefore, that curcumin and chalcones possess overlapping biological activity profiles.

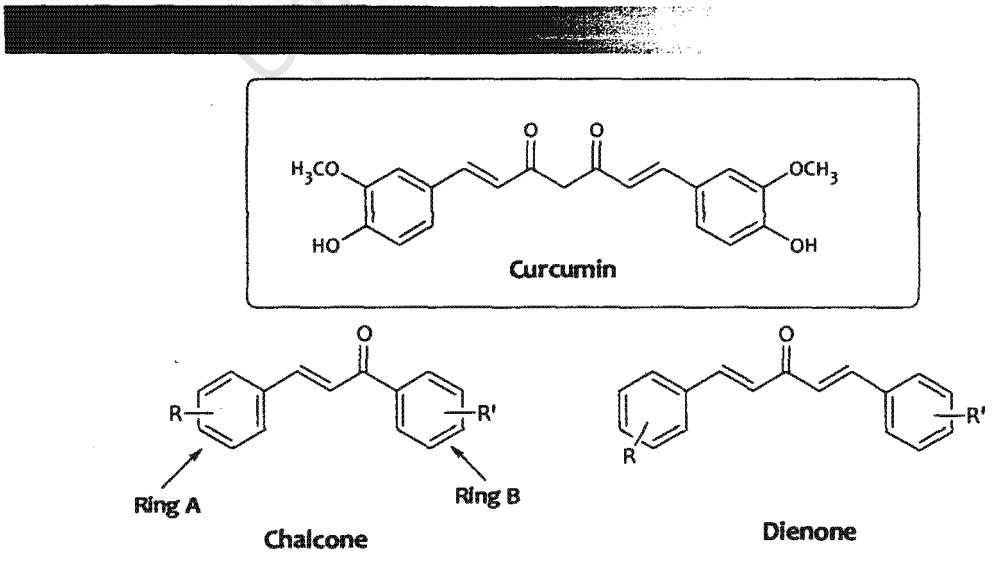

Figure 2.12: General structures of curcumin-related compounds chalcones and dienones

Reverse pharmacology offers an alternative means by which the molecular targets of biologically active compounds may be identified, and represents a major paradigm shift in drug discovery. Rather than apply a bioactive molecule in the identification of a molecular target, reverse pharmacology begins with the initial identification of potential protein targets (such as enzymes and receptors) by the application of bioinformatics tools that exploit the vast DNA-sequence databases provided by intensive genomic research. This process has been termed 'target mining'. The potential targets identified in this way are then cloned and exposed to candidate ligands, which may include natural products, in what has been termed as 'ligand fishing'. High-throughput screening (HTS) as well as virtual screening systems can also be designed based on such potential targets, and these can be used to screen physical and virtual libraries of both synthetic and naturally-derived molecules in the search for possible ligands [116]. As far as antimalarial drug discovery is concerned, this approach has been rendered quite feasible by the successful sequencing of the genome of the human malaria parasite *P. falciparum* [117], now available as a database for vaccine development and drug discovery applications [118].

It has been argued that libraries of natural products and their derivatives are actually better suited for such screens simply because they span a much broader chemical space than most synthetic compound libraries currently available for this purpose, and which are usually composed of collections of existing drugs or combinatorial libraries of 'drug-like' molecules [119]. This diversity evolves primarily from differences in the levels of chirality, degree of unsaturation, presence of complex ring systems and the ratios of heteroatoms such as nitrogen, oxygen, sulfur and halogens [120]. It has even been proposed that screening libraries should be intentionally optimized by adding to them molecules with biogenic or natural-product-like scaffolds [121].

Figure 2.10 schematically summarizes the inter-relationships between the various approaches to antimalarial drug discovery outlined in this Chapter, including some of the more modern approaches

2.9 Antimalarial drug discovery strategies applied in this study

This study applied some of the strategies outlined above in an attempt to identify novel, highly active antimalarial compounds. For example, natural product-inspired scaffolds were used in the design of the target compounds. Molecular hybridization was another of the strategies applied in this study - majority of the target compounds were designed as dual drugs. The study also utilized *in silico* (computational) and *in*

vitro physicochemical and ADME prediction to guide in the design and selection of target compounds for synthesis.

The natural product basis of the study is introduced in section 2.9.1 below; the approach to molecular hybridization and the selection of the hybrid components will be introduced and discussed in Chapter Three; the use of *in silico* and *in vitro* physicochemical and ADME predictions to guide target compound design is elaborated in Chapter Five.

2.9.1 Curcumin and chalcones

2.9.1.1 Introduction

As mentioned above, nature continues to be a rich source of chemical diversity for drug discovery [83,84]. Curcumin [*diferuloylmethane; 1,7-bis(4-hydroxy-3-methoxyphenyl)-1,6-heptadiene-3,5-dione*] is one such example of a bioactive compound of natural origin. It is the major one of three phenolic diketone molecules isolated from turmeric, the rhizomes of *Curcuma longa* L. (Zingiberaceae), the other two being demethoxycurcumin and bis-demethoxycurcumin [122]. These three compounds (as well as other structurally related synthetic and semi-synthetic compounds) are usually collectively referred to as curcuminoids.

In solution, these compounds exist as equilibrium mixtures of the symmetrical keto (diene-dione) and unsymmetrical enol tautomers (Figure 2.11); the enol tautomer predominates due to the dual stabilization effects of the resultant extended conjugation and intra-molecular hydrogen-bonding [123]. Interestingly, curcumin could also exist as a quinone-methide radical – the product of photo-catalyzed auto-oxidation in basic aqueous media [124].

Curcuma longa has for centuries been cultivated in India and other parts of Asia, and its rhizome (turmeric) used to impart colour and flavour to food as well as for medicinal purposes in the treatment of diabetic wounds, hepatic disorders, jaundice, anorexia, coryza, cough, rheumatoid arthritis among numerous other maladies [125]. These medicinal properties of turmeric have since been attributed to the curcuminoids present in it [126], and subsequent extensive studies of curcumin, the principle curcuminoid, have demonstrated a very diverse range of biological activities, as discussed below.

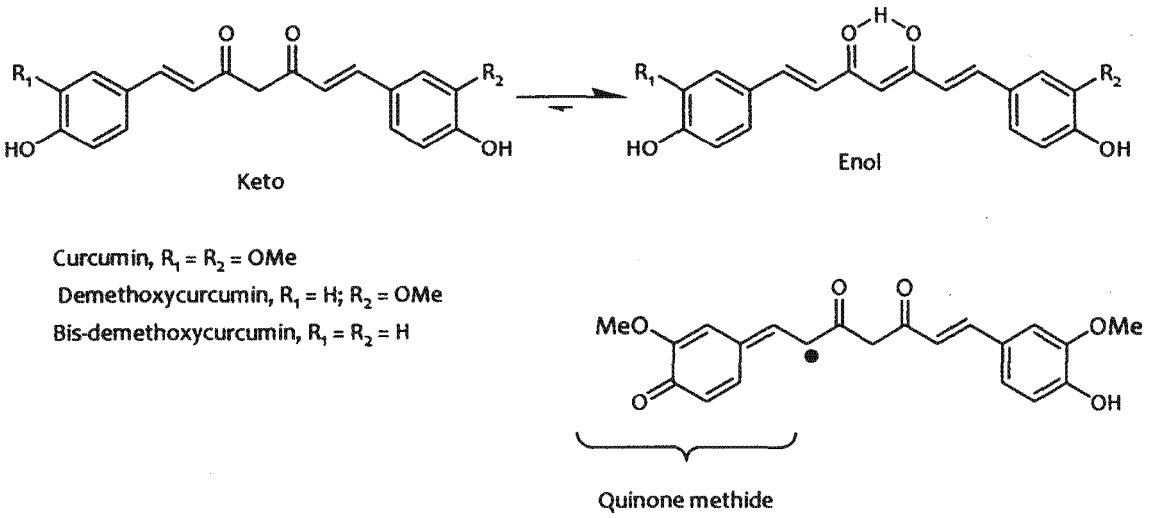

Figure 2.11: Structures of curcumin, demethoxycurcumin, and bis-demethoxycurcumin, showing their 'keto' and 'enol' forms [122,123] and the structure of the curcumin quinone-methide radical [124]

On the other hand, chalcones are 1,3-diarylprop-2-ene-1-ones, i.e. compounds containing two aromatic rings linked by an α,β-unsaturated carbonyl system in the form of a propenone chain, or compounds that contain this basic sub-structure [127]. The structural similarity of chalcones (and dienones) to curcumin is obvious (see Figure 2.12) both having two aryl rings linked by a chain that contains an α,β-unsaturated carbonyl system. It comes as no surprise, therefore, that curcumin and chalcones possess overlapping biological activity profiles.

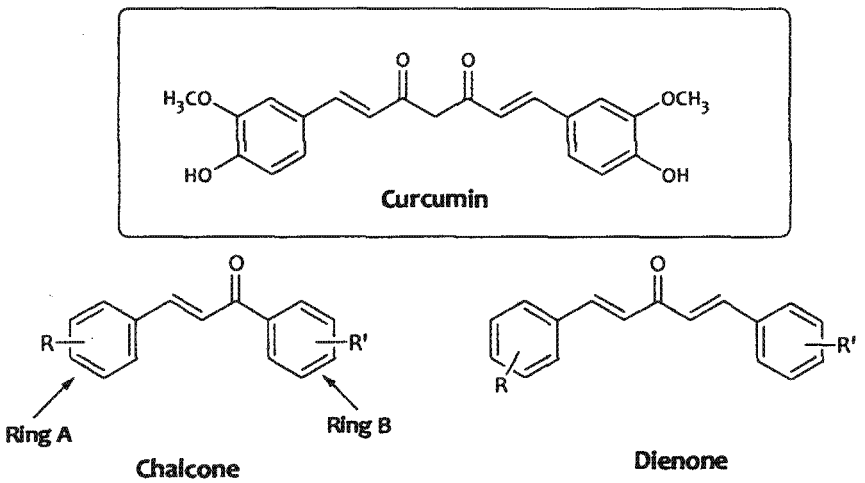

Figure 2.12: General structures of curcumin-related compounds chalcones and dienones

Scientific studies have shown curcumin to possess a variety of biological activities, including antioxidant [123], antiangiogenic [128] and anti-cancer [129] activity, as well as promotion of wound healing [125]. It has also been shown to possess anti-inflammatory [130,131] and anti-protozoal activity against *Trypanosoma* [132], *Leishmania* [133] and *Plasmodium* [134,135] parasites. Chalcones appear to be a privileged class of compounds, exhibiting a very diverse range of biological activities including anticancer [136,137], antioxidant [138], antibacterial [139], antiviral [140], anti-HIV [141], anti-TB [142], and antiprotozoal activity against *Giardia* [143], *Leishmania* [144,145] and *Plasmodium* [146,147] species.

2.9.1.2 Antimalarial activity of curcumin and chalcones

With regard to its antiplasmodial activity, *in vitro* studies have shown curcumin to inhibit the growth CQR *P. falciparum* in a dose-dependent manner, with an IC_{50} of ~5μM [134]. The current study reproduced these *in vitro* antimalarial results against both the CQR (Dd2) and the CQS (D10) strains (Chapter Four). However, the development of curcumin as an antimalarial is hampered by its relatively low potency and its poor oral bioavailability [148]; *in vivo* studies show up to 75% of orally administered curcumin is unabsorbed and excreted in faeces [126].

The study of chalcones as potential antimalarial agents was largely inspired by the discovery of the naturally occurring antimalarial chalcone, licochalcone A [101,102]. Extensive SAR studies on the antimalarial activity of chalcones, such as those by Glutteridge *et al.* [149] and Go *et al.* [146], have led to the identification of a very diverse range of synthetic chalcones with notable antimalarial activities, including halogenated, hydroxylated, alkoxylated and quinolinyl chalcones. These studies have suggested that:

- electron-withdrawing groups on ring A (e.g. 4-chloro, 2,3-dichloro, 2,4-dichloro and 2,4-difluoro substitutions) and electron-donating groups on the ring B (e.g. 2,4-dimethoxy and 2,3,4-trimethoxy substitutions) were associated with an increased *in vitro* antimalarial potency;
- replacement of ring A with a quinoline ring further enhanced antimalarial activity;
- alkoxylated chalcones were generally more active than hydroxylated chalcones;
- the α-βunsaturated enone linker was essential for activity [146,147,149-151].

2.9.1.3 Proposed mechanisms of antimalarial action

Curcumin has been experimentally shown to inhibit various mammalian isoforms of Sarcoplasmic Reticulum Calcium ATPase (SERCA) pumps, possibly by stabilizing the interaction between the nucleotide binding and phosphorylation domains, precluding ATP binding [152]. Inhibition of the *P. falciparum* SERCA (PfATP6) could therefore be a possible basis for its observed antimalarial activity, which is similar to one of the proposed mechanisms of action of the highly active artemisinin-derived antimalarials.

Other possible mechanisms of action of both curcumin and chalcones have been proposed based on the empirical evaluation of their structures. For example, these compounds may interfere with hemozoin formation by interacting with heme to prevent polymerization. This could be by π-π stacking interactions facilitated by the two phenyl ring systems, and which could allow for stacking interactions with heme. In the case of curcumin (and hydroxylated chalcones), inhibition of hemozoin formation could also result from hydrogen bonding between the enolic and phenolic hydroxyl groups on curcumin and the terminal carboxylate groups on heme, or from iron chelation involving the coordination of the central iron of the haem by the β-diketonate group on curcumin [153].

Another possible mechanism of action is the inhibition of the cysteine proteases involved in the hydrolysis of globulin. This non-reversible inhibition would be the result of curcumin or chalcones covalently binding with the enzymes *via* a 1,4-conjugate addition reaction, in which the thiol group of the cysteine residue within the enzyme's active site, in its thiolate form, acts as a nucleophile and attacks the α,β-unsaturated carbonyl system of curcumin as shown in Figure 2.13 [154].

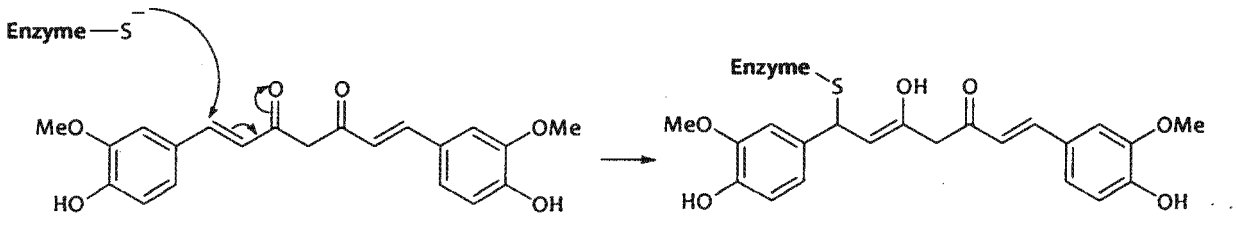

Figure 2.13: Schematic representation of the proposed 1,4-conjugate addition of the thiolate group of an enzyme and the α,β- unsaturated carbonyl system of curcumin

Other probable antimalarial mechanisms of action of chalcones include inhibition of the *P. falciparum* cyclin-dependent kinase PfMRK [155] or possible inhibition of protozoal fumarate reductase [156].

In spite of its low antimalarial potency, curcumin remains an attractive potential lead compound for the design and (semi)synthesis of potential antimalarial compounds [135]. Curcumin in itself was not applied in the synthesis of hybrid compounds in this study, but rather the two classes of structurally related compounds, chalcones and dienones, were used for this purpose.

2.10 Research questions, Aims and Objectives

Research question

The research question that this study aimed to answer was whether it would be possible to identify novel curcumin-related hybrid compounds with *in vitro* and *in vivo* antimalarial activity. An attendant question was whether it would be possible to elucidate the pharmacokinetics and mechanism(s) of action of selected target compounds.

Objective

The overall objective was to identify novel hybrid compounds containing scaffolds that are structurally related to the natural product curcumin, and which possess *in vitro* and *in vivo* antimalarial potency.

Specific aims

- To design and synthesize novel hybrid compounds as potential antimalarial agents which contain scaffolds that are structurally related to the natural product curcumin (Chapter Three).
- To pharmacologically evaluate the synthesized compounds *in vitro* for antimalarial activity and possible mechanisms of action (Chapter Four).
- To apply *in silico* (computational) techniques to guide the design of derivatives of the more active compounds with potentially superior physicochemical and/or ADMET properties for subsequent synthesis, *in vitro* antimalarial testing and mechanistic studies (Chapter Five).
- To elucidate the pharmacokinetic profiles and evaluate the *in vivo* antimalarial activities of the most promising compounds using the mouse model (Chapter Six).

References

1. R G Ridley. Medical need, scientific opportunity and the drive for antimalarial drugs. *Nature* (2002) 415 686-693.

2. C Biot and K Chibale. Novel approaches to antimalarial drug discovery. *Infect. Disord. Drug Targets* (2006) 6 173-204.

3. WHO. Guidelines for the treatment of malaria. *WHO* (2006)

4. G Edwards and G A Biagini. Resisting resistance: dealing with the irrepressible problem of malaria. *Brit. J. Clin. Pharmacol.* (2006) 61 (6) 690-693.

5. N White. Antimalarial drug resistance and combination chemotherapy. *Phil. Trans. R. Soc. Lond.* (1999) B354 739-749.

6. T K Mutabingwa. Artemisinin-based combination therapies (ACTs): Best hope for malaria but inaccessible to the needy. *Acta Trop.* (2005) 95 305-315.

7. WHO. Guidelines for the treatment of malaria - 2nd Edition. *WHO* (2010)

8. N J White. Qinghaosu (Artemisinin): The Price of Success. *Science* (2008) 320 330-334.

9. K I Barnes and N J White. Population biology and antimalarial resistance: The transmission of antimalarial drug resistance in *Plasmodium falciparum*. *Acta Trop.* (2005) 94 230-240.

10. N J White. Assessment of the Pharmacodynamic Properties of Antimalarial Drugs *In Vivo*. *Antimicrob. Agents Chemother.* (1997) 41 (7) 1413-1422.

11. D N Durrheim. Artemisinin-class combination therapy for malaria - unresolved ethical and technical issues. *Trop. Med. Infect. Dis.* (2004) 2 185-188.

12. A Nzila. The past, present and future of antifolates in the treatment of *Plasmodium falciparum* infection. *J. Antimicrob. Chemother.* (2006) 57 1043-1054.

13. H C Carrington, A F Crowther, D G Davey, A A Levi, and F L Rose. A metabolite of paludrine with high antimalarial activity. *Nature* (1951) 168 1080.

14. P A Winstanley, E K Mberu, I S F Szwandt, A M Breckenridge, and W M Watkins. In Vitro Activities of Novel Antifolate Drug Combinations against *Plasmodium falciparum* and Human Granulocyte CFUs. *Antimicrob. Agents Chemother.* (1995) 39 (4) 948-952.

15. A T Hudson. Atovaquone — a novel broad-spectrum anti-infective drug. *Parasitol. Today* (1993) 9 (2) 66-68.

16. W T Hughes. The role of Atovaquone tablets in treating *Pneumocystis carinii* pneumonia. *J. Acquir. Immune Defic. Syndr. Hum. Retrovirol.* (1995) 8 247-252.

17. I K Srivastava, H Rottenberg, and A B Vaidya. Atovaquone, a Broad Spectrum Antiparasitic Drug, Collapses Mitochondrial Membrane Potential in a Malarial Parasite. *J. Biol. Chem.* (1997) 272 (7) 3961-3966.

18. I K Srivastava and A B Vaidya. A Mechanism for the Synergistic Antimalarial Action of Atovaquone and Proguanil. *Antimicrob. Agents Chemother.* (1999) 43 (6) 1334-1339.

19. C J Canfield, M Pudney, and W E Gutteridge. Interactions of atovaquone with other antimalarial drugs against *P. falciparum in vitro*. *Experim. Parasitol.* (1995) 80 373-381.

20. P D Radloff, J Phillips, M Nkeyi, D Hutchinson, and P G Kremsner. Atovaquone and proguanil for *Plasmodium falciparum* malaria. *Lancet* (1996) 347 1511-1514.

21. N Olivieri, G M Brittenham, D matsui, M Berkovitch, L M Blendis, R G Cameron, R A McClelland, P P Liu, D M Templeton, and G Koren. Iron-chelation therapy with oral deferiprone in patients with thalassemia major. *New Engl. J. Med.* (1995) 332 (14) 918-922.

22. N Olivieri and G M Brittenham. Iron-Chelating Therapy and the Treatment of Thalassemia. *Blood* (1997) 89 (3) 739-761.

23. C B Modell and J Beck. Long-term desferrioxamine therapy in thalassemia. *Ann. New York Acad. Sci.* (2006) 232 201-210.

24. G F Mabeza, M Loyevsky, V R Gordeuk, and G Weiss. Iron Chelation Therapy for Malaria: A Review. *Pharmacol. Therap.* (1999) 81 (1) 53-75.

25. D G Heppner, P E Hallaway, G J Kontoghiorghes, and J W Eaton. Antimalarial Properties of Orally Active Iron Chelators. *Blood* (1988) 72 (1) 358-361.

26. V Gordeuk, P E Thuma, G M Brittenham, S Zulu, G Simwanza, A Mhangu, G Flesch, and D Parry. Iron Chelation With Desferrioxamine B in Adults With Asymptomatic *Plasmodium falciparum* Parasitemia. *Blood* (1992) 79 (2) 308-312.

27. T J Egan and C H Kaschula. Strategies to reverse drug resistance in malaria. *Curr. Opin. Infect. Dis.* (2007) 20 (6) 598-604.

28. P Rasoanaivo, D Ramanitrahasimbola, and S Ratsimamanga-Urverg. Leads and botanicals from plants in Madagascar. *Personal communication* (2010)

29. P Rasoanaivo, S Ratsimamanga-Urverg, R Milijaona, H Rafatro, A Rakoto-Ratsimamanga, C Galeffi, and M Nicoletti. *In vitro* and *in vivo* chloroquine-potentiating action of *Strychnos myrtoides* alkaloids against chloroquine-resistant strains of *Plasmodium* resistant malaria. *Planta Medica* (1993) 60 13-16.

30. P Rasoanaivo, S Ratsimamanga-Urverg, H Rafatro, D Ramanitrahasimbola, G Palazzino, C Galeffi, and M Nicoletti. Alkaloids of *Hernandia voyronii*: chlorquine-potentiating activity and structure elucidation of Herveline D. *Planta Medica* (1998) 64 58-62.

31. D Ramanitrahasimbola, P Rasoanaivo, and H Vial. Malagashanine potentiates chloroquine antimalarial activity in drug resistant *Plasmodium* malaria by modifying both its efflux and influx. *Mol. Biochem. Parasitol* (2006) 146 58-67.

32. H Rafatro, D Ramanitrahasimbola, P Rasoanaivo, S Ratsimamanga-Urverg, A Rakoto-Ratsimamanga, and F Frappier. Reversal Activity of the Naturally Occurring Chemosensitizer Malagashanine in *Plasmodium* Malaria. *Biochem. Pharmacol.* (2000) 59 1053-1061.

33. M Frédérich, M Hayatte, M Tits, P de Mol, and L Angenot. Reversal of chloroquine and mefloquine resistance in *Plasmodium falciparum* by two monoindole alkaloids, Icajine and Isoretuline. *Planta Medica* (2001) 67 523-527.

34. F Frappier, A Jossang, J Soudon, F Calvo, P Rasoanaivo, S Ratsimamanga-Urverg, J Saez, and J Schrevel. Bisbenzylisoquinolines as Modulators of Chloroquine Resistance in *Plasmodium falciparum* and Multidrug Resistance in Tumor Cells. *Antimicrob. Agents Chemother.* (1996) 40 (6) 1476-1481.

35. P A Tamez, D Lantvit, E Lim, and J M Pezzuto. Chemosensitizing action of cepharanthine against drug-resistant human malaria, *Plasmodium falciparum*. *J. Ethnopharmacol.* (2005) 98 137-142.

36. J A Martiney, A Cerami, and A F G Slater. Verapamil Reversal of Chloroquine Resistance in the Malaria Parasite *Plasmodium falciparum* is Specific for Resistant Parasites and Independent of the Weak Base Effect. *J. Biol. Chem.* (1995) 270 (38) 22393-22398.

37. G O Gbotosho, O A Ogundahunsi, C T Happi, D E Kyle, L Gerena, W K Milhous, A Sowunmi, A M J Oduola, and L A Salako. The effects of α1-acid glycoprotein on the reversal of chloroquine resistance in *Plasmodium falciparum*. *Annal. Tropic. Med. Parasitol.* (2006) 100 (7) 571-578.

38. A M J Oduola, A Sowunmi, W K Milhous, T G Brewer, D E Kyle, L Gerena, R N Rossan, L A Salako, and B G Schuster. *In vitro* and *in vivo* reversal of chloroquine resistance in *Plasmodium falciparum* with promethazine. *Am. J. Trop. Med. Hyg.* (1998) 58 (5) 625-629.

39. G O Gbotosho, C T Happi, A.Sijuade, O A T Ogundahunsi, A Sowunmi, and A M J Oduola. Comparative study of interactions between chloroquine and chlorpheniramine or promethazine in healthy volunteers: a potential combination-therapy phenomenon for resuscitating chloroquine for malaria treatment in Africa. *Annal. Tropic. Med. Parasitol.* (2008) 102 (1) 3-9.

40. W Peters, R Ekong, B L Robinson, D C Warhurst, and Xing-Qing Pan. Antihistaminic drugs that reverse chloroquine resistance in *Plasmodium falciparum*. *Lancet* (1989) 334-335.

41. Z He, L Chen, J You, L Qin, and X Chen. Antiretroviral protease inhibitors potentiate chloroquine antimalarial activity in malaria parasites by regulating intracellular glutathione metabolism. *Experim.Parasitol.* (2009) 123 122-127.

42. M F M Khairul, T H Min, J H Low, C H Che Nasriyyah, A N A'shikin, M N Norazmi, M Ravichandran, and S S Raju. Fluoxetine potentiates Chloroquine and Mefloquine effects on multi-drug resistant *Plasmodium falciparum in Vitro*. *Jap. J. Inf. Dis.* (2009) 59 329-331.

43. S G Evans, N Butkow, C Stilwell, M Berk, N Kirchmann, and I Havlik. Citalopram Enhances the Activity of Chloroquine in Resistant *Plasmodium in Vitro* and *in Vivo*. *J. Pharmacol. Experim. Therapeut.* (1998) 286 (1) 172-174.

44. T H Min, M F M.Khairul, J H Low, C H Che Nasriyyah, A N A'shikin, M N Norazmi, M Ravichandran, and S S Raju. Roxithromycin potentiates the effects of chloroquine and mefloquine on multidrug-resistant *Plasmodium falciparum in vitro*. *Experim. Parasitol.* (2007) 115 387-392.

45. A D van Schalkwyk, J C Walden, and P J Smith. Reversal of Chloroquine Resistance in *Plasmodium falciparum* using Combinations of Chemosensitizers. *Antimicrob. Agents Chemother.* (2001) 45 (11) 3171-3174.

46. F Chouteau, D Ramanitrahasimbola, P Rasoanaivo, and K Chibale. Exploiting a basic chemosensitizing pharmacophore hypothesis. Part 1: Synthesis and biological evaluation of novel arylbromide and bicyclic chemosensitizers against drug-resistant malaria parasites. *Bioorg. Med. Chem. Lett.* (2005) 15 3024-3028.

47. A K Bhattacharjee, D E Kyle, and J L Vennerstrom. Structural Analysis of Chloroquine Resistance Reversal by Imipramine Analogs. *Antimicrob. Agents Chemother.* (2001) 45 (9) 2655-2657.

48. Chung-Pu Wu, D A van Schalkwyk, D Taylor, P J Smith, and K Chibale. Reversal of chloroquine resistance in *Plasmodium falciparum* by 9*H*-xanthene derivatives. *Int. J. Antimicrob. Agents* (2005) 26 170-175.

49. J X Kelly, M J Smilkstein, R A Cooper, K D Lane, R A Johnson, A Janowsky, R A Dodean, D J Hinrichs, R Winter, and M Riscoe. Design, Synthesis, and Evaluation of 10-N-Substituted Acridones as Novel Chemosensitizers in *Plasmodium falciparum*. *Antimicrob. Agents Chemother.* (2007) 51 (11) 4133-4140.

50. Y Osa, S Kobayashi, Y Sato, Y Suzuki, K Takino, T Takeuchi, Y Miyata, M Sakaguchi, and H Takayanagi. Structural Properties of Dibenzosuberanylpiperazine Derivatives for Efficient Reversal of Chloroquine Resistance in *Plasmodium chabaudi*. *J. Med. Chem* (2003) 46 1948-1956.

51. S Yeh, P J Smith, and K Chibale. Dual-acting diamine antiplasmodial and chloroquine resistance modulating agents. *Biochem. Pharmacol.* (2006) 72 156-165.

52. S J Burgess, A Selzer, J X Kelly, M J Smilkstein, M K Riscoe, and D H Peyton. A Chloroquine-like Molecule Designed to Reverse Resistance in *Plasmodium falciparum*. *J. Med. Chem* (2006) 49 5623-5625.

53. N October, N D Watermeyer, V Yardley, T J Egan, K Ncokazi, and K Chibale. Reversed chloroquines based on the 3,4-dihydropyrimidin-2(*1H*)-one scaffold: synthesis and evaluation of antimalarial, β–hematin inhibition and cytotoxic activity. *ChemMedChem* (2008) 3 (11) 1649-1653.

54. J X Kelly, M J Smilkstein, R Brun, S Wittlin, R A Cooper, K D Lane, A Janowsky, R A Johnson, R A Dodean, R Winter, D J Hinrichs, and M K Riscoe. Discovery of dual function acridones as new antimalarial chemotype. *Nature* (2009) 459 (7244) 270-273.

55. T N K Raju. The Nobel Chronicles: 1988 - James Whyte Black, (b 1924), Gertrude Elion (1918-99), and George H Hitchings (1905-98). *Lancet* (2000) 355 1022.

56. J R Proudfoot. Drugs, Leads, and Drug-Likeness: An Analysis of Some Recently Launched Drugs. *Bioorg. Med. Chem. Lett.* (2002) 12 1647-1650.

57. R G Ridley, W Hofheinz, H Matile, C Jaquet, A Dorn, R Masciadri, S Jolidin, W F Richter, A Guenzi, M-A Girometta, H Urwyler, W Huber, S Thaithong, and W Peters. 4-Aminoquinoline Analogs of Chloroquine with Shortened Side Chains Retain Activity against Chloroquine-Resistant *Plasmodium falciparum*. *Antimicrob. Agents Chemother.* (1996) 40 (8) 1846-1854.

58. D De, F M Krogstad, L D Byers, and D J Krogstad. Structure-Activity Relationships for Antiplasmodial Activity among 7-Substituted 4-Aminoquinolines. *J. Med. Chem.* (1998) 41 4918-4926.

59. C H Kaschula, T J Egan, R Hunter, N Basilico, S Parapini, D Taramelli, E Pasini, and D Monti. Structure-Activity Relationships in 4-Aminoquinoline Antiplasmodials. The Role of the Group at the 7-Position. *J. Med. Chem.* (2002) 45 3531-3539.

60. P G Bray, S R Hawley, M Mungthin, and S A Ward. Physicochemical properties correlated with drug resistance and the reversal of drug resistance in *Plasmodium falciparum*. *Molec. Pharmacol.* (1996) 50 1559-1566.

61. D C Warhurst. Understanding resistance to antimalarial 4-aminoquinolines, cinchona alkaloids and the highly hydrophobic arylaminoalcohols. *Curr. Sci.* (2007) 92 (11) 1556-1560.

62. M A L Blackie, V Yardley, and K Chibale. Synthesis and evaluation of phenylequine for antimalarial activity *in vitro* and *in vivo*. *Bioorg. Med. Chem. Lett.* (2010) 20 1078-1080.

63. P Beagley, M A L Blackie, K Chibale, C Clarkson, R Meijboom, J R Moss, P J Smith, and H Su. Synthesis and antiplasmodial activity *in vitro* of new ferrocene-chloroquine analogues. *Dalton Trans.* (2003) 3046-3051.

64. P Beagley, M A L Blackie, K Chibale, C Clarkson, J R Moss, and P J Smith. Synthesis and antimalarial activity *in vitro* of new ruthenocene-chloroquine analogues. *Dalton Trans.* (2002) 4426-4433.

65. M A L Blackie, P Beagley, S L Croft, H Kendrick, J R Moss, and K Chibale. Metallocene-based antimalarials: An exploration into the influence of the ferrocenyl moiety on *in vitro* antimalarial activity in chloroquine-sensitive and chloroquine-resistant strains of *Plasmodium falciparum*. *Bioorg. Med. Chem.* (2007) 15 6510-6516.

66. K J Raynes, P A Stocks, P M O'Neill, B K Park, and S A Ward. New 4-Aminoquinoline Mannich Base Antimalarials. 1. Effect of an Alkyl Substituent in the 5'-Position of the 4'-Hydroxyanilino Side Chain. *J. Med. Chem.* (1999) 42 2747-2751.

67. J X Kelly, M J Smilkstein, R Brun, S Wittlin, R A Cooper, K D Lane, A Janowsky, R A Johnson, R A Dodean, R Winter, D J Hinrichs, and M K Riscoe. Discovery of dual function acridones as new antimalarial chemotype. *Nature* (2009) 459 (7244) 270-273.

68. J Guillon, P Grellier, M Labaied, P Sonnet, J-M Legér, R Déprez-Poulain, I Forfar-Bares, P Dallemagne, N Lemaitre, F Péhourcq, J Rochette, C Sergheraert, and C Jarry. Synthesis, Antimalarial Activity, and Molecular Modeling of New Pyrrolo[1,2-*a*]quinoxalines, Bispyrrolo[1,2-*a*]quinoxalines, Bispyrido[3,2-*e*]pyrrolo[1,2-*a*]pyrazines, and Bispyrrolo[1,2-*a*]thieno[3,2-*e*]pyrazines. *J. Med. Chem.* (2004) 47 1997-2009.

69. D K Taylor, T D Avery, B W Greatrex, E R T Tiekink, I G Macreadie, P I Macreadie, A D Humphries, M Kaikanidis, E N Fox, N Klonis, and L Tilley. Novel Endoperoxide Antimalarials: Synthesis, Heme Binding, and Antimalarial Activity. *J. Med. Chem.* (2004) 47 1833-1839.

70. M P Crespo, T D Avery, E Hanssen, E Fox, T V Robinson, P Valente, D K Taylor, and L Tilley. Artemisinin and a Series of Novel Endoperoxide Antimalarials Exert Early Effects on Digestive Vacuole Morphology. *Antimicrob. Agents Chemother.* (2008) 52 (1) 98-109.

71. K J Saliba, and K Kirk. Clotrimazole inhibits the growth of *Plasmodium falciparum in vitro*. *Trans. R. Soc. Trop. Med. Hyg.* (1998) 92 (6) 666-667.

72. T Tiffert, H Ginsburg, M Krugliak, B C Elford, and V L Lew. Potent antimalarial activity of clotrimazole in *in vitro* cultures of *Plasmodium falciparum*. *Proc. Natl. Acad. Sci. USA.* (2000) 97 (1) 331-336.

73. S Gemma, G Campiani, S Butini, G Kukreja, B P Joshi, M Persico, B Catalanotti, E Novellino, E Fattorusso, V Nacci, L Savini, D Taramelli, N Basilico, G Morace, V Yardley, and C Fattorusso. Design and Synthesis of Potent Antimalarial Agents Based on Clotrimazole Scaffold: Exploring an Innovative Pharmacophore. *J. Med. Chem.* (2007) 50 595-598.

74. D A Carache, S R Hörtner, A Bertogg, C Binkert, D Bur, H P Märki, A Dorn, and F Diederich. *De Novo* Design, Synthesis, and *In Vitro* Evaluation of a New Class of Nonpeptidic Inhibitors of the Malarial Enzyme Plasmepsin II. *ChemBioChem.* (2002) 11 1137-1141.

75. T Heikillä, S Thirumalairajan, M Davies, M R Parsons, A G McConkey, C W G Fishwick, and A P Johnson. The first *de novo* designed inhibitors of *Plasmodium falciparum* dihydroorotate dehydrogenase. *Bioorg. Med. Chem. Lett.* (2006) 16 88-92.

76. M L Baniecki, D F Wirth, and J Clardy. High-Throughput *Plasmodium falciparum* Growth Assay for Malaria Drug Discovery. *Antimicrob. Agents Chemother.* (2007) 51 (2) 716-723.

77. Y Kurosawa, A Dorn, M Kitsuji-Shirane, H Shimada, T Satoh, H Matile, W Hofheinz, R Masciadri, M Kansy, and R G Ridley. Hematin Polymerization Assay as a High-Throughput Screen for Identification of New Antimalarial Pharmacophores. *Antimicrob. Agents Chemother.* (2000) 44 (10) 2638-2644.

78. T S Haque, A G Skillman, C E Lee, H Habashita, I Y Gluzman, T J A Ewing, D E Goldberg, I D Kuntz, and J A Ellman. Potent, Low-Molecular-Weight Non-Peptide Inhibitors of Malarial Aspartyl Protease Plasmepsin II. *J. Med. Chem.* (1999) 42 1428-1440.

79. M A Phillips, R Gujjar, N A Malmquist, J White, F E Mazouni, J Baldwin, and P K Rathod. Triazolopyrimidine-Based Dihydroorotate Dehydrogenase Inhibitors with Potent and Selective Activity against the Malaria Parasite *Plasmodium falciparum*. *J. Med. Chem.* (2008) 51 3649-3653.

80. D Plouffe, A Brinker, C McNamara, K Henson, N Kato, K Kuhen, A Nagle, F Adrián, J T Madzen, P Anderson, T Nam, N S Gray, A Chatterjee, J Janes, S F Yan, R Trager, J S Caldwell, P G Schultz, Y Zhou, and E A Winzeler. *In silico* activity profiling reveals the mechanism of action of antimalarials discovered in a high-throughput screen. *Proc. Natl. Acad. Sci. USA.* (2008) 105 (26) 9059-9064.

81. P V Desai, A Patny, Y Sabnis, B Tekwani, J Gut, P J Rosenthal, A Srivastava, and M Avery. Identification of Novel Parasitic Cysteine Protease Inhibitors Using Virtual Screening. 1. The ChemBridge Database. *J. Med. Chem.* (2004) 47 6609-6615.

82. P V Desai, A Patny, J Gut, P J Rosenthal, B Tekwani, A Srivastava, and M Avery. Identification of Novel Parasitic Cysteine Protease Inhibitors by Use of Virtual Screening. 2. The Available Chemical Directory. *J. Med. Chem.* (2006) 49 1576-1584.

83. H Itokawa, S L Morris-Natschke, T Akiyama, and K-H Lee. Plant-derived natural product research aimed at new drug discovery. *J. Nat. Med.* (2008) 62 263-280.

84. D J Newman, G M Cragg, and K M Snader. Natural Products as Sources of New Drugs over the Period 1981-2002. *J. Nat. Prod.* (2003) 66 1022-1037.

85. M-W Wang, X Hao, and K Chen. **Biological screening of natural products and drug innovation in China.** *Phil. Trans. R. Soc. B.* (2007) 362 1093-1105.

86. D L Klayman. **Quinghaosu (artemisinin): An antimalarial drug from China.** *Science* (1985) 228 1049-1055.

87. S Saxena, N Pant, D C Jain, and R S Bhakuni. **Antimalarial agents from plant sources.** *Curr. Sci.* (2003) 85 (9) 1314-1329.

88. R K Haynes. **From Artemisinin to New Artemisinin Antimalarials: Biosynthesis, Extraction, Old and New Derivatives, Stereochemistry and Medicinal Chemistry Requirements.** *Curr. Top. Med. Chem.* (2006) 6 509-537.

89. K Kaur, M Jain, T Kaur, and R Jain. **Antimalarials from nature.** *Bioorg. Med. Chem.* (2009) 17 3229-3256.

90. K Gademann and J Kobylinska. **Antimalarial Natural Products of Marine and Freshwater Origin.** *Chem. Record* (2009) 9 187-198.

91. R Batista, A J Silva Jnr, and A B Oliviera. **Plant-Derived Antimalarial Agents: New Leads and Efficient Phytomedicines. Part II. Non-Alkaloidal Natural Products.** *Mol.* (2009) 14 3037-3072.

92. S A Charman, S Arbe-Barnes, I Bathurst, R Brun, M Campbell, W N Charman, F C Chiu, J Chollet, J C Craft, D J Creek, Y Dong, H Matile, M Maurer, J Morizzi, T Nguyen, P Papastogiannidis, C Scheurer, D M Shackleford, K Sriraghavan, L Stingelin, Y Tang, H Urwyler, X Wang, K L White, S Wittlin, L Zhou, and J L Vennerstrom. **Synthetic ozonide drug candidate OZ439 offers new hope for a single-dose cure of uncomplicated malaria.** *Proc. Natl. Acad. Sci.* (2011) 108 (11) 4400-5.

93. J L Vennerstrom, S Arbe-Barnes, R Brun, S A Charman, F C Chiu, J Chollet, Y Dong, A Dorn, D Hunziker, H Matile, K McIntosh, M Padmanilayam, T J Santo, C Scheurer, B Scorneaux, Y Tang, H Urwyler, S Wittlin, and W N Charman. **Identification of an antimalarial synthetic trioxolane drug development candidate.** *Nature* (2002) 430 (7002) 900-904.

94. F A Kuehl, Jr, C F Spencer, and K Folkers. **Alkaloids of *Dichroa febrifuga* Lour.** *J. Am. Chem. Soc.* (1948) 70 2091-2093.

95. S Jiang, Q Zeng, M Gettayacamin, A Tungtaeng, S Wannaying, A Lim, P Hansukjariya, C O Okunji, S Zhu, and D Fang. **Antimalarial Activities and Therapeutic Properties of Febrifugine Analogs.** *Antimicrob. Agents Chemother.* (2005) 49 (3) 1169-1176.

96. R K Pettit. **Culturability and Secondary Metabolite Diversity of Extreme Microbes: Expanding Contribution of Deep Sea and Deep-Sea Vent Microbes to Natural Product Discovery.** *Mar. Biotechnol.* (2010) Online publication DOI 10.1007/s10126-010-9294-y.

97. **Dictionary of Natural Products.** (2010) (http://dnp.chemnetbase.com/intro/index.jsp)

98. J Lei and J Zhou. **A Marine Natural Product Database.** *J. Chem. Inf. Comput. Sci.* (2002) 42 742-748.

99. A Ishih, T Suzuki, M Watanabe, T Miyase, and M Terada. **Combination Effects of Chloroquine with the Febrifugine and Isofebrifugine Mixture against a Blood-induced Infection with Chloroquine-resistant *Plasmodium berghei* NK65 in ICR Mice.** *Phytother. Res.* (2003) 17 1234-1236.

100. J J Walsh and A Bell. Hybrid Drugs for Malaria. *Curr. Pharm. Des.* (2009) 15 2970-2985.

101. M Chen, T G Theander, S B Christensen, L Hviid, L Zhai, and A Kharazmi. Licochalcone A, a New Antimalarial Agent, Inhibits In Vitro Growth of the Human Malaria Parasite *Plasmodium falciparum* and Protects Mice from *P. yoelii* Infection. *Antimicrob. Agents Chemother.* (1994) 38 (7) 1470-1475.

102. A Kharazmi. Discovery of oxygenated chalcones as novel antimalarial agents. *Ann. Trop. Med. Parasotol.* (1997) 91 (1) S-91-S-95.

103. R Ferrer, G Lobo, N Gamboa, J Rodrigues, C Abramjuk, K Jung, M Lein, and J E Charris. Synthesis of [(7-Chloroquinolin-4-yl)amino]chalcones: Potential Antimalarial and Anticancer Agents. *Sci. Pharm.* (2009) 77 725-741.

104. E K Kerns and L Di. Drug-like Properties: Concepts, Structure, Design and Methods: from ADME to Toxicity Optimization. *Academic Press/Elselvier* (2008) (1st Edition)

105. D Projean, B Baune, R Farinotti, J-P Flinois, P Beaune, A-M Taburet, and A Ducharme. *In vitro* metabolism of chloroquine: identification of CYP2C8, CYP3A4 and CYP2D6 as the main isoforms catalyzing *N*-desethylchloroquine formation. *Drug Met. Disp.* (2003) 31 (6) 748-754.

106. S Fu, A Björkman, B Wåhlin, D Ofori-Adjei, O Ericsson, and F Sjöqvist. *In vitro* activity of chloroquine, the two enantiomers of chloroquine, desethylchloroquine and pyronaridine against *Plasmodium falciparum*. *Br. J. Clin. Pharmacol.* (1986) 22 93-96.

107. S Hirai, H Kikuchi, H-S Kim, K Begum, Y Wataya, H Tasaka, Y Miyazawa, K Yamamoto, and Y Oshima. Metabolites of Febrifugine and Its Synthetic Analogue by Mouse Liver S9 and Their Antimalarial Activity against *Plasmodium* Malaria Parasite. *J. Med. Chem.* (2003) 46 4351-4359.

108. S Zhu, L Meng, Q Zhang, and L Wei. Synthesis and evaluation of febrifugine analogues as potential antimalarial agents. *Bioorg. Med. Chem. Lett.* (2006) 16 1854-1858.

109. S Zhu, Q Zhang, C Gudise, L Wei, E Smith, and Y Zeng. Synthesis and biological evaluation of febrifugine analogues as potential antimalarial agents. *Bioorg. Med. Chem.* (2009) 17 4496-4502.

110. M Pucheault. Natural products: chemical instruments to apprehend biological symphony. *Org. Biomol. Chem.* (2008) 6 424-432.

111. G G Harrigan, D J Brackett, and L G Boros. Medicinal Chemistry, Metabolic Profiling and Drug Target Discovery: A Role for Metabolic Profiling in Reverse Pharmacology and Chemical Genetics. *Mini-Rev. Med. Chem.* (2005) 5 13-20.

112. M B Cassera, E F Merino, V J Peres, E A Kimura, G Wunderlich, and A M Katzin. Effect of fosmidomycin on metabolic and transcript profiles of the methylerythritol phosphate pathway in *Plasmodium falciparum*. *Mem. Inst. Oswaldo Cruz* (2007) 102 (3) -377.

113. R Teng, P R Junankar, W A Bubb, C Rae, P Mercier, and K Kirk. Metabolite profiling of the intraerythrocytic malaria parasite *Plasmodium falciparum* by 1H NMR spectroscopy. *NMR Biomed.* (2009) 22 292-302.

114. T Böttcher, M Pitscheider, and S A Sieber. Natural Products and Their Biological Targets: Proteomic and Metabolomic Labeling Strategies. *Angew. Chem. Int. Ed.* (2010) 49 2680-2698.

115. D C Greenbaum, A Baruch, M Grainger, Z Bozdech, K F Medzihradszky, J Engel, J DeRisi, A A Holder, and M Bogyo. A role for the protease Falcipain 1 in host cell invasion by the human malaria parasite. *Science* (2002) 298 2002-2006.

116. T Takenaka. Classical vs reverse pharmacology in drug discovery. *B. J. U. International.* (2001) 88 (2) 7-10.

117. M J Gardner, N Hall, E Fung, O White, M Berriman, R W Hyman, J M Carlton, A Pain, K E Nelson, S Bowman, I T Paulsen, K James, J A Eisen, K Rutherford, S L Salzberg, A Craig, S Kyes, M-S Chan, V Nene, S J Shallom, B Suh, J Peterson, S Angiouli, M Pertea, J Allen, J Selengut, D Haft, M W Mather, A B Vaidya, D M A Martin, A H Fairlamb, M J Fraunholz, D S Roos, S A Ralph, G I McFadden, G M Subramanian, C Mungall, J C Venter, D J Carruci, S L Hoffman, C Newbold, R W Davis, C M Fraser, and B Barrell. Genome sequence of the human malaria parasite *Plasmodium falciparum*. *Nature* (2002) 419 498-511.

118. The Plasmodium Genome Database Collaborative. PlasmoDB: An integrative database of the *Plasmodium falciparum* genome. Tools for accessing and analyzing finished and unfinished sequence data. *Nucleic Acids Res.* (2001) 29 (1) 66-69.

119. R A Bauer, J M Wurst, and D S Tan. Expanding the range of 'druggable' targets with natural product-based libraries: an academic perspective. *Curr. Opin. Chem. Biol.* (2010) 14 301-314.

120. M Feher and J M Schmidt. Property Distributions: Differences between Drugs, Natural Products, and Molecules from Combinatorial Chemistry. *J. Chem. Inf. Comput. Sci.* (2003) 43 218-227.

121. J Hert, J J Irwin, C Laggner, M J Keiser, and B K Shoichet. Quantifying Biogenic Bias in Screening Libraries. *Nat. Chem. Biol.* (2009) 5 (7) 479-483.

122. H B Rasmussen, S B Christensen, L P Kvist, and A Karazmi. A simple and efficient separation of curcumins, the antiprotozoal constituents of *Curcuma longa*. *Planta Med.* (2000) 66 396-398.

123. W M Weber, L A Hunsaker, S F Abcouwer, L M Deck, and D L Vander Jagt. Anti-oxidant activities of curcumin and related enones. *Bioorg. Med. Chem.* (2005) 13 3811-3820.

124. M Griesser, V Pistis, T Suzuki, N Tejera, D A Pratt, and C Schneider. Autoxidative and cyclooxygenase-2 catalyzed transformation of the dietary chemopreventive agent curcumin. *J. Biol. Chem.* (2011) 286 1114-1124.

125. H P T Ammon and M A Wahl. Pharmacology of *Curcuma longa*. *Planta Med.* (1991) 57

126. R K Maheshwari, A K Singh, J Gaddipati, and R C Srimal. Multiple biological activities of curcumin: A short review. *Life Sci.* (2006) 78 2081-2087.

127. Z Nowakowska. A review of anti-infective and anti-inflammatory chalcones. *Eur. J. Med. Chem.* (2007) 42 125-137.

128. T P Robinson, T Ehlers, R B Hubbard IV, X Bai, J L Arbiser, D J Goldsmith, and J P Bowen. Design, synthesis and biological evaluation of angiogenesis inhibitors: aromatic enone and dienone analogues of curcumin. *Bioorg. Med. Chem. Lett.* (2003) 13 115-117.

129. B B Aggarwal, A Kumar, and A C Bharti. Anticancer potential of curcumin: preclinical and clinical studies. *Anticancer Res.* (2003) 23 363-398.

130.A N Nurfina, M S Reksohadiprodjo, H Timmermen, U A Jenie, D Sugiyanto, and H van der Goot. Synthesis of some symmetrical curcumin derivatives and their antiinflammatory activity. *Eur. J. Med. Chem.* (1997) 32 321-328.

131. L Camacho-Barquero, I Villegas, J M Sánchez-Calvo, E Talero, S Sánchez-Fidalgo, V Motilva, and C A Lastra. Curcumin, a *Curcuma longa* constituent, acts on MAPK p38 pathway modulating COX-2 and iNOS expression in chronic experimental colitis. *Int. Immunopharmacol.* (2007) 7 333-342.

132.M Nose, T Koide, Y Ogihara, Y Yabu, and N Ohta. Trypanosomal effecta of curcumin *in vitro*. *Biol. Pharm. Bull.* (1998) 21 (6) 643-645.

133.T Koide, M Nose, Y Ogihara, and N Ohta. Leishmanicidal effect of curcumin *in vitro*. *Biol. Pharm. Bull.* (2002) 25 (1) 131-133.

134.R C Reddy, P G Vatsala, V G Keshamouni, G Padmanaban, and P N Rangarajan. Curcumin for malaria therapy. *Biochem. Bioph. Res. Co.* (2005) 326 472-474.

135.D N Nandakumar, V A Nagaraj, P G Vathsala, P Rangarajan, and G Padmanaban. Curcumin-Artemisinin combination therapy for malaria. *Antimicrob. Agents Chemother.* (2006) 50 (5) 1859-1860.

136.N J Lawrence, R P Patterson, L-L Ooi, D Cook, and S Ducki. Effects of α-substitutions on structure and biological activity of anticancer chalcones. *Bioorg. Med. Chem. Lett.* (2006) 16 5844-5848.

137.A Modzelewska, C. Pettit, G Achanta, N E Davidson, P Huang, and S R Khan. Anticancer activities of novel chalcone and bis-chalcone derivatives. *Bioorg. Med. Chem.* (2006) 14 3491-3495.

138.O P Sharma. Antioxidant activity of curcumin and related compounds. *Biochem. Pharmacol.* (1976) 25 1811-1812.

139.S F Nielsen, T Boesen, M Larsen, K Schønning, and H Kromann. Antibacterial chalcones--bioisosteric replacement of the 4'-hydroxy group. *Bioorg. Med. Chem.* (2004) 12 3047-3054.

140.B Malhotra, J C Onyilagha, A Bohm, G H N Towers, D James, J B Harborne, and C J French. Inhibition of tomato ringspot virus by flavonoids. *Phytochem.* (1996) 43 (6) 1271-1276.

141. Q Wang, Z-H Ding, J-K Liu, and Y-T Zheng. Xanthohumol, a novel anti-HIV-1 agent purified from Hops *Humulus lupulus*. *Antiviral Res.* (2004) 64 189-194.

142.Y-M Lin, Y Zhou, M T Flavin, L-M Zhou, W Nie, and F-C Chen. Chalcones and Flavonoids as Anti-Tuberculosis Agents. *Bioorg. Med. Chem.* (2002) 10 2795-2802.

143.L Pérez-Arriaga, M L Mendoza-Magaña, R Cortés-Zárate, A Corona-Rivera, L Bobadilla-Morales, R Troyo-Sanromán, and M N Ramírez-Herrera. Cytotoxic effects of curcumin on *Giardia lamblia* trophozoites. *Acta Trop.* (2006) 98 152-161.

144.P Boeck, C A B Falcão, P C Leal, R A Yunes, V C Filho, E C Torres-Santos, and B Rossi-Bergman. Synthesis of chalcone analogs with increased antileishmanial activity. *Bioorg. Med. Chem.* (2006) 14 1538-1545.

145.M Chen, S B Christensen, T G Theander, and A Kharazmi. **Antileishmanial Activity of Licochalcone A in Mice Infected with *Leishmania major* and in Hamsters Infected with *Leishmania donovani*.** *Antimicrob. Agents Chemother.* (1994) 38 (6) 1339-1344.

146.M Liu, P Wilairat, and M-L Go. **Antimalarial alkoxylated and hydroxylated chalcones: structure-activity relationship analysis.** *J. Med. Chem.* (2001) 44 4443-4452.

147.R Li, G L Kenyon, F E Cohen, X Chen, B Gong, J N Dominguez, E Davidson, G Kurzban, R E Miller, E O Nuzum, P J Rosenthal, and J H McKerrow. ***In Vitro* Antimalarial Activity of Chalcones and Their Derivatives.** *J. Med. Chem.* (1995) 38 5031-5037.

148.P Anand, A B Kunnumakkara, R A Newman, and B B Aggarwal. **Bioavailability of Curcumin: Problems and Promises.** *Mol. Pharm.* (2007) 4 (6) 807-818.

149.C E Gutteridge, D A Nichols, S M Curtis, D S Thota, J V Vo, L Gerena, G Montip, C O Asher, D S Diaz, C A DiTusa, K Smith, and A K Bhattacharjee. ***In vitro* and *in vivo* efficacy and *in vitro* metabolism of 1-phenyl-3-aryl-2-propen-1-ones against *Plasmodium falciparum*.** *Bioorg. Med. Chem. Lett.* (2006) 16 5682-5686.

150.J N Dominguez, J E Charris, G Lobo, N G de Dominguez, M M Moreno, F Riggione, E Sanchez, J Olson, and P J Rosenthal. **Synthesis of quinolinyl chalcones and evaluation of their antimalarial activity.** *Eur. J. Med. Chem.* (2001) 36 555-560.

151. M Liu, P Wilairat, S L Croft, A L-C Tan, and M-L Go. **Structure–Activity Relationships of Antileishmanial and Antimalarial Chalcones.** *Bioorg. Med. Chem.* (2003) 11 2729-2738.

152.J G Bilmen, S Z Khan, M Javed, and F Michelangeli. **Inhibition of the SERCA Ca^{2+} pumps by curcumin.** *Eur. J. Biochem.* (2001) 268 6318-6327.

153.Y Jiao, J Wilkinson IV, E C Pietsch, J L Buss, W Wang, R Planalp, F M Torti, and S V Torti. **Iron chelation in the biological activity of curcumin.** *Free Radical Bio. Med.* (2006) 40 1152-1160.

154.Z Kunakbaeva, R Carrasco, and I Rozas. **An approximation of the mechanism of inhibition of cysteine proteases: nucleophilic sulphur addition to Michael acceptor type compounds.** *J. Mol. Struct-Theochem* (2003) 626 209-216.

155.J A Geyer, S M Keenan, C L Woodard, P A Thompson, L Gerena, D A Nichols, C E Gutteridge, and N C Waters. **Selective inhibition of Pfmrk, a Plasmodium falciparum CDK, by antimalarial 1,3-diaryl-2-propenones.** *Bioorg. Med. Chem. Lett.* (2009) 19 1982-1985.

156.M Chen, L Zhai, S B Christensen, T G Theander, and A Kharazmi. **Inhibition of Fumarate Reductase in *Leishmania major* and *L. donovani* by Chalcones.** *Antimicrob. Agents Chemother.* (2001) 45 (7) 2023-2029.

In the context of trying to circumvent antimalarials drug resistance, hybridization is quite an attractive strategy particularly when the pharmacophores/active molecules being merged possess independent modes of antimalarial action. Application of dual drugs developed in this way would be akin to applying the individual bioactive molecules in combination [2], thereby borrowing from the highly rated combination therapy approach which advises against mono-therapy and advocates for the co-administration of two (or more) antimalarial agents [3] (*see* **Chapter One**). In addition, such an approach would avoid the frequent problem of having to consider the different pharmacokinetic profiles of individual drugs when administered as simple combinations [2].

Although there are no examples of antimalarial dual drugs in clinical use so far, a number of highly active molecules have been identified using this approach. For example, compounds named trioxaquines have been developed by covalently linking a 1,2,4-trioxane motif (borrowed from the highly active natural sesquiterpene artemisinin, **Figure 3.1**) to a 4-aminoquinoline moiety (borrowed from chloroquine and other aminoquinoline-based antimalarials) *via* an appropriate spacer. This strategy combined the potential heme-alkylating peroxide entity with the 4-aminoquinoline entity, known to enhance accumulation in the acidic food vacuole of the parasite and act by interfering with hemozoin formation. The most active of these were ODC 182 and ODC 188 (**Figure 3.1**) with IC_{50} values <40 nM against FcB1 (CQR) and FcM29 (also CQR) *P. falciparum* strains [4]. Another set of dual drugs was designed to target both the glutathione (GSH) regeneration system and the heme detoxification pathway. Compounds **GRQ1** and **GRQ2** (**Figure 3.1**) were therefore prepared by linking a glutathione reductase (GR) inhibitor to a 4-aminoquinoline moiety *via* an ester bond that was revealed to be sufficiently stable in biological compartments but prone to acid hydrolysis in the food vacuole of the parasite. These compounds were found to be quite active, with ED50 values <30 nM against CQR *P. falciparum* [5].

These examples, along with others such as antimalarial primaquine-statin double-drugs (that inhibit the malarial parasite Plasmepsin II enzyme, one of the aspartic proteases involved in haemoglobin degradation) [6], illustrate the potential of molecular hybridization as a strategy for the development of novel antimalarial agents. This study therefore sought to exploit this potential, investigating the antimalarial activity of hybrid compounds consisting of curcumin-related compounds linked to other rationally selected entities, as described in the sections that follow.

CHAPTER THREE

DESIGN AND SYNTHESIS OF CHALCONE- AND DIENONE-BASED HYBRID COMPOUNDS

3.1 Preamble

This chapter contains the work done to address the first specific aim of the study, which was: To design and synthesize novel hybrid compounds as potential antimalarial agents which contain scaffolds that are structurally related to the natural product curcumin.

The chapter begins by introducing the concept of hybrid compounds/dual drugs and its application as a strategy for (antimalarial) drug discovery. It goes on to examine the 1,3-dipolar cycloaddition reaction of azides and acetylenes as a convenient molecular hybridization strategy. What follows is an account of the rational selection of chalcones, dienones, AZT and chloroquinoline as suitable entities in the design of target antimalarial hybrid compounds, after which the synthesis and ^{1}H-NMR characterization of the target compounds is reported and discussed.

3.2 Hybrid compounds/dual drugs

As mentioned in Chapter One, the development of resistance by the malaria parasite to the bulk of therapeutic agents available clinically has become one of the leading impediments in the efforts to control this disease. As a direct result of this, great efforts have been made towards the development of new, highly efficacious therapeutic agents that do not suffer from this liability.

One of the strategies employed in this quest for novel drugs is molecular hybridization (see section 2.8.1), which is the rational design of new molecules involving the adequate fusion of pharmacophoric sub-units recognized and derived from two or more known bioactive molecules [1]. Such pharmacophoric units would consist of the molecular frameworks that bear those structural features thought to be responsible for the observed pharmacological activity of the original compounds; their selection would therefore be aimed at maintaining the said pharmacological characteristics, with their subsequent fusion, usually *via* a covalent linker, potentially transferring and combining these characteristics into the final target molecules (referred to as hybrid compounds or dual drugs) [1,2].

In the context of trying to circumvent antimalarials drug resistance, hybridization is quite an attractive strategy particularly when the pharmacophores/active molecules being merged possess independent modes of antimalarial action. Application of dual drugs developed in this way would be akin to applying the individual bioactive molecules in combination [2], thereby borrowing from the highly rated combination therapy approach which advises against mono-therapy and advocates for the co-administration of two (or more) antimalarial agents [3] (*see* **Chapter One**). In addition, such an approach would avoid the frequent problem of having to consider the different pharmacokinetic profiles of individual drugs when administered as simple combinations [2].

Although there are no examples of antimalarial dual drugs in clinical use so far, a number of highly active molecules have been identified using this approach. For example, compounds named trioxaquines have been developed by covalently linking a 1,2,4-trioxane motif (borrowed from the highly active natural sesquiterpene artemisinin, **Figure 3.1**) to a 4-aminoquinoline moiety (borrowed from chloroquine and other aminoquinoline-based antimalarials) *via* an appropriate spacer. This strategy combined the potential heme-alkylating peroxide entity with the 4-aminoquinoline entity, known to enhance accumulation in the acidic food vacuole of the parasite and act by interfering with hemozoin formation. The most active of these were ODC 182 and ODC 188 (**Figure 3.1**) with IC_{50} values <40 nM against FcB1 (CQR) and FcM29 (also CQR) *P. falciparum* strains [4]. Another set of dual drugs was designed to target both the glutathione (GSH) regeneration system and the heme detoxification pathway. Compounds GRQ1 and GRQ2 (**Figure 3.1**) were therefore prepared by linking a glutathione reductase (GR) inhibitor to a 4-aminoquinoline moiety *via* an ester bond that was revealed to be sufficiently stable in biological compartments but prone to acid hydrolysis in the food vacuole of the parasite. These compounds were found to be quite active, with ED50 values <30 nM against CQR *P. falciparum* [5].

These examples, along with others such as antimalarial primaquine-statin double-drugs (that inhibit the malarial parasite Plasmepsin II enzyme, one of the aspartic proteases involved in haemoglobin degradation) [6], illustrate the potential of molecular hybridization as a strategy for the development of novel antimalarial agents. This study therefore sought to exploit this potential, investigating the antimalarial activity of hybrid compounds consisting of curcumin-related compounds linked to other rationally selected entities, as described in the sections that follow.

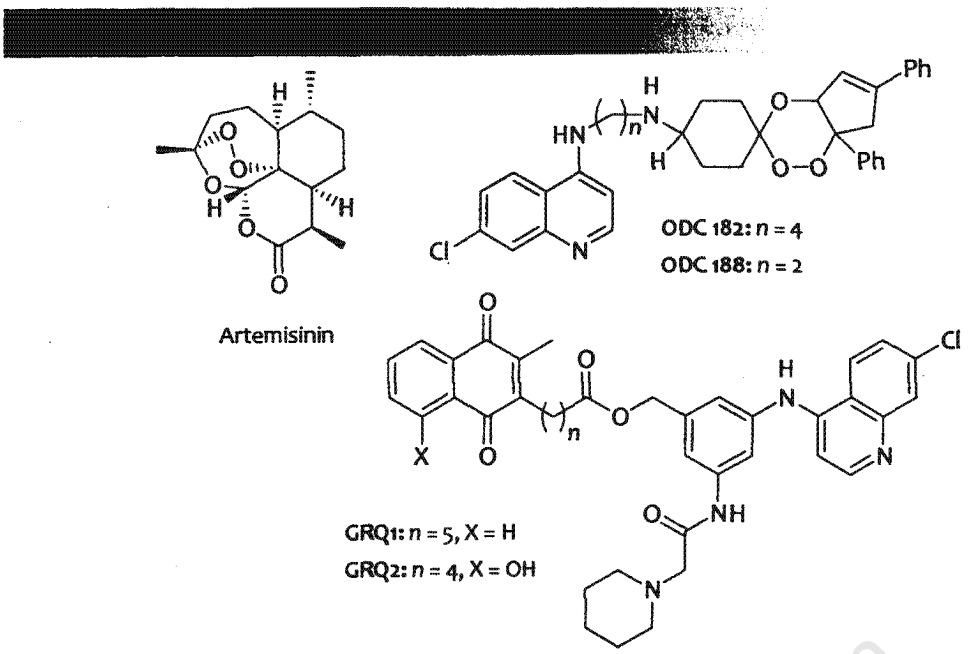

Figure 3.1: Structures of artemisinin and selected antimalarial hybrid compounds [4,5]

3.3 Selection of a suitable hybridization strategy

3.3.1 Introduction to Click Chemistry

Click chemistry is a modular approach to chemical transformations that applies practical and reliable chemical reactions to connect a diversity of structures bearing a wide variety of functional groups [7,8]. It encompasses several groups of reactions including cycloaddition reactions, nucleophilic ring-opening reactions, carbonyl chemistry of the non-aldol type and addition to carbon–carbon multiple bonds (Figure 3.2). As described by Sharpless *et al.* [8], click reactions must be of wide scope, give consistently high yields with a variety of starting materials, be easy to perform, be insensitive to oxygen or water, use only readily available reagents and offer simple reaction work-up and product isolation. Robust chemistry of this nature offered a convenient hybridization strategy for application in this study, and the 1,3-dipolar cycloaddition reactions were considered for this purpose.

1,3-Dipolar cycloadditions are exergonic fusion processes that involve the reaction of 1,3-dipoles and dipolarophiles to yield a variety of 5 -membered heterocycles [9,10]. As the name suggests, a 1,3-dipole is a molecule that has both a nucleophilic site and an electrophilic site in a 1,3-relation; this generally refers to molecules containing one or more heteroatoms and which possess at least one mesomeric structure in the form of a

charged dipole (in a 1,3-relation). A typical example of such a structure is an azide (Figure 3.3A).

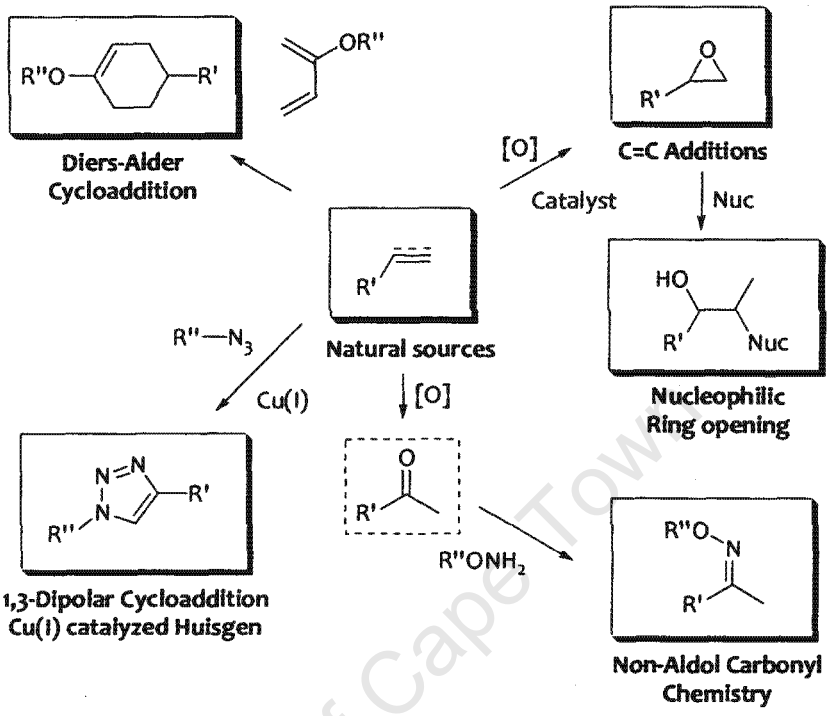

Figure 3.2: A selection of click chemistry reactions [11]

The second reaction component, the dipolarophile, is a source of two π-electrons, and generally refers to a structure with a double or triple bond e.g. an alkyne, alkene or carbonyl group [9]. The cycloaddition of azides and alkynes to yield 1,2,3-triazoles is arguably the most widely applied member of this class of reactions, largely due to the ease with which the azide can be introduced and subsequently carried unscathed through many synthetic steps. It also appears to be the only 1,3-dipole that is practically devoid of any side reactions. However, there are always concerns about the safety of working with organic azides due to their potentially explosive nature [12,13].

This type of reaction was first described by R. Huisgen [10] and classically involves the concerted movement of six electrons in a suprafacial manner – 4 π-electrons from the 1,3-dipole and 2 π-electrons from the dipolarophile [9,10]. Figure 3.3B illustrates the mechanism of the classical (non-catalyzed) Huisgen 1,3-dipolar cycloaddition reaction using the azide and alkyne as the 1,3-dipole and dipolarophile, respectively, to yield a mixture of the 1,4- and 1,5-substituted-1,2,3-triazoles.

3.3.2 Cu(I) catalyzed cycloaddition reaction of azides and terminal alkynes

Under thermal (non-catalyzed) conditions, this 1,3-dipolar cycloaddition reaction of alkynes and azides requires extended reaction times (hours to days), significant heating, and affords a mixture of both 1,4- and 1,5-regioisomers (Figure 3.3C); this is because the activation energy barriers for the concerted process leading to the generation of both isomers are very close, 25.7 and 26.0 kcal/mol for the 1,4- and 1,5-regioisomers, respectively [7,12,14,15]. However, this reaction has since been revolutionalized by the independent discoveries by the research groups led by Sharpless [12] and Meldal [16] that the use of Cu(I) catalysis resulted in higher yields, stability to various solvents (including water) and pH, tolerance to most functionalities, faster reactions under milder reaction conditions, and, unlike the prior uncatalyzed reaction, yielded only the 1,4-disubstituted regioisomer [7,8,17]. As a result, the Cu(I)-catalyzed 1,3-dipolar cycloaddition reaction of azides and terminal alkynes now met the general requirements of a click chemistry reaction (as defined in Section 3.3.1).

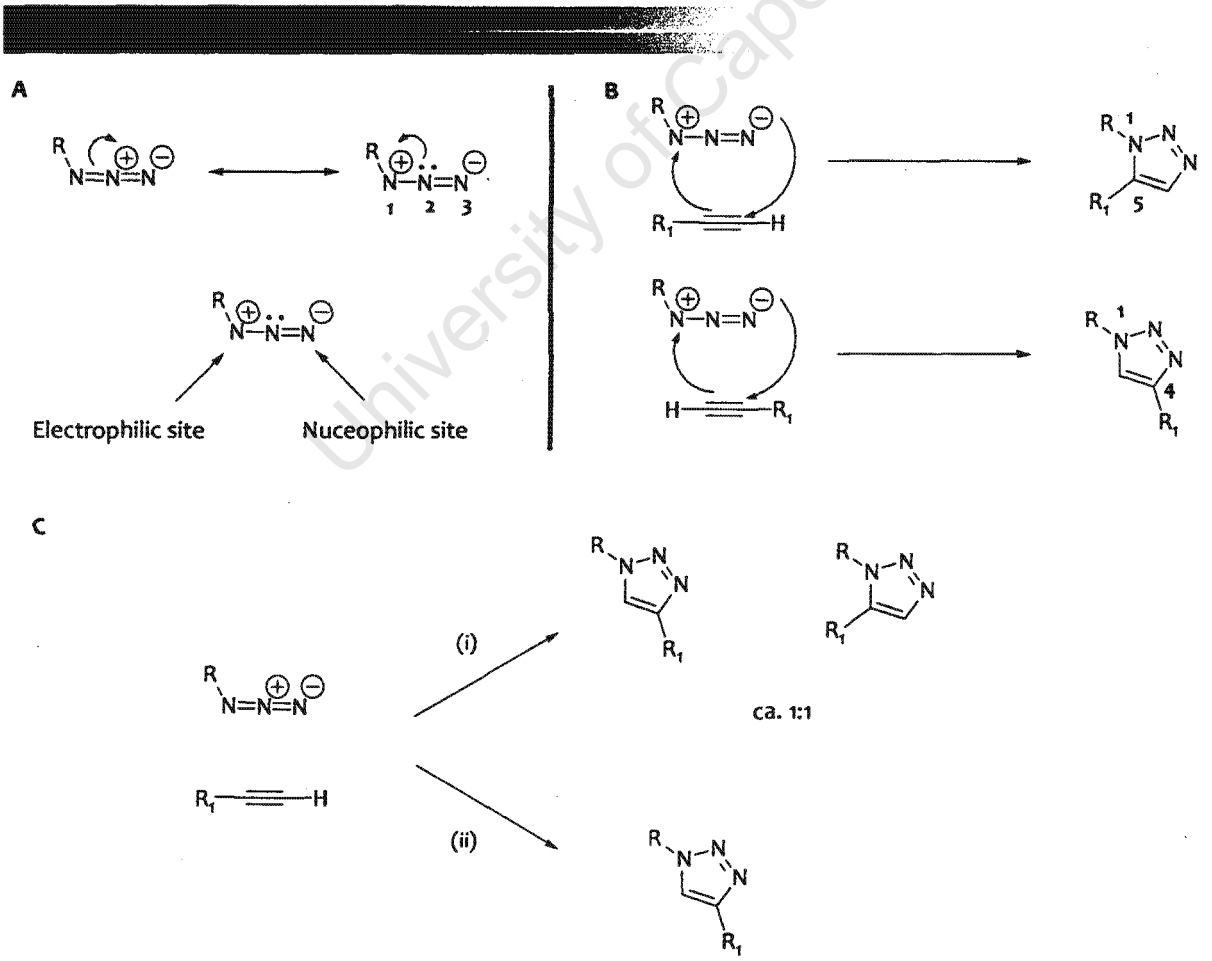

Figure 3.3: A: mesomeric forms of the azide showing the 1,3-dipole; B: mechanism of the classical Huisgen cycloaddition reaction showing the concerted movement of electrons and the resultant regioisomers; C: products of the azide-alkyne cycloaddition reaction under thermal (i) and Cu(I)-catalyzed (ii) conditions: (i) 80 – 120 °C, 12-60 hrs; (ii) Cu(I), rt, 12-24 hrs [7]

Sharpless and coworkers (2002) [12] indicated that the generation of the Cu(I) catalyst *in situ* by the reduction of Cu(II) salts (such as $Cu(OAc)_2$, but more commonly $CuSO_4.5H_2O$) is the preferable approach as Cu(II) salts tend to be less costly and are often purer that Cu(I) salts; ascorbic acid or sodium ascorbate have proven to be excellent reducing agents for this purpose. Direct sources of Cu(I) such as $CuOTf.C_6H_6$ [12], CuI [18], $[Cu(NCCH_3)_4][PF_6]$ [19], $Cu(OEt)_3I$ and $Cu(PPh_3)_3Br$ [20] can be used directly in the absence of a reducing agent. However, these reactions usually require acetonitrile as co-solvent and one equivalent of a nitrogen base (for example 2,6-lutidine, triethylamine, diisopropylethylamine, or pyridine), which, along with the exclusion of oxygen, tend to minimize the formation of undesired by-products observed with direct Cu(I) catalysis. One of the primary by-products of direct Cu(I) catalysis are the diacetylenes, resulting from the Cu(I)-catalyzed oxidative homocoupling of terminal acetylenes *via* their corresponding Cu(I)-acetylides, a reaction discovered by Carl Glaser in 1869, and termed the Glaser reaction [21]. In addition to generating the catalyst from a Cu(II) source, a slight excess of ascorbic acid/ascorbate prevents formation of these oxidative coupling by-products [15].

As alluded to earlier, the reaction tolerates a wide range of solvents. Typically, water is used along with a variety of co-solvents ranging from the water-miscible *tert*-butanol [7,12], ethanol [7,22], DMSO and DMF [17], to the water-immiscible THF [7], and DCM [23,24]. Microwave conditions have also been applied successfully for the generation of 1,2,3-triazoles [20,25]. In an attempt to simplify the experimental conditions even further, the one-pot synthesis of 1,2,3-triazoles from alkyl halides, sodium azide and alkynes has been successfully carried out [17].

The proposed catalytic cycle for the cycloadditon reaction is shown in Figure 3.4 The sequence begins with the coordination of the alkyne to the Cu(I) species, displacing one of the solvent ligands (e.g. water) and forming the copper acetylide I. This would explain why this reaction is not observed with internal alkynes. The azide then displaces a second solvent ligand, binding to the copper *via* the nitrogen proximal to the carbon as in II. After this, the terminal azide nitrogen then attacks the C-2 carbon of the acetylide, forming the six-membered Cu(III) metallacycle III. An energy favoured ring contraction then occurs to generate IV, and finally the release of the formed triazole and regeneration of the Cu(I) catalyst completes the catalytic cycle. This proposed mechanism explains the experimentally observed regioselectivity of the reaction, and is supported by extensive density functional theory (DFT) calculations which strongly disfavour the concerted cycloaddition (B-direct) under conditions of Cu(I) catalysis [12,15].

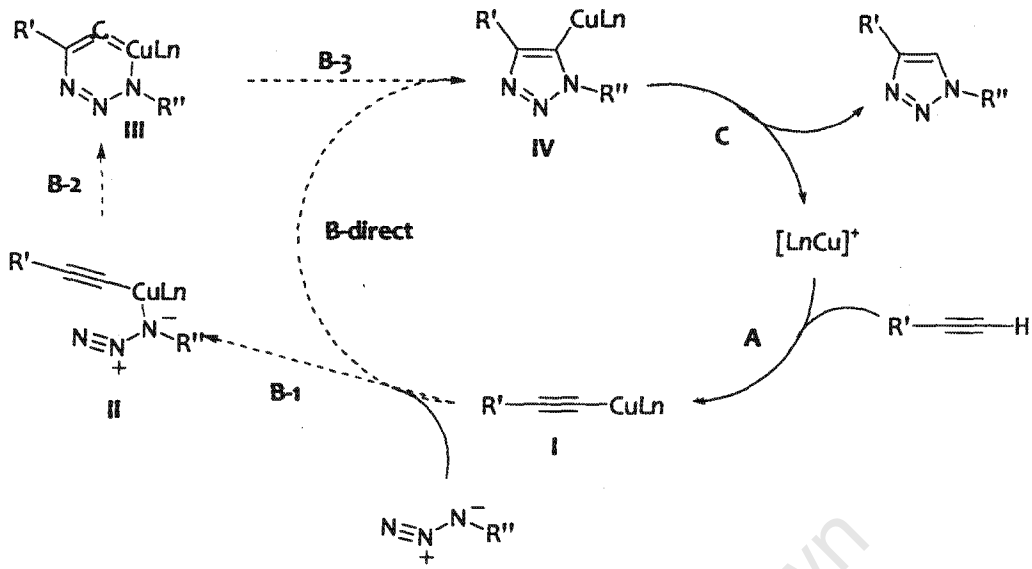

Figure 3.4: Proposed mechanism of the Cu(I)-catalyzed 1,3-dipolar cycloaddition reaction of azides and terminal alkynes [12].

The robust nature and experimental simplicity of this Cu(I)-catalyzed reaction has allowed for its wide application not just in mainstream organic chemistry, but also in medicinal chemistry/drug discovery for the synthesis of bioactive molecules and generation of libraries of drug-like scaffolds possessing the triazole ring [26,27]. It has also found application in biomedical research for such functions as cell-surface labeling [28], activity-based protein profiling (ABPP) [11] and DNA labeling [8]. Its application in drug discovery has led to the identification of triazole-containing compounds with interesting biological activities such as protozoal cysteine protease inhibition [26] and HIV-1 protease inhibition [27] activity.

Based on these positive reports, the current study therefore applied the Cu(I)-catalyzed cycloaddition of azides and terminal alkynes in the synthesis of selected hybrid compounds.

3.4 Selection of the entities for hybridization

3.4.1 Chalcones as curcumin-related compounds

Chalcones are structurally related to curcumin (Figure 2.12), both having two aryl rings linked by a chain that contains an α,β-unsaturated carbonyl system (in the form of a heptadienone chain for curcumin and a propenone chain for chalcones). Also, chalcones can be readily synthesized and have been shown to exhibit notable *in vivo*

and *in vitro* antimalarial activity [29,30]. Based on this, chalcones were chosen as the first class of curcumin-related compounds for this study.

3.4.2 Dienones as curcumin-related compounds

Dienones are also structurally related to curcumin (Figure 2.12), both having two aryl rings joined by an α,β-unsaturated carbonyl system (in the form of a pentadienone chain for dienones). However, no reports on the investigation of the potential antimalarial activity of this class of compounds could be found in available literature. In an attempt to fill this gap, and considering their structural likeness to curcumin, dienones were selected as the second class of curcumin-related compounds for synthesis in this study.

3.4.3 3'-azido-2',3'-dideoxythymidine, AZT (Zidovudine®)

AZT (Figure 3.5) is a nucleoside reverse-transcriptase inhibitor (NRTI), and was the first antiretroviral agent to be approved for use in HIV infection [31]. The rationale for the selection of AZT as an entity for hybridization was that it is relatively hydrophilic [32], and hybridization to chalcones or dienones could yield hybrid compounds with enhanced hydrophilicity (relative to the chalcone or dienone parent compounds), a factor that could enhance their *in vitro* and *in vivo* antimalarial activity, as well as their oral bioavailability. In addition, AZT is a nucleoside (deoxythymidine) analogue; nucleosides are biological molecules that are known to be actively transported into mammalian cells [33], and therefore linking AZT to the chalcones or dienones could potentially take advantage of this trans-membrane transport mechanism to further improve the oral bioavailability of the target molecules, as well as facilitate their delivery to their intracellular site of action.

It is acknowledged that AZT too has its oral bioavailability challenges arising from poor absorption, enzymatic transformation within the intestinal cells and significant first-pass effect. However, hybridization to chalcones/dienones (which may be considered to be at the other end of the physicochemical spectrum) could yield more balanced hybrid compounds that could potentially exhibit improved bioavailability profiles.

Furthermore, hybridization of the potentially antimalarial chalcones and dienones to a molecule with intrinsic anti-HIV activity could very well lead to the identification of molecules that exhibit both antimalarial and anti-HIV activity. This is particularly interesting considering that in sub- Saharan Africa, the high burden of both malaria and

HIV translates into high incidences of co-infection in many regions [34]. This overlap in the distribution of HIV and malaria also occurs in other regions of the world, such as Southeast Asia, Latin America and the Caribbean [35].

Finally, AZT bears an azide functionality that could be conveniently exploited in its hybridization to other entities *via* click chemistry.

3.4.4 7-Chloroquinoline

Several potent, quinoline-based antimalarial drugs have been used clinically for decades e.g. chloroquine and amodiaquine. The 7-chloroquinoline moiety, a main antimalarial pharmacophore present in this class of antimalarials, is thought to confer antimalarial potency to these compounds by facilitating binding to heme and consequently inhibiting hemozoin formation [36]. This study therefore aimed at exploiting this feature by incorporating the 7-chloroquinoline moiety into hybrid molecules with chalcones and dienones.

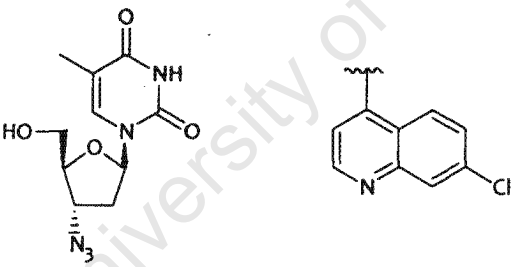

AZT (3.4) 7-chloro-quinoline (4-substituted)

Figure 3.5: Structures of AZT (3.4) and 4-substituted-7-chloro-quinoline.

3.5 Chalcones

3.5.1 Selection of Chalcones for synthesis and hybridization

There were two main considerations in the selection of the chalcones to be synthesized:

- The rational selection of the substitution patterns for the two phenyl rings of the chalcones;
- The convenient introduction of the terminal alkyne in readiness for subsequent hybridization.

The selection of the chalcones for synthesis was guided by, firstly, the substitution pattern on curcumin (which bears the 4-hydroxy-3-methoxy substitution pattern on both phenyl rings, Figure 2.11) and, secondly, by the reported SAR results of two extensive studies on hydroxylated and alkoxylated chalcones by Glutteridge *et al.* 2006 [29] and Liu *et al.* 2001 [30] (section 2.9.1.2).

Based on these, and coupled with the range of starting materials (acetophenones and benzaldehydes) readily available to us, a small series of alkoxylated and halogenated chalcones was selected for synthesis. The approach used was to vary the substitutions on one of the rings (as shown in Table 3.1) while maintaining the 4-hydroxy-3-methoxy substitution pattern (derived from curcumin) on the opposite ring, i.e. varying the substituents on ring A while retaining the 4-hydroxy-3-methoxy substitution on ring B, and vice versa. The hydroxy group would then allow for the convenient introduction of the terminal acetylene group *via* a simple alkylation reaction as shown in Scheme 3.2, thereby yielding acetylenic chalcones ready for the anticipated hybridization to the appropriate azide-bearing entities.

Table 3.1: Table showing the selected substitutions to be applied in chalcone synthesis

Ring A substitutions	Ring B substitutions
2,4-dimethoxy	4'-methoxy
2,3,4-trimethoxy	2',4'-dimethoxy
2,4-dichloro	2',3',4'-trimethoxy
4-flouro	
2,4-difluoro	

In order to maintain the 4-hydroxy-3-methoxy substitutions on ring A, 4-hydroxy-3-methoxy benzaldehyde (vanillin, 3.5) was condensed with the appropriate acetophenones; for similar substitution on ring B, 1-(4-Hydroxy-3-methoxy-phenyl)-ethanone (acetovanillone, 3.6) was condensed with the selected benzaldehydes.

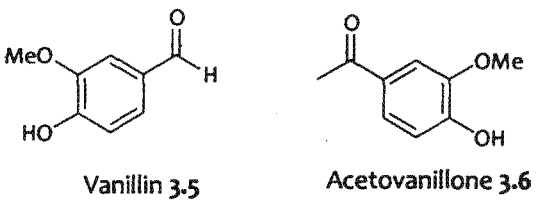

Vanillin 3.5 Acetovanillone 3.6

Figure 3.6: Structures of vanillin 3.5 and acetovanillone 3.6.

The selection of the chalcones for synthesis was guided by, firstly, the substitution pattern on curcumin (which bears the 4-hydroxy-3-methoxy substitution pattern on both phenyl rings, Figure 2.11) and, secondly, by the reported SAR results of two extensive studies on hydroxylated and alkoxylated chalcones by Glutteridge *et al.* 2006 [29] and Liu *et al.* 2001 [30] (section 2.9.1.2).

Based on these, and coupled with the range of starting materials (acetophenones and benzaldehydes) readily available to us, a small series of alkoxylated and halogenated chalcones was selected for synthesis. The approach used was to vary the substitutions on one of the rings (as shown in Table 3.1) while maintaining the 4-hydroxy-3-methoxy substitution pattern (derived from curcumin) on the opposite ring, i.e. varying the substituents on ring A while retaining the 4-hydroxy-3-methoxy substitution on ring B, and vice versa. The hydroxy group would then allow for the convenient introduction of the terminal acetylene group *via* a simple alkylation reaction as shown in Scheme 3.2, thereby yielding acetylenic chalcones ready for the anticipated hybridization to the appropriate azide-bearing entities.

Table 3.1: Table showing the selected substitutions to be applied in chalcone synthesis

Ring A substitutions	Ring B substitutions
2,4-dimethoxy	4'-methoxy
2,3,4-trimethoxy	2',4'-dimethoxy
2,4-dichloro	2',3',4'-trimethoxy
4-flouro	
2,4-difluoro	

In order to maintain the 4-hydroxy-3-methoxy substitutions on ring A, 4-hydroxy-3-methoxy benzaldehyde (vanillin, 3.5) was condensed with the appropriate acetophenones; for similar substitution on ring B, 1-(4-Hydroxy-3-methoxy-phenyl)-ethanone (acetovanillone, 3.6) was condensed with the selected benzaldehydes.

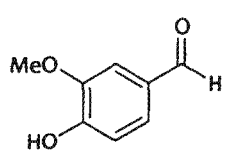

Vanillin 3.5

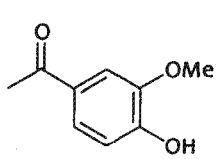

Acetovanillone 3.6

Figure 3.6: Structures of vanillin 3.5 and acetovanillone 3.6.

3.5.2 Synthesis of Chalcones

Chalcones are typically synthesized by the Claisen-Schmidt condensation of appropriately substituted benzaldehydes and acetophenones [9,29,30,37]. In general, this reaction involves the acid or base-catalyzed condensation of two different carbonyl compounds, one acting as the nucleophile in its enol or enolate form, and the other acting as the electrophile. It therefore requires that one of the carbonyl compounds be capable of enolization, while the other carbonyl compound be incapable of enolizing and be more electrophilic than the enolizable partner [9].

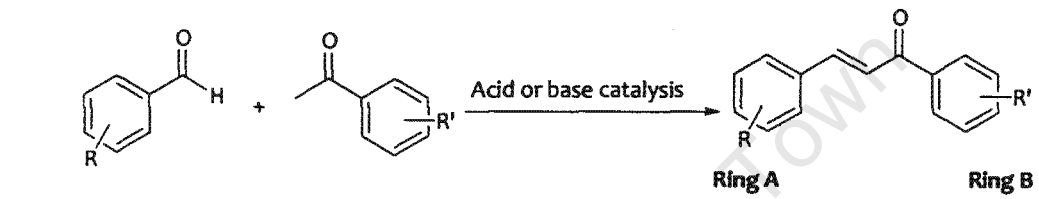

Scheme 3.1: General scheme showing the synthesis of chalcones

In the case of the synthesis of chalcones, the acetophenone is the enolizable carbonyl compound, while the benzaldehyde is the more electrophilic, non-enolizable carbonyl compound. The mechanism for this reaction is outlined in Figure 3.7.

In acidic conditions, the reaction begins with the acid-mediated keto-enol tautomerization of the enolizable acetophenone, resulting in the formation of the neutral enol I. The enol then attacks the electrophilic carbonyl carbon of the benzaldehyde (made more electrophilic by the protonation of the adjacent oxygen) to form the aldol intermediate II. Due to steric and electronic factors, ketones are less reactive than aldehydes, and the enol attacks the benzaldehyde preferentially to any un-enolized acetophenone that may be present. The aldol intermediate then dehydrates *via* the E2 mechanism to yield the more stable α,β-unsaturated system of the final chalcone III, while regenerating the acid catalyst [9].

In basic conditions, the reaction begins with the base abstracting the acidic α-proton of the acetophenone, forming the enolate IV; the benzaldehyde lacks any α-protons, and hence lacks the ability to enolize. The resulting enolate then preferentially attacks the benzaldehyde to form the aldol intermediate V. The resulting aldol then dehydrates

via the E1cB mechanism to yield the α,β-unsaturated system of the final chalcone product VI, while regenerating the base catalyst [9].

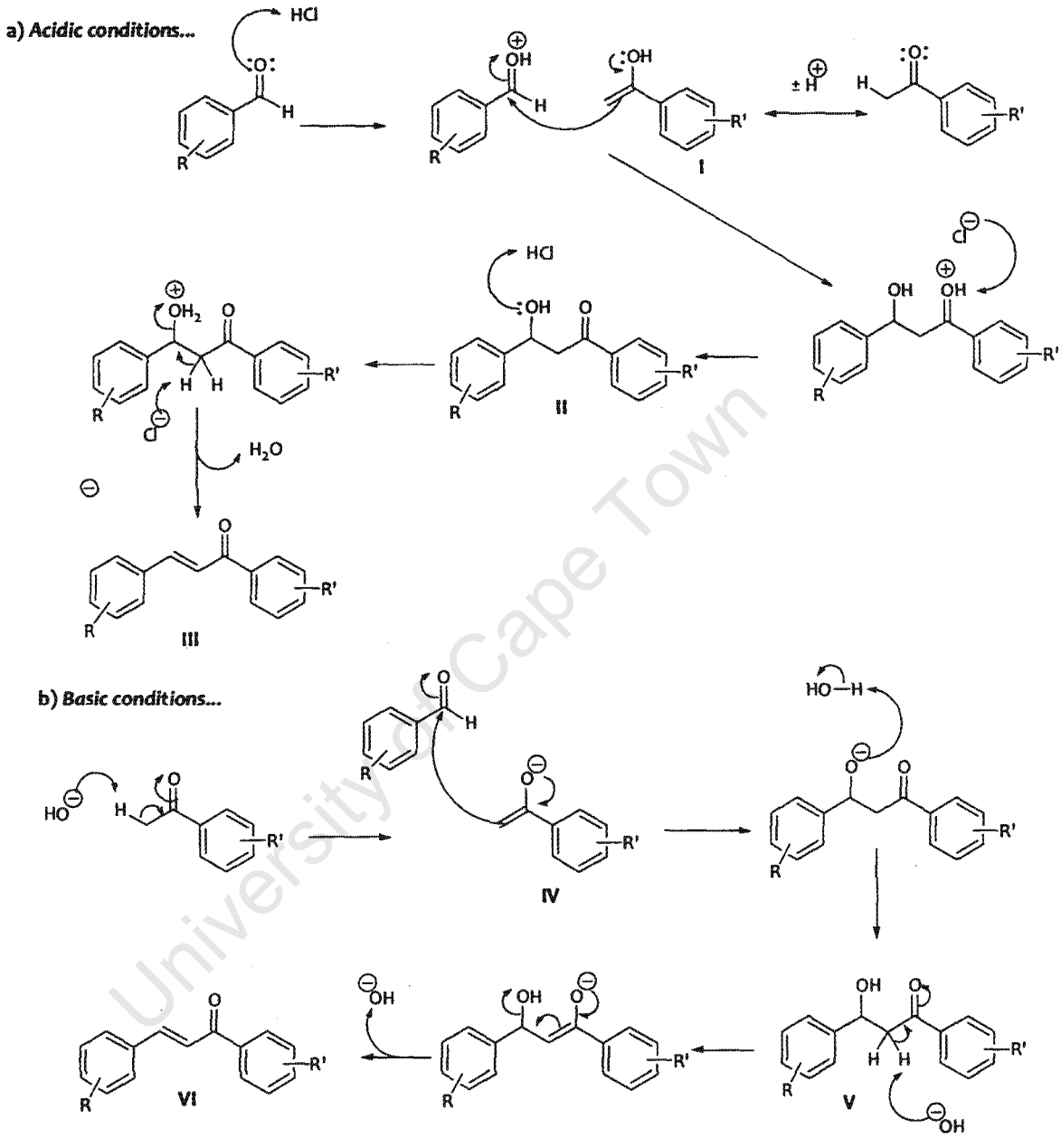

Figure 3.7: Schematic diagram showing the mechanism for the synthesis of chalcones under a) acid, and b) base-catalyzed, conditions [9].

By far the most popular method of chalcone synthesis is the base-catalyzed condensation [37], probably because of the associated shorter reaction times and the relatively higher yields. However, it has been reported that, in the synthesis of hydroxylated chalcones, protection of any *para*-hydroxyl groups (such as the ones on 3.5 and 3.6) prior to the base-catalyzed condensation is necessary for improved yields [30]. This is probably due to the dissociation of the acidic phenolic proton in the basic

reaction medium – the proton's inherent acidic nature (being a phenolic proton) is further enhanced by the presence of the *para* carbonyl substituent (aldehyde or ketone), which is electron withdrawing and attracts *ortho* and *para* electrons [38]. The resulting negative charge of the phenoxide would then be delocalised into the ring and the electron-withdrawing carbonyl system, as shown by the two extreme resonance structures below.

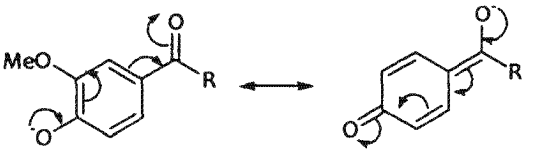

R=H: benzaldehyde
R=CH_3: acetophenone

Figure 3.8: Resonance structures of deprotonated 4-hydroxylated benzaldehyde and/or acetophenone.

The result of this would be, for the benzaldehyde, decreased electrophilicity of the carbonyl carbon and, for the acetophenone, decreased acidity of the α-protons necessary for abstraction by the base during enolization. This, coupled with the fact that some of the base required for the catalysis of the aldol reaction will have been consumed in deprotonating the phenolic hydroxyl group, probably explains the low yields observed during base-catalyzed chalcone synthesis from un-protected hydroxylated benzaldehydes and/or acetophenones. This problem is avoided either by the use of acid catalysis [39], or by protection of the *para*-hydroxy group prior to the base catalyzed condensation. This protection is generally as tetrahydropyranyl (THP), methoxymethyl (MOM), or methoxyethoxymethyl (MEM) ethers [30,40].

For this study, this potential problem was avoided by the O-alkylation of the phenolic hydroxyl groups of the vanillin 3.5 and acetovanillone 3.6 prior to the base-catalyzed Claisen-Schmidt condensation reaction (Scheme 3.2). As it was intended to further derivatize these chalcones by "ligation" of an azide and a terminal alkyne *via* click chemistry, this O-alkylation involved replacing the phenolic proton with a 2-propynyl chain; this effectively eliminated the acidic phenolic proton, and at the same time introduced the terminal alkyne necessary for the click chemistry to follow.

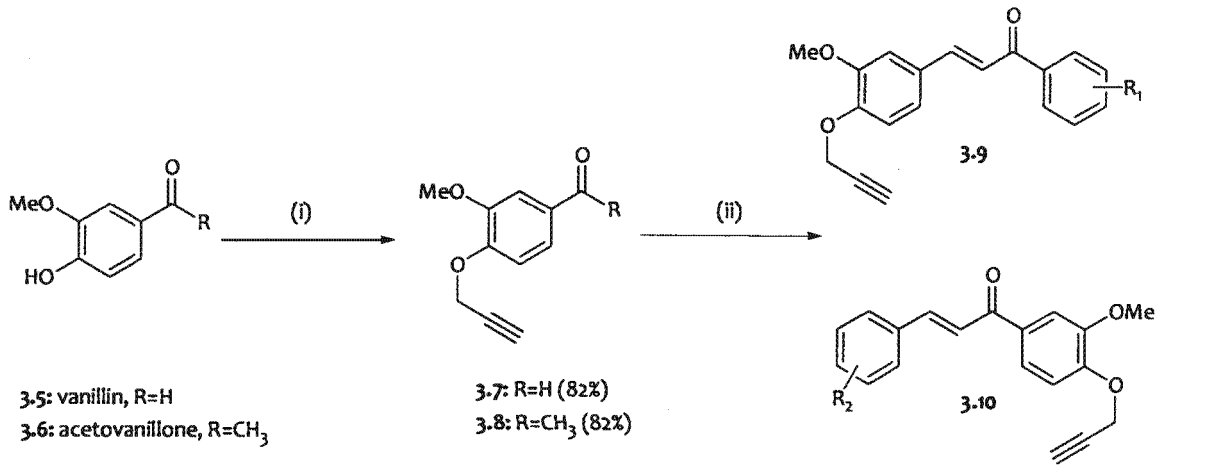

Scheme 3.2: *Reagents and conditions:* (i) propargyl bromide, K_2CO_3, DMF, 30 °C, 18hrs; (ii) appropriate acetophenones (for 3.7) or benzaldehydes (for 3.8), 2.5M NaOH, MeOH, 70 °C, 3-6 hrs.

The synthesis of the targeted acetylenic chalcones 3.9 and 3.10 was therefore a two-step procedure as shown in Scheme 3.2. The first step was the alkylation reaction, involving the reaction of 3.5 or 3.6 with 1.5 eq of propargyl bromide in anhydrous DMF and in the presence of 1.5 eq of anhydrous K_2CO_3. This reaction yielded the respective acetylenes 3.7 and 3.8 in good yield after purification by recrystallization from DCM/Hexane mixtures. The second step was the Claisen-Schmidt condensation of 3.7 and 3.8 with the appropriately substituted benzaldehydes and acetophenones. The method reported by Liu *et al.* 2001 [30] was modified for this purpose, and involved the reaction of 3.7 and 3.8 with an equimolar amount of the appropriate benzaldehyde/acetophenone in methanol, in the presence of aqueous NaOH as catalyst. The products were then purified by silica gel column chromatography to furnish the pure target acetylenic chalcones 3.9 and 3.10 in good yields, as shown in Table 3.2.

Table 3.2: Yields of acetylenic chalcones 3.9 and 3.10.

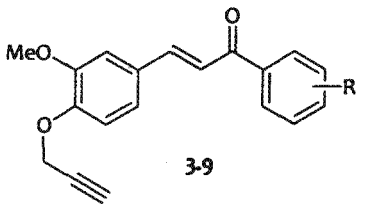

3-9

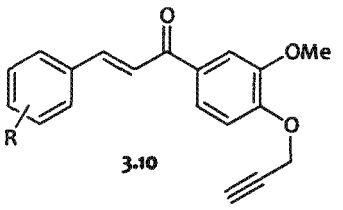

3-10

Compound code	R	Yield (%)
3.9a	4'-OMe	76
3.9b	2',4'-diOMe	90
3.9c	2',3',4'-triOMe	84
3.10a	2,4-diOMe	89
3.10b	2,3,4-triOMe	78
3.10c	2,4-diCl	79
3.10d	4-F	88
3.10e	2,4-diF	85

3.6 Dienones

3.6.1 Selection of dienones for synthesis and hybridization

The dienones selected for synthesis were to bear similar substitution patterns to the acetylenic chalcones described previously. This would enable a direct SAR comparison of the *in vitro* (and possibly *in vivo*) activities of similarly substituted chalcones and dienones, where the only difference between the pairs of compounds compared would be the length of the chain linking the two aromatic rings.

3.6.2 Synthesis of dienones

The retrosynthetic analysis of the target acetylenic dienones, outlined in Scheme 3.3, shows that these compounds could be generally synthesized by sequential condensation, i.e. the condensation of 3.7 and acetone to yield the acetylenic enone 3.11, which would then be condensed with various appropriately substituted benzaldehydes to yield the target acetylenic dienones 3.12.

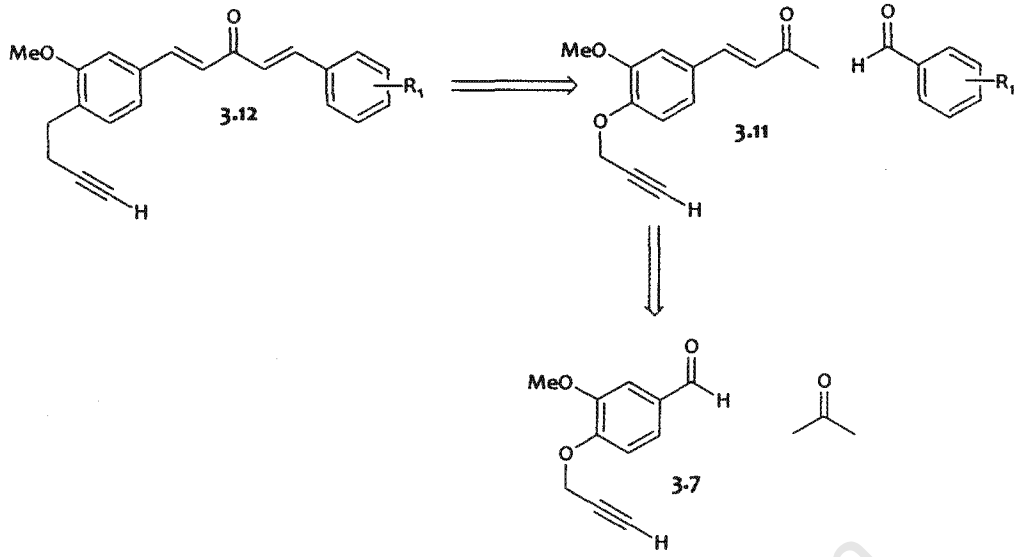

Scheme 3.3: Retrosynthetic analysis of dienones

The condensation of acetone, itself an enolizable carbonyl compound, to 3.7 is quite similar to that carried out in the synthesis of chalcones, and was carried out using the (modified) method reported by Ramachandra and Subbaraju, 2006 [41]. Intermediate 3.7 was stirred in acetone (as reagent and solvent) in the presence of aqueous 2.5M NaOH at room temperature for 6 hours. The crude product of the reaction was purified by silica column chromatography to yield 3.11 in 71% yield.

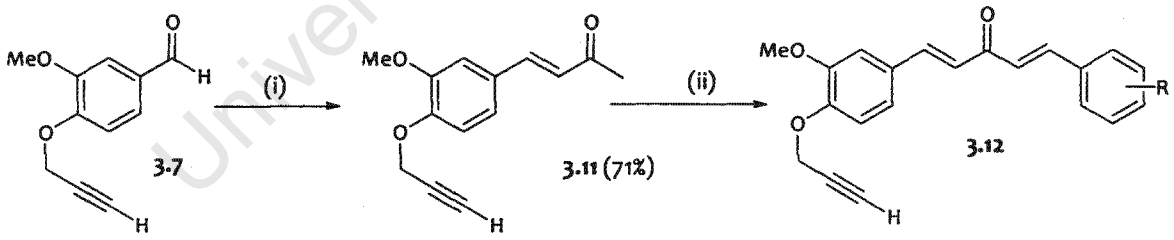

R = 4-methoxy, 2,4-dimethoxy, 2,3,4-trimethoxy, 2,4-dichloro, 4-fluoro. 2,4-difluoro

Scheme 3.4: *Reagents and conditions:* (i) acetone, 2.5M NaOH, r.t., 6 hrs; (ii) appropriate benzaldehydes, BF_3-Et_2O, dioxane, 50 °C, 16 hrs.

It had been envisaged that the second set of condensation reactions (of the enone intermediate 3.11 and the appropriately substituted benzaldehydes) would be carried out under similar conditions. However, when this was attempted, the reaction yielded an un-resolvable mixture of products, possibly due to competing side reactions such as the Cannizzaro reaction [9].

However, this condensation was successfully carried out by applying a method reported for the synthesis of chalcones and which makes use of boron-trifluoride etherate (BF_3-Et_2O) as a Lewis-acid catalyst [42]. The reaction conditions are shown in Scheme 3.4, and involved the reaction of **3.11** with 1.1 eq of the appropriate benzaldehyde in the presence of 1.5 eq BF_3-Et_2O; the reaction was carried out in anhydrous dioxane under a nitrogen atmosphere. The crude products were purified by silica gel column chromatography (EtOAc/Hexane) to yield the target acetylenic dienone products. The respective yields are given in Table 3.3.

The reasons for the relatively low yields for this final step of the dienone synthesis are unclear. However, during the purification of these compounds by silica column chromatography (necessary to separate the target molecule from the residual benzaldehyde starting material that was used in a slight excess), a significant amount of baseline material was observed, suggesting the possibility of the formation of complexes and other decomposition products during the course of the reaction.

The proposed mechanism for this reaction is outlined in Figure 3.9. The Lewis acid, boron trifluoride, coordinates to the carbonyl oxygen of the benzaldehyde to form I, thereby increasing the electron-withdrawing effect of this oxygen; this in turn increases the electrophilicity of the adjacent carbonyl carbon, making it even more susceptible to nucleophilic attack by the enol tautomeric form of **3.11**. The result is the intermediate II, equivalent to the aldol intermediates described in Fig. 3.7 above. During the aqueous work-up of this reaction, this intermediate undergoes the equivalent of a dehydration reaction to yield the target dienone **3.12**.

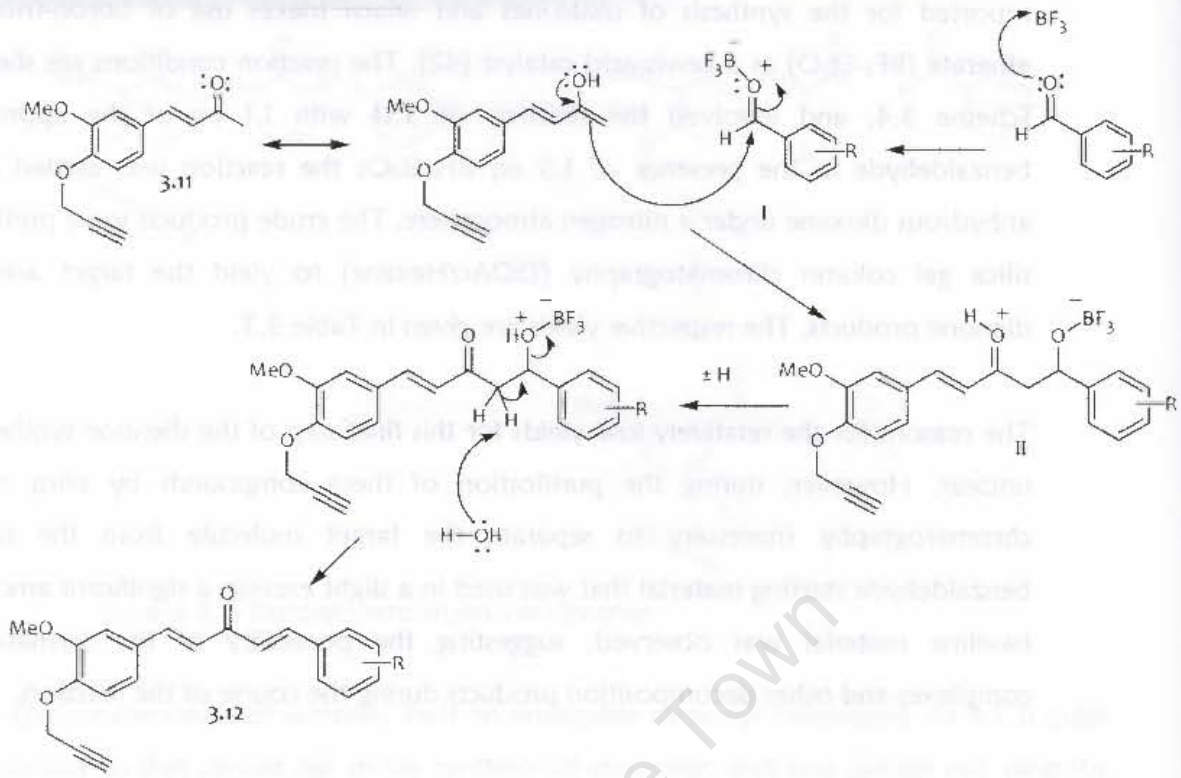

Figure 3.9: Proposed mechanism of the condensation of the enone intermediate and a benzaldehyde.

Table 3.3: Yields of acetylenic dienones 3.12

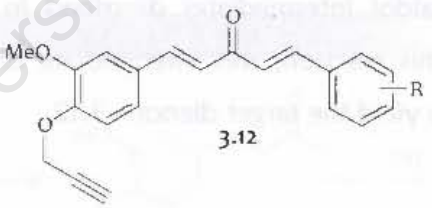

Compound code	R	Yield (%)
3.12a	4'-OMe	39
3.12b	2',4'-diOMe	49
3.12c	2',3',4'-triOMe	47
3.12d	2,4-diCl	65
3.12e	4-F	45
3.12f	2,4-diF	43

3.7 Synthesis of the 4-azido-7-chloro-quinoline

Whereas AZT already bears the azide group and is, as it were, ready for "clicking", the 4-azido-7-chloro-quinoline 3.13 was furnished by applying the method described by de Souza *et al.* 2009 [43], whereby 4,7-dichloroquinoline was reacted with 2 eq of NaN_3 in anhydrous DMF at 65 °C for 6 hours. Crystallization of the product from DCM/hexane mixtures afforded 3.13 in 86% yield (Scheme 3.5).

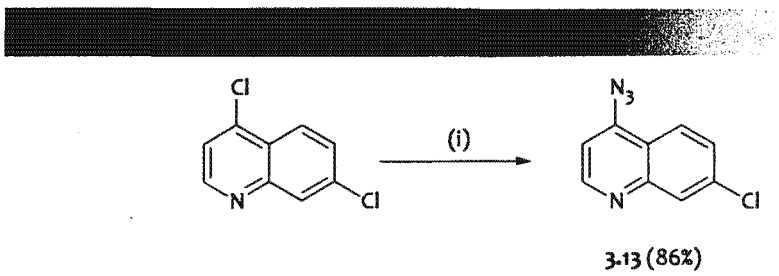

3.13 (86%)

Scheme 3.5: *Reagents and conditions:* (i) NaN_3, DMF, 65 °C, 6 hrs.

3.8 Synthesis of the Triazoles

As outlined in section 3.5 above, the primary synthetic aim was to apply the Cu(I)-catalyzed cycloaddition reaction of azides (AZT 3.4 and 4-azido-7-chloroquinoline 3.13) and alkynes (the acetylenic chalcones 3.9 and dienones 3.12) to yield the target triazolyl chalcone/AZT, chalcone/chloroquinoline, dienone/AZT and dienone/chloroquinoline hybrid compounds. The Cu(I) required for catalysis would be generated by the *in situ* reduction of Cu(II) to Cu(I) by sodium ascorbate.

With the entities for hybridization already synthesized as described above (AZT was kindly provided by Cipla Ltd.), the cycloaddition reaction was then carried out using the (modified) procedure reported by Feldman *et al.* 2004 [17]. Equimolar amounts of the relevant azide and acetylenic compound were dissolved in DMF, after which 1 M sodium ascorbate (0.4 eq) and 1 M $CuSO_4$ (20 mol%) were added sequentially, in that order. The reaction mixture was then stirred vigorously at 65° C for 24 hrs. Purification was by silica gel column chromatography.

The chalcone hybrid compounds 3.14 – 3.17 were synthesized by the reaction of the acetylenic chalcones 3.9 and 3.10 with either 3.4 or 3.13 using the procedure described above.

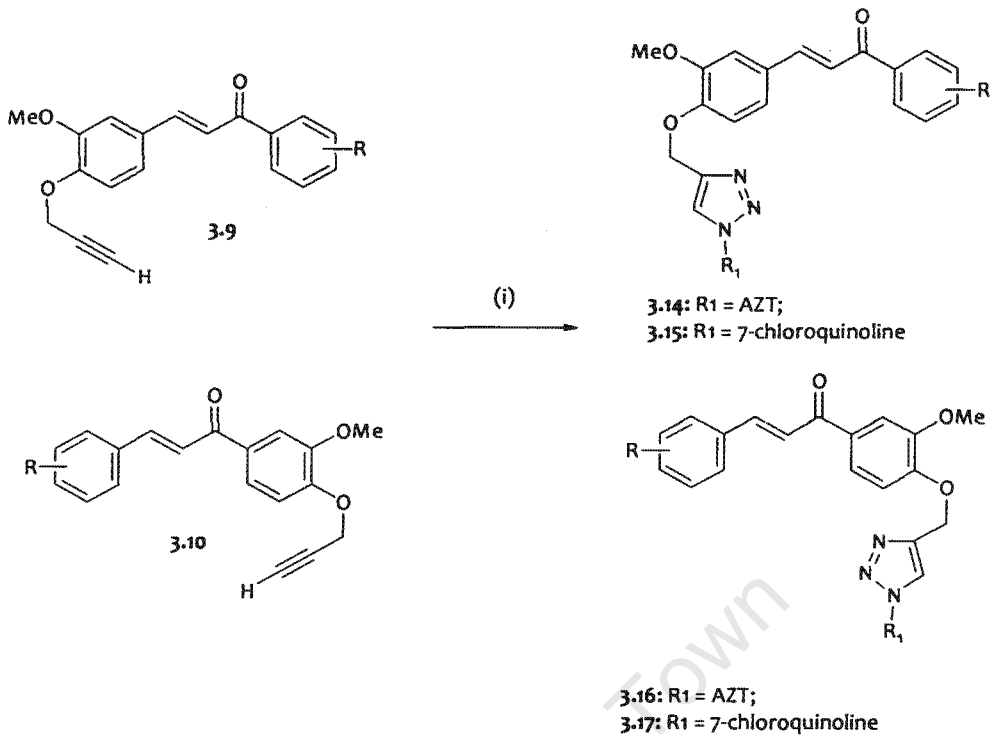

Scheme 3.6: *Reagents and conditions:* (i) 3.4 or 3.13, 1M Na ascorbate, 1M $CuSO_4.5H_2O$, DMF, 65 °C, 24hrs.

However, the synthesis of the target dienone hybrid compounds was approached in a slightly different way (Scheme 3.7); these were synthesized by initially reacting acetylenic enone intermediate 3.11 with either 3.4 or 3.13 to generate the enone-triazole derivatives 3.18 and 3.19, and then subsequently condensing these intermediates with the appropriate benzaldehydes using boron-trifluoride etherate as catalyst as already described above to yield the target hybrid dienone derivatives 3.20 and 3.21.

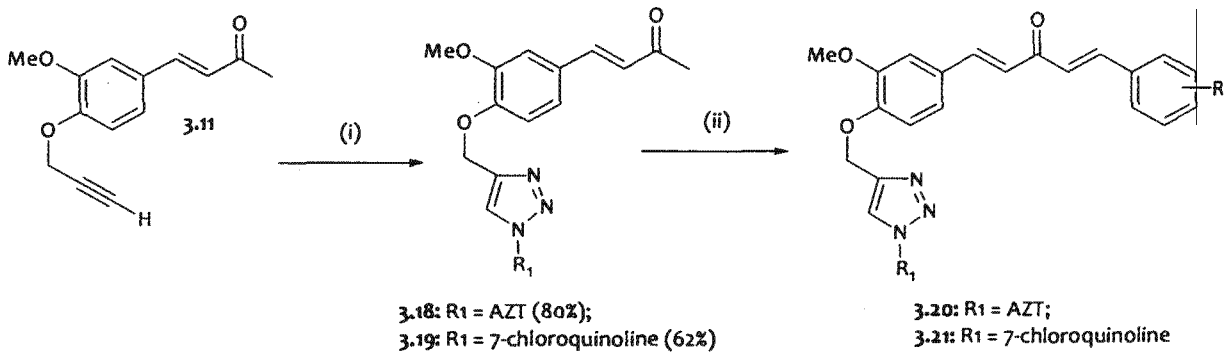

Scheme 3.7: *Reagents and conditions:* (i) 3.4 or 3.13, 1M Na ascorbate, 1M $CuSO_4.5H_2O$, DMF, 65 °C, 24hrs; (ii) appropriate benzaldehydes, BF_3-Et_2O, dioxane, 50 °C, 16 hrs.

The yields of the chalcones and dienone hybrid compounds are tabulated below. The relatively low yields observed for the chalcone click reactions was probably the direct consequence of difficulties in isolating and purifying the target compounds. The crude product of the reaction (precipitated out of the reaction mixture by the gradual addition of cold water) was particularly difficult to manipulate, and showed a limited solubility in common organic solvents; this then led to product losses during purification by column chromatography. Attempts at purification by crystallization were unsuccessful.

However, sufficient amounts of the target compounds were isolated for *in vitro* antimalarial assays, and for this reason no attempts were made at this stage to optimize the reaction conditions and isolation methods.

Table 3.4: Yields of chalcones hybrid compounds **3.14** - **3.17**

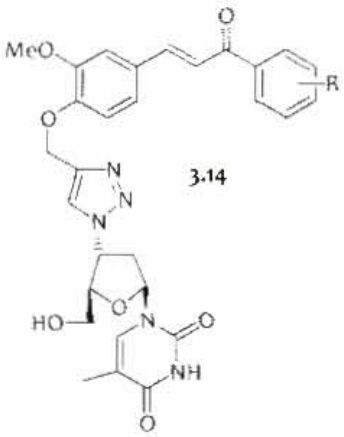

3.14

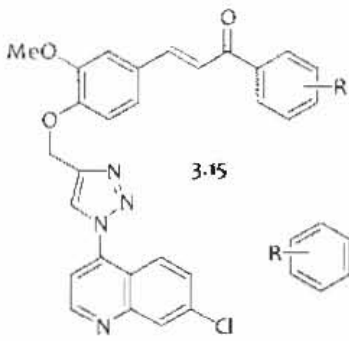

3.15

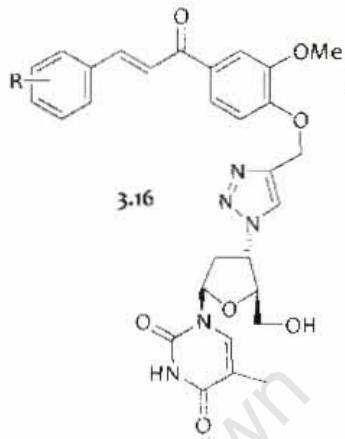

3.16

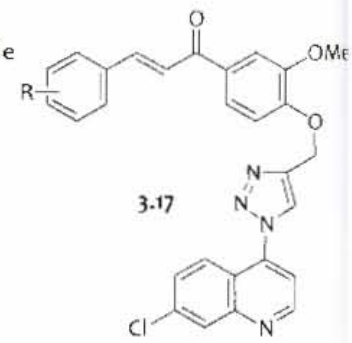

3.17

Compound code	R	Yield (%)
3.14a	4'-OMe	50
3.14b	2',4'-diOMe	47
3.14c	2',3',4'-triOMe	46
3.15a	4'-OMe	58
3.15b	2',4'-diOMe	51
3.15c	2',3',4'-triOMe	54
3.16a	2,4-diOMe	44
3.16b	2,3,4-triOMe	51
3.16c	2,4-diCl	45
3.16d	4-F	48
3.16e	2,4-diF	44
3.17a	2,4-diOMe	41
3.17b	2,3,4-triOMe	54
3.17c	2,4-diCl	52
3.17d	4-F	52
3.17e	2,4-diF	38

Table 3.5: Yields of dienone hybrid compounds 3.20 - 3.21

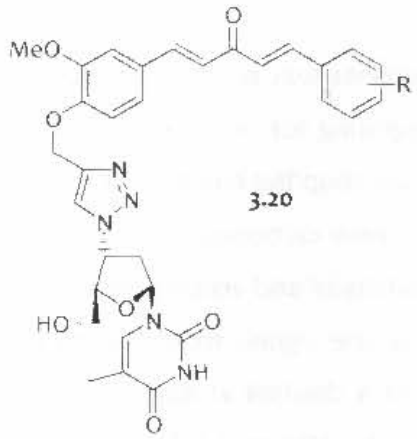

3.20

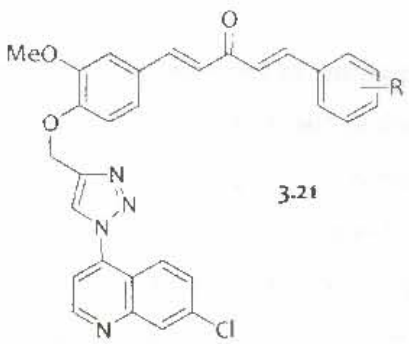

3.21

Compound code	R	Yield (%)
3.20a	4'-OMe	42
3.20b	2',4'-diOMe	52
3. 20c	2',3',4'-triOMe	40
3. 20d	2,4-diCl	58
3. 20e	4-F	32
3. 20f	2,4-diF	31
3. 21a	4'-OMe	36
3. 21b	2',4'-diOMe	33
3. 21c	2',3',4'-triOMe	33
3. 21d	2,4-diCl	42
3. 21e	4-F	38
3. 21f	2,4-diF	31

3.9 Characterization of the Target Compounds

All compounds were characterized by ^{1}H-NMR, ^{13}C-NMR, Mass Spectrometry, IR Spectroscopy, Elemental analysis and melting point determination.

However, in this section the focus will be on ^{1}H-NMR, with particular attention being paid to signal peaks that were diagnostic for each set of target compounds. The full characterization data for each of the synthesized compounds is reported in the Experimental chapter (Chapter 8).

3.9.1 Acetylenic chalcones

Confirmation of the formation of the chalcones was by the presence of two distinct doublets in the ^{1}H-NMR spectra, each integrating for one proton, lying in the region between δ 7 – 8 ppm, and sharing a ^3J-*trans* coupling constant of between 15-16 Hz. These signals confirm the formation of the new carbon-carbon double bond (with a *trans* geometry) between the parent benzaldehyde and acetophenone. Also distinct on the spectra of the acetylenic chalcones are the signals from the terminal acetylene group: a triplet at approximately δ 2.5 and a doublet at approximately δ 4.8, both sharing an allylic ^4J coupling constant of 2 - 3 Hz (**Figure 3.10**).

The aromatic signals from the different chalcones varied depending on the differing substitution patterns of the two aromatic rings. The full spectroscopic characterization of these compounds compared well with literature reports [30].

3.9.2 Acetylenic dienones

Confirmation of the dienones was by the presence of two pairs of distinct doublets similar to those observed for the chalcones – they occur as two pairs simply because the dienones possess two α-β unsaturated carbonyl systems (sharing the same carbonyl group). The signals from the terminal acetylene group – the triplet and the doublet – were also present on the spectra of the acetylenic dienones. (**Figure 3.11**)

3.9.3 Triazole hybrid compounds

Empirical analysis of the ^{1}H-NMR to confirm presence of the triazole products was by noting:

- The presence of signals attributable to the two parent entities;
- The absence of the triplet at about δ 2.5 ppm and integrating for one proton that corresponded to the terminal acetylenic proton of the parent acetylenic entities;
- The appearance of a singlet integrating for one proton appearing at about δ 8.1 ppm, attributed to the single proton on the triazole ring;
- The signal at approximately δ 5.5 ppm and integrating for two protons corresponding to the two methylene protons on the carbon adjacent to the triazole ring (and initially on the 2-propynyl side chain of the chalcone). The signal is now a singlet due to the absence of the terminal acetylenic proton that these protons were coupling with. (**Figure 3.12**)

3.10 Conclusion

The concepts of molecular hybridization and click chemistry were introduced and discussed, after which is given a description of how they were applied in the design, synthesis and characterization of chalcone/AZT, chalcone/chloroquinoline, dienone/AZT and dienone/chloroquinoline hybrid compounds as potential antimalarial agents. The target compounds, as well as selected intermediates, were then assayed for *in vitro* antimalarial activity – the results are reported and discussed in the chapter that follows, along with results from limited mechanistic studies.

δ (ppm)	Multiplicity	J (Hz)	H#
7.60	d	15.7	H-a
7.37	d	15.7	H-b
4.79	d	2.4	H-5
2.53	t	2.4	H-6

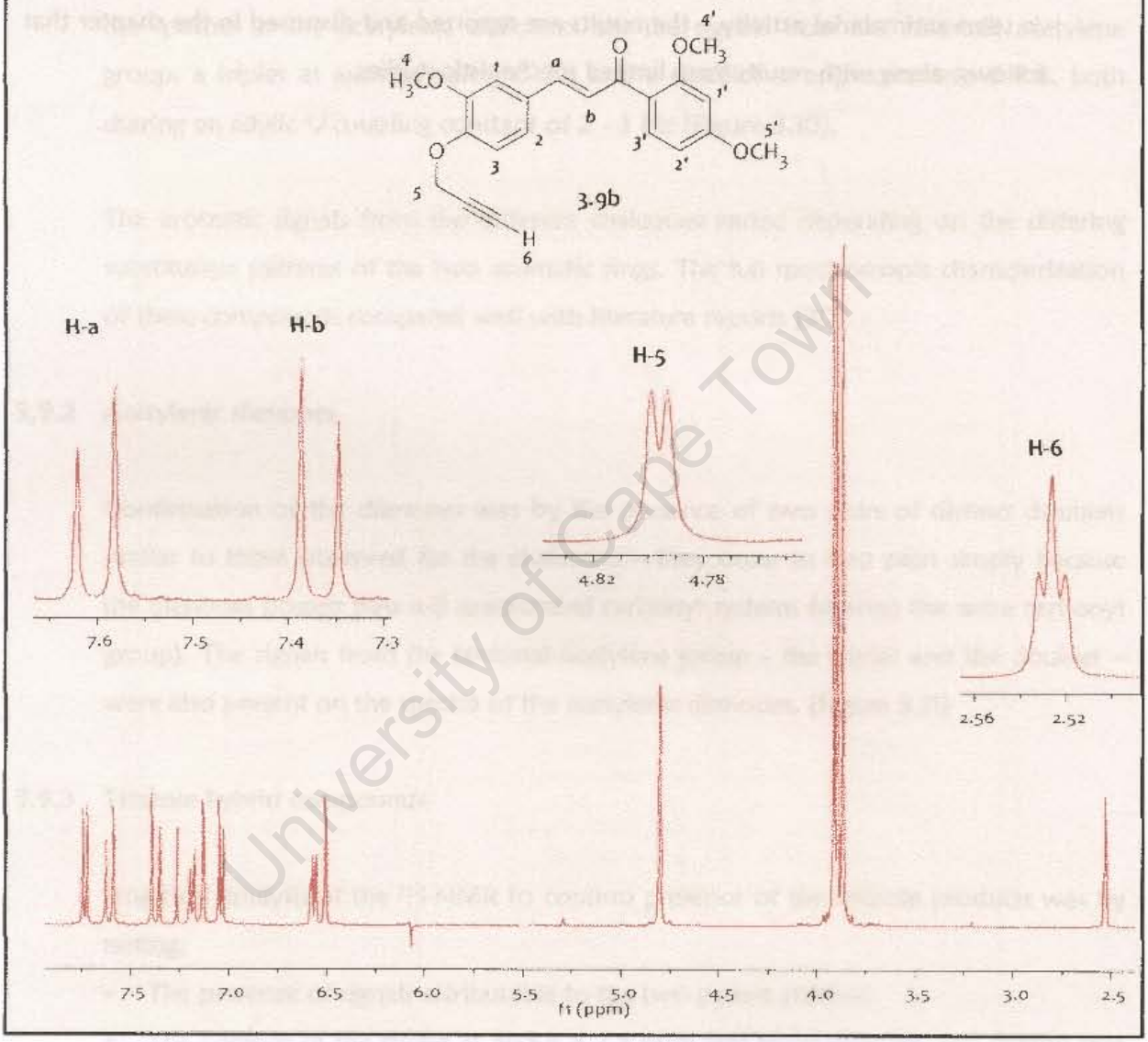

Figure 3.10: Example of an H-NMR spectrum for an acetylenic chalcone.

δ (ppm)	Multiplicity	J (Hz)	H#
7.94	d	16.1	H-a'
7.68	d	15.9	H-a
7.07	d	16.0	H-b'
6.99	d	15.8	H-b
4.82	d	2.4	H-5
2.55	t	2.4	H-6

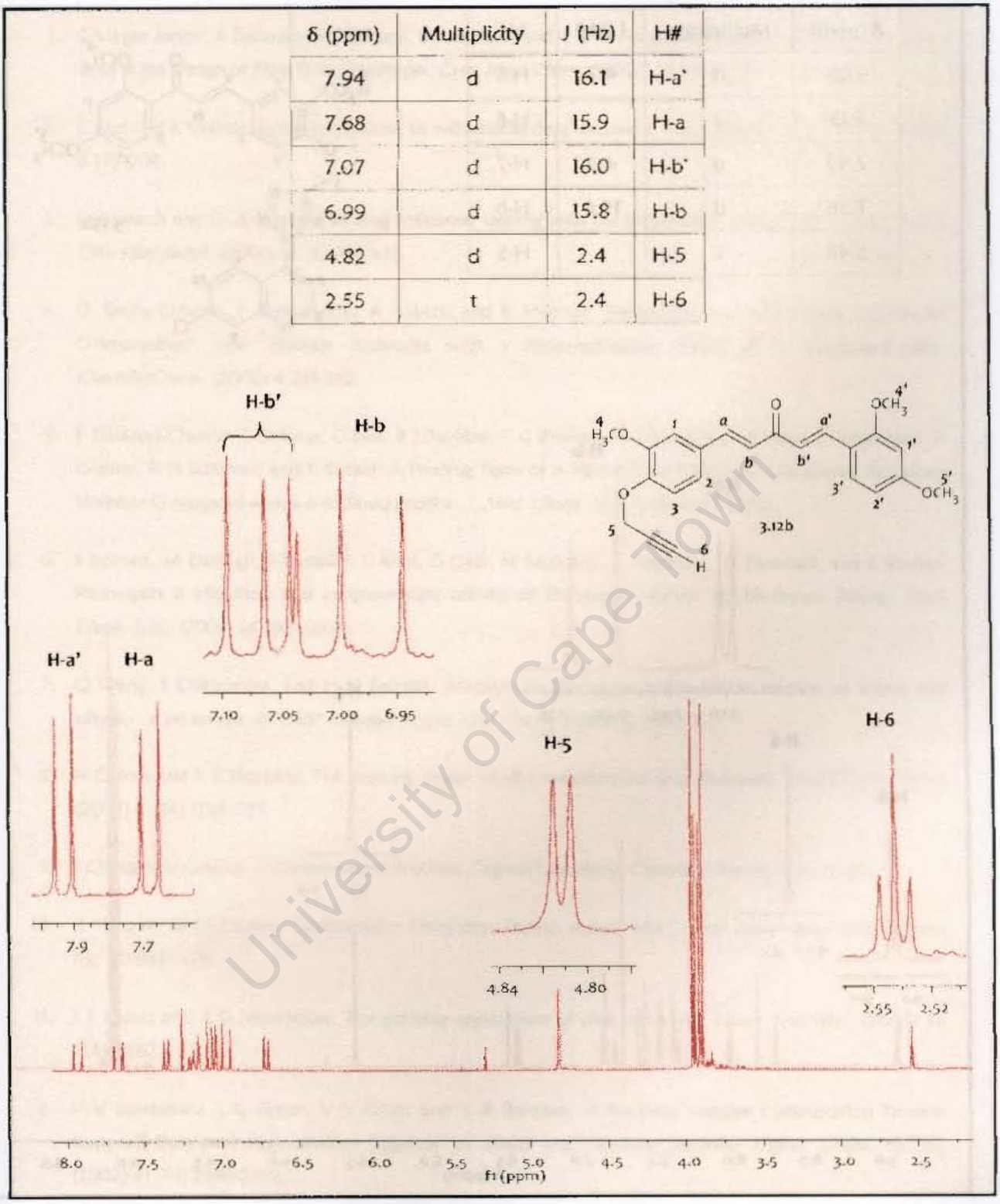

Figure 3.11: Example of an H-NMR spectrum for an acetylenic dienone.

δ (ppm)	Multiplicity	J (Hz)	H#
9.05	d	4.7	H-8
8.13	s	-	H-6
7.49	d	4.6	H-7
7.38	d	15.6	H-b
5.48	s	-	H-5

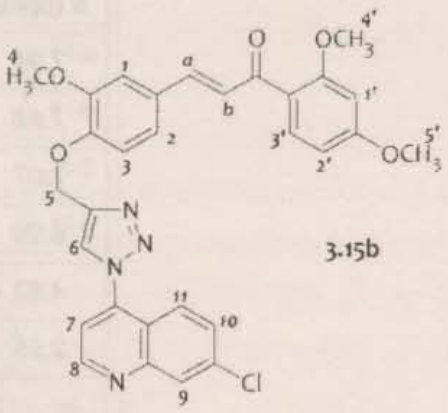

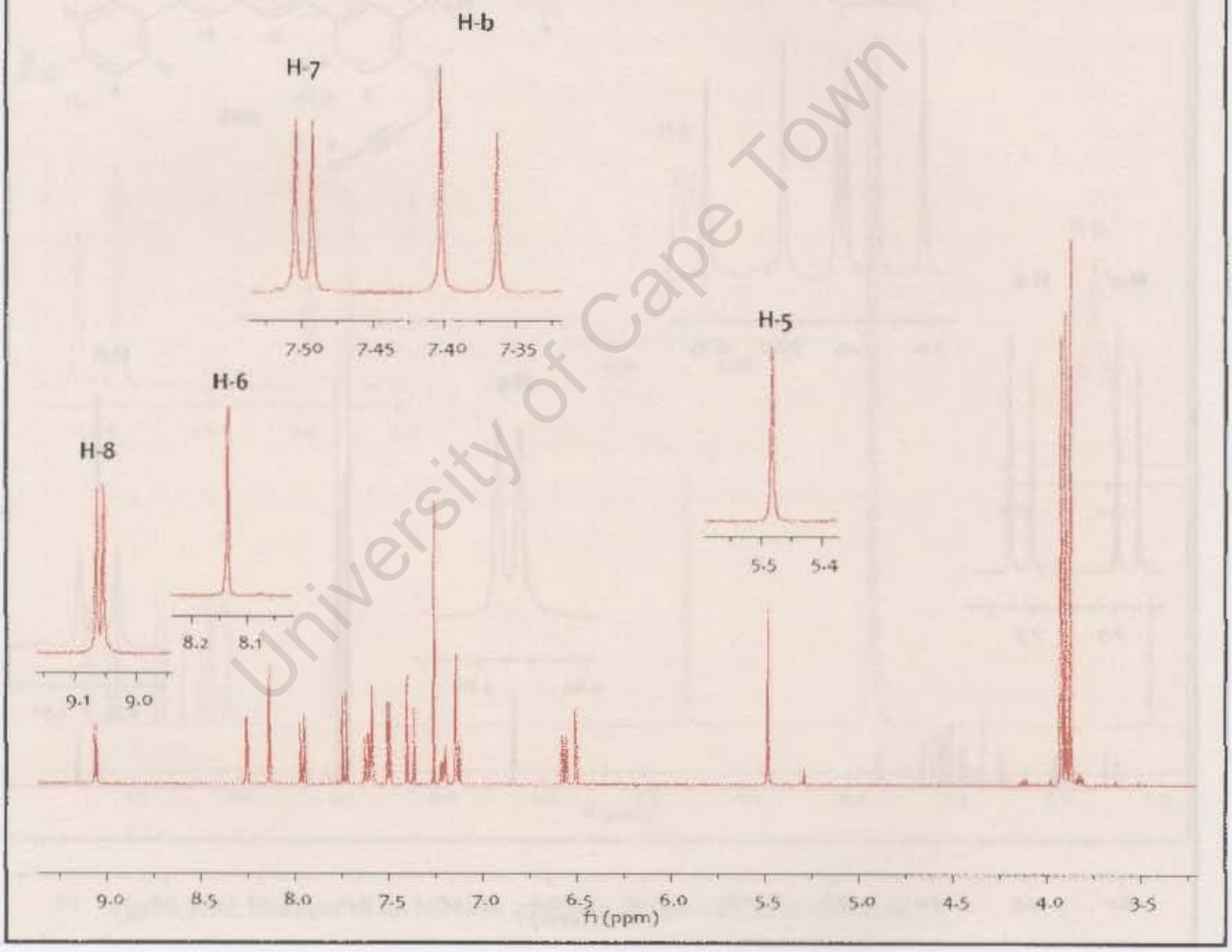

Figure 3.12: Example of an H-NMR spectrum for a quinoline triazole derivative of a chalcone.

References

1. C Viegas Junior, A Danuello, V S Bolzani, E J Barreiro, and C A M Fraga. Molecular Hybridization: A Useful Tool in the Design of New Drug Prototypes. *Curr. Med. Chem.* (2007) 14 1829-1852.

2. C Biot and K Chibale. Novel approaches to antimalarial drug discovery. *Infect. Disord. Drug Targets* (2006) 6 173-204.

3. G Edwards and G. A Biagini. Resisting resistance: dealing with the irrepressible problem of malaria. *Brit. J. Clin. Pharmacol.* (2006) 61 (6) 690-693.

4. O Dechy-Cabaret, F Benoit-Vical, A Robert, and B Meunier. Preparation and antimalarial activities of "Trioxaquines", new modular molecules with a trioxaneskeleton linked to a 4-aminoquinoline. *ChemBioChem.* (2000) 4 281-283.

5. E Davioud-Charvet, S Delarue, C Biot, B Schwöbel, C C Boehme, A Müssigbrodt, L Maes, C Sergheraert, P Grellier, R H Schirmer, and K Becker. A Prodrug Form of a Plasmodium falciparum Glutathione Reductase Inhibitor Conjugated with a 4-Anilinoquinoline. *J. Med. Chem.* (2001) 44 4268-4276.

6. S Romeo, M Dell'Agli, S Parapini, L Rizzi, G Galli, M Mondani, A Sparatore, D Taramelli, and E Bosisio. Plasmepsin II inhibition and antiplasmodial activity of Primaquine–Statine 'double-drugs'. *Bioorg. Med. Chem. Lett.* (2004) 14 2931-2934.

7. Q Wang, S Chittaboina, and H N Barnhill. Advances in 1,3-dipolar cycloaddition reaction of azides and alkynes - a prototype of "Click" Chemistry. *Lett. Org. Chem.* (2005) 2 293-301.

8. H C Kolb and K B Sharpless. The growing impact of click chemistry on drug discovery. *Drug Discov. Today* (2003) 8 (24) 1128-1137.

9. J Clayden, N Greeves, S Warren, and P Wothers. Organic Chemistry. *Oxford University Press* (2001)

10. R Huisgen. *In* 1,3-Dipolar Cycloaddition Chemistry. *Padwa, A.(ed), Vol.1, New York, John Wiley & Sons, Inc.* (1984) 1-176.

11. J E Moses and A D Moorhouse. The growing applications of click chemistry. *Chem. Soc. Rev.* (2007) 36 1249-1262.

12. V V Rostovtsev, L G Green, V V Fokin, and K B Sharpless. A Stepwise Huisgen Cycloaddition Process: Copper(I)-Catalyzed Regioselective "Ligation" of Azides and Terminal Alkynes. *Angew. Chem. Int. Ed.* (2002) 41 (14) 2596-2599.

13. R H Wiley and J Moffat. Preparation and Polymerization of Vinyl Azide. (1957) 22 995-996.

14. G C Patton. Development and applications of click chemistry. *http://chemistry.illinois.edu/research/organic/seminar extracts/2004_2005/08_Patton_Abstract.pdf* (2004)

15. F Himo, T Lovell, R Hilgraf, V V Rostovtsev, L Noodleman, K B Sharpless, and V V Fokin. Copper(I)-catalyzed synthesis of azoles. DFT study predicts unprecedented reactivity and intermediates. *J. Am. Chem. Soc.* (2005) 127 210-216.

16. C W Tornøe, C Christensen, and M Meldal. Peptidotriazoles on Solid Phase: [1,2,3]-Triazoles by Regiospecific Copper(I)-Catalyzed 1,3-Dipolar Cycloadditions of Terminal Alkynes to Azides. *J. Org. Chem.* (2002) 67 3057-3064.

17. A K Feldman, B Colasson, and V V Fokin. One-pot synthesis of 1,4-disubstituted 1,2,3-triazoles from *in situ* generated azides. *Org. Lett.* (2004) 6 (22) 3897-3899.

18. A Ray, K Manoj, M M Bhadbhade, R Mukhoypadhyay, and A.Bhattacharjya. Cu(I)-Catalyzed cycloaddition of constrained azido-alkynes: access to 12- to 17-membered monomeric triazolophanes incorporating furanoside rings. *Tetrahedron Lett.* (2006) 47 2775-2778.

19. B Gerard, J Ryan, A B Beeler, and J A Porco Jr. Synthesis of 1,4,5-trisubstituted-1,2,3-triazoles by coppercatalyzed cycloaddition-coupling of azides and terminal alkynes. *Tetrahedron* (2006) 62 6405-6411.

20. M Malkoch, K Schleicher, E Drockenmuller, C J Hawker, T P Russel, P Wu, and V.F.Fokin. Structurally Diverse Dendritic Libraries: A Highly Efficient Functionalization Approach Using Click Chemistry. *Macromolecules* (2005) 38 3663-3678.

21. M D Cameron and G E Bennet. Use of Amines in the Glaser Coupling Reaction. *J. Org. Chem.* (1957) 22 557-558.

22. R Manetsch, A Krasinski, Z Radic, J Raushel, P Taylor, K B Sharpless, and H C Kolb. *In Situ* Click Chemistry: Enzyme Inhibitors Made to Their Own Specifications. *J. Am. Chem. Soc.* (2004) 126 12809-12818.

23. E N da Silva Jr, R F S Menna-Barreto, M C F R Pinto, R F S Silva, D V Teixeira, M C B V de Souza, C A D Simone, S L D Castro, V F Ferreira, and A V Pinto. Naphthoquinoidal [1,2,3]-triazole, a new structural moiety active against *Trypanosoma cruzi*. *Eur. J. Med. Chem.* (2008) 43 1774-1780.

24. B-Y Lee, S.R.Park, H B Jeon, and K S Kim. A new solvent system for efficient synthesis of 1,2,3-triazoles. *Tetrahedron Lett.* (2006) 47 5105-5109.

25. P Appakkuttan, W Dehaen, V F Fokin, and E V Eycken. A Microwave-Assisted Click Chemistry Synthesis of 1,4-Disubstituted 1,2,3-Triazoles via a Copper(I)-Catalyzed Three-Component Reaction. *Org. Lett.* (2004) 6 (23) 4223-4225.

26. C W Tornoe, S J Sanderson, J C Mottram, G H Coombs, and M Meldal. Combinatorial Library of Peptidotriazoles: Identification of [1,2,3]-triazole inhibitors against a recombinant *Leishmania mexicana* cysteine protease. *J. Comb. Chem.* (2004) 6 312-324.

27. A Brik, J Muldoon, Y-C Lin, J H Elder, D S Goodsell, A J Olson, V.V.Fokin, K.B.Sharpless, and C-H Wong. Rapid Diversity-Oriented Synthesis in Microtiter Plates for *In Situ* Screening of HIV Protease Inhibitors. *ChemBioChem.* (2003) 4 1246-1248.

28. A J Link and D A Tirrell. Cell Surface Labeling of *Escherichia coli* via Copper(I)-Catalyzed [3+2] Cycloaddition. *J. Am. Chem. Soc.* (2003) 125 11164-11165.

29. C E Gutteridge, D A Nichols, S M Curtis, D S Thota, J V Vo, L Gerena, G Montip, C O Asher, D S Diaz, C A DiTusa, K Smith, and A K Bhattacharjee. *In vitro* and *in vivo* efficacy and *in vitro* metabolism of 1-phenyl-3-aryl-2-propen-1-ones against *Plasmodium falciparum*. *Bioorg. Med. Chem. Lett.* (2006) 16 5682-5686.

30. M Liu, P Wilairat, and M-L Go. Antimalarial alkoxylated and hydroxylated chalcones: structure-activity relationship analysis. *J. Med. Chem.* (2001) 44 4443-4452.

31. S C Piscitelli and M A Polis. An update on drug interactions with zidovudine. *AIDS Patient Care STD* (1998) 12 (9) 687-690.

32. D C Bibby, W N Charman, S A Charman, M N Iskander, and C J H Porter. Synthesis and evaluation of 5' alkyl ester prodrugs of zidovudine for directed lymphatic delivery. *Int. J. Pharm.* (1996) 144 61-70.

33. D A Griffith and S M Jarvis. Nucleoside and nucleobase transport systems of mammalian cells. *Biochim. Biophys. Acta* (1996) 1286 153-181.

34. WHO. Malaria and HIV interactions and their implications for Public Health Policy. (2004)

35. T S Skinner-Adams, J S McCarthy, D L Gardiner, and K T Andrews. HIV and malaria co-infection: interactions and consequences of chemotherapy. *Trends Parasitol.* (2008) 24 (6) 264-271.

36. T J Egan. Structure-function relationships in chloroquine and related 4-aminoquinoline antimalarials. *Mini Rev. Med. Chem.* (2001) 1 113-123.

37. Marek T Konieczny, W Konieczny, M Sabisz, A Skladanowski, R Wakiec, E Augustynowicz-Kopec´, and Z Zwolska. Acid-catalyzed synthesis of oxathiolone fused chalcones. Comparison of their activity toward various microorganisms and human cancer cells line. *Eur. J. Med. Chem.* (2007) 42 729-733.

38. Gy Siphos and F Sirokmán. Chalcone formation from different substituted acetophenones and *p*-hydroxybenzaldehyde. *Nature* (1964) 4931 489.

39. W D Seo, J H Kim, J E Kang, H W Ryu, M J Curtis-Long, H S Lee, M S Yang, and K H Park. Sulfonamide chalcone as a new class of a-glucosidase inhibitors. *Bioorg. Med. Chem. Lett.* (2005) 15 5514-5516.

40. M-L Go, X Wu, and X L Liu. Chalcones: An Update on Cytotoxic and Chemoprotective Properties. *Curr. Med. Chem.* (2005) 12 483-499.

41. M S Ramachandra and G V Subbaraju. Synthesis and bioactivity of novel caffeic acid esters from *Zuccagnia punctata*. *J. Asian Nat. Prod. Res.* (2006) 8 (8) 683-688.

42. T Narender and K P Reddy. A simple and highly efficient method for the synthesis of chalcones by using borontrifluoride etherate. *Tetrahedron Lett.* (2007) 48 3177-3180.

43. M V N de Souza, K C Pais, C R Kaiser, M A Peralta, M de L Ferreira, and M C S Lourenco. Synthesis and *in vitro* antitubercular activity of a series of quinoline derivatives. *Bioorg. Med. Chem.* (2009) 17 1474-1480.

CHAPTER FOUR

IN VITRO ANTIMALARIAL EVALUATION AND MECHANISTIC STUDIES

4.1 Preamble

This chapter contains the work done to address the second specific aim of the study, which was: To pharmacologically evaluate the synthesized compounds *in vitro* for antimalarial activity and possible mechanisms of action.

This chapter therefore focuses on the *in vitro* antimalarial assays applied in the current study. After a brief introduction, the assays of the synthesized compounds will be described, and the results reported and discussed. The chapter ends with a brief description of, and the results from, limited mechanistic studies on a selected number of the target compounds.

4.2 Introduction

Bioassays are quantitative procedures that determine the effect of a substance, or mixture of substances, on a biological system. They are performed either *in vitro* or *in vivo*, and as such may involve the use of animal models, isolated organs and tissues, whole cell cultures or sub-cellular systems/molecular targets, principally enzymes and receptors. Their main purpose is to quantify the relative 'activity' or 'potency' of a substance, i.e. its capacity to elicit the intended biological effect, and which may be expressed relative to a standard substance of known potency. This is determined by observing or objectively evaluating a given measurable parameter at a set interval from the bioassay starting point. As expected, the biological effect of a substance generally increases with increasing concentration (within limits), and the determination of the biological effect of a substance over a suitable range of concentrations usually enables the generation of analyzable 'dose-response' data [1,2].

4.3 *In Vitro* Antimalarial assays

Consistent with the specific aims of this study, the target compounds were evaluated for their *in vitro* antimalarial activity against both chloroquine sensitive (CQS) and chloroquine resistant (CQR) strains of *P. falciparum*. The strains used for the assays were the D10 (CQS) and Dd2 (CQR) strains. In addition, samples of the compounds

were also tested against the (CQR) W2 strain of *P. falciparum* in the laboratories of Prof. P. J. Rosenthal at the University of California, San Francisco (UCSF).

4.3.1 *In vitro* antimalarial testing

4.3.1.1 Culturing of the malaria parasite *in vitro*

The asexual erythrocytic stages of the parasites were maintained in continuous *in vitro* culture by the (modified) method described by Trager and Jensen, 1976 [3]. Briefly, the parasites were maintained at between 2 – 10% parasitemia in type O-positive human erythrocytes (Groote Schuur Hospital, Cape Town, South Africa); these were suspended in complete culture medium composed of 10.4g/L RPMI 1640 culture medium (Biowhittaeker) supplemented with 4 g/L glucose, 6 g/L HEPES buffer, 0.088 g/L hypoxanthine, 5 g/L albumax, 1% sodium bicarbonate and 0.05 g/L gentamicin. The cultures were incubated at physiological temperature, 37°C, under an atmosphere of 3% O_2, 4% CO_2 and 93% N_2. The culture medium was replaced daily, and parasitemia was determined from Giemsa stained blood smears of the cultures.

The cultured parasites were, whenever necessary, synchronized (maintained in phase) by treatment with 5% D-sorbitol (Sigma) at the ring stage of their development, applying the (modified) method described by Lambros and Vanderberg, 1979 [4].

4.3.1.2 Assay procedure

Chloroquine diphosphate (Sigma) was used as the positive control/reference compound in all experiments, with a stock solution of 2 mg/mL prepared in Millipore water. The test compounds were prepared as initial 20 mg/mL stock solutions in DMSO, sonicated to enhance solubility as required. These stock solutions were stored at -20 °C.

The assays were carried out in 96-well micro-titre plates (Greiner). Each plate could accommodate duplicate determinations of chloroquine and three test compounds (Figure 4.1). The stock solutions were aseptically diluted in complete medium to furnish working solutions of appropriate, pre-determined starting concentrations, i.e. for chloroquine, 200 ng/mL for D10 assays and 2000 ng/mL for Dd2 assays; the solutions of test compounds were similarly diluted to a starting concentration of 200 μg/mL. For those test compounds that exhibited relatively high activity in preliminary

assays, this starting concentration was lowered to 100 µg/mL, 20 µg/mL and 2 µg/mL, as appropriate.

		Blank	Neg. cont	Serial dilution of chloroquine/test compound.									
		Col 1	Col 2	Col 3	Col 4	Col 5	Col 6	Col 7	Col 8	Col 9	Col 10	Col 11	Col 12
CQ	Row A												
	Row B												
Cpd 1	Row C												
	Row D												
Cpd 2	Row E												
	Row F												
Cpd 3	Row G												
	Row H												

Figure 4.1: Figure showing the assay layout of the 96 well micro-titer plate for *in vitro* antimalarial testing.

200 µL of these working solutions were then transferred into the wells in column 3 (in duplicate), after which two-fold serial dilutions were carried out in complete medium across the plates. The outcome was that the wells in columns 3 – 12 contained 100 µL of the compound solutions in serially reducing concentrations. 100 µL of complete medium was added to each of the wells in columns 1 and 2.

Synchronized parasites were harvested in the trophozoite stage of development, and the parasitemia and hematocrit adjusted to 2% by addition of appropriate amounts of unparasitized erythrocytes and complete medium, respectively. 100 µL of these parasitized erythrocytes (2% parasitemia, 2% hematocrit) was then added to each of the wells in columns 2 – 12. 100 µL of unparasitized erythrocytes (2% hematocrit) was added to each of the wells in column 1. The final volumes in each well were therefore 200 µL. In this way, the parasites in columns 3 – 12 were exposed to a serially decreasing concentration of chloroquine and the various test compounds in a manner that could be used to determine the concentration of each compound that would inhibit the growth/viability of the parasites by 50% (IC_{50}).

The plates were then incubated for 48 hours at 37 °C in airtight gas chambers under a gas environment of 3% O_2, 4% CO_2 and 93% N_2.

The final layout of a typical 96-well assay plate is depicted in Figure 4.1:

- Wells in column 1 contained un-parasitized erythrocytes (1% hematocrit); this was the blank: no parasites, no test compounds.
- Wells in column 2 contained parasitized erythrocytes (2% parasitemia, 1% hematocrit); this was the negative control, essentially a row in which the parasites were not exposed to either chloroquine or any of the test compounds.
- Wells in column 3 contained parasitized erythrocytes (2% parasitemia, 1% hematocrit) and either 100ng/mL chloroquine (1000ng/mL for Dd2 assays) or 100 µg/mL (or lower) of the test compounds, in duplicate;
- Wells in columns 4 to 12 contained parasitized erythrocytes (2% parasitemia, 1% hematocrit) as well as the two-fold serial dilutions of chloroquine/test compounds starting from column 3.

The concentration of DMSO that the parasites were exposed to during these assays did not exceed 0.5%v/v, thereby ensuring no solvent-induced adverse effects on parasite survival, and in so doing maintaining the validity of the assays.

4.3.1.3 Quantitation and analysis based on pLDH activity

In vitro antimalarial assay protocols are generally based on either microscopic detection of Giemsa-stained slides, flow cytometry, ^{3}H-hypoxanthine uptake inhibition, fluorescence (such as the SYBR Green I-based fluorescence assay) or, as for this study, determination of parasite lactate dehydrogenase (pLDH) activity for their assessment of compound efficacy against *P. falciparum* [5,6].

Lactate dehydrogenase (LDH) catalyses the reduction of pyruvate to lactate with the concomitant oxidation of NADH to NAD+. This enzyme is particularly vital for the malaria parasite as the NAD+ that it regenerates is essential for the continuation of glycolysis, the biochemical pathway upon which the parasite is dependent for the generation of its energy in the form of ATP [7]. pLDH has an intrinsically higher rate of catalysis than human LDH; in addition, when the NAD+ analog 3-acetylpyridine adenine dinucleotide (APAD) is used as co-factor, pLDH exhibits a several hundred-fold higher catalytic conversion of lactate to pyruvate than human LDH, with the concomitant reduction of APAD to APADH [8]. Based on this, the activity of pLDH can be selectively detected in the presence of human LDH [9], and this was applied in the development of an *in vitro* antimalarial assay protocol by Makler and co-workers,

1993 [10]. This pLDH assay was found to be rapid, robust, selective, easy to perform, cheaper than the ^{3}H-hypoxanthine uptake protocols, yielded reproducible results and allowed for the freezing of the assay plates at -20 °C until it was convenient to run the assays [10].

The current study therefore applied this approach to indirectly determine the inhibition of growth of the parasites exposed to the various test compounds relative to the unexposed parasites (the negative control described above). This was done by colorimetrically quantifying pLDH activity using the light sensitive reagent mixture of nitroblue tetrazolium (NBT)/phenazine ethosulphate (PES), which, in the presence of APADH, is reduced to a strongly colored blue formazan product. The intensity of the blue color was proportional to the amount of blue formazan product formed, which was directly proportional to the amount of APADH present, which in turn was proportional to the level of pLDH activity present. This level of pLDH activity was dependent on the number of viable parasites still present at the end of the incubation period.

After the 48 hour incubation period, the assay plates were retrieved from the gas chambers, and the contents of each well were re-suspended. Maintaining the same layout as the assay plate, 15 μL of the re-suspended mixtures were then transferred to a separate 96-well plate containing 100 μL of Malstat reagent (1 ml/L triton, 0.33 g/L APAD and 3.3 g/L TRIS buffer) in each well. 25 μL of NBS/PES solution was then added into each well, after which the plates were allowed to develop for 5 – 10 minutes in the dark. The absorbance of the formazan products in each well was then measured at 620 nm on a 7520 Microplate reader from Cambridge Technology Inc, or on a Modulus microplate reader from Turner Biosystems.

The absorbance data from the colorimetric assays was then transformed to represent percentage viability by adjusting for the absorbance in the blank and control wells; this data was then analyzed using GraphPad Prism® Version 4 software to yield semi-logarithmic dose-response curves and the corresponding IC_{50} values for the compounds.

For studies with the W2 strain, assays were conducted as previously reported (Shenai *et al.* 2003) [11] with parasites cultured in standard medium including 10% human serum; parasite development was assessed with a FACS-based assay, as previously described (Sijwali and Rosenthal, 2004) [12].

4.3.2 *In vitro* antimalarial assay results

4.3.2.1 Acetylenic chalcones

Table 4.1: IC_{50} values of the acetylenic chalcones **3.9** and **3.10** against the D10, Dd2 and W2 strains of *P. falciparum*

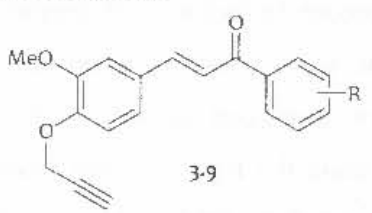

3.9

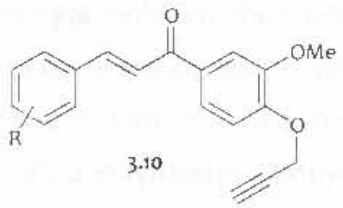

3.10

Compound code	R	D10 IC_{50} (μM)	Dd2 IC_{50} (μM)	W2 IC_{50} (μM)
3.9a	4'-OMe	9.7	13.5	8.4
3.9b	2',4'-diOMe	3.4	4.3	3.8
3.9c	2',3',4'-triOMe	7.7	2.8	7.0
3.10a	2,4-diOMe	>20	14.5	9.7
3.10b	2,3,4-triOMe	4.1	2.4	6.7
3.10c	2,4-diCl	3.3	2.8	5.0
3.10d	4-F	7.2	7.7	>20
3.10e	2,4-diF	>20	5.2	9.4
(CQ)	-	0.017	0.097	0.069

NB: these are average values from two independent determinations, each carried out in duplicate

As pointed out earlier, the IC_{50} values represent the concentration of a compound that inhibits the growth/viability of the parasites by 50%, and thereby provide a means of comparing the activities of different compounds; the lower the IC_{50} value, the more active the compound is.

From Table 4.1, it can be seen that the acetylenic chalcones exhibited moderate *in vitro* antimalarial activity relative to the reference compound chloroquine, with IC_{50} values generally falling in the lower micromolar region. Compounds **3.10a** and **3.10e** were inactive against the D10 strain of *P. falciparum*, as was **3.10d** against the W2 strain, at the highest concentrations tested (IC_{50} >20 μM). Excluding these three results, it would appear that the activity of these series of compounds is conserved across the three strains of parasites, with IC_{50} values of between 2.4 – 14.5 μM; this would suggest similar susceptibility of both the chloroquine sensitive and chloroquine resistant strains of the parasite to the antimalarial activity of these compounds. No particular trends could be delineated with respect to the different substitution patterns.

4.3.2.2 Chalcones hybrid compounds

Table 4.2: IC_{50} values of the chalcone hybrid compounds 3.14 - 3.17 against the D10, Dd2 and W2 strains of *P. falciparum*

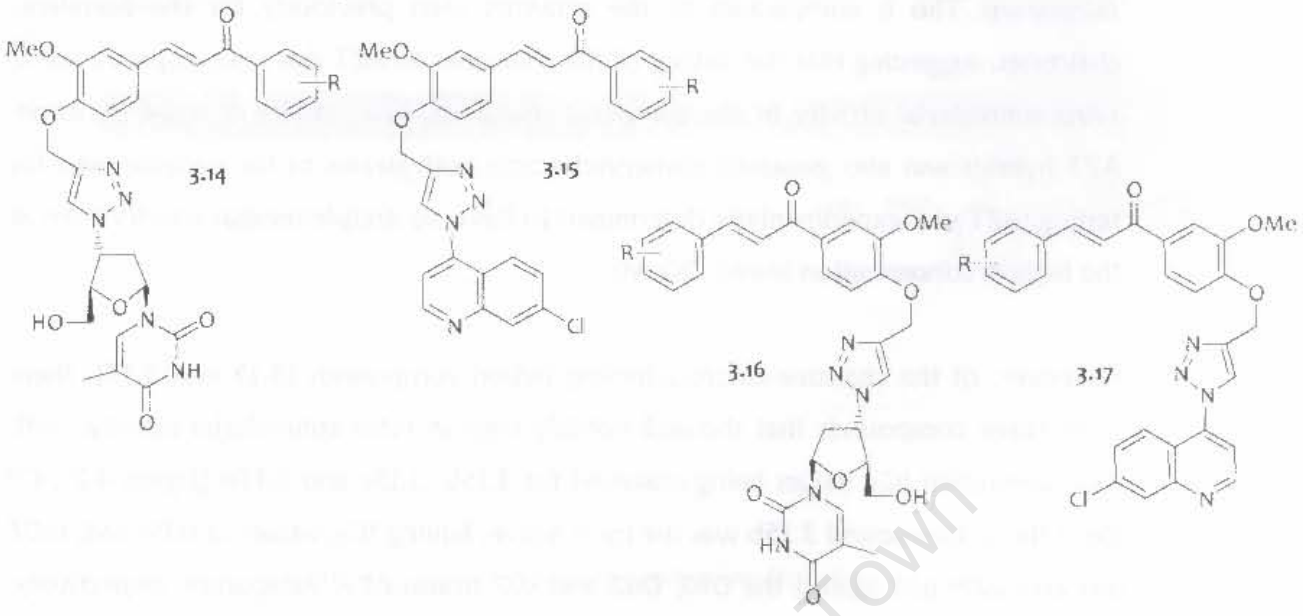

Compound code	R	D10 IC_{50} (μM)	Dd2 IC_{50} (μM)	W2 IC_{50} (μM)
3.14a	4'-OMe	2.9	6.1	8.0
3.14b	2',4'-diOMe	1.5	4.4	5.4
3.14c	2',3',4'-triOMe	3.3	3.7	5.4
3.15a	4'-OMe	0.6	2.2	5.0
3.15b	2',4'-diOMe	0.04	0.07	0.09
3.15c	2',3',4'-triOMe	0.4	0.4	0.6
3.16a	2,4-diOMe	10.2	11.8	9.0
3.16b	2,3,4-triOMe	5.4	3.8	7.1
3.16c	2,4-diCl	3.7	1.9	8.4
3.16d	4-F	7.3	6.1	6.6
3.16e	2,4-diF	3.9	4.8	7.1
3.17a	2,4-diOMe	5.2	11.7	6.6
3.17b	2,3,4-triOMe	0.3	0.3	0.5
3.17c	2,4-diCl	6.0	1.9	11.5
3.17d	4-F	7.4	1.6	6.9
3.17e	2,4-diF	4.1	2.1	10.6
(CQ)	-	0.017	0.097	0.069

NB: these are average values from two independent determinations, each carried out in duplicate

From Table 4.2, it can be seen that the chalcone-AZT hybrid compounds 3.14 and 3.16 exhibited moderate *in vitro* antimalarial activity, with IC_{50} values within the lower micromolar region and ranging from 1.5 – 11.8 μM for the three strains of *P. falciparum*. This is comparable to the activities seen previously for the acetylenic chalcones, suggesting that the linking of the chalcones to AZT does not improve the *in vitro* antimalarial activity of the acetylenic chalcones. The activity of these chalcone-AZT hybrids was also generally conserved across both strains of the parasite used for testing. AZT was experimentally determined to have no antiplasmodial activity even at the highest concentration tested (20μM).

However, of the chalcone-chloroquinoline hybrid compounds (3.15 and 3.17), there were three compounds that showed notably high *in vitro* antimalarial activity, with sub-micromolar IC_{50} values being observed for 3.15b, 3.15c and 3.17b (Figure 4.2). Of these three, compound 3.15b was the most active, having IC_{50} values of 0.04 μM, 0.07 μM and 0.09 μM against the D10, Dd2 and W2 strains of *P. falciparum*, respectively. Interestingly, these three compounds were either di- or tri-methoxylated chalcone-chloroquinoline hybrids; none of the halogenated chalcone-chloroquinoline hybrid compounds exhibited sub-micromolar IC_{50} values.

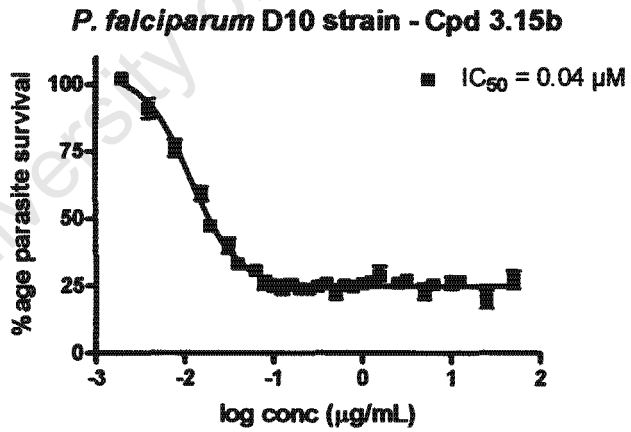

Figure 4.2: Example of a typical dose response curve – specifically for data from the assay of compound 3.15b against D10 *P. falciparum*.

The presence of the chloroquinoline moiety on the three more active compounds is most likely responsible for the improved activity that these compounds exhibit; this would be no surprise since, as mentioned previously, this sub-structure is present in a variety of antimalarial drug classes, ranging from the aminoquinolines (e.g. chloroquine, amodiaquine) to the quinoline-methanols (e.g. quinine, mefloquine), and is thought to confer antimalarial potency to these compounds by facilitating binding to intra-parasitic heme and consequently inhibiting hemozoin formation [13]. However, it

should be noted that this significant improvement in activity was not universal, as shown by the fact that the other hybrid compounds in this class had *in vitro* activities comparable with those of the acetylenic chalcones and the chalcone-AZT hybrid derivatives.

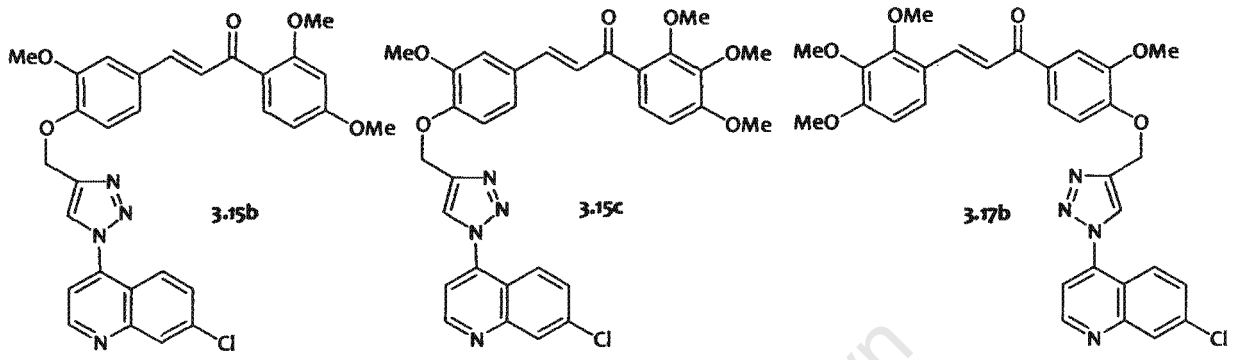

Figure 4.3: Figure showing the three chalcone derivatives that were most active *in vitro*

4.3.2.3 Acetylenic dienones

Table 4.3: IC_{50} values of the acetylenic enone **3.11** and acetylenic dienones **3.12** the D10, Dd2 and W2 strains of *P. falciparum*

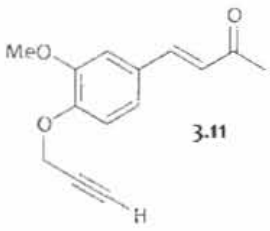

3.11

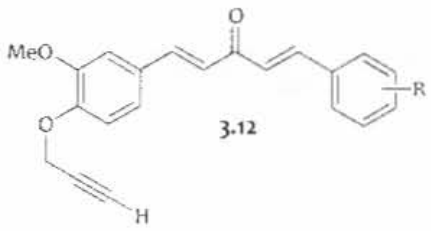

3.12

Compound code	R	D10 IC_{50} (μM)	Dd2 IC_{50} (μM)	W2 IC_{50} (μM)
3.11	-	9.7	7.5	>20
3.12a	4'-OMe	11.8	10.7	>20
3.12b	2',4'-diOMe	5.4	4.0	18.9
3.12c	2',3',4'-triOMe	0.9	1.4	9.2
3.12d	2,4-diCl	9.2	9.0	>20
3.12e	4-F	9.8	6.5	21.5
3.12f	2,4-diF	11.9	9.3	>20
(CQ)	-	0.017	0.097	0.069

NB: these are average values from two independent determinations, each carried out in duplicate

From Table 4.3, it can be seen that the acetylenic dienones exhibited moderate *in vitro* antimalarial activity against the D10 and Dd2 strains, with IC_{50} values generally falling in the lower micromolar range of 0.9 – 11.9 μM. However, these compounds tend to be noticeably less active against the W2 strain of *P. falciparum*, with compounds **3.12a**, **3.12d** and **3.12f** showing no detectable antimalarial activity against this strain at the maximum concentration tested.

The most active compound of this series was **3.12c**, the tri-methoxylated acetylenic dienone, which had an IC_{50} of 0.9 μM against *P. falciparum* D10. Interestingly, the acetylenic enone intermediate **3.11** also showed moderate antimalarial activity comparable to that of the acetylenic chalcones, with IC_{50}s of 9.7 μM and 7.5 μM against *P. falciparum* D10 and Dd2, respectively. This would suggest that for chalcones and dienones, the most basic structure/pharmacophore required to exhibit antimalarial activity could be the phenyl-propenone moiety.

4.3.2.4 Dienones hybrid compounds

Table 4.4: IC_{50} values of the dienone hybrid compounds 3.20 - 3.21 against the D10, Dd2 and W2 strains of *P. falciparum*

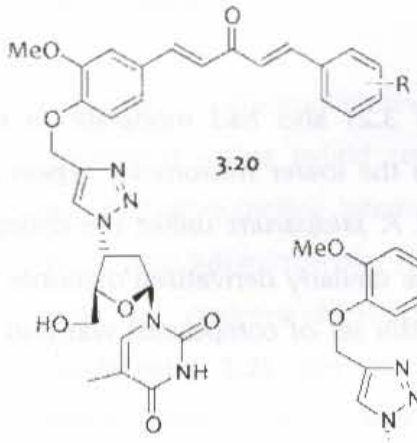

3.20

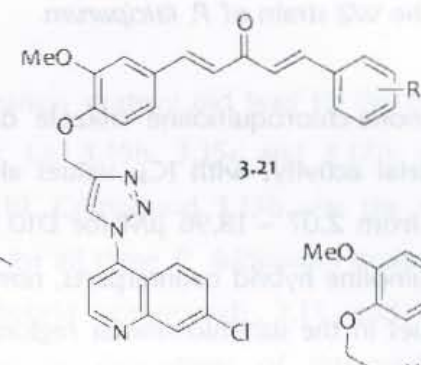

3.21

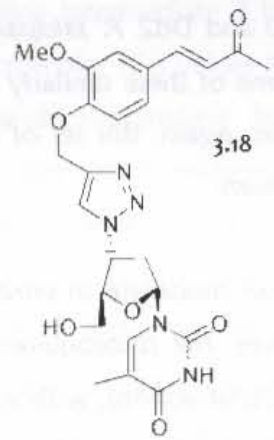

3.18

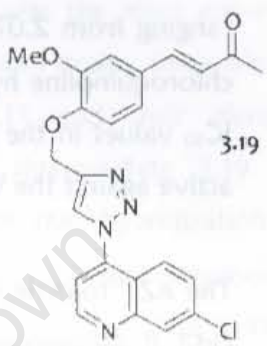

3.19

Compound code	R	D10 IC_{50} (μM)	Dd2 IC_{50} (μM)	W2 IC_{50} (μM)
3.18	-	12.0	16.4	ND
3.19	-	0.8	0.7	ND
3.20a	4'-OMe	2.8	1.5	18.2
3.20b	2',4'-diOMe	1.3	1.2	14.5
3. 20c	2',3',4'-triOMe	1.3	2.4	8.3
3. 20d	2,4-diCl	1.4	1.7	9.1
3. 20e	4-F	1.7	2.6	ND
3. 20f	2,4-diF	1.4	1.7	12.4
3. 21a	4'-OMe	3.0	2.1	5.3
3. 21b	2',4'-diOMe	5.1	6.4	>20
3. 21c	2',3',4'-triOMe	2.5	2.1	18.5
3. 21d	2,4-diCl	19.0	16.8	>20
3. 21e	4-F	9.4	9.3	>20
3. 21f	2,4-diF	10.2	6.5	>20
(CQ)	-	0.017	0.097	0.069

NB: these are average values from two independent determinations, each carried out in duplicate

The dienone-AZT triazole derivatives **3.20** had moderate *in vitro* antimalarial activity, with IC_{50} values also within the lower micromolar region and ranging from 1.2 – 2.8 μM for the D10 and Dd2 strains of *P. falciparum*. As was previously observed for the acetylenic dienones, the dienone-AZT hybrids also tend to be noticeably less active against the W2 strain of *P. falciparum*.

The dienone-chloroquinoline triazole derivatives **3.21** also had moderate *in vitro* antimalarial activity, with IC_{50} values also within the lower micromolar region and ranging from 2.07 – 18.96 μM for D10 and Dd2 *P. falciparum*; unlike the chalcone-chloroquinoline hybrid counterparts, none of these similarly derivatized dienones had IC_{50} values in the sub-micromolar region. Again, this set of compounds was also less active against the W2 strain of *P. falciparum*.

The AZT triazole intermediate **3.18** shows moderate *in vitro* activity against D10 and Dd2 *P. falciparum*; interestingly, however, the chloroquinoline triazole intermediate **3.19** shows notably high *in vitro* antimalarial activity, with sub-micromolar IC_{50} values against these two strains of the parasite. It would therefore appear that the introduction of the chloroquinoline sub-structure is associated with a marked increase in *in vitro* antimalarial activity of the acetylenic enone intermediate **3.11**, which is not surprising for reasons already pointed out; this is not the case when AZT is introduced.

4.3.3 Discussion

The moderate *in vitro* antimalarial activity observed for the acetylenic chalcones **3.9** and **3.10** is very much in line with the published results for alkoxylated chalcones, which have been reported as having IC_{50} values in the high nanomolar to low micromolar ranges [14,15]; this activity does not seem to be compromised by the presence of the acetylene substitution.

It is interesting to note that the acetylenic dienones exhibit comparable antimalarial activity to the acetylenic chalcones. As has been noted previously, this is probably attributable to the presence of the common phenyl propenone sub-structure in both these series of compounds, as the acetylenic enone intermediate **3.11** also exhibits comparable *in vitro* antimalarial activity.

The AZT hybrid compounds of both the chalcones and dienones did not exhibit notably higher *in vitro* antimalarial activity relative to their acetylenic precursors, though the retention of activity in most cases is still noteworthy. It is therefore possible

that the envisaged benefits of the AZT hybridization strategy, which were primarily the increased solubility and possibly enhanced oral bioavailability of these compounds, may only become apparent through pharmacokinetic profiling or *in vivo* antimalarial efficacy assays.

However, the chloroquinoline-hybridization strategy did lead to the identification of significantly active hybrid compounds, i.e. **3.15b**, **3.15c** and **3.17b**, as well as the enone-chloroquinoline intermediate **3.19**. Compound **3.15b** was the most active of these, with sub-micromolar IC_{50} values for all three *P. falciparum* strains. Interestingly, both the chalcone-chloroquinoline hybrid compounds **3.15** and their dienone counterparts **3.21** can be considered as derivatives of intermediate **3.19** *via* modifications on its α-carbon. It is also intriguing to note that hybridization to chloroquinoline did not lead to a similarly remarkable activity in all these compounds; instead, only the three methoxylated chalcones mentioned previously had notably improved activity. This indicates that the group on the terminal α-carbon of **3.19** is crucial for the retention of activity, and some groups could actually negate any beneficial effects that the chloroquinoline moiety confers (as is the case with the halogenated chalcone-chloroquinoline and the dienone-chloroquinoline hybrid compounds).

No obvious trends were observed as far as the influence of the different substitution patterns of the chalcones or dienones on antimalarial activity is concerned. The only valid comment that could be made in this regard is that, of all the compounds with notable antimalarial activity/sub-micromolar IC_{50} values, none of them were halogenated compounds.

In conclusion, the most promising candidate for further development based on *in vitro* antimalarial potency was **3.15b**, and this compound was therefore prioritized for subsequent pharmacokinetic profiling and *in vivo* antimalarial efficacy assays. In anticipation of this, compound **3.15b** was evaluated for its cytotoxicity against the Chinese Hamster Ovarian (mammalian) cell line. No cytotoxicity was observed at the highest concentration (100 μM) tested.

It is acknowledged that pharmacokinetic and/or *in vivo* efficacy profiling of representative AZT-based hybrid compounds would have been useful for proof-of-principle, i.e. to test the hypothesis on the potential beneficial effects *in vivo* of hybridization to the hydrophilic nucleoside AZT. However, due to mainly time

constraints, this was not carried out during the course of this study, but has been earmarked for future follow-up (see section 7.2).

4.4 Mechanistic studies

A limited mechanistic investigation was carried out on some of the compounds so far synthesized and tested in an attempt to elucidate their possible mechanisms of action. The compounds for this investigation were selected from among the chalcone-chloroquinoline hybrid compounds **3.15** and **3.17**, as these were the hybrid compounds that had yielded the most active compounds, such as **3.15b**. Compound **3.9b**, the acetylenic chalcone precursor of **3.15b**, was also included for investigation, as was curcumin.

The mechanisms of action considered for investigation were based on literature accounts of the possible mechanisms by which chalcones and quinoline-containing compounds exerted their antimalarial activities.

4.4.1 Inhibition of hemozoin (β-hematin) formation

As mentioned in Chapter One, hemoglobin degradation is the principle way by which the malaria parasite secures its supply of iron [16] and amino acids [17] vital for its survival. Heme, one of the by-products of this metabolic process, is toxic to the parasite, and accumulation of heme within the parasite would be lethal. The parasite therefore detoxifies heme mainly *via* its conversion to hemozoin (malaria pigment), an inert, crystalline form of heme [18]. Inhibition of hemozoin formation therefore is an attractive target for antimalarial drugs, and quinoline-based antimalarials such as chloroquine and amodiaquine are proposed to exert their antimalarial activity *via* this mechanism [18-20]. On the strength of this, the chalcone-chloroquinoline hybrid compounds were investigated for their potential to inhibit hemozoin formation.

Assays have been designed to estimate the ability of compounds to inhibit hemozoin formation [20]. The assay described by Ncokazi and Egan, 2004 [21] is one such assay, which colorimetrically quantifies the ability of a compound to inhibit the conversion of hematin to β-hematin, the synthetic equivalent of hemozoin. The IC_{50} values from this assays represent the number of molar equivalents of the test compound, relative to hematin, that are required to inhibit its conversion to β-hematin by 50% - the lower the IC_{50}, the more potent the compound is at inhibiting β-hematin formation.

constraints, this was not carried out during the course of this study, but has been earmarked for future follow-up (see section 7.2).

4.4 Mechanistic studies

A limited mechanistic investigation was carried out on some of the compounds so far synthesized and tested in an attempt to elucidate their possible mechanisms of action. The compounds for this investigation were selected from among the chalcone-chloroquinoline hybrid compounds **3.15** and **3.17**, as these were the hybrid compounds that had yielded the most active compounds, such as **3.15b**. Compound **3.9b**, the acetylenic chalcone precursor of **3.15b**, was also included for investigation, as was curcumin.

The mechanisms of action considered for investigation were based on literature accounts of the possible mechanisms by which chalcones and quinoline-containing compounds exerted their antimalarial activities.

4.4.1 Inhibition of hemozoin (β-hematin) formation

As mentioned in Chapter One, hemoglobin degradation is the principle way by which the malaria parasite secures its supply of iron [16] and amino acids [17] vital for its survival. Heme, one of the by-products of this metabolic process, is toxic to the parasite, and accumulation of heme within the parasite would be lethal. The parasite therefore detoxifies heme mainly *via* its conversion to hemozoin (malaria pigment), an inert, crystalline form of heme [18]. Inhibition of hemozoin formation therefore is an attractive target for antimalarial drugs, and quinoline-based antimalarials such as chloroquine and amodiaquine are proposed to exert their antimalarial activity *via* this mechanism [18-20]. On the strength of this, the chalcone-chloroquinoline hybrid compounds were investigated for their potential to inhibit hemozoin formation.

Assays have been designed to estimate the ability of compounds to inhibit hemozoin formation [20]. The assay described by Ncokazi and Egan, 2004 [21] is one such assay, which colorimetrically quantifies the ability of a compound to inhibit the conversion of hematin to β-hematin, the synthetic equivalent of hemozoin. The IC_{50} values from this assays represent the number of molar equivalents of the test compound, relative to hematin, that are required to inhibit its conversion to β-hematin by 50% - the lower the IC_{50}, the more potent the compound is at inhibiting β-hematin formation.

The selected compounds were submitted for this assay, which was carried out by Dr. K. Ncokazi in the laboratories of Prof. Timothy J. Egan at the Dept. of Chemistry, UCT. The results are presented in Table 4.5.

4.4.2 Inhibition of Falcipain-2, a plasmodial cysteine protease

The subsequent breakdown of the globulin component of hemoglobin into smaller peptide fragments is known to involve the activity of cysteine proteases, principally Falcipain 2 and Falcipain 3 [22,23]. These enzymes therefore offer themselves as targets for potential antimalarial agents. Plasmodial cysteine proteases, and in particular Falcipain 2, have been proposed as such [24,25], and efforts have been made to develop cysteine protease inhibitors as novel antimalarial agents [26]. Several quinolinyl chalcones have been identified that actually inhibited plasmodial cysteine proteases (contained in soluble parasite extracts) at micromolar concentrations, though there was no correlation between this inhibition and the *in vitro* antimalarial activities of the compounds [27].

On this basis, the selected chalcone-chloroquinoline hybrid compounds were submitted for recombinant Falcipain-2 inhibition assays, which were carried out by Dr. J. Gut in the laboratories of Prof. P. J. Rosenthal at the University of California, San Francisco (UCSF), USA. The results are also presented in Table 4.5.

4.4.3 Inhibition of sorbitol-induced hemolysis

Infection of human erythrocytes with the malaria parasite induces the activation of channels, dubbed new permeability pathways (NPPs), hitherto absent in the erythrocyte membrane. These channels allow for the influx of electrolytes and essential nutrients (such as amino-acids, nucleosides and sugars) required by the parasite while allowing the efflux of metabolic waste products extruded by the parasite [28,29]. The fact that these channels are absent in non-parasitized cells and are essential for the survival of the intracellular parasite make them an attractive target for novel antimalarial agents [30].

Inhibition of sorbitol-induced lysis of infected erythrocytes is an experimental technique used to assess compounds for their potential to inhibit these NPPs [31]. Briefly, when a parasitized erythrocyte is exposed to an isosmolar solution of sorbitol, the sorbitol (which is one of the solutes that can pass through the NPPs) is taken up *via* these NPPs and accumulates in the erythrocyte. What follows is a rise in intracellular

osmotic pressure, and the resultant osmosis of water into the erythrocyte causes it to swell and ultimately lyse. The assay is based on the observed fact that less lysis is observed in erythrocytes exposed to inhibitors of NPPs relative to erythrocytes not exposed to NPP inhibitors; the more potent the inhibitor, the less the observed lysis.

A study of some of the chalcones from a series of alkoxylated and hydroxylated chalcones (mentioned in Chapter Three, Section 3.5.1, [32,33]) for their inhibition of sorbitol-induced lysis of parasitized red blood cells found that most of the good inhibitors of sorbitol-induced lysis were also active antiplasmodial agents. However, not all active antiplasmodial agents inhibited sorbitol-induced lysis. This, along with the fact that the chalcones were not exceptionally potent inhibitors of the parasite induced channels relative to other known inhibitors, strongly suggested the presence of alternative antimalarial mechanisms of action. Some chalcones with poor *in vitro* antimalarial activity were good inhibitors of sorbitol-induced lysis [31].

The selected chalcone-chloroquinoline hybrid compounds were therefore evaluated for inhibition of sorbitol-induced lysis of infected erythrocytes. The method described by Go *et al.* 2004 [31] was applied for this assay, with modifications, in our UCT laboratories.

Briefly, chloroquine-sensitive *P. falciparum* D10 was cultured as described in section 4.3.1.1, and trophozoite-stage infected erythrocytes (10% parasitemia) were harvested by centrifugation (750 r.p.m., 3 min), washed twice with a solution of NaCl (150 mM) – HEPES (20 mM) (pH 7.4; 304 mosM), and suspended in the same solution to give a hematocrit of about 50%.

Test compounds were dissolved in dimethylsulfoxide (DMSO) to give 10 mM stock solutions, which were diluted further with a solution comprising 300 mM sorbitol – 20 mM HEPES (pH 7.4; 345 mosM) to give the test solutions of 100 μM.

In 10 mL screw-cap centrifuge tubes, 100 μL of the test solutions were separately combined with an additional 700 μL of the sorbitol-HEPES buffer and 200 μl of the parasitized cell suspension in NaCl-HEPES buffer. The final concentration of the test compounds was 10 μM. For the negative control, 800 μL of the sorbitol-HEPES buffer and 200 μl of the parasitized cell suspension in NaCl-HEPES buffer were transferred into a 10 mL screw-cap centrifuge tube. For the blank, 800 μL of the sorbitol-HEPES buffer and 200 μl of non-parasitized erythrocyte suspension (50% hematocrit) in NaCl-HEPES buffer were transferred into a 10 mL screw-cap centrifuge tube. The mixtures were incubated at 37°C for 15 min and centrifuged, and aliquots of the supernatant (100 μL) were dispensed into 96-well plates. The absorbances at 560 nm

With the exception of 3.17a which was inactive at the highest concentration tested, the submitted compounds showed inhibition of β-hematin formation to varying degrees. The most potent compound was 3.15c, with an IC_{50} of 0.2 equivalents. Interestingly curcumin and the acetylenic chalcone 3.9b were also more potent inhibitors of β-hematin formation than chloroquine, with IC_{50} values of 0.3 and 0.5 equivalents, respectively. Compound 3.15b, the most potent compound *in vitro*, was only slightly more potent (IC_{50} 1.6 equiv.) than chloroquine, as was 3.17e with a similar IC_{50}. 3.17b and 3.17d were less potent inhibitors of β-hematin formation than chloroquine. Though the chalcone component of the hybrid compounds could contribute to their potency as inhibitors of β-hematin formation (the chalcone 3.9 was a potent β-hematin inhibitor, for example), no obvious structural features could be identified that could account for why some of the hybrid compounds were significantly more potent β-hematin inhibitors than others.

There was also no consistent correlation between β-hematin inhibition and *in vitro* antimalarial potency, as the more potent inhibitors of β-hematin formation were not necessarily the more potent compounds *in vitro*. This implies the possible influence of other factors; one such factor could be the degree of accumulation within the parasite digestive vacuole, which is the definitive site of hemoglobin catabolism and therefore the site of action of hemozoin inhibitors. Chloroquine accumulates considerably within the parasite digestive vacuole by both saturable [34,35] and non-saturable (pH-dependent) [13,36,37] mechanisms, a factor that undoubtedly contributes to its antimalarial potency. The lower *in vitro* antimalarial activity (relative to chloroquine) of those target compounds showing comparable or superior β-hematin inhibition could therefore suggest the absence of equivalent accumulation mechanisms, resulting in lower concentrations at the site of action (digestive vacuole) and ultimately in relatively lower *in vitro* antimalarial efficacies. The target compounds were notably not as basic as the dibasic chloroquine, which would rule out pH-dependent accumulation as a possible mechanism of accumulation for these compounds.

However, the fact that some of the compounds were quite potent inhibitors of β-hematin formation (in several cases more active than chloroquine) would suggest that this is a primary mechanism by which these compounds exert their antimalarial activity, though the presence of other mechanisms of action is also quite possible.

The compounds showed only moderate inhibition of Falcipain 2, with IC_{50} values in the lower micromolar region; this is relative to E64, a known potent inhibitor of

were then determined and used to estimate the amount of hemoglobin released and, by extension, the degree of sorbitol-induced hemolysis. The absorbances of the control and blank wells were determined concurrently, and corrections to the absorbances measured in the test wells were made as appropriate. The percentage inhibition of sorbitol-induced lysis was then calculated for each test compound, and the results are presented in Table 4.5.

4.4.4 Results

Table 4.5: Results from the mechanistic studies

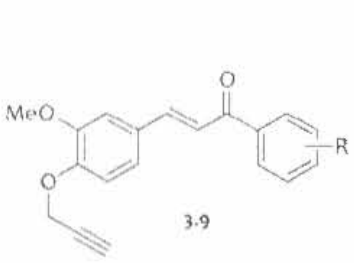

3.9

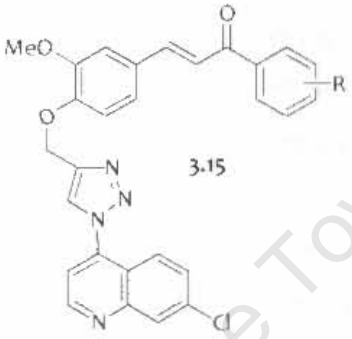

3.15

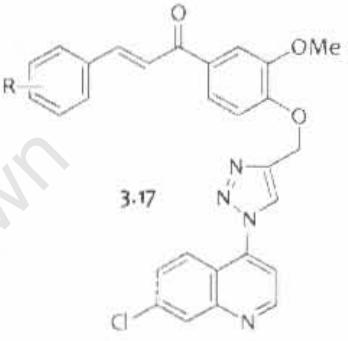

3.17

Compound code	R	D10 IC_{50} (μM)	Dd2 IC_{50} (μM)	W2 IC_{50} (μM)	β-hematin inhibition (IC_{50} in equiv.)[a]	Falcipain-2 inhibition IC_{50} (μM)[b]	%age Sorbitol-induced hemolysis inhibition.[c,d]
3.9b	2',4'-diOMe	3.4	4.3	3.8	0.5	>50	58.8
3.15b	2',4'-diOMe	0.04	0.07	0.09	1.6	10.8	15.4
3.15c	2',3',4'-triOMe	0.4	0.4	0.6	0.2	15.7	7.1
3.17a	2.4-diOMe	5.2	11.7	6.6	Inactive	24.3	11.6
3.17b	2.3.4-triOMe	0.3	0.3	0.5	4.1	11.9	11.3
3.17d	4-F	7.4	1.6	6.9	4.8	12.7	<1
3.17e	2,4-diF	4.1	2.1	10.6	1.6	13.1	10.0
Curcumin	-	5.6	4.1	-	0.3	5.2	25.3
CQ	-	0.017	0.097	0.069	1.91	-	-
E64	-	-	-	-	-	0.055	-

[a]: The IC_{50}s are averages of triplicate determinations and are reported in equivalents of the drug relative to hematin.

[b]: The IC_{50}s are averages of duplicate determinations and are reported in μM.

[c]: Average percentage inhibition from duplicate determinations of sorbitol-induced lysis by the test compounds at a concentration of 10 μM.

[d]: Furosemide, the typical positive control for this assay, was unfortunately unavailable at the time the assay was being carried out.

Falcipain 2 with an IC_{50} of 0.055 μM. Interestingly, curcumin was the most active of the selected compounds submitted for this assay, with a moderate IC_{50} of 5.2 μM. Compound 3.9b, the acetylenic chalcone precursor of the highly active hybrid compound 3.15b, did not inhibit Falcipain 2 at the highest concentration tested (50 μM).

Again, there was no consistent correlation between Falcipain 2 inhibition and *in vitro* antimalarial potency as the more potent compounds *in vitro* were not necessarily the more potent inhibitors of Falcipain 2. For example compound 3.15b, which showed the highest antimalarial activity *in vitro*, was not the most potent inhibitor of Falcipain 2. In addition, the relatively low potencies of the compounds as Falcipain 2 inhibitors suggests that this is not a primary mechanism of antimalarial action of these compounds, though inhibition of the enzyme may still contribute to their overall observed antimalarial activity.

The most potent inhibitor of sorbitol-induced lysis was actually the acetylenic chalcone 3.9, which inhibited hemolysis by 58%. The rest of the molecules tested were poor inhibitors of sorbitol-induced lysis; curcumin inhibited hemolysis by 25%, while the chalcone-chloroquinoline hybrid compounds inhibited hemolysis by ≤ 15%. This probably discounts inhibition of NPPs as a mechanism of action for the hybrid compounds, though this mechanism of action could possibly contribute to the moderate *in vitro* potency observed for 3.9.

4.4.5 Conclusion

The results above suggest that inhibition of hemozoin formation is likely to contribute to the antimalarial activity of the target compounds. This is particularly so for the hybrid compounds 3.15b, 3.15c and 3.15e, which were all comparably or more potent than chloroquine in inhibiting β-hematin formation. This would not be surprising as these hybrid compounds also contain the chloroquinoline moiety. Inhibition of Falcipain 2 could also contribute to the overall observed antimalarial activities of these compounds, albeit to a limited extent. Inhibition of parasite-induced transport channels does not appear to be a notable mechanism of action for these compounds.

The lack of correlation between these proposed mechanisms of action and the observed *in vitro* antimalarial activities of these compounds suggests the possibility of either the existence of additional mechanisms of action, varying contributions of the various proposed mechanisms of action to the overall observed antimalarial activity, or of other factors that influence the *in vitro* antimalarial activities of these compounds such as varying degrees of lysosomal accumulation within the malaria parasite.

Also worth mentioning is that curcumin appears to be a potent inhibitor of β-hematin formation (IC_{50} 0.3 equiv.), as well as a moderate inhibitor of Falcipain 2 and parasite-induced permeability pathways. This would suggest the likelihood that these mechanisms, possibly among others, contribute to the overall antimalarial activity of this natural product.

References

1. A Meager. Measurement of cytokines by bioassays: Theory and application. *Methods* (2006) 38 237-252.

2. Atta-ur-Rahman, M I Choudhary, and W J Thomson. Bioassay techniques for drug development. *Harwood Academic Publishers, Taylor & Francis e-Library* (2005)

3. W Trager and J B Jensen. Human malaria parasites in continuous culture. *Sci. New Series* (1976) 193 (4254) 673-675.

4. C Lambros and J P Vanderberg. Synchronization of *Plasmodium falciparum* erythrocyte stages in culture. *J. Parasitol.* (1979) 65 (3) 418-420.

5. J D Johnson, R A Dennull, L Gerena, M Lopez-Sanchez, N E Roncal, and N C Waters. Assessment and Continued Validation of the Malaria SYBR Green I-Based Fluorescence Assay for Use in Malaria Drug Screening. *Antimicrob. Agents Chemother.* (2007) 51 (6) 1926-1933.

6. D A Fidock, P J Rosenthal, S L Croft, R Brun, and S Nwaka. Antimalarial efficacy screening: *in vitro* and *in vivo* protocols. *MMV* (2004) (Supplemental file)

7. A Chaikuad, V Fairweather, R Connors, T Joseph-Horne, D Turgut-Balik, and R L Brady. Structure of lactate dehydrogenase from *Plasmodium vivax* complexes with NADH and APADH. *Biochem.* (2005) 44 16221-16228.

8. M S Gomez, R C Piper, L A Hunsaker, R E Royer, L M Deck, M T Makler, and D L V Jagt. Substrate and cofactor specificity and selective inhibition of lactate dehydrogenase from the malarial parasite *P. falciparum*. *Mol. Biochem. Parasitol.* (1997) 90 235-246.

9. M T Makler and D J Hinrichs. Measurement of the lactate dehydrogenase activity of *Plasmodium falciparum* as an assessment of parasitemia. *Am. J. Trop. Med. Hyg.* (1993) 48 (2) 205-210.

10. M T Makler, J M Ries, J A Williams, J E Bancroft, R C Piper, B L Gibbins, and D J Hinrichs. Parasite lactate dehydrogenase as an assay for *Plasmodium falciparum* drug sensitivity. *Am. J. Trop. Med. Hyg.* (1993) 48 (6) 739-741.

11. B R Shenai, B J Lee, A Alvarez-Hernandez, P Y Chong, C D Emal, R J Neitz, W R Roush, and P J Rosenthal. Structure-Activity Relationships for Inhibition of Cysteine Protease Activity and Development of *Plasmodium falciparum* by Peptidyl Vinyl Sulfones. *Antimicrob. Agents Chemother.* (2003) 47 (1) 154-160.

12. P S Sijwali and P J Rosenthal. Gene disruption confirms a critical role for the cysteine protease falcipain-2 in hemoglobin hydrolysis by *Plasmodium falciparum*. *Proc. Natl. Acad. Sci. USA.* (2004) 101 (13) 4384-4389.

13. T J Egan. Structure-function relationships in chloroquine and related 4-aminoquinoline antimalarials. *Mini Rev. Med. Chem.* (2001) 1 113-123.

14. M Liu, P Wilairat, and M-L Go. Antimalarial alkoxylated and hydroxylated chalcones: structure-activity relationship analysis. *J. Med. Chem.* (2001) 44 4443-4452.

References

1. A Meager. Measurement of cytokines by bioassays: Theory and application. *Methods* (2006) 38 237-252.

2. Atta-ur-Rahman, M I Choudhary, and W J Thomson. Bioassay techniques for drug development. *Harwood Academic Publishers, Taylor & Francis e-Library* (2005)

3. W Trager and J B Jensen. Human malaria parasites in continuous culture. *Sci. New Series* (1976) 193 (4254) 673-675.

4. C Lambros and J P Vanderberg. Synchronization of *Plasmodium falciparum* erythrocyte stages in culture. *J. Parasitol.* (1979) 65 (3) 418-420.

5. J D Johnson, R A Dennull, L Gerena, M Lopez-Sanchez, N E Roncal, and N C Waters. Assessment and Continued Validation of the Malaria SYBR Green I-Based Fluorescence Assay for Use in Malaria Drug Screening. *Antimicrob. Agents Chemother.* (2007) 51 (6) 1926-1933.

6. D A Fidock, P J Rosenthal, S L Croft, R Brun, and S Nwaka. Antimalarial efficacy screening: *in vitro* and *in vivo* protocols. *MMV* (2004) (Supplemental file)

7. A Chaikuad, V Fairweather, R Connors, T Joseph-Horne, D Turgut-Balik, and R L Brady. Structure of lactate dehydrogenase from *Plasmodium vivax* complexes with NADH and APADH. *Biochem.* (2005) 44 16221-16228.

8. M S Gomez, R C Piper, L A Hunsaker, R E Royer, L M Deck, M T Makler, and D L V Jagt. Substrate and cofactor specificity and selective inhibition of lactate dehydrogenase from the malarial parasite *P. falciparum*. *Mol. Biochem. Parasitol.* (1997) 90 235-246.

9. M T Makler and D J Hinrichs. Measurement of the lactate dehydrogenase activity of *Plasmodium falciparum* as an assessment of parasitemia. *Am. J. Trop. Med. Hyg.* (1993) 48 (2) 205-210.

10. M T Makler, J M Ries, J A Williams, J E Bancroft, R C Piper, B L Gibbins, and D J Hinrichs. Parasite lactate dehydrogenase as an assay for *Plasmodium falciparum* drug sensitivity. *Am. J. Trop. Med. Hyg.* (1993) 48 (6) 739-741.

11. B R Shenai, B J Lee, A Alvarez-Hernandez, P Y Chong, C D Emal, R J Neitz, W R Roush, and P J Rosenthal. Structure-Activity Relationships for Inhibition of Cysteine Protease Activity and Development of *Plasmodium falciparum* by Peptidyl Vinyl Sulfones. *Antimicrob. Agents Chemother.* (2003) 47 (1) 154-160.

12. P S Sijwali and P J Rosenthal. Gene disruption confirms a critical role for the cysteine protease falcipain-2 in hemoglobin hydrolysis by *Plasmodium falciparum*. *Proc. Natl. Acad. Sci. USA.* (2004) 101 (13) 4384-4389.

13. T J Egan. Structure-function relationships in chloroquine and related 4-aminoquinoline antimalarials. *Mini Rev. Med. Chem.* (2001) 1 113-123.

14. M Liu, P Wilairat, and M-L Go. Antimalarial alkoxylated and hydroxylated chalcones: structure-activity relationship analysis. *J. Med. Chem.* (2001) 44 4443-4452.

15. C E Gutteridge, D A Nichols, S M Curtis, D S Thota, J V Vo, L Gerena, G Montip, C O Asher, D S Diaz, C A DiTusa, K Smith, and A K Bhattacharjee. *In vitro* and *in vivo* efficacy and *in vitro* metabolism of 1-phenyl-3-aryl-2-propen-1-ones against *Plasmodium falciparum*. *Bioorg. Med. Chem. Lett.* (2006) 16 5682-5686.

16. P J Rosenthal and S R Meshnick. Hemoglobin catabolism and iron utilization by malaria parasites. *Mol. Biochem. Parasitol.* (1996) 83 131-139.

17. J Liu, E S Istivan, I Y Gluzman, J Gross, and D E Goldberg. *Plasmodium falciparum* ensures its amino acid supply with multiple acquisition pathways and redundant proteolytic enzyme systems. *Proc. Natl. Acad. Sci. USA.* (2006) 103 (23) 8840-8845.

18. I Weissbuch and L Leiserowitz. Interplay Between Malaria, Crystalline Hemozoin Formation, and Antimalarial Drug Action and Design. *Chem. Rev.* (2008) 108 4899-4914.

19. S Kumar, M Guha, V Choubey, P Maity, and U Bandyopadhay. Antimalarial drugs inhibiting hemozoin ([]-hematin) formation: a mechanistic update. *Life Sci.* (2007) 80 813-828.

20. B L Tekwani and L A Walker. Targeting hemozoin synthesis pathway for new antimalarial drug discovery: technologies for *in vitro* []-hematin formation assay. *Comb. Chem. High Throughput Screening* (2005) 8 63-79.

21. K Ncokazi and T Egan. A colorimetric high-throughput []-hematin inhibition screening assay for use in the search for antimalarial compounds. *Anal. Biochem.* (2005) 338 306-319.

22. P J Rosenthal. Cysteine proteases of malaria parasites. *Int. J. Epidemiol.* (2004) 34 1489-1499.

23. R Bhaskar and P J Rosenthal. Reducing requirements for hemoglobin hydrolysis by *Plasmodium falciparum* cysteine proteases. *Mol. Biochem. Parasitol.* (2002) 122 99-104.

24. J H McKerrow, J C Engel, and C R Caffrey. Cysteine Protease Inhibitors as Chemotherapy for Parasitic Infections. *Bioorg. Med. Chem.* (1999) 7 639-644.

25. B-K Na, T-S Kim, P J Rosenthal, J-K Lee, and Y Kong. Evaluation of cysteine proteases of *Plasmodium vivax* as antimalarial drug targets: sequence analysis and sensitivity to cysteine protease inhibitors. *Parasitol. Res.* (2004) 94 312-317.

26. B J Lee, A Singh, P Chiang, S J Kemp, E A Goldman, M I Weinhouse, G P Vlasuk, and P J Rosenthal. Antimalarial Activities of Novel Synthetic Cysteine Protease Inhibitors. *Antimicrob. Agents Chemother.* (2003) 47 (12) 3810-3814.

27. J N Dominguez, J E Charris, G Lobo, N G de Dominguez, M M Moreno, F Riggione, E Sanchez, J Olson, and P J Rosenthal. Synthesis of quinolinyl chalcones and evaluation of their antimalarial activity. *Eur. J. Med. Chem.* (2001) 36 555-560.

28. S M Huber, C Lang, F Lang, and C Duranton. Organic osmolyte channels in malaria-infected erythrocytes. *Biochem. Biophys. Res. Com.* (2008) 376 514-518.

29. H M Staines, C Rae, and K Kirk. Increased permeability of the malaria-infected erythrocyte to organic cations. *Biochim. Biophys. Acta* (2000) 1463 88-98.

30. K Kirk and H A Horner. In search of a selective inhibitor of the induced transport of small solutes in *Plasmodium falciparum*-infected erythrocytes: effects of arylaminobenzoates. *Biochemistry* (1995) 311 761-768.

31. M L Go, M Liu, P Wilairat, P J Rosenthal, K J Saliba, and K Kirk. Antiplasmodial Chalcones Inhibit Sorbitol-Induced Hemolysis of *Plasmodium falciparum*-Infected Erythrocytes. *Antimicrob. Agents Chemother.* (2004) 48 (9) 3241-3245.

32. M Liu, P Wilairat, and M-L Go. Antimalarial Alkoxylated and Hydroxylated Chalones: Structure-Activity Relationship Analysis. *J. Med. Chem.* (2001) 44 4443-4452.

33. M Liu, P Wilairat, S L Croft, A L-C Tan, and M-L Go. Structure–Activity Relationships of Antileishmanial and Antimalarial Chalcones. *Bioorg. Med. Chem.* (2003) 11 2729-2738.

34. H Ginsburg and M Krugliak. Chloroquine - some open questions on its antimalarial mode of action and resistance. *Drug Resist. Updates* (1999) 2 180-187.

35. P G Bray, M Mungthin, R G Ridley, and S Ward. Access to Hematin: The Basis of Chloroquine Resistance. *Mol. Pharmacol.* (1998) 54 170-179.

36. A Yayon, Z I Cabantchik, and H Ginsburg. Susceptibility of human malaria parasites to chloroquine is pH dependent . *Proc. Natl. Acad. Sci. USA.* (1985) 82 2784-2788.

37. P H Schlesinger, D J Krogstad, and B L Herwaldt. Antimalarial Agents: Mechanisms of Action. *Antimicrob. Agents Chemother.* (1988) 32 (6) 793-798.

CHAPTER FIVE

INTEGRATION OF *IN SILICO* TOOLS IN THE IDENTIFICATION OF *IN VITRO* HITS WITH SUPERIOR PREDICTED PHYSICOCHEMICAL AND ADME PROPERTIES

5.1 Preamble

This chapter contains the work done to address the third specific aim of the study, which was: To apply *in silico* (computational) techniques to guide the design of derivatives of the more active compounds with potentially superior physicochemical and/or ADME properties for subsequent synthesis as well as *in vitro* and *in vivo* antimalarial testing and mechanistic studies.

The chapter begins by briefly introducing *in silico* (computational) prediction of physicochemical and ADME (Absorption, Distribution, Metabolism and Excretion), as well as the main determinants of oral bioavailability. It then goes on to describe the *in silico*-guided design of proposed analogs, as well as the subsequent synthesis, characterization and *in vitro* antimalarial testing of the selected analogs. The chapter then concludes with a brief description of, and the results from, limited mechanistic studies on selected analogs.

5.2 *In silico* (computational) prediction of physicochemical and ADME properties

It is widely acknowledged that challenging ADME properties significantly hamper the development of many promising compounds into leads and drug candidates [1,2]. This has led to an increased interest in the early determination (and/or prediction) of ADME properties of compounds, and it is therefore becoming increasingly routine for compounds to be simultaneously filtered *in vitro* for potency and *in silico* (and *in vitro*) for suitable ADME properties [1].

Of interest to the current study was the application of *in silico* tools in the prediction of ADME and physicochemical properties of compounds. *In silico* ADME prediction models and tools complement *in vitro* and *in vivo* ADME efforts by facilitating the characterization of the ADME properties of compounds prior to their synthesis. In other words, a reliable ADME predictive model can be applied on a set of proposed compounds to identify those that are more likely to have favorable pharmacokinetic properties, thereby enabling their prioritization for synthesis and subsequent *in vitro*

and/or *in vivo* biological evaluation [2]. Such an approach would save time and resources by focusing synthetic and experimental evaluation efforts on a smaller number of more promising compounds.

Any property of a particular molecule is encoded in its structure. A molecule's structure can be resolved into a complement of molecular descriptors, which are essentially measured or calculated properties of the molecule e.g. molecular weight, polar surface area, etc. It therefore follows that the properties of a molecule can be deduced from molecular descriptors derived from its structure, and that for different properties, the sets of molecular descriptors that would be employed would be different [3]. Many *in silico* prediction tools, including the tools used in the current study, are based on this concept, and apply molecular descriptors (and the 3-D molecular interaction fields used to generate these molecular descriptors) as inputs in building the mathematical/statistical models that are then applied in the prediction of physicochemical and ADME properties of compounds. Properties that may be predicted in this way include solubility, LogP/LogD, passive permeability, metabolic stability, plasma protein binding and volume of distribution.

It is noted that this process is not as straight-forward as it would appear to be [3]. For example, a variety of models can be developed to predict the same property, and the predictive capacity of such models would be inherently different. This predictive capacity would vary depending on the molecular descriptors used as inputs in the building of the individual models, the mathematical/statistical approach applied (and attendant assumptions made) in building the model, the chemical diversity/chemical space covered by the set of compounds used to train each model, and/or the quality of the data accompanying the training set of compounds. Furthermore, the prediction of ADME parameters is quite challenging because of the complicated nature of the actual *in vivo* ADME processes resulting from the complexities of participating organs and the simultaneous involvement of multiple mechanisms [1,2,4].

A recognition of these limitations implies that results from such predictions should not be over-interpreted, and has even led to proposals for the estimation of the applicability domain and prediction accuracy of models prior to their actual utilization for a given set of compounds [5].

However, despite these challenges, computational tools developed for the prediction of physicochemical and ADME properties have been successfully applied in the

characterization of compounds, with their results being corroborated by *in vitro* and/or *in vivo* ADME assays. For example, MetaSite®, which was one of the tools used in the current study, was used to predict the sites of metabolism of several derivatives of the non-steroidal anti-inflammatory drug (NSAID) indomethacin. MetaSite® accurately predicted the sites of metabolism of the range of derivatives studied, with the predictions found to be in close agreement with the results from *in vitro* and *in vivo* metabolism experiments carried out on the derivatives [6].

The current study applied available *in silico* prediction tools in the characterization of compounds proposed for synthesis and which were based on promising compounds identified from the *in vitro* antimalarial assays described in the preceding Chapter. A deliberate attempt was made not to over-interpret the predictions, but rather use them only as a guide in determining whether or not the proposed compounds were likely to be improvements on the parent compounds. An attempt was also made to experimentally corroborate some of the predictions.

5.3 The Tools

Three software packages, with varying but complementary capabilities, were available for use in the *in silico* prediction of various physicochemical and ADME parameters. These were:

- VolSurf+®: this software package computes 3D molecular interaction fields of molecules, and then compresses and converts these fields into a range of molecular descriptors that numerically characterize size, shape, polarity, and hydrophobicity of the molecules. Descriptors of this kind generated for extensive databases of diverse compounds are then utilized in the generation of mathematical/statistical models which can be applied for the prediction of various physicochemical and ADME parameters of compounds, such as aqueous solubility, LogP (n-octanol/water), LogD (at various pHs), Caco2 permeability, metabolic stability, etc [7,8].
- MetaSite®: this is an automated tool for the rapid prediction of the possible site(s) of metabolism of molecules by hepatic cytochromes (which constitute the bulk of the enzymes involved in drug metabolism in the liver) during phase I metabolism. MetaSite® also provides the structures of the predicted metabolites along with a probability ranking derived from the site of metabolism predictions. In addition to predicting the site of metabolism, this software package also highlights the atoms or

groups in the molecule that contribute to the prediction (i.e. that help direct the molecule into the cavity of the cytochrome's active site such that the predicted site of metabolism is in proximity to the catalytic centre) [6,9].

- **MoKa®:** this is a software tool that enables the quick and accurate prediction of the pKa of ionizable compounds; in addition, it also predicts (and graphically represents) the relative species abundance at various pHs [10].

5.4 The main determinants of oral bioavailability

The main aim of the derivatization exercise was to identify analogs with optimized oral bioavailability. This is because, for antimalarial drugs, oral administration is often the desired route for their delivery as it enhances patient compliance while reducing formulation and administration costs. This is important considering the financial challenges facing much of the population most affected by malaria [11]. It was therefore necessary to first identify the main properties/parameters that would need to be addressed.

The overall proportion of an orally administered drug that is delivered into systemic circulation (i.e. its oral bioavailability) is dependent on the outcome of several main factors, as shown in Figure 5.1.

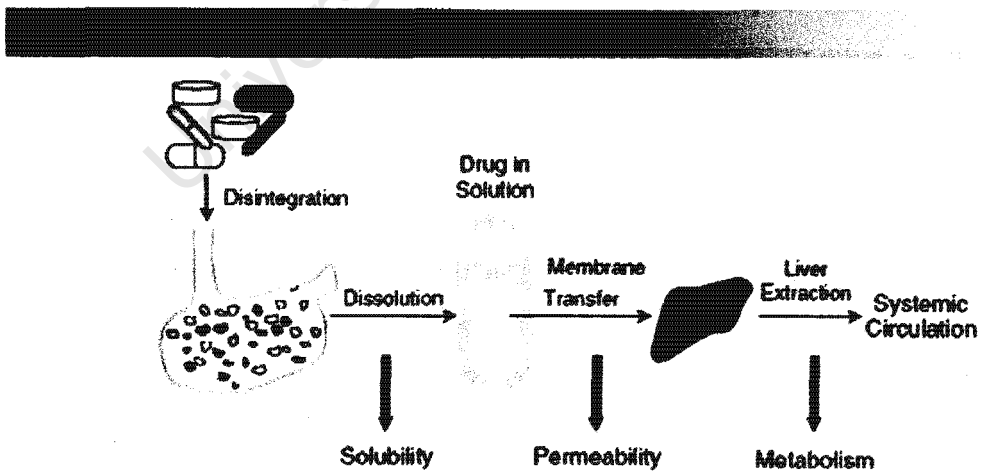

Figure 5.1: Figure showing the various processes between the oral administration of a drug and its delivery into systemic circulation [12]

5.4.1 Solubility

The compound must be in solution before it can be absorbed; it could either be dissolved in an aqueous system prior to administration, or administered as a solid or suspension dosage form whereby it is expected to dissolve into the mainly aqueous contents of the gastro-intestinal (G.I.) tract after administration. The degree to which a compound dissolves (i.e. its intrinsic solubility) and which would directly impact on its oral bioavailability is dependent on, among other things, its chemical structure and (in the case of ionizable compounds) the pH of the aqueous environment that it is dissolving in [12,13].

5.4.2 Permeability

Once in solution, the compound then diffuses to the wall of the G.I. tract, through which it permeates and enters the G.I. blood circulation. Biological membranes are essentially lipid bi-layers, and hence permeation through the G.I. wall involves the partitioning of the compound between aqueous phases (G.I. contents, intracellular cytosol and blood plasma) and lipid phases (biological membranes). The permeability of compounds through the G.I. tract wall is therefore dependent on their relative affinities for aqueous and lipophilic phases, a characteristic that is usually represented by the logarithm of the organic solvent/water partition coefficient (i.e. LogP). For ionizable compounds, this partition coefficient is pH dependent and usually expressed as the LogD of the compound, which is essentially its LogP at a specified pH [12].

It is no surprise, therefore, that LogP/LogD has been identified as a critical physicochemical property that influences oral bioavailability, and has been included in proposed guidelines for the design of compounds with favorable oral bioavailability such as the Lipinski 'rule of 5' [14].

The higher the lipophilicity of the compound, the higher it's LogP/LogD, and hence the faster it's expected permeation through biological membranes; however, increased lipophilicity is obviously at the expense of aqueous solubility, as depicted in Figure 5.2 below. Therefore, the aim is usually to strike a balance between the two antagonistic properties, with LogP range of 0 – 3 being proposed as optimal [12]; this and other similar ranges are usually viewed more as guidelines rather than absolute cutoffs [15].

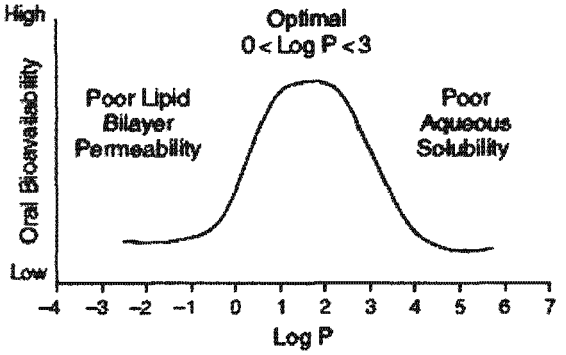

Figure 5.2: The relationship between aqueous solubility, LogP and oral bioavailability [12]

5.4.3 Metabolic stability

Once in the G.I. circulation, the compound is then carried through to the liver *via* the hepatic portal vein. The liver is the primary metabolic and detoxification organ of the body, responsible for the chemical transformation and elimination of the majority of xenobiotics. This implies that any drug/compound must survive hepatic metabolism during this initial passage through the liver (referred to as *first pass metabolism*) in order to enter systemic circulation [12,16]. The metabolic stability of an orally administered compound is therefore crucial in determining the proportion of the compound that survives this first-pass metabolism.

The above description is by no means exhaustive, and represents a very simplified version of the oral absorption process that does not take into account the effects of, for example, G.I. contents, active transport, efflux pumps, G.I. metabolism, etc [13]. Nevertheless, these three fundamental properties have a direct and apparent bearing on the oral bioavailability of compounds, and as such need to be addressed as early as possible in any drug discovery initiative.

5.5 Strategies to improve oral bioavailability

In general, strategies for improving the oral bioavailability of a compound involve either the use of formulations and/or the rational structural modification of the compound, i.e. the design and synthesis of related compounds predicted to have more favourable physicochemical and ADME profiles relative to the parent compound, and which retain biological activity.

Both these approaches have been considered in the current study, though this Chapter focuses on the latter of the two. Formulations as a strategy will be introduced and discussed in Chapter Six, along with the findings from the actual PK and *in vivo* efficacy determinations.

5.6 Design and characterization of proposed analogs

5.6.1 Selection of compounds for derivatization

As mentioned in Chapter Four above, compound 3.15b was the most promising of the target compounds so far synthesize based on *in vitro* antimalarial results. The next logical step would therefore have been to examine the PK and efficacy profiles of the compound under *in vivo* conditions.

However, one of the main concerns about this compound (and which was a feature shared by all the tested compounds) was its poor aqueous solubility. This poor solubility necessitated the use of up to 10% DMSO as co-solvent (along with extended periods of sonication and agitation) during sample preparation prior to the *in vitro* antimalarial assays. As mentioned above, aqueous solubility, along with permeability and metabolic stability, is a key determinant of oral bioavailability, and therefore the aqueous solubility challenges of the compound observed during the *in vitro* procedures could possibly have a detrimental effect on its oral bioavailability.

In anticipation of such a situation, the primary focus was therefore to design and synthesize analogs of 3.15b with improved aqueous solubility. The other parameters outlined above that are also necessary for good oral bioavailability would be considered as well. Promising analog(s) would then be synthesized and evaluated *in vivo* alongside 3.15b.

However, it was apparent from the outset that this compound had notable constraints with respect to its chemical tractability, with the range of possible analogs somewhat limited (without deviating significantly from the parent structure or adding significantly to its molecular weight). With this in mind, the intermediate 3.19, which also showed notable *in vitro* antimalarial activity, was selected along with 3.15b (Figure 5.3). This was due to its potential for a more diverse range of analogs afforded by the open-ended nature of the butenone side-chain.

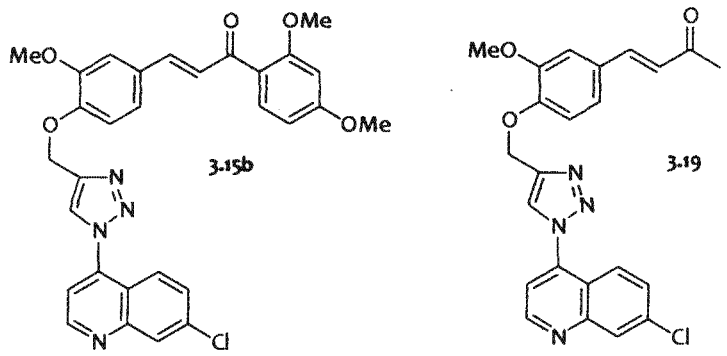

Figure 5.3: Structures of compounds selected for structural modification (3.15b and 3.19)

The evaluation of such potentially enhanced compounds based on the two selected compounds was to be guided by the *in silico* (computational) tools, as described below.

5.6.2 Selection of characterization parameters

Considering the myriad of possible physicochemical and ADME descriptors that could be predicted using the software tools available, it was necessary to first identify a manageable but adequate complement of these parameters that would be considered in the characterization of the selected compounds as well as guide in the design and evaluation of any subsequently proposed analogs.

The set of parameters to be derived was based on:

- The overall objective of the derivatization process, which was to enhance oral bioavailability.
- The range of physicochemical parameters that could be generated by the software packages available, and that can be directly and meaningfully interpreted.
- The range of ADME parameters that could be generated by the software packages available; these are limited by the number of in-built predictive models.

Critical for oral bioavailability and an obvious limitation of the two selected compounds, solubility (represented as the logarithm of the molar aqueous solubility at 25°C and at a specified pH, LogS) was therefore chosen as one of the parameters for characterization.

LogD was also selected as another parameter for characterization. This represents the logarithm of the partition coefficient between an organic phase and water at a specified pH, and gives a measure of the lipophilicity/hydrophilicity balance of the compound, taking into account the presence of any ionizable groups.

In addition, Caco2 permeation, which represents one of the *in vitro* methods available for assessing permeability (and which could be predicted by the software available), was also selected as a parameter for characterization. This parameter describes the ability of a compound to traverse across a Caco2 epithelial cell monolayer (under the assumption of passive, transcellular permeation); the output of the prediction of this parameter is qualitative, indicating a good, intermediate or poor ability to permeate through the epithelial cells.

Metabolic stability is crucial in estimating the proportion of the compound that would survive first-pass hepatic metabolism and, for this reason, was selected as a characterization criterion of interest. This predicted metabolic stability provides an estimate of the metabolic stability of a compound when a predetermined concentration of the compound is incubated for 60 minutes with a fixed concentration of the enzymes at 37°C. The interpretation of the output of this predictive model is also qualitative.

In addition, pKa predictions and site of metabolism predictions were also determined to provide support information, as appropriate.

5.6.3 Design and characterization of proposed analogs

In order to design analogs of 3.15b and 3.19, it was necessary to first identify the core structural feature(s) of the compounds that would be retained in the analogs with a view to maintaining the observed antimalarial activity. The choice of what sub-structures would be retained based on the anticipated mechanisms of action of the compounds.

Literature, along with the limited mechanistic studies so far carried out in this study (section 4.4) indicated that inhibition of hemozoin formation and, to a lesser extent, Falcipain 2 inhibition could be possible mechanisms of action of this type of compounds. For this reason, the core structural features identified for retention were the chloroquinoline moiety and either the phenyl-butenone moiety (for 3.19) or the chalcone moiety (for 3.15b) (Figure 5.4)- the chloroquinoline moiety for its potential role in hemozoin inhibition, and the chalcone and phenyl-butenone moieties for their

possible dual roles in malarial cysteine-protease inhibition [17], and in facilitating inhibition of hemozoin formation through π-π stacking interactions.

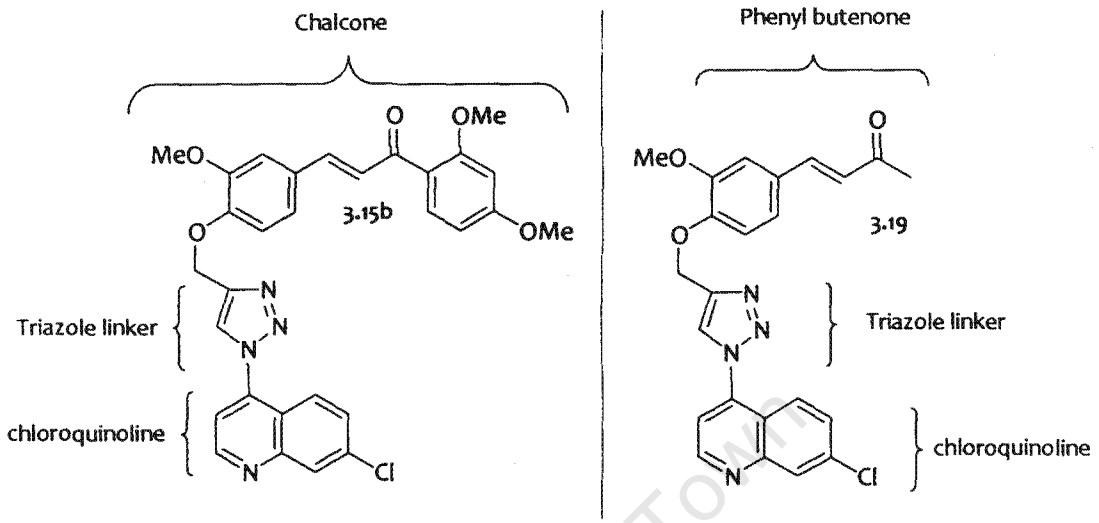

Figure 5.4: Figure showing the core structural features of 3.15b and 3.19

With these core features in mind, the sites on these two compounds that offer themselves for convenient modification/replacement were the triazole ring (here considered as a linker between the chloroquinoline and chalcone/phenyl-butenone groups), as well as the terminal carbon of the butenone side chain of 3.19.

5.6.3.1 Replacement of the triazole ring:

With the primary goal being to improve aqueous solubility, the types of structural modifications that would facilitate this improvement were considered, such as the introduction of ionizable groups, the reduction of LogP, and the introduction of polar groups and groups capable of hydrogen bonding [12]. Synthetic accessibility was an attendant consideration.

Figure 5.5 shows the first set of proposed analogs, in which the triazole linker has been replaced with a variety of other linkers.

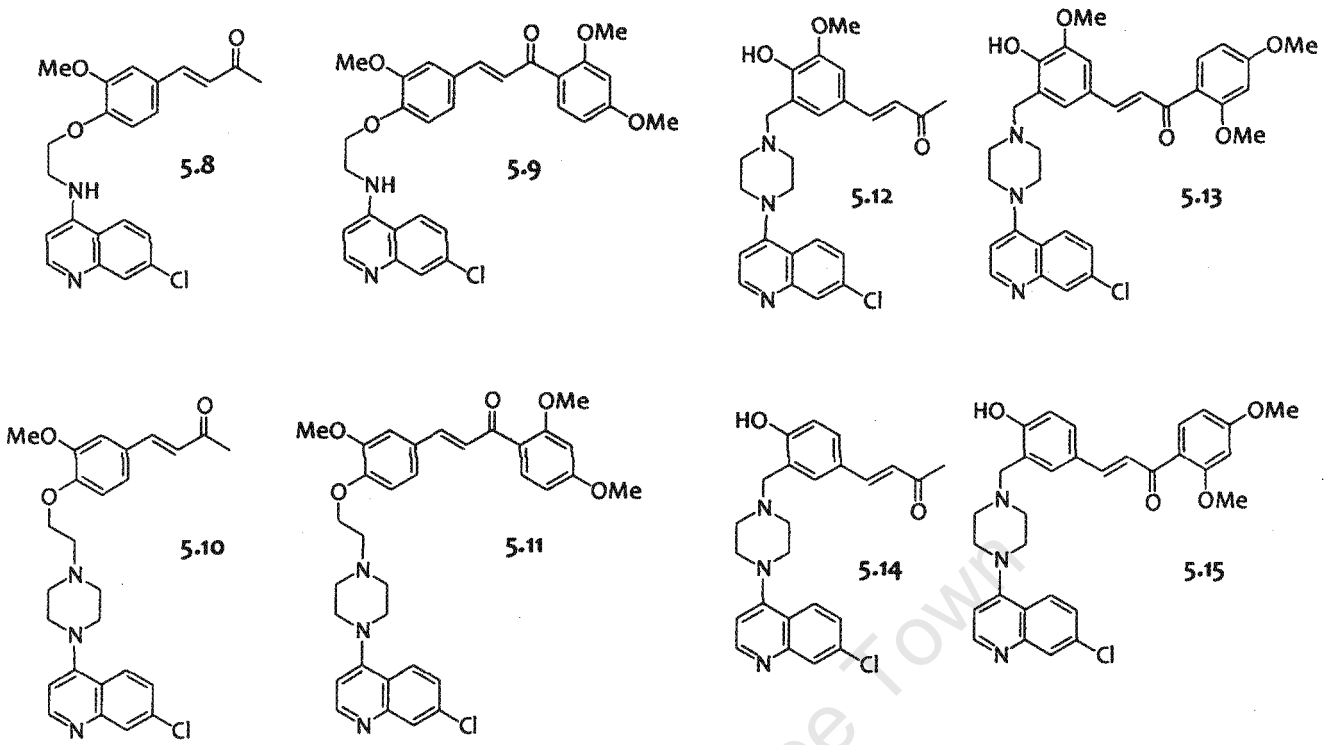

Figure 5.5: Figure showing the structures of the analogs of 3.19 and 3.15b derived from replacement of the triazole linker

Compounds 5.8 and 5.10 were analogs of 3.19 in which the triazole linker has been replaced with the amino-ethoxy linker and the piperazinyl-ethoxy linker, respectively. Compounds 5.9 and 5.11 are the equivalent analogs of 3.15b.

The piperazinyl-methyl linker was introduced for compounds 5.12 and 5.13; however, rather than have the linker attaching at the 4-O position of the chalcone/phenyl-propenone sub-unit (as was the case with 5.8 – 5.11), the point of attachment was at the 5-position, leaving the 4-hydroxy-group untouched. This introduced a little more diversity into the analogs proposed.

The proposed compounds 5.14 and 5.15 were analogs of 5.12 and 5.13, respectively, in which the 3-methoxy group has been omitted, again to introduce some diversity to the analogs as well as introduce the possibility for even further structural modifications at the 3-position (see Figure 5.13)

In the proposed analogs, the amino-alkyl or piperazinyl-based linkers all introduce the 4-amino-substitution on the chloroquinoline sub-unit. The introduction of a 4-amino group on the chloroquinoline ring enhances the pKa of the nitrogen on the quinoline ring, thereby increasing its basicity and enhancing ionization at this position; the resultant compounds are thus more polar and this in turn enhances their (pH-

dependent) solubility. This feature has been successfully exploited in the formulation of chloroquine and amodiaquine, both of which are available as water-soluble salts.
In addition, the piperazinyl-based linkers possess a second protonatable nitrogen, further enhancing the possible ionization of the analogs bearing this type of linkers.

The incorporation of an ionizable centre, such as an amine or similar function, is a recognized strategy of improving water solubility of compounds [18]. Though this is the most common way of increasing solubility and ultimately bioavailability of poorly-soluble compounds [19], this type of pH dependent solubility comes with its own set of limitations and concerns. A drastic change in pH would result in a loss of solubility, and the result could be the precipitation of such a compound out of solution.

In addition, some molecules cannot traverse across the highly lipophilic biological membranes in the charged state, implying that complete ionization of such compounds, while being advantageous at improving solubility, could be detrimental to absorption and oral bioavailability - this is particularly so for acidic compounds. However, the partitioning of basic compounds is reportedly highly favored and independent of the degree of ionization. This is believed to be due to electrostatic interactions with charged membrane phospholipids such as the acidic phospholipid phosphatidylserine; this property is not shared with acidic compounds [18].

However, most organic molecules are usually weak acids or bases, thereby ensuring the existence of an equilibrium between the ionized and non-ionized forms of the compound at intermediate pHs. This implies the continued presence of the non-ionized species that can cross the biological membranes, and which is continually replenished from the reservoir of the ionized species by readjustment of the equilibrium as absorption progresses. Such equilibria would be favoured by the rather gradual pH transition of G.I. contents as they move along the G.I. tract.

5.6.4 *In silico* characterization of 3.15b, 3.19 and the proposed analogs

As the two compounds selected for derivatization 3.15b and 3.19 (as well as the proposed analogs) were chloroquinoline-based compounds, it was thought prudent to select the clinically approved chloroquinoline-based drugs amodiaquine and chloroquine (Figure 5.6) as benchmarks for the characterizations. In other words, chloroquine and amodiaquine would be characterized along with the study compounds to allow for comparison of the results, and in this way inferences could be

made on how these compounds compared with the two established drugs. A deliberate attempt was made not to over-interpret the prediction results, but rather use them only as a guide in determining whether or not the proposed compounds were likely to be improvements on the parent compounds 3.15b and 3.19, and to highlight any potential liabilities.

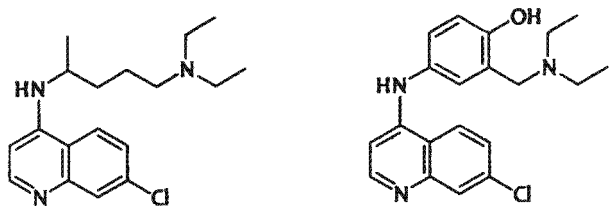

Fig. 5.6: Chloroquine and amodiaquine, examples of chloroquinoline-based antimalarial drugs

Characterization of the compounds and the two reference drugs yielded the following highlights:

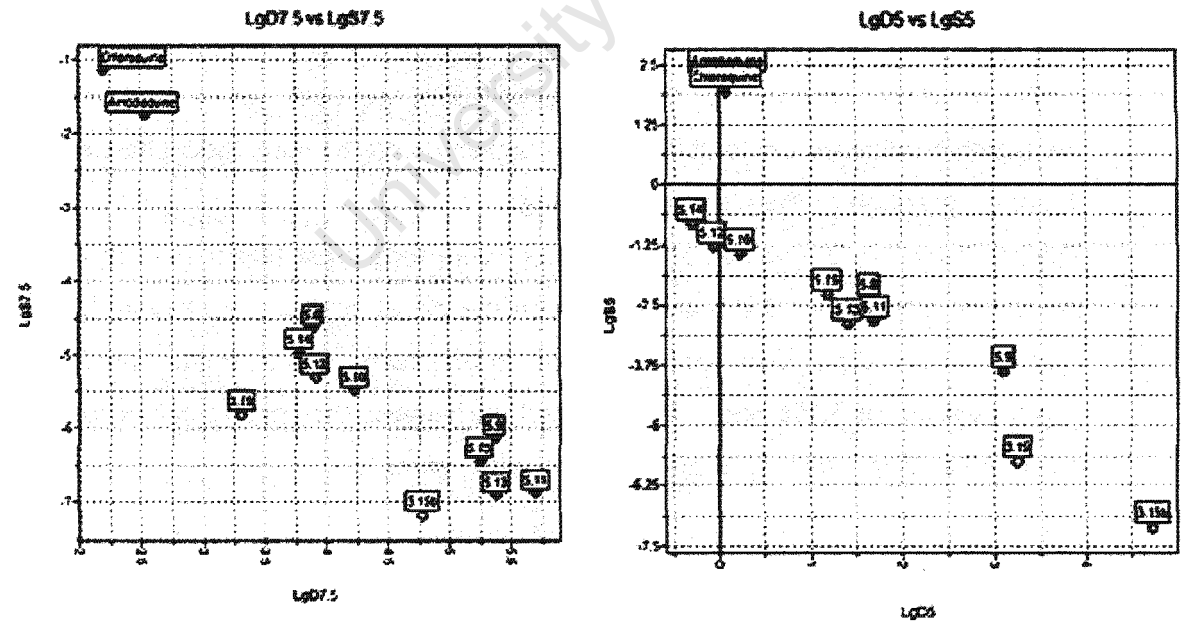

Fig. 5.7: Plots of predicted solubility (expressed as the logarithm, log S) against the predicted n-Octanol-water partition coefficient (also expressed as the logarithm, log D) at pH 5.0 and at pH 7.5

- Chloroquine and amodiaquine show significantly superior predicted aqueous solubility both at approximately physiological pH (pH 7.5) and at pH 5.0 when compared to **3.15b**, **3.19** and the proposed analogs (**Figure 5.7**).
- At both pH 5.0 and 7.5, **3.15b** showed the lowest predicted solubility; **3.19** was predicted to be more soluble than **3.15b**, and this is most likely as a result of its lower molecular weight. Expectedly, a similar trend is seen for the proposed compounds, whereby analogs of **3.19** are predicted to be more soluble than the corresponding analogs of **3.15b**.
- At pH 7.5, the predicted solubilities of the proposed analogs were only slightly higher than those of the parent compounds. However, and as anticipated, there is a significant influence of pH on the predicted solubilities of the proposed compounds – the predicted solubilities were significantly higher at pH 5.0 than at pH 7.5. This is attributable to the fact that these compounds, being basic, would exist predominantly in their ionised state at lower pH levels, rendering them more soluble. Analysis on MoKa® indicated that compounds **5.8 – 5.15** are predicted to be >90% ionised at pH 5.0.
- The number of protonable centres was also found to influence this pH dependent solubility. For example, among the analogs of **3.19**, the piperazinyl analogs **5.10**, **5.12** and **5.14** (which have two protonable centres) were found to have higher predicted solubilities than the amino-ethoxy analog **5.8**. This was despite the fact that these three piperazinyl derivatives have higher molecular weights than **5.8**. A similar trend was observed for the analogs of **3.15b**, and both can be attributed to the positive influence on solubility of the higher charge to mass ratio afforded by the di-protonation of the piperazinyl analogs.
- The predicted $LogD_{7.5}$ values of the analogs were somewhat higher than those of the parent compounds **3.15b** and **3.19**, with the piperazinyl analogs having higher $LogD_{7.5}$ values than their amino-ethoxy counterparts. Whereas the predicted $LogD_{5.0}$ values for **3.15b** and **3.19** remained unchanged, the $LogD_{5.0}$ values for the proposed analogs were significantly lower, with values ≥ 3.1.

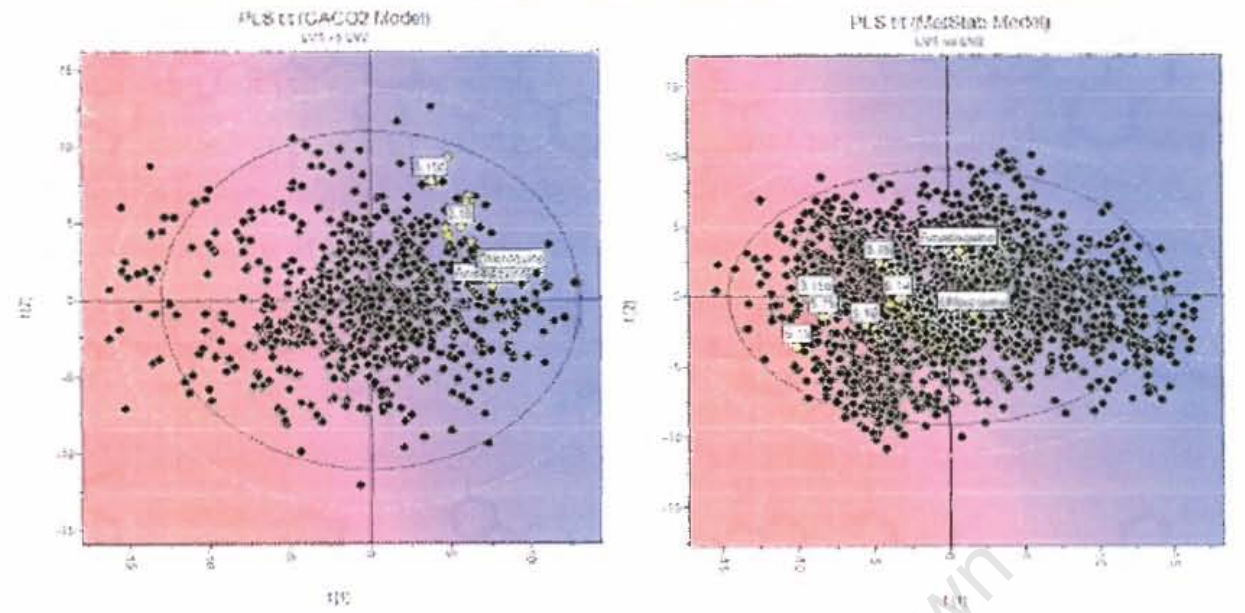

Fig. 5.8: Plots showing the proposed analogs projected onto the PLS models used to predict Caco2 permeability and metabolic stability – the black dots represent the compounds comprising the models' training data sets while the yellow dots represent the test compounds: the blue regions indicate acceptable predicted permeability/metabolic stability while the red zones indicate poor predicted properties.

- Prediction and interpretation of Caco2 permeability was essentially qualitative. When projected onto the two-dimensional PLS plot of the database of compounds used to generate the in-built Caco2 permeation model, all the compounds (along with chloroquine and amodiaquine) show acceptable Caco2 permeation - they fall within the blue zone of the plot (Figure 5.8).
- Amodiaquine and chloroquine are predicted to have intermediate metabolic stability, falling somewhat between the blue and red zones on the PLS plot (Fig. 5.8). However, the two are predicted to be more stable to metabolism than the test compounds.
- 3.15b is predicted to be less stable to hepatic metabolism than 3.19. The proposed analogs are also shown to have relatively low predicted metabolic stabilities, particularly compounds 5.11, 5.15 and 5.10.

  Site of metabolism analysis was carried out on MetaSite® in an attempt to shed light on these findings (Figure 5.9).

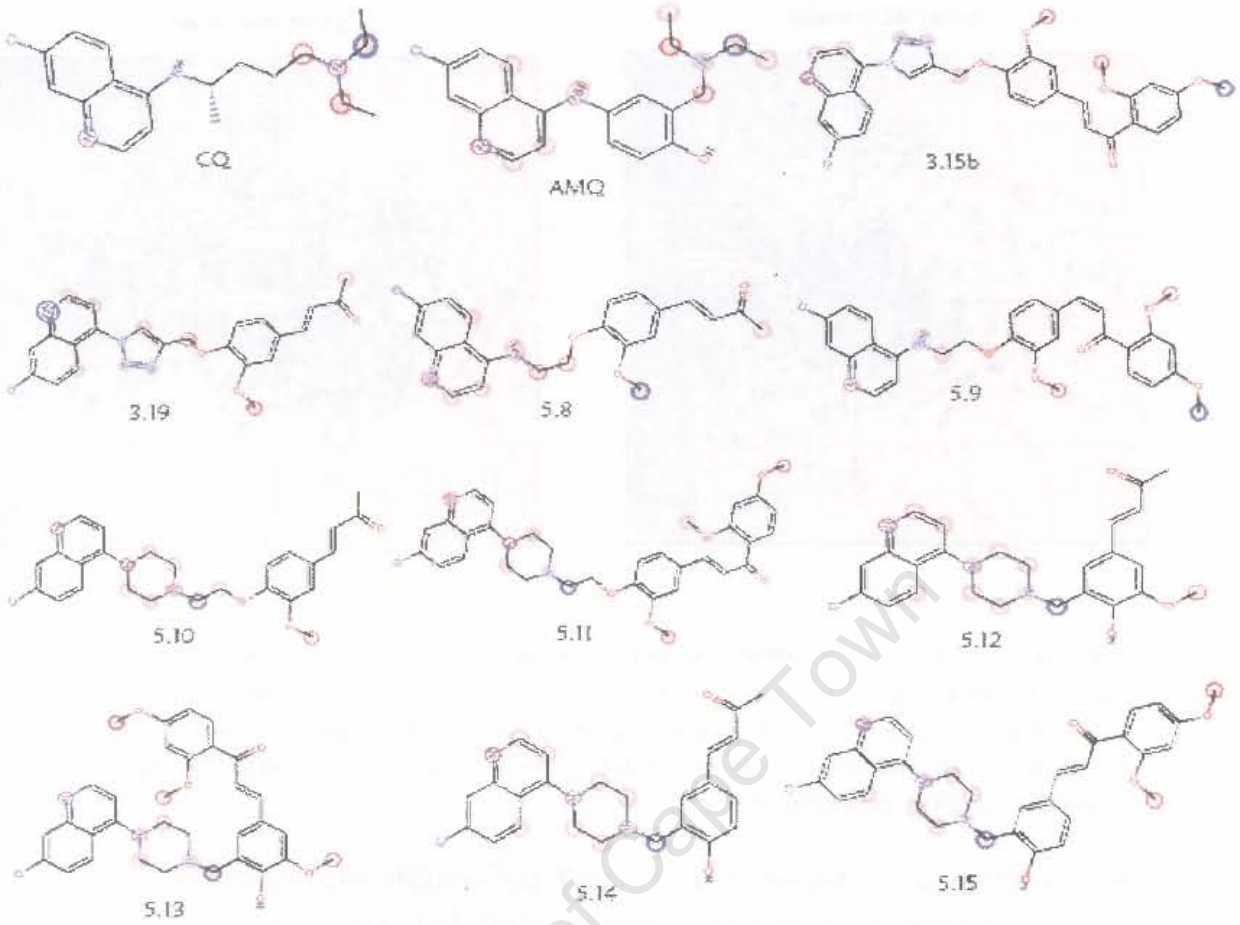

Fig. 5.9: Output from MetaSite® showing the predicted sites of metabolism on the various analogs. The blue ring indicates the predicted main site of metabolism; red and pink rings indicate other predicted possible sites of metabolism (the more intense the color, the more likely the site).

- N-dealkylation of the nitrogen-containing side-chain is the principle route of metabolism for chloroquine and amodiaquine as predicted by MetaSite®. This is in agreement with reported experimental findings, with their main metabolites identified as N-desethylchloroquine and N-desethylamodiaquine, respectively [20,21]. N-oxidation of the quinoline nitrogen (highlighted by MetaSite® as a possible site of metabolism) does not seem to be a favoured route of metabolism for this class of compounds.
- The main route of metabolism for 3.15b is predicted as being O-demethylation of the *para*-methoxy group on ring B - this group is absent in 3.19. O-demethylation on ring A and N-oxidation of the quinoline ring are the main routes of metabolism predicted for 3.19, but these may not be as efficient as O-demethylation on ring B, and this is probably why this compound is predicted to be more stable to metabolism than 3.15b.

- N-dealkylation of the nitrogen-containing linkers was predicted as a possible route of metabolism for the proposed analogs. The piperazinyl-based linkers (present in 5.10 - 5.15) appeared to be predicted as being particularly susceptible to N-dealkylation, and is possibly why these compounds were predicted as being relatively unstable to metabolism. A combination of this and the additional possibility of O-demethylation on ring B for 5.11 is probably why this compound was predicted to be the least stable of them all.
- The amino-ethoxy linker (present in 5.8 – 5.9) appears to be somewhat less susceptible to N-dealkylation, and was not predicted as the primary route of metabolism for these compounds, which are among the relatively more stable analogs.

In summary, compounds 3.15b and 3.19 showed poor predicted solubility profiles, a factor that could be detrimental to their potential oral bioavailability as well as their distribution once absorbed. They had acceptable predicted Caco2 permeation when compared to the reference compounds chloroquine and amodiaquine, though their metabolic stability was predicted to be lower.

The proposed analogs had improved predicted solubilities relative to their parent compounds, particularly at lower pH, and this was a feature that could possibly be utilized during their solubilization for PK studies. The analogs also maintained acceptably high predicted Caco2 permeability. The main alert was their possible metabolic instability, primarily due to N-dealkylation of the nitrogen-containing linkers or O-demethylation of the ring B of the chalcone derivatives.
The analogs were nevertheless synthesized for *in vitro* antimalarial evaluation, to establish if they retained antimalarial activity. In addition, experimental solubility determination and *in vitro* metabolism studies were also carried, and the results compared to those from the *in silico* predictions

5.7 Synthesis and characterization of the proposed analogs

5.7.1 Synthesis

The hydroxylated enones (5.1 and 5.3) and chalcones (5.2 and 5.4) were intermediates in the synthesis of these compounds; the synthesis of these intermediates is depicted in Scheme 5.1, and involved the acid-catalyzed Claisen-Schmidt reaction.

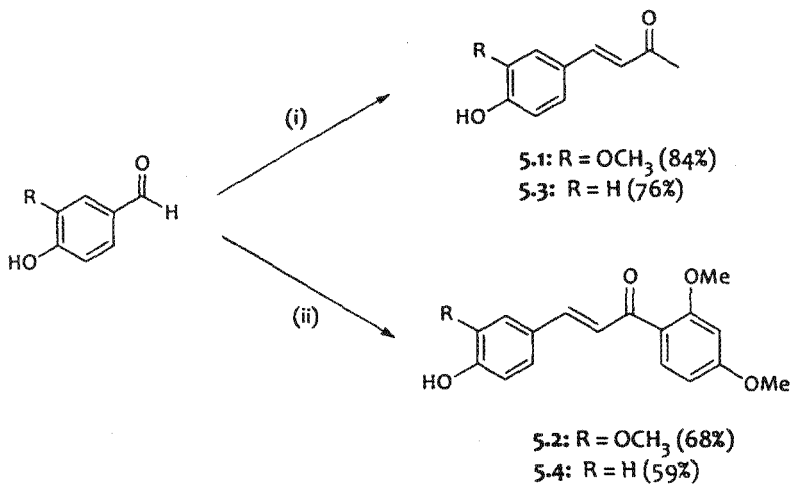

Scheme 5.1: *Reagents and conditions:* (i) acetone, 5M HCl, rt, 24 hrs; (ii) 2',4'-dimethoxy acetophenone, 5M HCl, MeOH, 50 °C, 24 hrs.

Vanillin or 4-hydroxybenzaldehyde was stirred in acetone (as reagent and solvent) in the presence of aqueous 5M HCl at room temperature for 24 hours. The crude product of the reaction was purified by silica column chromatography to furnish the pure products 5.1 and 5.3 in good yields. The synthesis of the chalcones 5.2 and 5.4 involved the reaction of vanillin or 4-hydroxybenzaldehyde with 1.1 equivalents of the 2'4'-dimethoxy-acetophenone in methanol, in the presence of aqueous HCl as catalyst. The crude products were then purified by silica gel column chromatography to furnish the pure chalcone intermediates in average yields.

Scheme 5.2 shows the synthesis of the target analogs 5.8 – 5.11. The required hydroxylated quinoline intermediates 5.5 and 5.6 were afforded by typical aromatic substitution reactions using the (modified) method reported by Singh *et al.* 1971 [22]. Briefly, 4,7-dichloroquinoline was heated with excess ethanolamine or with 1 equivalent of 1-(2-hydroxyethyl)piperazine in the presence of potassium carbonate to yield the target intermediates in moderate to good yield after purification by crystallization.

The intermediates 5.5 and 5.6 were then coupled to either 5.1 or 5.2 to yield the target compounds 5.8 – 5.11. This coupling was achieved by applying the Mitsunobu reaction, a convenient, one-step S_N2 reaction using 1.2 equivalents of triphenylphosphine (PPh_3) and 1.2 equivalents of diisopropyl azodicarboxylate (DIAD) (Scheme 5.2) as described by Debaene *et al.* 2007 [23].

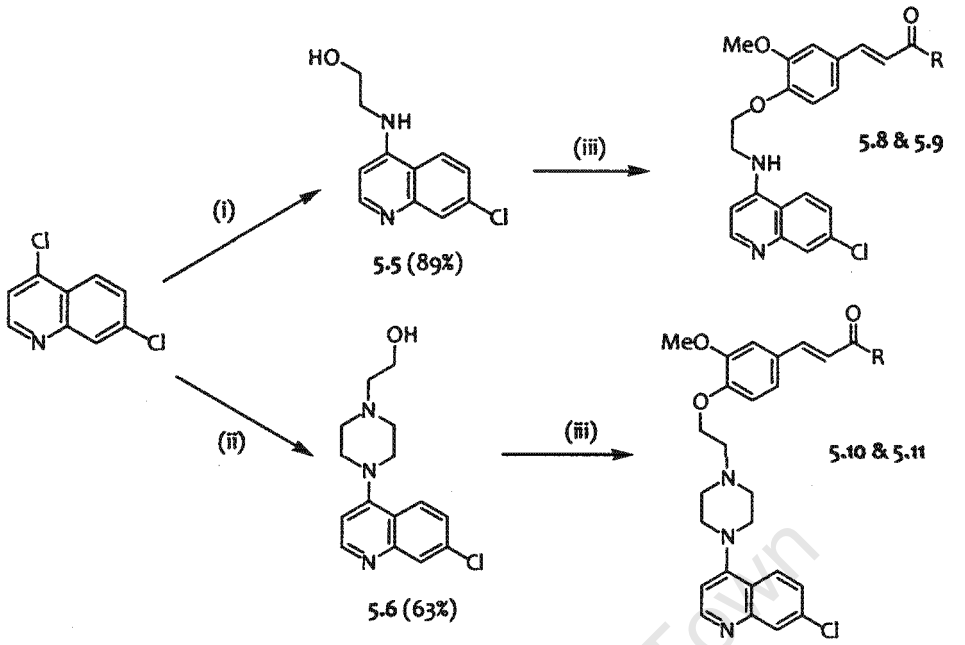

Scheme 5.2: *Reagents and conditions:* (i) ethanolamine, 130 °C, 5 hrs; (ii) 1-(2-hydroxyethyl)piperazine, K_2CO_3, DMF, 80 °C, 24 hrs; (iii) 5.1, 5.2, 5.3 or 5.4, PPh_3, DIAD, DCM, 0 °C – rt, 6 hrs.

Table 5.1: Yields of analogs 5.8 – 5.11

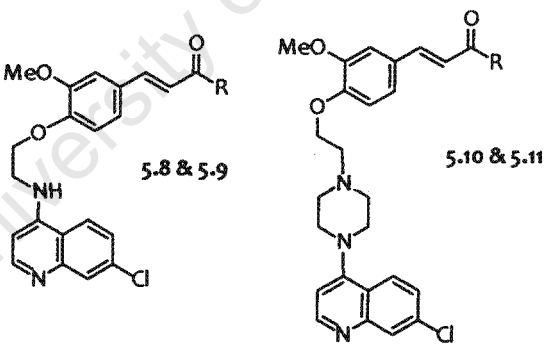

Compound code	R	Yield (%)
5.8	CH_3	73
5.9	2',4'-diMeOPhe	60
5.10	CH_3	68
5.11	2',4'-diMeOPhe	74

The application of the Mitsunobu reaction avoided the need to initially and separately convert the hydroxyl group of the aminoquinoline intermediates into a good leaving group (such as a toluenesulfonyl or methanesulfonyl ester) prior to the S_N2 reaction with 5.1 or 5.2. As detailed in the mechanism below (Figure 5.10), the hydroxyl group

is converted *in situ* into a good leaving group bearing a (positively charged) phosphonium species.

The reaction begins with the nucleophilic addition of PPh_3 to the diisopropyl azodicarboxylate to yield the charged species I that bears a nitrogen anion stabilized by the adjacent carbonyl group. This anion then deprotonates the hydroxylated quinoline, and the resulting alkoxide immediately attacks the positively-charged phosphorous atom, yielding a phosphonium derivative of the alcohol (II) and displacing the charged species III that also bears a nitrogen anion stabilized in the same way as the first. This S_N2 reaction at phosphorous is driven by ionic attraction and the strong affinity between oxygen and phosphorous.

The displaced anion is basic enough to deprotonate the phenolic hydroxyl group (of 5.1 or 5.2), and the resulting phenoxide then attacks the phosphonium derivative II to yield the target compound and triphenylphosphine oxide as a by-product, with the formation of the highly stable P=O double bond being the driving force for this reaction [24].

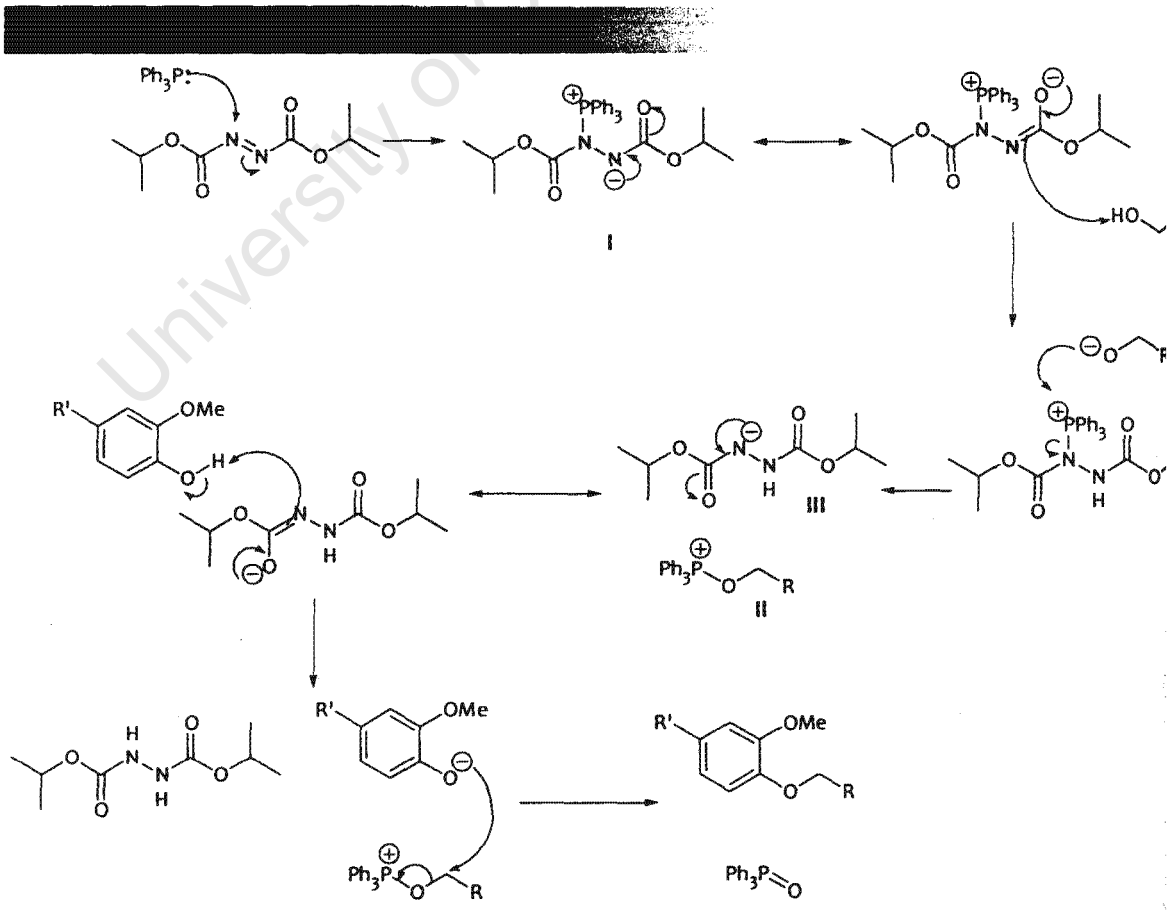

Figure 5.10: Proposed mechanism for the Mitsunobu reaction [24]

The synthesis of the proposed analogs 5.12 – 5.15 began with the synthesis of the piperazinyl intermediate 5.7 *via* an aromatic substitution reaction of 4,7-dichloroquinoline and 6 equivalents of piperazine, in the presence of potassium carbonate, using the (modified) method reported by Singh *et al.* 1971 [22]. Purification by silica gel column chromatography afforded 5.7 in good yield.

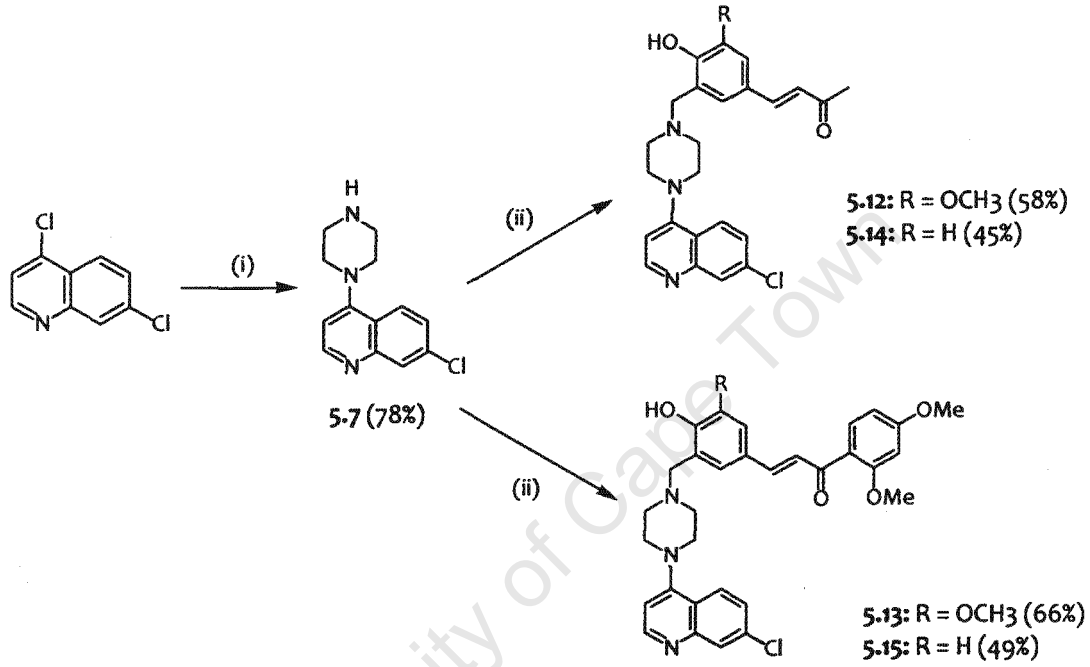

Scheme 5.3: *Reagents and conditions:* (i) piperazine, K_2CO_3, NMP, 135 °C, 4 hrs; (ii) 5.1, 5.2, 5.3 or 5.4, HCHO, EtOH, reflux at 110 °C, 12 hrs.

The Mannich reaction was then applied to furnish the target analogs using the (modified) method described by Chipeleme *et al.* 2007 [25]. This involved the refluxing of the appropriate phenolic intermediate (5.1 – 5.4) and 1 equivalent of 5.7 in ethanol in the presence of 10 equivalents of aqueous formaldehyde for 12 hours. The crude products were then purified by silica gel column chromatography to afford the pure target compounds in average yields, which could be partly attributed to the fact that these reactions did not proceed to completion even with the use of a large excess of formaldehyde or after extended refluxing.

A typical Mannich reaction usually involves an enolizable aldehyde or ketone, a secondary amine, formaldehyde (either as paraformaldehyde or as its aqueous solution) and a catalytic amount of acid [24]. For the Mannich reaction on phenolic compounds (such as the one described above), the enolizable carbonyl compound is

replaced by the phenolic compound, and no external acid catalyst is added; the acidic phenolic proton provides the required acid catalyst.

The proposed mechanism for this reaction is described below (Fig. 5.11):

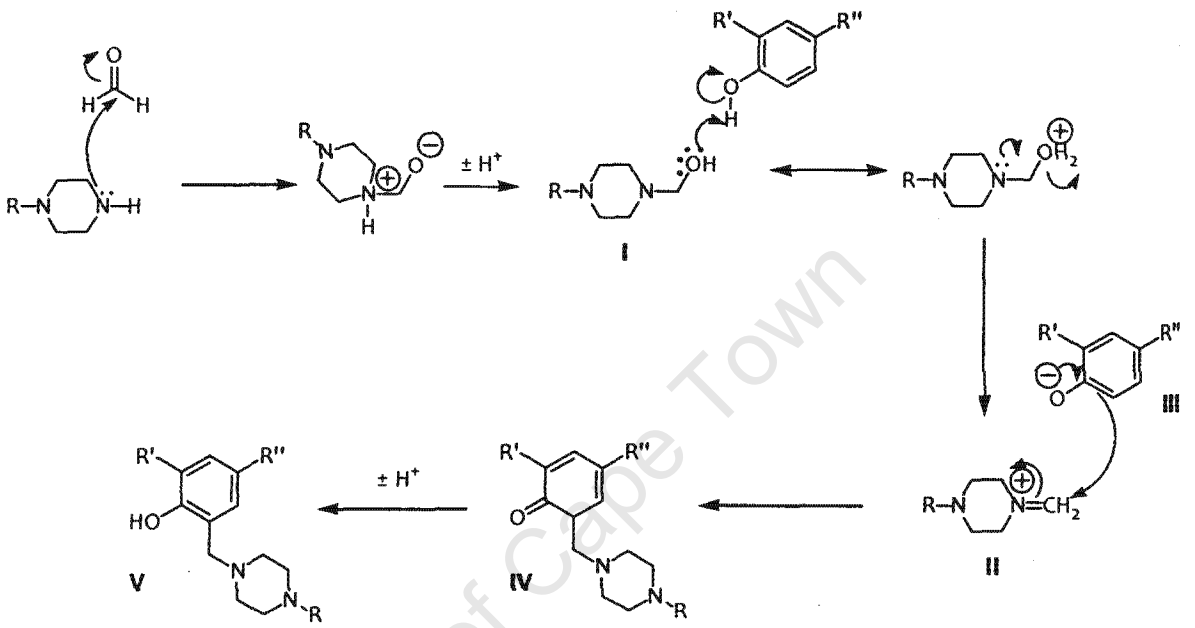

Figure 5.11: Proposed mechanism for the Mannich reaction of phenolic compounds

As with the typical Mannich reaction, this proposed mechanism involves the preliminary formation of an iminium ion intermediate (II); the reaction begins with the nucleophilic secondary amine attacking the highly electrophilic formaldehyde. A proton transfer yields the neutral intermediate I, which then undergoes acid-mediated dehydration facilitated by the acidic phenolic compound. The resulting iminium intermediate II then undergoes nucleophilic attack by the charged phenolic intermediate III (which can be seen to act as a nucleophilic enolate species) to yield the intermediate IV. The dehydration and subsequent nucleophilic addition are driven by the elevated temperatures of the reaction, which is carried out under reflux conditions. A proton transfer, driven by the restoration of the aromaticity of the phenyl ring, finally yields the target phenolic Mannich base V.

5.7.2 ^{1}H-NMR analysis

The ^{1}H-NMR spectra of the target compounds bore distinct features of the different components of these hybrid compounds, i.e. the quinoline ring, the amino-ethoxy or piperazinyl linker, and the enone or chalcone components.

The spectrum for compound 5.9 is used here as an example for discussion. Features of this spectrum (Fig. 5.12) include:

- A distinct pair of doublets – the first appearing at approximately δ 8.57 ppm, and the second at approximately δ 6.48 ppm – each integrating for one proton and sharing a coupling constant of 5.3 Hz. These are signature signals corresponding to the quinoline protons H-9 and H-8, respectively.
- The presence of another set of two distinct doublets, each integrating for one proton, lying in the region between δ 7 – 8 ppm and sharing a ^3J-*trans* coupling constant of between 15 - 16 Hz. These corresponded to protons H-a and H-b, and were diagnostic of the α-β-unsaturated system present in the chalcone component of the compound.
- A triplet at approximately δ 4.4 and a quartet at approximately δ 3.7, each integrating for two protons and corresponding to the methylene protons (H-5 and H-6, respectively) of the amino-ethoxy linker.

δ (ppm)	Multiplicity	J (Hz)	H#
8.57	d	5.3	H-9
7.61	d	15.7	H-a
7.39	d	15.7	H-b
6.48	d	5.3	H-8
4.39	t	5.2	H-5
3.72	q	5.2	H-6

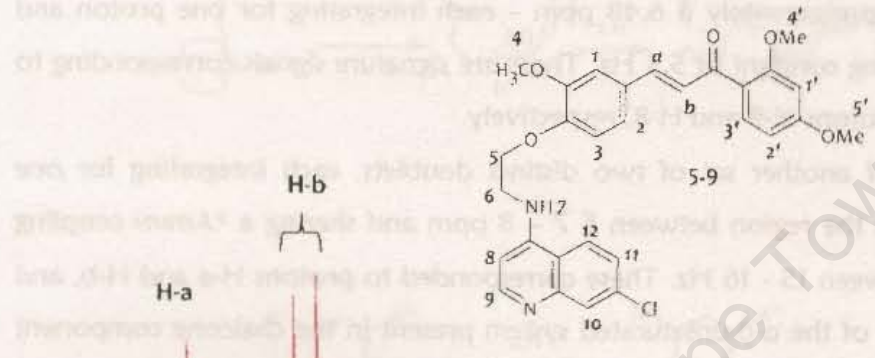

5-9

Figure 5.12: ^{1}H-NMR analysis of compound 5.9

5.8 Results from the experimental determination of *in silico*-predicted properties

5.8.1 Solubility

To corroborate the *in silico* solubility predictions described above, samples of some of the synthesized compounds were submitted for the experimental evaluation of this property. These determinations were carried out by Roslyn Thelingwani in the laboratories of Prof. Collen Masimirembwa at the African Institute of Biomedical Science & Technology (AiBST) in Harare, Zimbabwe.

Solubility was determined using a turbidimetric assay, which is a plate-based assay for determining aqueous solubility. It is based on the fact that, for any given compound, a precipitate begins to form when maximum solubility is reached, and this formation of a precipitate can be detected using UV-Vis spectrophotometry.

Experimentally, concentrations of 0, 1, 2, 4, 6, 10, 20, 30, 50, 70, 90 and 100μM are prepared for each compound by dilutions in aqueous buffer of stock solutions prepared in DMSO. These dilutions are effected such that the final concentration of DMSO does not exceed 2%. In order to determine the pH-dependent solubilities of ionizable compounds, the assay may be performed at different pH simply by altering the buffer used.

These solutions are incubated at a given temperature, in this case 37 °C, and their absorbances determined at 620 nm. Plots of absorbance versus concentration are then used to determine the concentration at maximum solubility, which is the solubility when precipitation begins to occur. This is read off at the point of inflection on the plot, i.e. the point at which absorbance begins to rise with increasing concentration rather than remain constant and relatively negligible, and which indicates that maximum concentration has been reached (and that surplus compound is precipitating out, leading to the observed rise in absorbance).

The results for the solubility experiments at both pH 4.0 and physiological pH (pH 7.4) are given in Table 5.2. The following guide was used in the ranking of the compounds: <10 = insoluble; >10 - 20 = mild; >20 - 50 = moderate; >50 - 100 = soluble; >100 = highly soluble. Two controls were used: niclosamide (insoluble) and paracetamol (soluble).

Table 5.2: Results from the experimental solubility determinations at pH 4 and pH 7

Compound	Solubility pH 4 (μM)	Solubility pH 7.4 (μM)	Interpretation
Paracetamol	>100	>100	Highly Soluble
Niclosamide	6	10	Insoluble
3.15b	4	4	Insoluble
3.19	20	70	Mild at pH 4 and soluble at pH 7.4
5.8	90	90	Soluble at both pH 7.4 and pH4
5.9	>100	20	Highly soluble at pH 4 and mild at pH 7.4
5.10	>100	10	Highly soluble at pH 4 and insoluble at pH 7.4
5.11	>100	1	Highly soluble at pH 4 and insoluble at pH 7.4
5.12	>100	20	Highly soluble at pH 4 and insoluble at pH 7.4
5.13	90	20	Soluble at pH 4 and insoluble at pH 7.4
5.14	90	20	Soluble at pH 4 and mild at pH 7.4
5.15	90	20	Soluble at pH 4 and insoluble at pH 7.4

The experimental results show similar trends to those observed from the *in silico* predictions.

- Compound 3.15b was poorly soluble in aqueous media, and this solubility was not enhanced at lower pH; 3.19 was more soluble than 3.15b, though this solubility appeared to be lower at pH 4.0 than at pH 7.4. The possible reasons for this are not clear.
- With the exception of 5.11, the analogs showed slightly improved solubilities at pH 7.4 relative to 3.19, though these solubilities were still poor. However, all the analogs showed remarkably higher solubilities at pH 4.0, which was to be expected as these compounds would be ionized at this pH. Compound 5.8, which had the lowest molecular weight of all the analogs, showed a similarly high solubility at pH 7.4 as it did at pH 4.0. The other analogs showed a significantly higher solubility at low pH than they did at pH 7.4.

The tentative conclusions that were drawn from the *in silico* solubility predictions were therefore supported by these experimental results.

5.8.2 Metabolism and metabolic stability

To corroborate the site-of-metabolism and metabolic stability predictions, samples of some of the synthesized compounds were submitted to the laboratories of Prof. Susan Charman at the Centre for Drug Candidate Optimization (CDCO), Monash University, Australia, for *in vitro* metabolism studies. The aim of these studies was to determine the *in vitro* metabolic stability of 3.15b, 3.19, and 5.8 – 5.15 in both human and mouse liver microsomes as a preliminary indication of their likely *in vivo* metabolic clearance, and to identify potential metabolic products for comparison with the predicted routes of metabolism of these compounds.

The metabolic stability assays were performed by separately incubating the test compounds at 37°C (in duplicate, substrate concentrations 1 μM) with human or mouse liver microsomes (0.4 mg/mL protein concentration). The metabolic reaction was initiated by the addition of an NADPH-regenerating system (containing 1 mg/mL NADP, 1 mg/mL glucose 6-phosphate, 1 U/mL glucose 6-phosphate dehydrogenase) and quenched at various time points over the incubation period by the addition of acetonitrile. NADPH is the cofactor required for CYP450-mediated metabolism. Additional samples with the dual cofactors NADPH and UDPGA (the latter being the cofactor for glucuronidation) were also included in the incubations for the qualitative assessment of the potential for glucuronide formation. Control samples (containing neither NADPH nor UDPGA) were included to monitor for potential degradation in the absence of cofactors.

The concentrations of the substrates after the various periods of incubation were quantified by LC-MS against standard curves prepared in blank microsomal matrix. The MS scan data from the metabolic stability assay of each compound was screened for the presence of fragments corresponding to putative metabolites; data acquisition was conducted in MS scan mode (spectra acquired from 100 to 1000 Daltons). It should be noted that the identities of the putative metabolites were not confirmed by dedicated MS-MS experiments.

The results for the *in vitro* metabolism studies are summarized in Table 5.3. Two peaks were observed for 3.19, 5.10 and 5.11 during chromatographic LC-MS analysis, most likely indicating *cis* - *trans* isomerism occurring under assay conditions. The rates of degradation for each individual peak were therefore determined.

Table 5.3: Results from the *in vitro* metabolism studies

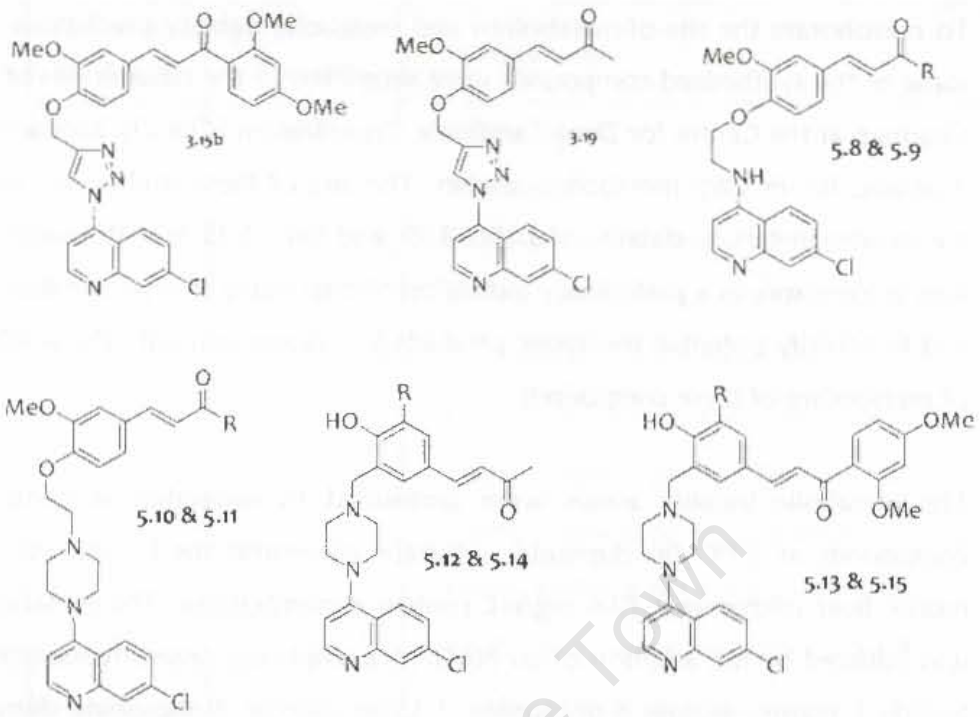

Compound		R	Degradation half-life (min)		Microsome-Predicted Extraction ratio (E_H)		Metabolites detected
			Human	Mouse	Human	Mouse	
3.15b		-	51.1	56.8	0.65	0.57	P+16
3.19	Peak 1	-	7.4	10.8	0.93	0.88	Not Detected
	Peak 2		9.1	6.2	0.91	0.92	
5.8		CH_3	10.5	13.4	0.90	0.85	P-218
5.9		2',4'-diOCH_3-	17.5	12.7	0.85	0.86	P+16 (x2), P+32 (x2), P-14, P+16+176
5.10	Peak 1	CH_3	14.2	6.7	0.87	0.92	P-14, P-218
	Peak 2		9.8	5.6	0.91	0.93	
5.11	Peak 1	2',4'-diOMe-Phe	11.5	9.8	0.89	0.89	P+16 (x4), P-14 (x2) P-340
	Peak 2		93.2	149.8	0.51	0.34	
5.12		OCH_3	16.9	14.0	0.85	0.84	P+16, P-204, P+176
5.13		OCH_3	37.0	11.8	0.72	0.87	P-14 (x2), P-326, P+176
5.14		H	7.5	15.0	0.93	0.84	P+16, P-174, P+176
5.15		H	58.6	45.4	0.62	0.63	P+16 (x2), P-14, P-296 P+176
Chloroquine			>250	177.0	<0.28	0.31	Not Undertaken

With respect to metabolic stability, the compounds examined exhibited varying degradation half-lives in human and mouse microsomes. However, all of the compounds exhibited similar extraction ratios (E_H values) in both human and mouse liver microsomes; E_H values take into account the different liver masses (g liver/kg body mass) and hepatic flow rates (mL/min/kg) of both species, and therefore the similarities in these values suggested that there are no significant inter-species differences in the relative rates of metabolism of these compounds.

Most of the compounds exhibited high E_H values (>0.7), suggesting notable susceptibility to hepatic metabolism. This is particularly apparent when compared to the relatively low values for chloroquine (≤0.31), and is in agreement with the predicted metabolic stability of this set of compounds, which were predicted to be less stable than chloroquine to hepatic metabolism. Notably, 3.15b and 5.15 had intermediate E_H values, as did the isomer of 5.11 corresponding to peak 2, indicating relatively better metabolic stability.

The majority of the test compounds showed no measurable degradation in the microsomal matrix devoid of cofactors (i.e. controls), suggesting that there was no major non-cofactor dependent metabolism contributing to their overall rate of metabolism in liver microsomes (i.e. metabolism by enzymes other than hepatic cytochromes and transferases). The only exceptions were 3.19 (peak 2) and 5.10 (peak 2), both of which demonstrated apparent non-cofactor dependent degradation (which was not observed for the other isomer), potentially indicating a stereo-specific process.

With respect to routes/sites of metabolism, the metabolite profiles of all the examined compounds were found to be similar across the two species tested. Oxygenation, O-demethylation and N-dealkylation appeared to be the predominant pathways. This was remarkably consistent with the site-of-metabolism predictions derived from MetaSite® (Figure 5.9), where these three were the major routes of metabolism predicted for this set of compounds. However, there were some differences between the predicted routes of metabolism and detected metabolites for some of the compounds; for example, no predicted O-demethylation metabolites were detected for 3.15b and 5.8, and no N-dealkylation metabolite was detected for 5.9.

For compounds with the piperazine linkers (5.10 – 5.15) a common metabolite with *m/z* of 248 Daltons was found, consistent with N-dealkylation of the side chain from the piperazine. For 5.8, N-dealkylation of the amino-ethoxy linker was observed, resulting in the generation of a metabolite with *m/z* 179 Daltons; this was not observed for 5.9, which also bears an amino-ethoxy linker. The putative metabolites from these N-dealkylation reactions are shown in Figure 5.13.

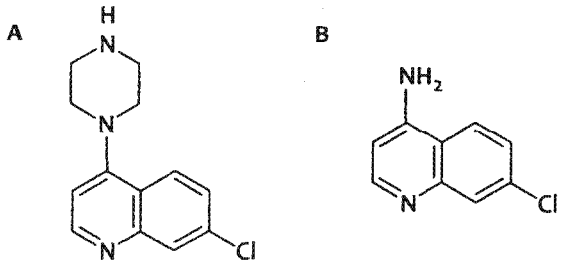

Figure 5.13: Figure showing the structures of the putative metabolites of 5.10 – 5.15 (A) and 5.8 (B)

The potential of the test compounds to undergo primary glucuronidation was assessed in the microsomal incubation by the addition of the cofactor UDPGA. There was no major increase in the rate of degradation of 3.15b, 5.8, 5.9 and 5.11 (or chloroquine) in microsomal samples containing NADPH and UDPGA relative to NADPH alone, suggesting that these compounds were not susceptible to primary glucuronidation in the microsomal test system. For 3.19 and 5.10, the impact of UDPGA on the overall rate of metabolism could not be assessed, as the rate of NADPH-dependent degradation alone was too rapid. For these two compounds, there were no putative metabolites detected having molecular weights consistent with glucuronidation.
However, there was evidence of primary glucuronidation for 5.12 – 5.15 in the microsomal assay, where there was an increase in the relative rates of degradation of test compounds in the presence of UDPGA and/or the detection of a putative metabolite with a molecular weight consistent with glucuronide conjugation (P+176). All these compounds bear a free phenolic –OH group, and it therefore is somewhat expected that they are substrates for glucuronidation. This route of metabolism was not predicted by MetaSite®, which only predicts cytochrome-mediated phase I metabolism.

In summary, there was no evidence of significant inter-species differences in the relative rates of metabolism of these compounds. However, most of the compounds exhibited high E_H values (>0.7), suggesting notable susceptibility to hepatic metabolism. Oxygenation, O-demethylation and N-dealkylation appeared to be the predominant metabolic pathways, which was consistent with the site-of-metabolism predictions derived from MetaSite®. There was also evidence of primary glucuronidation for 5.12 – 5.15.

5.9 *In vitro* antimalarial assays

5.9.1 Results and discussion

Analogs **5.8 – 5.15**, along with the phenolic intermediates **5.1** and **5.2** and the chloroquinoline intermediates **5.5 – 5.7** were tested for *in vitro* antimalarial activity as described in Chapter Four above. The results of these assays are presented in Table 5.4 and discussed below.

Table 5.4: IC_{50} values of the analogs 5.8 – 5.15 as well as selected intermediates against the D10, Dd2 and W2 strains of *P. falciparum*

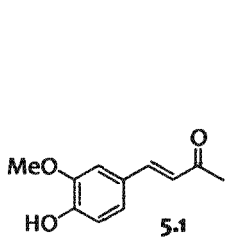

5.1

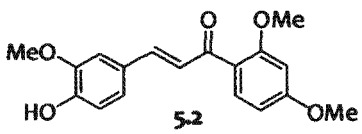

5.2

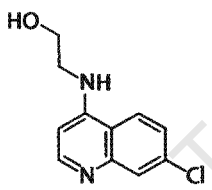

5.5

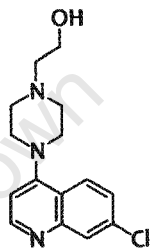

5.6

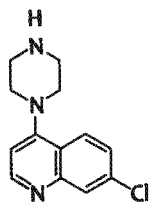

5.7

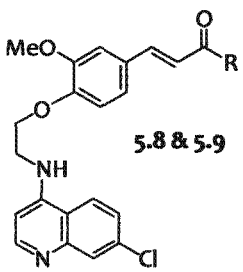

5.8 & 5.9

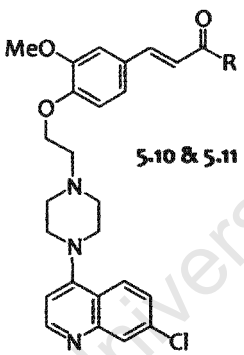

5.10 & 5.11

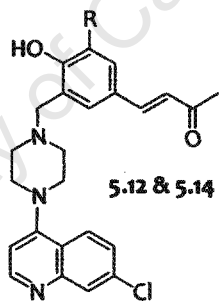

5.12 & 5.14

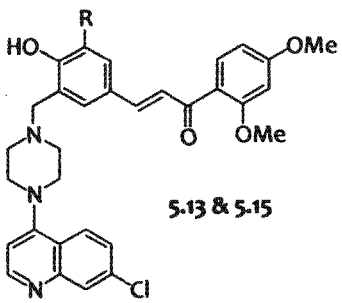

5.13 & 5.15

Compound code	R	D10 IC_{50} (μM)	Dd2 IC_{50} (μM)	W2 IC_{50} (μM)
5.1	-	>20	>20	>10
5.2	-	5.3	7.3	>10
5.5	-	2.6	1.0	0.2
5.6	-	5.2	3.8	1.0
5.7	-	0.7	0.9	0.3
5.8	CH_3	1.0	1.5	0.1
5.9	2',4'-diOCH_3-Phe	0.8	1.0	0.4
5.10	CH_3	1.2	1.1	0.5
5.11	2',4'-diOMe-Phe	1.2	0.5	0.6
5.12	OCH_3	1.0	1.7	0.5
5.13	OCH_3	0.5	0.5	0.4
5.14	H	1.7	3.1	0.7
5.15	H	0.6	0.5	0.3
(3.19)	-	0.8	0.7	ND
(3.15b)	-	0.04	0.07	0.09
(CQ)	-	0.017	0.097	0.069

NB: these are average values from two independent determinations, each carried out in duplicate

The hydroxylated enone intermediate 5.1 showed negligible antimalarial activity *in vitro* across all three strains at concentrations ≥10 μM. However, the chalcone intermediate 5.2 showed moderate antimalarial activity against D10 and Dd2 *P. falciparum*, but showed negligible activity against W2 *P. falciparum* even at 10 μM concentration.

The chloroquinoline-based intermediates 5.5, 5.6 and 5.7 showed antimalarial activity *in vitro*, with 5.7 showing sub-micromolar IC_{50} values against all three strains of *P. falciparum*.

All the target analogs exhibited notable antimalarial activity, with IC_{50} values in the lower micro-molar to mid nano-molar range. This indicated that replacement of the triazole linker in 3.15b and 3.19 with the selected nitrogen-containing linkers was associated with retention of antimalarial activity, though none were as active as 3.15b.

The related analogs 5.13 and 5.15 were the most active of the analogs; both were chalcone derivatives with piperazinyl linkers, and had IC_{50} values between 0.3 – 0.6 μM against all three strains of *P. falciparum*. 5.11 was also quite active, with mid-nanomolar IC_{50} values against the CQR Dd2 and W2 *P. falciparum* strains.

These results demonstrated that these compounds were indeed viable candidates for preliminary PK profiling and *in vivo* antimalarial assays. However, due to time and resource constraints, only two compounds were selected for this:

- Compound 3.15b, the most active of the compounds so far synthesized and tested.
- Compound 5.13, an analog of 3.15b, and which was one of the more active analogs identified.

In anticipation of this exercise, both compounds were evaluated for their cytotoxicity against the Chinese Hamster Ovarian (mammalian) cell line. No cytotoxicity was observed at the highest concentration (100 μM) tested.

Furthermore, there was the added possibility of tracking one of the predicted metabolites of 5.13 during the PK studies. Intermediate 5.7 was predicted by MetaSite® as the main metabolite of 5.13, and was also identified during *in vitro* metabolism studies as a putative metabolite arising from N-dealkylation of the piperazinyl linker (see section 5.8.2). The fact that it exhibits notable *in vitro* antimalarial potency implies that this intermediate/metabolite could very well contribute to any observed *in vivo* antimalarial activity of 5.13, and thereby offset any potential liabilities of the compound arising from its susceptibility to metabolism *via* this route. Using the synthesized 5.7 as reference, it would be possible to follow its PK profile alongside that of 5.13 (following the administration of 5.13 only), and in this way provide an additional dimension to the PK profiling of 5.13.

5.9.2 Summary and conclusions

3.15b and 3.19 were selected for structural modification with the aim of identifying analogs with improved solubility and which retained antimalarial potency. Eight analogs were proposed, and these were characterized *in silico* for selected physicochemical and ADME parameters. These analogs were predicted to have improved solubilities relative to the parent compounds, particularly at low pH; they retained acceptable predicted Caco2 permeabilities, but were identified as possible substrates for N-dealkylation by hepatic cytochromes.

These proposed analogs were then synthesized and tested, and were found to exhibit notable *in vitro* antimalarial activity. 5.13 and 5.15 were the most active of the analogs. 5.7, an intermediate in the synthesis (and a predicted metabolite) of some of the analogs was also found to exhibit notable antimalarial activity *in vitro*.

Compounds 3.15b and 5.13 (Figure 5.14) were thereafter selected for preliminary PK profiling and *in vivo* antimalarial testing. The possible simultaneous PK profiling of 5.7 alongside 5.13 was an additional reason for the selection of 5.13. This is reported and discussed in the following Chapter.

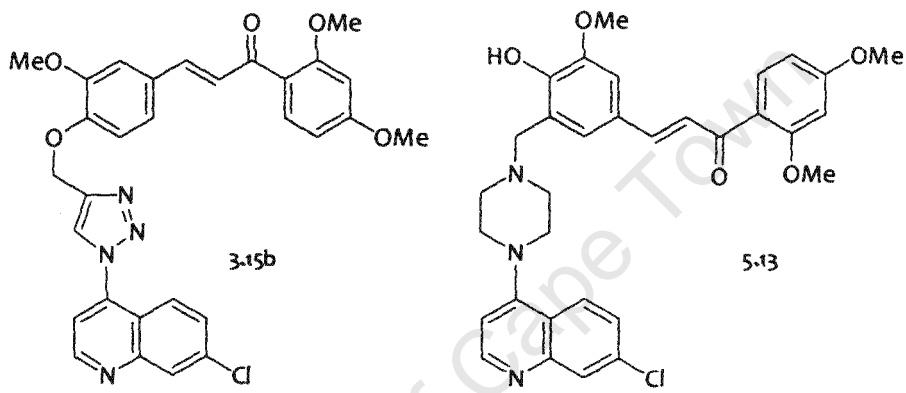

Figure 5.14: Figure showing the structures of the two compounds selected for pharmacokinetic profiling and *in vivo* antimalarial efficacy studies

The proposed analogs were by no means exhaustive, but represented analogs that did not represent significant deviations from the molecules known to be active, and were therefore more likely to retain activity. They represented a small range of compounds that could be conveniently synthesized, and which offered possible improvements on certain physicochemical and/or ADME properties of the parent compounds, particularly solubility. In addition, they opened up possibilities for even further derivatization in future, as highlighted in Figure 5.15.

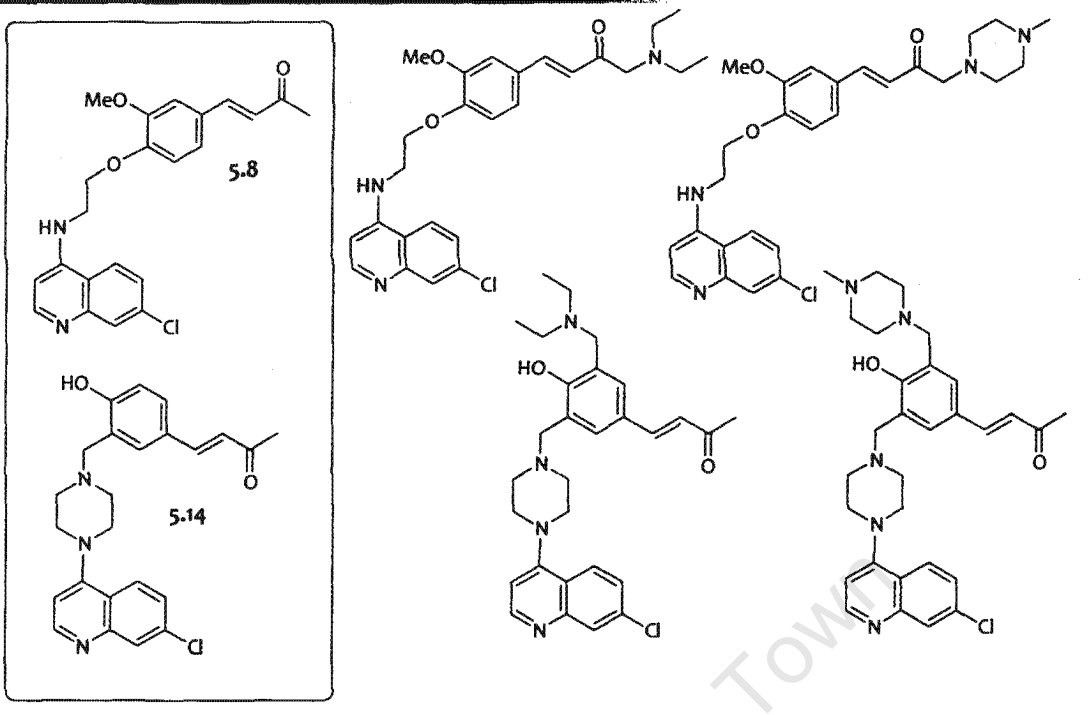

Figure 5.15: Figure showing a few examples of possible further derivatization of some of the analogs already synthesized

5.10 Mechanistic studies

5.10.1 Results

Analogs 5.8 – 5.15, along with the chloroquinoline intermediates 5.5 and 5.7 were put through the same mechanistic studies as described in Chapter Four above. The results of these assays are presented in Table 5.4 and discussed below.

Compounds 5.8 - 5.15 were all very potent inhibitors of β-hematin formation, more potent than chloroquine. They all had comparable, sub-micromolar IC_{50} values, with compounds 5.11 and 5.15 (which were some of the more active of these analogs *in vitro*) having the lowest values of 0.2 equivalents. This indicates the notable potential of these compounds to inhibit hemozoin formation, and suggests that this could be a primary mechanism of antimalarial action of these compounds. The intermediates 5.5 - 5.7 showed only moderate inhibition of β-hematin formation.

The analogs showed moderate to poor inhibition of Falcipain 2 relative to E64; analogs 5.9, 5.11, 5.13, 5.14 and 5.15 had lower micromolar IC_{50} values, while the other compounds tested did not show appreciable Falcipain 2 inhibition even at a concentration of 50 μM. The relatively low potencies of these compounds as Falcipain 2 inhibitors suggests that this is not the primary mechanism of antimalarial action of these compounds, though inhibition of the enzyme may still contribute to the overall observed antimalarial activity of some of them.

These analogs tested were poor inhibitors of sorbitol-induced lysis, with 5.12 showing the highest % inhibition of only 17%. This would discount inhibition of NPPs as a mechanism of action for these analogs.

Table 5.5: Results from the mechanistic studies

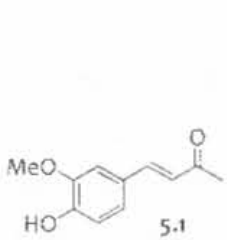

5.1

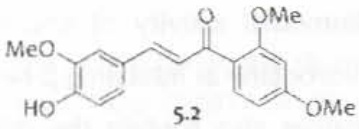

5.2

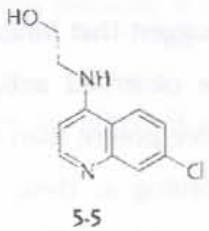

5.5

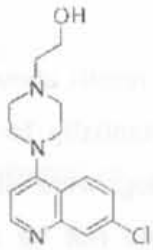

5.6

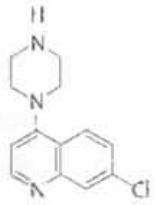

5.7

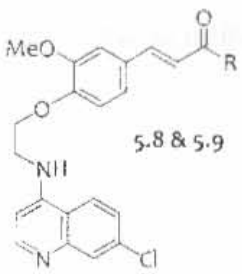

5.8 & 5.9

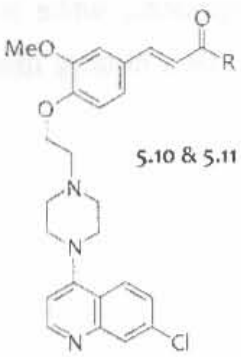

5.10 & 5.11

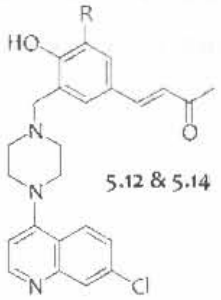

5.12 & 5.14

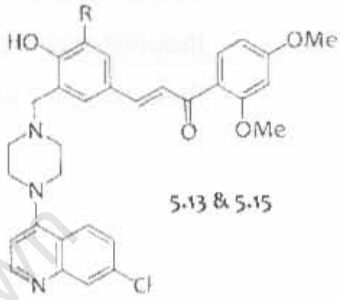

5.13 & 5.15

Compound code	R	β-hematin inhibition (IC_{50})[a]	Falcipain-2 Inhibition IC_{50} (μM)[b]	%age Sorbitol-induced hemolysis inhibition.[c]
5.5	-	4.9	>50	0.9
5.6	-	3.9	>50	ND
5.7	-	5.2	>50	5.8
5.8	CH_3	0.6	>50	12.3
5.9	diMeO-Phe	0.3	22.9	ND
5.10	CH_3	0.5	>50	ND
5.11	diMeO-Phe	0.2	11.7	ND
5.12	OCH_3	0.5	>50	16.8
5.13	OCH_3	0.3	9.1	3.9
5.14	H	0.5	29.9	11.6
5.15	H	0.2	10.0	ND
CQ	-	1.91	-	-
E64	-	-	0.055	-

[a]: The IC_{50}s are averages of triplicate determinations and are reported in equivalents of the drug relative to hematin.

[b]: The IC_{50}s are averages of duplicate determinations and are reported in μM.

[c]: Percentage inhibition of sorbitol-induced lysis by the test compounds at a concentration of 10 μM.

ND: Not determined

5.10.2 Summary and conclusions

The results above suggest that inhibition of hemozoin formation is likely to contribute substantially to the observed antiplasmodial activity of analogs 5.8 – 5.15. These analogs were all more potent than chloroquine at inhibiting β-hematin formation. This would not be surprising as these analogs also contain the chloroquinoline moiety. Inhibition of Falcipain 2 could also contribute to a limited extent to the overall observed antimalarial activities of these compounds, while inhibition of parasite-induced transport channels does not appear to be a notable mechanism of action for these compounds.

References

1. D Butina, M D Segall, and K Frankcombe. Predicting ADME properties *in silico*: methods and models. *Drug Discov. Today* (2002) 7 (11) S83-S88.

2. H Yu and A Adedoyin. ADME-Tox in drug discovery: integration of experimental and computational technologies. *Drug Discov. Today* (2003) 8 (18) 852-861.

3. H Sun. A Universal Molecular Descriptor System for Prediction of LogP, LogS, LogBB, and Absorption. *J. Chem. Inf. Comput. Sci.* (2004) 44 748-757.

4. F Lombardo, E Gifford, and M Y Shalaeva. *In Silico* ADME Prediction: Data, Models, Facts and Myths. *Mini Rev. Med. Chem.* (2003) 3 861-875.

5. I V Tetko, P Bruneau, H-W Mewes, D C Rohrer, and G I Poda. Can we estimate the accuracy of ADME–Tox predictions? *Drug Discov. Today* (2006) 11 (15/16) 700-707.

6. D Boyer, J N Bauman, D P Walker, B Kapinos, K Karki, and A S Kalgutkar. Utility of MetaSite in Improving Metabolic Stability of the Neutral Indomethacin Amide Derivative and Selective Cyclooxygenase-2 Inhibitor 2-(1-(4-Chlorobenzoyl)-5-methoxy-2-methyl-1H-indol-3-yl)-N-phenethyl-acetamide. *Drug Metab. Dispos.* (2009) 37 (5) 999-1008.

7. G Cruciani, P Crivori, P A Carrupt, and B Testa. Molecular fields in quantitative structure-permeation relationships: the VolSurf approach. *J. Mol. Struct-Theochem* (2000) 503 17-30.

8. G Cruciani, M Pastor, and W Guba. VolSurf: a new tool for the pharmacokinetic optimization of lead compounds. *Eur. J. Pharm. Sci.* (2000) 11 (2) S29-S39.

9. G Cruciani, E Carosati, B de Boeck, K Erithajulu, C Mackie, T Howe, and R Vianello. Understanding metabolism in human cytochromes from the perspective of the chemist. *J. Med. Chem.* (2005) 48 6970-6979.

10. F Milletti, L Storchi, G Sforna, and G Cruciani. New and original pKa prediction method using Grid Molecular Interaction Fields. *J. Chem. Inf. Mod.* (2007) 47 (6) 2172-2181.

11. S Ray, P B Madrid, P Catz, S E LeValley, M J Furniss, L L Rausch, R K Guy, J L DeRisi, L V Iyer, C E Green, and J C Mirsalis. Development of a New Generation of 4-Aminoquinoline Antimalarial Compounds Using Predictive Pharmacokinetic and Toxicology Models. *J. Med. Chem.* (2010) 53 3685-3695.

12. E K Kerns and L Di. Drug-like Properties: Concepts, Structure, Design and Methods: from ADME to Toxicity Optimization. (2008) 1st Edition. Academic Press/Elselvier

13. I L O Buxton. Pharmacokinetics and pharmacodynamics: the dynamics of drug absorption, distribution, action, and elimination. *In: Goodman and Gilman's The Pharmacological Basis of Therapeutics* (2006) 11th Edition. Edited by L L Brunton. McGraw-Hill: Medical Publishing Division. New York

14. C A Lipinski, F Lombardo, B W Dominy, and P J Feeney. Experimental and computational approaches to estimate solubility and permiability in drug discovery and development settings. *Adv. Drug Deliv. Rev.* (2001) 46 3-26.

CHAPTER SIX

PHARMACOKINETIC AND *IN VIVO* ANTIMALARIAL EFFICACY STUDIES

6.1 Preamble

This chapter contains the work done to address the fourth and final specific aim of the study, which was: To elucidate the pharmacokinetic profiles and evaluate the *in vivo* antimalarial efficacy of the most promising compounds using the mouse model.

This chapter therefore reports the pharmacokinetic profiling and *in vivo* antimalarial assays of the two compounds identified in Chapter Five. After brief introductions, the pharmacokinetic analysis and *in vivo* antimalarial assays of 3.15b and 5.13 are described, and the results discussed.

6.2 The use of animal models for preliminary PK and efficacy investigations

The use of laboratory animals for preliminary pharmacokinetic and efficacy experiments is generally carried out as part of the pre-clinical drug development process. Preliminary pharmacokinetic experiments are aimed at investigating the time course of the test compound in a living organism. In other words, such studies investigate the influence of physiological and anatomical factors on the disposition of the test compound after its administration to a living organism. *In vivo* efficacy studies aim to demonstrate the ability of the test compound to exert its anticipated pharmacological effect in an appropriate disease model under the influence of the physiological and anatomical factors alluded to above. Other effects of the test compound, such as toxicity and carcinogenicity, may also be investigated through such studies.

The overall aim of these studies is to serve as an aid in assessing the potential of the test compound to exhibit acceptable pharmacokinetic, pharmacodynamic and toxicity profiles should they be administered to human beings, and is almost invariably a procedural and ethical requirement before any clinical testing may be allowed to proceed in humans.

The murine malaria disease model has been extensively used for *in vivo* antimalarial efficacy testing, and this was the model applied in this study (section 6.6). Preliminary PK profiling of the two compounds was also carried out in mice, and was done prior

to the *in vivo* efficacy testing. In this way, the results from the PK studies were available to establish the ability of the compounds to access systemic circulation after administration and the best formulation to use for the *in vivo* efficacy studies, as well as to guide in the interpretation of the results from the various dosing regimens to be used during the *in vivo* efficacy studies.

6.3 Formulations

As mentioned in section 5.5 (Chapter Five), some of the general strategies for improving the oral bioavailability of a compound involve either the use of appropriate formulations and/or the rational structural modification of the compound. Structural modification as a strategy has been discussed in Chapter Five. The use of formulations is introduced below.

In PK and *in vivo* experiments, the formulation of test compounds (i.e. the way the compound is prepared for administration) is an important consideration. For example, a study of the *in vivo* efficacy of some endoperoxide antimalarials in murine and simian (monkey) models demonstrated significant differences in the efficacy of some of the test compounds (ranging from curative to negligible activity) arising from the different formulations used in the study. The compounds were administered either as simple water solutions, as water solutions with 10% DMSO as co-solvent, as oil solutions (e.g. in sesame oil), and as formulations incorporating gelatin or carboxymethylcellulose as a standard suspending vehicle (SSV). The differences in the *in vivo* efficacies observed were linked to the varying levels of bioavailability afforded by the different formulations [1].

Ideally, compounds are best administered as solutions in water/aqueous media. Highly water soluble compounds therefore pose no formulation challenges as they can be prepared as simple solutions in water or normal saline for parenteral and/or oral administration.

Adjustment of pH can be used to render poorly soluble but ionizable compounds soluble in appropriately buffered aqueous systems. For example, basic compounds such as compound 5.13 can be prepared in appropriate buffer solutions of low pH in which they become protonated/charged, thereby rendering them more soluble in aqueous media. This is a recognized strategy for the formulation of hydrophobic but ionizable compounds, with the pH range of 4.0 – 9.0 being regarded as acceptable for routine discovery *in vivo* studies [2,3]. Compound 5.3 was therefore to be formulated in

isotonic sodium acetate buffer pH 4.0 for PK and *in vivo* studies; this buffer has been safely and successfully applied for *in vivo* experiments in mice, rats, dogs and monkeys [4]. For comparison, 5.13 would also be formulated in water with 10% DMSO as a water-miscible organic co-solvent.

For poorly water-soluble compounds that are non-ionizable within the pH range appropriate for *in vivo* studies (such as compound 3.15b), the use of mixed-phase formulations is an additional approach available for their formulation. These are lipid-based formulations, which have long been recognized as alternative strategies for the delivery of lipophilic drugs with aqueous solubility and oral bioavailability challenges [5]. Many lipid-based formulations, such as SMEDDS (self-micro-emulsifying drug delivery system) and Pheroid formulations, are essentially stable oil-in-water (o/w) micro-emulsions – micro-droplets of a lipid phase (into which the lipophilic compound is entrapped) dispersed within an aqueous phase [5-7].

The Pheroid formulation (developed by the Department of Pharmaceutics, North-West University, South Africa) is a stable sub-micron emulsion composed of mainly ethyl esters of plant and essential fatty acids such as linoleic acid, linolenic acid, and oleic acid, emulsified in water saturated with nitric oxide (NO); the lipid droplets into which the hydrophobic compound is entrapped tend to be within the nano- to micro-meter size range [7,8]. On the other hand, the SMEDDS formulations consist of an oil phase (e.g. sesame oil, linoleic acid or its ethyl ester) dispersed as a micro-emulsion in an aqueous phase; these emulsions are stabilized by the combination of a surfactant, principally Tween 80, and a co-surfactant such as a PEG 400 or short chain alcohol (e.g. ethanol) [6,9].

These formulations enhance the oral absorption of highly lipophilic compounds by presenting the compound in a dissolved form (within the lipid droplets), and, as a result of the small droplet size and large number of droplets, concurrently providing a large interfacial surface area for drug release and absorption [6,7]. In addition, the specific components of some of these formulations may promote the intestinal lymphatic transport of drugs possibly by increasing membrane fluidity, thereby facilitating trans-cellular absorption; they may also open tight junctions to allow para-cellular transport [7,10]. Some formulations may interact with the transport and metabolic processes of the intestinal cells, thereby influencing drug uptake, efflux, disposition and the formation of metabolites within these cells [10]. Notably, the use of formulations also enables the parenteral (IV) administration of lipophilic compounds that could otherwise not be administered by this route.

In this regard, the Pheroid formulation (kindly provided by the Department of Pharmaceutics, North-West University, South Africa) and the SMEDDS formulation were used in the preparation of the compound 3.15b for *in vivo* evaluation in this study.

In summary, for the preliminary PK studies, compound 3.15b was separately formulated in Pheroid and SMEDDS formulation as well as in water with 10% DMSO as co-solvent. Compound 5.13 was formulated in isotonic sodium acetate buffer pH 4.0 as well as in water with 10% DMSO as co-solvent. In this way, the bioavailability results obtained for each compound using the various formulation strategies could be compared, and the most appropriate formulation strategy (i.e. the one affording the best oral bioavailability) would then be applied for the dosing of the compounds during the *in vivo* efficacy studies.

6.4 Pharmacokinetic studies

Pharmacokinetics (PK) is the study of the time course of the disposition of a drug within the body. This is based on determinations of the drug concentration in blood/plasma at different time points after administration of a drug. In general, it is the total drug concentration of the drug in plasma that is considered, and this is a combination of the fraction of the drug that is bound to plasma proteins and other blood components, as well as the free (unbound) fraction [11].

When a drug enters the body, several processes begin to almost simultaneously act on the drug; specifically, these processes are absorption, distribution, metabolism (biotransformation), and elimination/excretion (ADME) [11,12]. Therefore, the time course of a drug (i.e. its pharmacokinetics) is a reflection of the outcome of these processes on the drug after its administration.

Absorption is the movement of a drug from its site of administration into the central compartment (the blood), and the extent to which this occurs [12]. For example, a drug administered orally must traverse the GI mucosa to reach the blood; drugs administered topically must get past the skin barrier (epidermis and dermis). Absorption after parenteral administration is somewhat simpler: after intramuscular (IM) or sub-cutaneous (SC) administration, absorption involves simple diffusion along the concentration gradient from site of administration to the blood; intravenous (IV) administration circumvents any need for absorption as the drug is directly introduced into the blood [11,12].

Once in the blood, the drug exists in equilibrium between the free (unbound) fraction and the fraction bound to blood components, principally plasma proteins. The drug then distributes into the interstitial/intercellular and intracellular compartments of tissues. The extent to which a drug distributes into the tissues is dependent on both physiological factors (e.g. tissue perfusion and capillary permeability) and the drug's physicochemical properties (mainly its lipophilicity). Initially, the liver, kidney and other well-perfused organs receive most of the drug, whereas delivery to muscle, most other organs, the skin, and fat is slower and may take several hours. Only the free (unbound) fraction of the drug in plasma is available for distribution, and therefore one of the more important determinants of blood-tissue partitioning is the binding affinity of the drug to plasma proteins relative to tissue membranes and macromolecules [11,12].

Metabolism, by and large, generates more hydrophilic products (metabolites) of drugs and other xenobiotics, and in this way facilitates their more efficient excretion from the system in urine. This may be by the introduction or revelation of polar groups on these molecules in what is traditionally termed as phase I metabolism, or by the covalent conjugation of these molecules (or their phase I metabolites) to highly hydrophilic endogenous entities in what is referred to as phase II metabolism. Phase I metabolism mainly involves oxidation, reduction and hydrolysis reactions mainly carried out by enzymes of the cytochrome P450 family. Phase II metabolism usually leads to the formation of glucuronide, sulfate, glutathione, acetate or amino-acid conjugates by the action of the relevant transferase enzymes. The enzyme systems involved in the biotransformation of drugs are localized primarily in the liver, although every tissue examined has some metabolic activity, including the GI tract, kidneys, and lungs. Phase I metabolism usually results in loss of pharmacological activity of a drug, though in some cases the resulting metabolites may acquire or retain pharmacological activity (e.g. in the case of pro-drugs and active metabolites), or even exhibit toxic or altered pharmacological activity [11,12].

Drugs are eliminated from the body either unchanged or after their conversion to metabolites. The kidney is the most important organ for excreting drugs and their metabolites, and eliminates polar compounds more efficiently than substances with high lipid solubility. Lipophilic drugs tend to be reabsorbed quite efficiently by the kidneys, and it is for this reason that they are not readily eliminated until they are metabolized to more polar compounds. It is also noted that only the unbound fraction of the drug in plasma is available for renal clearance, and hence drugs with high plasma protein binding tend to be excreted relatively slowly by the kidney [11,12].

6.5 Preliminary PK profiling of compounds 3.15b and 5.13

As described in Chapter Five, compounds **3.15b** and **5.13** were selected for preliminary PK profiling and *in vivo* antimalarial testing. Compound **3.15b** was the most active target compound so far identified; compound **5.13** was one of the more active analogs of **3.15b**, had a significantly improved predicted (pH-dependent) solubility relative to **3.15b**, and was a potent inhibitor of hemozoin formation. The possible simultaneous PK profiling of **5.7**, a predicted metabolite of **5.13**, was an additional reason for the selection of **5.13** for these studies.

Briefly, the intention was to formulate the selected compounds appropriately, dose them individually (orally and/or otherwise) to healthy mice and determine the circulating concentrations of the compounds at different time points over a sufficient duration of time. The concentration-time profiles thus attained would enable a qualitative analysis of the absorption and elimination patterns of the two compounds, as well as a quantitative estimation of such parameters as half life ($t_{1/2}$), maximum concentration (Cmax), and time to maximum concentration (Tmax).

These results would also guide in the selection of appropriate formulation for each compound in the subsequent *in vivo* efficacy studies, and in the interpretation of the results from these assays.

6.5.1 Analytical methodology

The anticipated PK studies were envisaged to proceed *via* the following broad steps.

- Dosing of the mice *via* the appropriate route(s);
- Sampling of blood from the dosed mice at appropriate intervals;
- Liquid-liquid extraction to extract the compound from the blood plasma (an aqueous medium) into a suitable organic solvent;
- Determination of the concentration of the compound in the organic solvent;
- Calculation of the initial concentration of the compound in the blood sample, which would correspond to the circulating concentration of the compound at the time of sampling.
- Analysis of the resulting concentration – time profile.

However, prior to the dosing of the mice, it was necessary to develop suitable sample preparation and analytical methods capable of detecting and quantifying the two test

compounds 3.15b and 5.13 at low (nano-molar) concentrations from mouse whole-blood samples. These analytical methods were kindly developed and validated by Dr. Tracy Kellerman in our laboratories at the Division of Pharmacology, University of Cape Town.

The methods are summarized below.

6.5.1.1 Chromatography and Mass spectrometric conditions

An AB SCIEX API 3200 Triple Quadropole system (Applied Biosystems) was used for sample analysis. The instrument was equipped with a Turbo electro-spray ionization (ESI) source. The system was operated in positive ion mode. The spray voltage and source temperature were 5500 V and 450°C respectively. Nitrogen was used as the nebulizer and curtain gas and set to 50 and 20 (arbitrary) units, respectively. The argon collision gas pressure was set to 5 (arbitrary) units.

The MS-MS system was coupled to an Agilent 1200 Series HPLC System (Agilent Technologies), and both instruments were interfaced with a Lenovo® Windows® XP computer running Applied Biosystems Analyst Software version 1.5.

For the analysis of 3.15b (and 3.15c, here used as an internal standard), the system was fitted with a Supelco® Luna NX 100A (50 x 2.00mm) column, maintained at a temperature of 20 °C. Gradient elution was applied using binary mixtures of 2.5 mM ammonium bicarbonate (solvent A) and AcN (solvent B), at a flow rate of 0.6ml/min.

Table 6.1: Table showing the gradient elution applied for 3.15b and 3.15c

Time (min)	Flow rate (µl/min)	A (%)	B (%)
0.00	600	70	30
1.00	600	70	30
1.10	600	5	95
4.90	600	5	95
5.00	600	70	30
8.00	600	70	30

The LC-MS-MS system was operated at unit resolution in the multiple reaction monitoring (MRM) mode, monitoring the transition of the molecular ion m/z 557.08

to the product ion m/z 161.90 (quantifier) and 215.00 (qualifier) for **3.15b**, and 587.11 to the product ion m/z 162.00 (quantifier) and 215.00 (qualifier) for **3.15c**.

For the analysis of **5.13**, its proposed metabolite **5.7** and internal standard **5.8**, the system was fitted with a Phenomenex® Luna 5μ PFP 100A (50 x 2.00mm) column, maintained at a temperature of 20 °C. Gradient elution was applied using binary mixtures of 10 mM ammonium acetate (solvent A) and MeOH (solvent B), at a flow rate of 0.5ml/min.

Table 6.2: Table showing the gradient elution applied for **5.13**, **5.7** and **5.8**

Time (min)	Flow rate (μl/min)	A (%)	B (%)
0.00	500	28	72
1.00	500	28	72
1.10	500	3	97
5.00	500	3	97
5.10	500	28	72
8.50	500	28	72

The LC-MS-MS system monitored the transition of the molecular ion m/z 574.14 to the product ion m/z 189.00 (quantifier) and 248.15 (qualifier) for **5.13**, 248.10 to the product ion m/z 205.10 (quantifier) and 191.00 (qualifier) for **5.7** and 397.08 to the product ion m/z 205.20 (quantifier) and 178.10 (qualifier) for **5.8**.

Examples of the chromatograms from the analysis of the compounds are shown below (Figure 6.1).

A

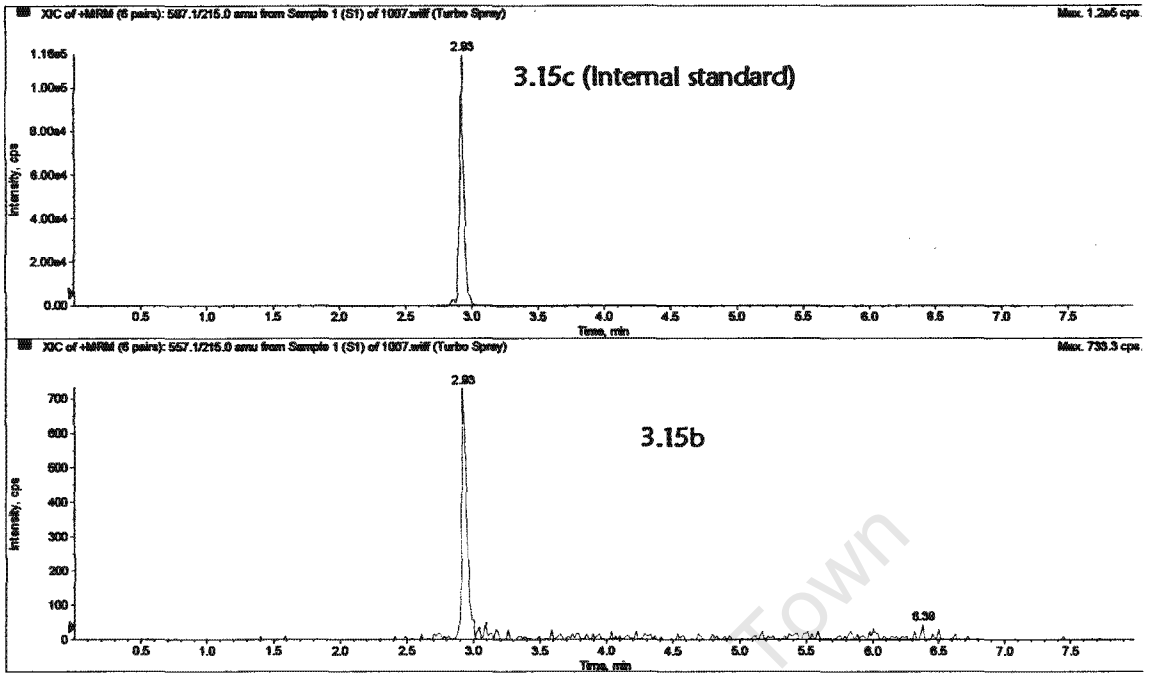

B:

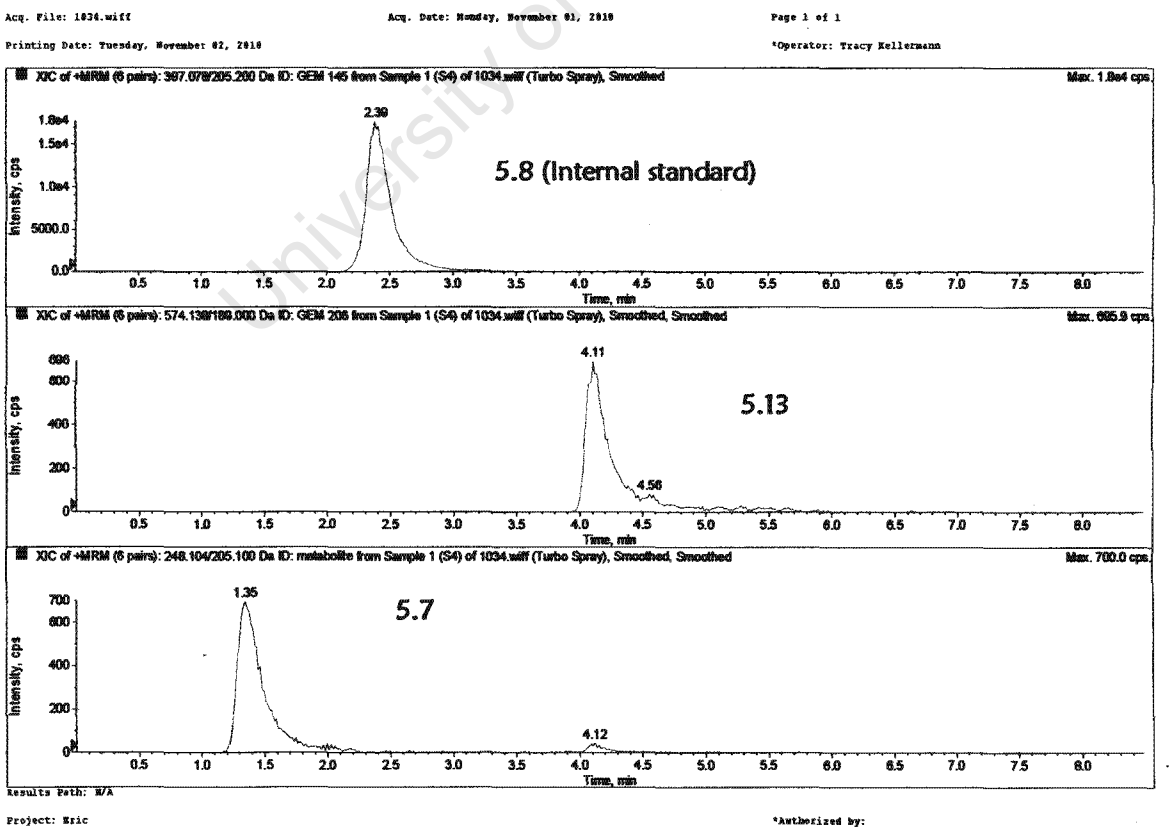

Figure 6.1: Sample chromatograms from the analysis: **A: 3.15b** and **3.15c** (as internal standard); **B: 5.13, 5.7** (putative metabolite) and **5.8** (as internal standard).

6.5.1.2 Preparation of Calibration Standard Solutions

Combined calibration standard solutions of **3.15b**, **5.7** and **5.13** in whole mouse blood were prepared as follows.

Three 1.0 mg/mL stock solutions (SS1) were prepared by separately dissolving 1 mg of **3.15b**, **5.7** or **5.13** in 1.0 mL DMSO. The solutions were vortexed for 1 min to complete dissolution. A 1:10 dilution in DMSO was carried out for each SS1 to yield SS2 solutions of 100 μg/mL. All stock solutions were kept frozen (-80 °C) when not in use.

20 μL of each of the three SS2 was added into the same 1940 μL mouse whole blood to yield 2 mL of the standard solution S9 containing 1000 ng/mL of each analyte, and which represented the upper limit of quantitation (ULOQ). The solution was vortexed for 1 min, after which 1 mL of this S9 was transferred to 1 mL of whole mouse blood to yield the 500 ng/mL S8. Similar 1:1 dilutions were continued down to the 3.9 ng/mL S1 (Table 6.3).

Fresh standard solutions were prepared for every batch run.

Table 6.3: Concentrations of calibration standards

Standard	S1 - LLOQ	S2	S3	S4	S5	S6	S7	S8	S9- ULOQ
Conc. (ng/ml)	3.9	7.8	15.6	31.3	62.5	125	250	500	1000

6.5.2 Dosing and sample collection

Male C57BLACK6 mice weighing 18 – 22g were sourced from the animal breeding facilities at the University of Cape Town (UCT), South Africa. The animals were housed in an accredited facility run on a 12-h light and dark cycle, and were allowed unrestricted access to food and water. All protocols for the animal studies conformed to the highest standards for the humane handling, care, and treatment of research animals and were approved by the UCT Animal Ethics Committee.

3.15b was administered to 5 mice per group as follows:

- 10% DMSO-water formulation at 20mg/kg by oral gavage:

- Pheroid formulation (3.8% Pheroid + 96.2% gassed water) at 20mg/kg by oral gavage;
- SMEDDS formulation (50% sesame oil, 15% water; 7% PEG400; 7% ethanol; 21% Tween 80) at 20mg/kg by oral gavage.
- 3.15b was also administered to 3 mice intravenously at 2mg/kg in 10% DMSO-water; injected into dorsal penis vein.

5.13 was administered to 5 mice per group as follows:

- 10% DMSO-water formulation at 20mg/kg by oral gavage;
- pH4 acetate buffer at 20mg/kg by oral gavage;
- 5.13 was also administered to 3 mice intravenously at 2mg/kg in 10% DMSO-water; injected into dorsal penis vein.

At the low concentration used for IV administration, the compounds remained in solution in 10% DMSO-water, and were therefore suitable for intravenous use. The volume administered for both oral and IV dosing was 200 μL.

Immediately before dosing (0 hrs), 15μl of whole blood was collected by making a small incision in the upper tail and collecting the blood in hepanarized tubes. The blood was immediately transferred to polypropylene vials on ice containing 50μl of pH9 Britton Robinson universal buffer after which they were vortexed and frozen at -80°C until analysis.

Each mouse then received an oral or IV dose as outlined above. Subsequently, 15 µL samples of blood were drawn as described above from each mouse at 0.5, 1, 2, 5, 8 and 24 hours after dosing. However, for the IV experiments, the first samples were drawn 5min after dosing; the remaining samples were then drawn at the same time points as indicated above.

All samples were immediately frozen at -80°C.

6.5.3 Extraction procedure

The same method was developed for the extraction of all the mouse blood samples (i.e. the calibration standards S1-S9 and the actual mouse blood samples from the PK experiments), with the only variation being the internal standard solution used for extraction. The general extraction procedure is described below.

The frozen samples were thawed in a water bath at 37°C. 15 μL of the calibration standards in mouse whole blood were transferred in duplicate to 1.5 mL polypropylene centrifuge vials containing 50 μL of universal buffer pH 9.0. The actual mouse blood samples from the PK experiments were already in the buffer pH 9.0, and were thus ready for extraction after thawing.

To each of these mixtures, 250 μL of ethyl acetate containing the appropriate internal standard was added - for the extraction of samples of 3.15b, a 50 ng/mL solution of 3.15c in ethyl acetate was used as the extraction solvent; for the extraction of samples of 5.7 and 5.13, a 25 ng/mL solution of 5.8 in ethyl acetate was used as the extraction solvent.

The vials were capped, vortexed for 1 min, and the mixtures clarified by centrifugation at 13000 rpm for 5 minutes. 210 μL of the clear ethyl acetate supernatant was then carefully transferred from each vial into clean vials and dried under a steady stream of nitrogen. The residues were then re-dissolved in an AcN/water (75:25) mixture. These were then vortexed for 30 sec, transferred to low-volume glass inserts and placed into glass chromatography vials, ready for LC-MS-MS analysis (10 μL injection volume) using the method described above.

A pair of blank samples was prepared by transferring plain mouse whole blood (15 μL) into 50 μL of universal buffer pH 9.0 and extracting with ethyl acetate solution of the appropriate internal standard. A pair of double blanks was also prepared by transferring plain mouse whole blood (15 μL) into 50 μL of universal buffer pH 9.0 and extracting with plain ethyl acetate.

For both 3.15b and 5.13, the samples were extracted, prepared and analyzed as single batches.

6.5.4 Results

6.5.4.1 Calibration curves

For compound 3.15b, the calibration standards were analyzed (in duplicate) along with the unknown blood samples (from the PK experiments) as a single batch. The results from the LC-MS-MS analysis of the calibration standards were used in the generation of standard calibration curves which were then be applied in the

quantification of 3.15b in the unknowns. A similar approach was used for the simultaneous quantitation of 5.13 and 5.7.

Examples of the calibration curves are given below (Figure 6.2):

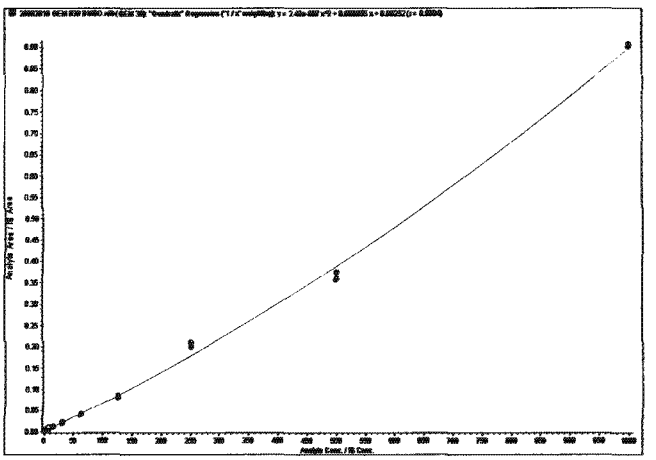

3.15b

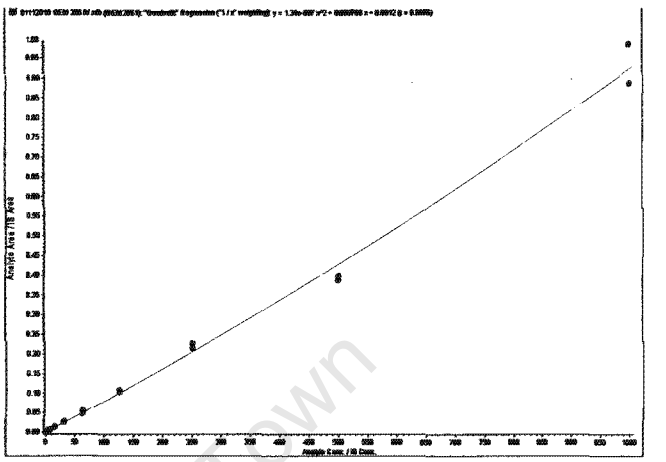

5.13

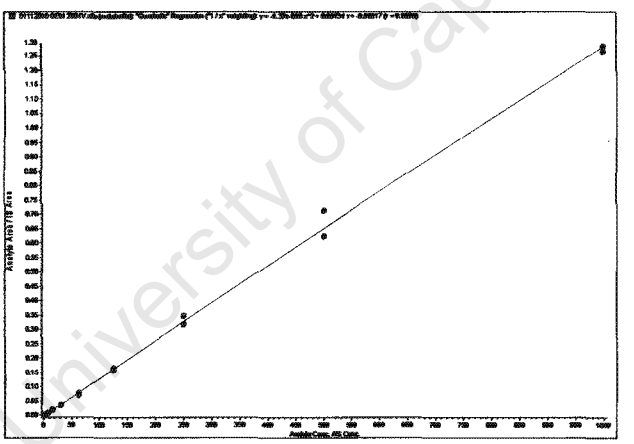

5.7

Figure 6.2: Examples of calibration curves for 3.15b, 5.13 and 5.7

All the calibration curves showed good fit, with r-squared values all > 0.9.

The quantitation of the unknown samples was done automatically by the Analyst Software version 1.5, using the generated calibration curves as reference.

6.5.4.2 Pharmacokinetic results for 3.15b

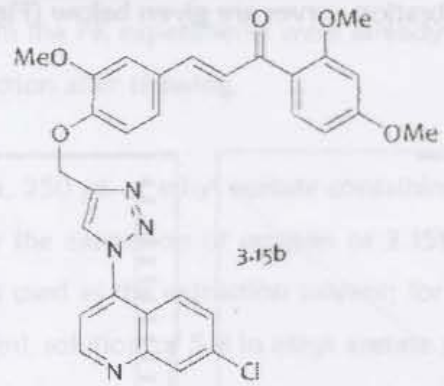

Compound 3.15b

The determined concentrations of 3.15b are shown in Table A1 (Appendix A). The average concentrations were then plotted against time of sampling to yield the concentration-time profiles shown in Figure 6.3 below.

A:

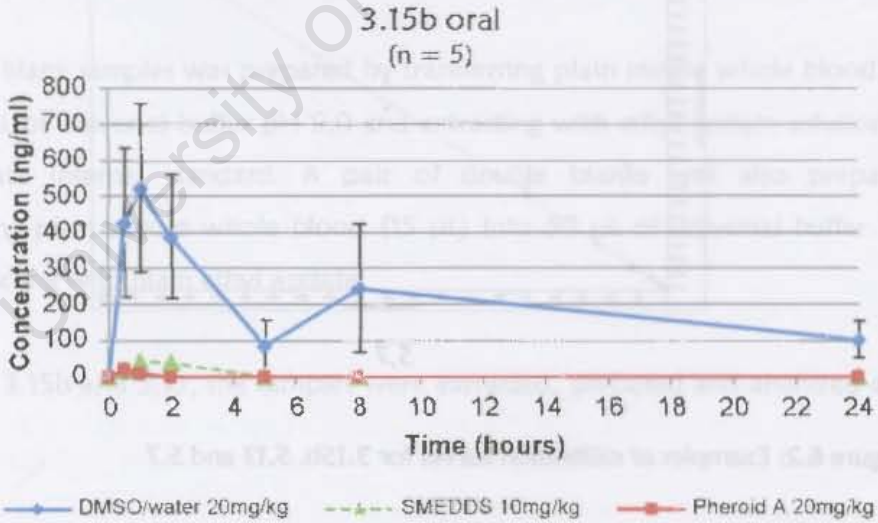

B:

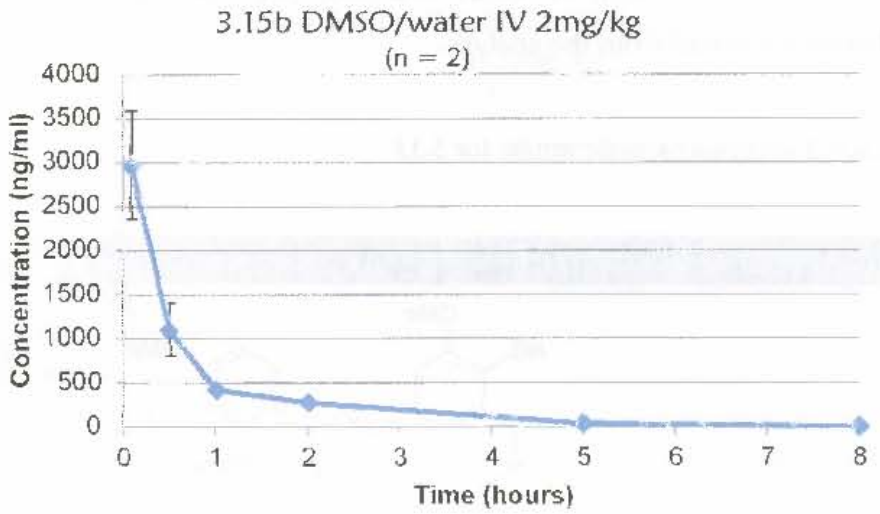

Figure 6.3: Graphs showing how circulating concentrations of 3.15b vary with time. A: after oral administration; B: after IV administration. (Error bars represent standard deviations.)

The 10%DMSO-water formulation yielded the highest exposure after oral dosing, with circulating concentrations reaching a maximum of 520 ng/mL. With this formulation, the compound exhibited a possible bi-phasic concentration-time profile, with two peak concentrations. Maximum circulating concentrations were achieved approximately 1 hour after dosing; these levels then fell gradually over 4 hours, reaching lows of just over 80 ng/mL about 5 hours post-dosing, before rising again to give a second peak concentration of approximately 240 ng/mL approximately 8 hours after dosing (however, the large error bar associated with this second peak introduces a degree of uncertainty around the observed bi-phasic profile). Concentration levels fell to below quantifiable levels within 24 hours after dosing. This bi-phasic profile did not allow for the modelling of the data and the estimation of descriptive PK statistics (e.g. half-life).

Exposure from the alternative formulations (SMEDDS and Pheroid) was, by comparison, very poor, with circulating concentrations never exceeding 50 ng/mL. No evidence of a bi-phasic PK profile with these formulations was observed.

As expected after IV administration, peak circulating concentrations of 3.15b were seen immediately after dosing – a maximum concentration of almost 3000ng/mL was observed. However, this concentration fell rapidly to just over 400 ng/mL after 1 hour. Basic PK analysis using WinNonLin version 4.1 estimated the half life of 3.15b as 1.1 hrs. This rapid decline then tapered off, and circulating concentrations fell more gradually, reaching approximately 40 ng/mL after 5 hours and falling to below quantifiable levels after 8 hours.

NB: the results from one of the mice used for the IV PK experiment were unusually lower than those from the other two mice (see Table A1, Appendix A), and were therefore omitted from the analysis.

6.5.4.3 Pharmacokinetic results for 5.13

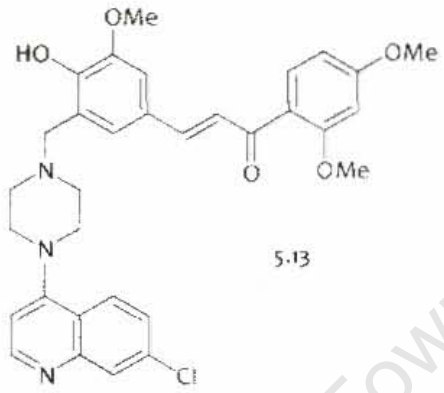

Compound 5.13

The determined concentrations of 5.13 are shown in Table A2 (Appendix A). Table A3 shows the concentrations of 5.7, the predicted metabolite, in the same samples. The average concentrations of both compounds are plotted against time of sampling to yield the concentration-time profiles shown in Figure 6.4 below.

A:

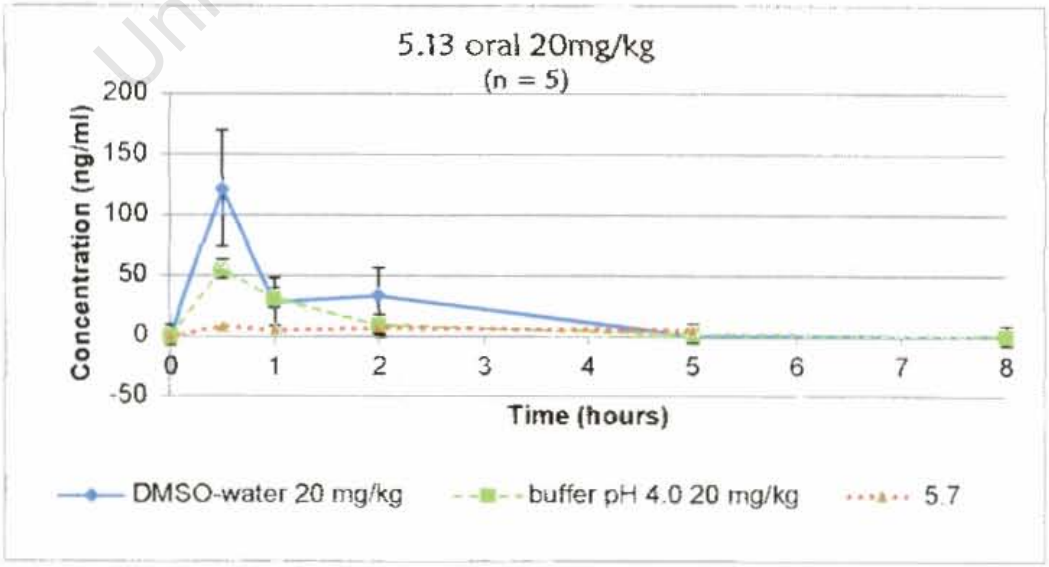

B:

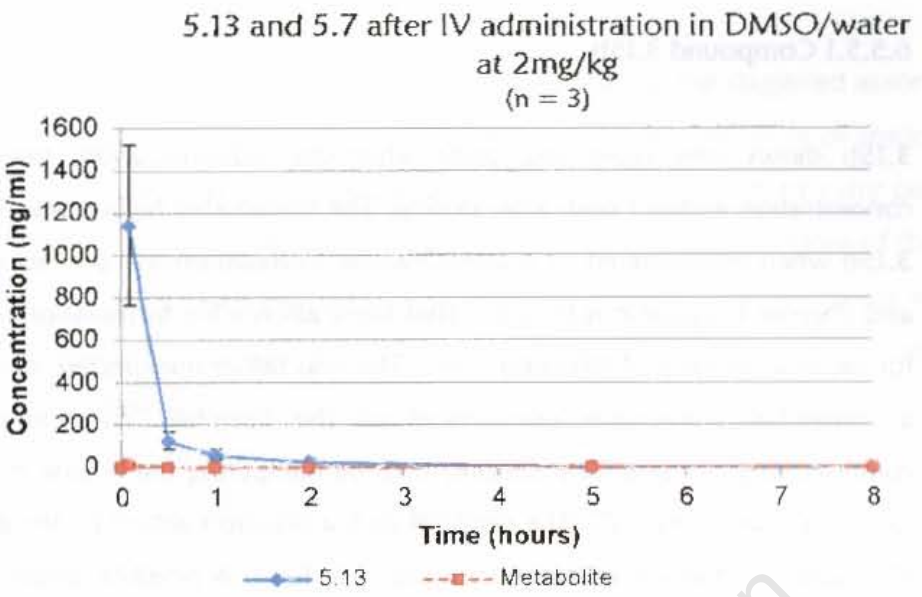

Figure 6.4: Graphs showing how circulating concentrations of 5.13 and 5.7 vary with time. A: after oral administration; B: after IV administration. (Error bars represent standard deviations.)

As was the case for 3.15b, the 10%DMSO-water formulation also yielded the highest exposure after oral dosing of 5.13, with circulating concentrations reaching a maximum of just over 250 ng/mL within 30 min of dosing. These levels then declined rapidly, down to approximately 60 ng/mL after 1 hour, and then more gradually to below detectable levels after 5 hours.

NB: the results from one of the mice used for the 5.13 DMSO-water oral experiment were unusually higher than those from the other four mice (see Table A2, Appendix A), and were therefore omitted from the analysis.

Exposure from the alternative formulation (acetate buffer pH 4.0) followed a similar trend but is, by comparison, relatively poor. The maximum circulating concentrations were just over 50 ng/mL.

As expected after IV administration, peak circulating concentrations of 5.13 were seen immediately after dosing. However, the maximum concentrations observed of approximately 1140 ng/mL were not as high as those observed for 3.15b. These levels also fell quite rapidly, down to just under 60 ng/mL within 1 hour, approximately 25 ng/mL after 2 hours and fell to below quantifiable levels after 5 hours. Basic PK analysis using WinNonLin version 4.1 estimated the half life of 5.13 as 0.6 hrs.

Interestingly, the predicted metabolite 5.7 was detected in circulation after both oral (10%DMSO-water formulation) and IV administration of 5.13. However, the detected levels of this metabolite were very low, and never exceeded 20 ng/mL.

6.5.5 Discussion of results

6.5.5.1 Compound 3.15b

3.15b shows very rapid absorption after oral administration, reaching maximum concentration within 1 hour after dosing. The remarkably higher oral bioavailability of 3.15b when administered as a DMSO-water formulation as opposed to the SMEDDS and Pheroid formulations indicates that these alternative formulations are not optimal for the oral delivery of this compound. This was rather unexpected, and could point to a somewhat irreversible entrapment of the lipophilic compound in the lipid component(s) of these formulations, thereby hampering the release of the compound for absorption in the GIT. The result of such a situation would be the almost complete elimination of the administered compound in feces. A possible conclusion from this is that perhaps the improvement or otherwise of the oral bioavailability of a compound by the use of formulations is compound-specific, dependent on the compound's unique properties and its interaction with the formulation.

A possible bi-phasic PK profile was also a notable feature of 3.15b after oral administration as a DMSO-water formulation. Multi-peak PK profiles usually result from either:

- entero-hepatic circulation, whereby the compound is excreted into the GIT in bile and thereafter gets reabsorbed;
- redistribution of the compound into body tissues, where it subsequently undergoes a concerted release from these reservoirs back into circulation; or
- staggered absorption, i.e. absorption in two separate sections of the GIT [3].

It would be expected that a compound that undergoes entero-hepatic circulation would still show features of biliary excretion and GI reabsorption even after IV administration. However, the PK profile of 3.15b after IV administration (Figure 6.3B) does not show evidence of a second wave of absorption, thereby suggesting that entero-hepatic circulation does not explain the bi-phasic PK profile observed after oral administration of 3.15b.

The appearance of the second peak in the PK profile of 3.15b after oral administration occurs approximately 8 hours after dosing, a period that is much too short to account for redistribution into bodily tissues and subsequent release. Furthermore, tissue redistribution would also occur after IV administration, and the absence of the bi-phasic PK profile after IV administration of 3.15b discounts tissue distribution and

subsequent release as the mechanism behind the PK profile observed after oral administration.

Therefore, the likely explanation for this PK profile would be the staggered absorption of 3.15b in two different sections of the GIT. For example, the first wave of absorption could occur in the more proximal portions of the GIT (the stomach or early parts of the small intestine), while the next phase could occur in more distal portions of the GIT (late small intestine or large intestine). The duration between the two peaks would also be consistent with GI motility and the movement of GI contents along the tract [3]. Such a phenomenon could also be facilitated by possible compound precipitation, followed by slower re-dissolution and delayed absorption; this is quite possible considering the poorly solubility of the compound.

The rapid decline in the circulating concentrations of 3.15b after IV administration, approximately six-fold within the first hour, indicates an extremely efficient clearance of the compound, possibly a combination of both hepatic and renal clearance. As discussed in Chapter 5 (Section 5.8.2), compound 3.15b was shown during *in vitro* metabolism studies to exhibit intermediate extraction ratios in both human and mouse microsomes. The main route of metabolism of this compound appeared to be oxygenation, most likely resulting in the N-oxide metabolite (putative metabolite P + 16). It is therefore quite possible that this biotransformation, and the subsequent renal excretion of the more polar oxygenated metabolite, could explain the rapid clearance of 3.15b from systemic circulation.

6.5.5.2 Compound 5.13

Compound 5.13 shows very rapid absorption after oral administration, reaching maximum concentration within 30 min after dosing. The DMSO-water formulation yielded the better exposure following oral administration of 5.13, affording maximum circulating concentrations over two times higher than those afforded after administration of the compound as a solution in acetate buffer pH 4.0. 5.13b was more soluble in buffer pH 4.0, forming a clear solution as opposed to a milky but stable suspension in DMSO-water; however, this improved solubility did not translate into the expected improved oral bioavailability. A possible explanation for this is based on the degree of ionization of the compound, as described below.

The rationale behind formulation of insoluble but ionizable compounds in appropriate buffers is to allow for their ionization and the improved solubility that this affords. However, many compounds cannot traverse the GIT membrane in their ionized state, particularly weakly acidic compounds. Therefore, and as discussed in section 5.6.3.1,

the presence of an equilibrium between the ionized and non-ionized states is crucial for absorption.

Compound 5.13 is predicted to be >90% ionized at pH 5.0, possibly higher at pH 4.0. It would be expected that this degree of ionization would fall gradually as the administered formulation moves along the GIT into the more alkaline small and large intestines; the increasing portion of the non-ionized compound would then be available for absorption. It is quite possible, however, that the volume of administered buffer was sufficiently large to actually modify the pH of the intestines, lowering the otherwise alkaline pH and keeping most of the compound in the ionized state. This is particularly probable considering the rather small size of mice, and even smaller volume of their GI tract, and could perhaps explain the lower oral bioavailability despite the observed improved solubility with this formulation.

Also noteworthy was that significantly higher exposure and circulating concentrations were observed for 3.15b compared to 5.13; the maximum circulating concentrations for 3.15b were approximately three times those observed for 5.13 when administered orally in similar formulations (DMSO-water). In this regard, 5.13 did not offer any of the anticipated improvement on the oral bioavailability of 3.15b. This is probably the result of the higher metabolic instability of 5.13 relative to 3.15b; based on the *in vitro* metabolism studies (section 5.8.2), 5.13 had a higher extraction ratio in both mouse and human microsomes, and was also susceptible to several routes of metabolism, including O-demethylation, N-dealkylation and glucuronide conjugation

The bi-phasic PK profile observed after the oral administration of 3.15b was not replicated for 5.13, possibly due to the distinctly different physicochemical properties of the two related compounds.

The rapid decline in the circulating concentrations of 5.13 after IV administration, approximately five-fold within the first hour, also indicates an extremely efficient clearance of the compound. As discussed in Chapter 5 (Section 5.8.2), compound 5.13 was shown during *in vitro* metabolism studies to exhibit relatively high extraction ratios in both human and mouse microsomes (E_H > 0.7). The main routes of metabolism of this compound appeared to be O-demethylation, N-dealkylation and glucuronide conjugation. It is therefore quite possible that this susceptibility to several routes of metabolism, could explain the rapid clearance of 5.13 from systemic circulation.

However, the detected levels of the predicted *N*-dealkylation metabolite 5.7 in circulation were very low, which could suggest that either this was not the primary

route of metabolism in mice, or that this particular metabolite was polar enough to be efficiently eliminated by the kidneys in urine before significantly accumulating in circulation.

No detailed statistical analysis of the PK results of these compounds was carried out. As described above, only qualitative analysis of the data was carried out, as this was sufficient to allow for a general comparison of the bioavailability of the two compounds and enable preliminary conclusions to be reached.

Of the various formulations used for the oral administration of 3.15b and 5.13, the 10%DMSO-water formulation afforded the best oral bioavailability for both compounds. This formulation was therefore selected for oral dosing of the compounds for the subsequent *in vivo* antimalarial efficacy studies, reported in the next section.

overall clearance; notably however, murine models with human hepatocytes (and which would ideally exhibit similar metabolic profiles) are under development [18].

In spite of these challenges, the murine malaria disease model continues to be extensively used for *in vivo* antimalarial efficacy testing. In this study, the *P. yoelii* murine malaria model was used for the *in vivo* efficacy studies of compounds 3.15b and 5.13.

6.6.2 *In vivo* antimalarial assays of compounds 3.15b and 5.13

Male C57BLACK6 mice weighing 18 – 22g were sourced from the animal breeding facilities at the University of Cape Town (UCT), South Africa. The animals were housed in an accredited facility run on a 12 hour light-dark cycle, and were allowed unrestricted access to food and water. All protocols for the animal studies conformed to the highest standards for the humane handling, care, and treatment of research animals and were approved by the UCT Animal Ethics Committee.

The chloroquine sensitive *Plasmodium yoelii N.* strain used in the study was sourced from WHO repository, University of Edinburgh, Scotland. The parasite strain was propagated in mice and maintained by serial passage of infected erythrocytes.

The antimalarial activity of the two compounds 3.15b and 5.13 was evaluated using the modified Peter's 4-day suppressive test [19]. Each mouse was inoculated intraperitoneally with 1×10^7 *P. yoelii*-infected erythrocytes suspended in 200 μL of phosphate-buffered saline. The mice were randomly divided into groups of five animals per cage and treated for 4 consecutive days (beginning on the day of infection, day zero) with daily oral doses of 20, 10 or 5 mg/kg/day of either 3.15b or 5.13 (10%DMSO/water formulation). Two control groups were used in each experiment; one was treated with chloroquine at a low non-curative dose (10mg/kg/day, orally) and the other group was left untreated. Coded blood smears were prepared from blood samples from all the mice on day 2 (second day post-infection) and examined to confirm if the infection had taken.

Thin blood smears were prepared from the tail blood obtained from each of the surviving mice on days 4, 7, and 10 after infection from the untreated controls and from treated animals. The levels of parasitemia were determined from the Giemsa-stained smears by counting the percentage of infected erythrocytes in 500 – 600

6.6 *In vivo* antimalarial efficacy studies

6.6.1 Introduction

As previously mentioned in section 6.2, the purpose of *in vivo* antimalarial efficacy studies is to investigate the ability of a test compound to exert its antimalarial activity within a living organism, where anatomical, physiological, immunological and other biological factors present in such a system also come into play.

Animal malaria models are usually applied for these studies, with the murine malaria model being the most widely used model [13]. *Plasmodium berghei, P. yoelii, P. vinckei* and *P. chabaudi* are four malaria species that infect African murine rodents that have been extensively used as malaria models for drug testing, malaria vaccine development and the study of immunopathological reactions and mosquito transmission [14,15]. Though phylogenetically distant, these species closely resemble human malaria parasites in terms of their basic biology. Biochemical and genetic processes, and hence similarities in drug susceptibility and mechanisms of drug resistance, appear to be relatively conserved between the different species [14].

The laboratory mice used for these studies are cheap, easily maintained and are usually well characterized through careful breeding. The murine malaria parasites used are usually well characterized clones, and the mouse model allows for experimentation with a range of different inoculation and treatment protocols.

The main disadvantage of using these models (and indeed any animal model) is the difficulty in extrapolating results from these models to actual humans [15]. In the application of these murine malaria models, two important considerations must be made.

First, the parasite species has been changed, and the test compound may be more or less potent against the murine parasite than the human parasite; it should be noted that, in an attempt to address this challenge, immune-compromised mice have been used to develop mouse 'humanized' murine malaria models (mice inoculated with human malaria parasites) [16,17]; these are yet to become widely available for routine drug discovery studies, possibly due to cost implications associated with the need to use immune-suppressed and/or genetically manipulated mice for this model - rodents are not normally susceptible to infection by human malaria parasites [15].

Second, host pharmacokinetics and metabolism may differ between mice and humans in terms of the extent and nature of the metabolism of a compound, as well as its

overall clearance; notably however, murine models with human hepatocytes (and which would ideally exhibit similar metabolic profiles) are under development [18].

In spite of these challenges, the murine malaria disease model continues to be extensively used for *in vivo* antimalarial efficacy testing. In this study, the *P. yoelii* murine malaria model was used for the *in vivo* efficacy studies of compounds 3.15b and 5.13.

6.6.2 *In vivo* antimalarial assays of compounds 3.15b and 5.13

Male C57BLACK6 mice weighing 18 – 22g were sourced from the animal breeding facilities at the University of Cape Town (UCT), South Africa. The animals were housed in an accredited facility run on a 12 hour light-dark cycle, and were allowed unrestricted access to food and water. All protocols for the animal studies conformed to the highest standards for the humane handling, care, and treatment of research animals and were approved by the UCT Animal Ethics Committee.

The chloroquine sensitive *Plasmodium yoelii N.* strain used in the study was sourced from WHO repository, University of Edinburgh, Scotland. The parasite strain was propagated in mice and maintained by serial passage of infected erythrocytes.

The antimalarial activity of the two compounds 3.15b and 5.13 was evaluated using the modified Peter's 4-day suppressive test [19]. Each mouse was inoculated intraperitoneally with 1×10^7 *P. yoelii*-infected erythrocytes suspended in 200 μL of phosphate-buffered saline. The mice were randomly divided into groups of five animals per cage and treated for 4 consecutive days (beginning on the day of infection, day zero) with daily oral doses of 20, 10 or 5 mg/kg/day of either 3.15b or 5.13 (10%DMSO/water formulation). Two control groups were used in each experiment; one was treated with chloroquine at a low non-curative dose (10mg/kg/day, orally) and the other group was left untreated. Coded blood smears were prepared from blood samples from all the mice on day 2 (second day post-infection) and examined to confirm if the infection had taken.

Thin blood smears were prepared from the tail blood obtained from each of the surviving mice on days 4, 7, and 10 after infection from the untreated controls and from treated animals. The levels of parasitemia were determined from the Giemsa-stained smears by counting the percentage of infected erythrocytes in 500 – 600

randomly counted erythrocytes. Weights, stress/discomfort and mortality were monitored daily in all groups during the post-inoculation period.

The antimalarial activity of the compounds was then evaluated based on the degree and duration of suppression of parasitemia, the rate of decline of the mouse body weights and duration of mouse survival after infection, compared to that of chloroquine, an established antimalarial.

6.6.3 Results

6.6.3.1 Compound 3.15b

A:

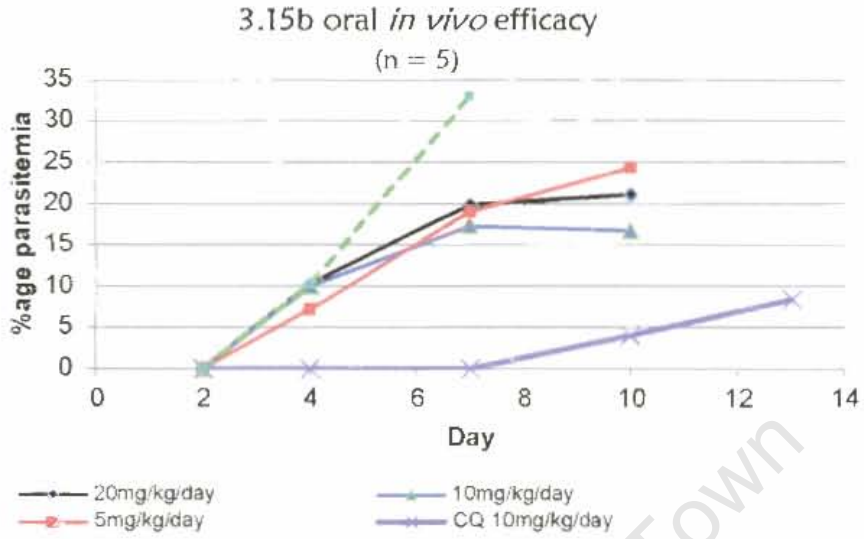

B:

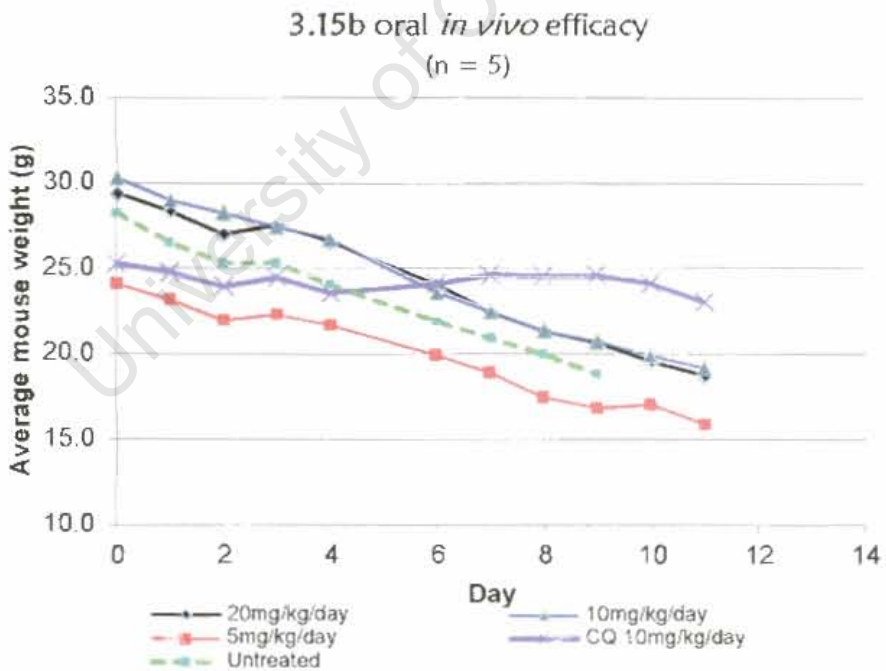

Figure 6.5: Graphs showing trends in %age parasitemia (A) and average mouse weights (B) after the oral administration of chloroquine and varying doses of 3.15b

There was no notable difference between the three dosing levels of 3.15b with respect to suppression of parasitemia; the rising trend in parasitemia was relatively similar between the three groups (Figure 6.5A).

The rate at which parasitemias rose was somewhat lower for the mice treated with 3.15b relative to the untreated controls, quite obvious after day 4. This suggested a present but limited level of suppression of parasitemia by 3.15b. However, this suppression was not comparable to that afforded by chloroquine; the group of mice treated with the non-curative dose of 10 mg/kg/day of chloroquine still had parasitemias lower than 5% even 10 days after infection.

The mice in the three groups treated with 3.15b, as well as the untreated controls, showed similar rates of decline in average mouse weights, which was used as a proxy indicator of the health and well-being of the mice. However, the weights of the chloroquine-treated mice did not change notably over the course of the study.

In terms of mouse survival, 2 mice from each of the three groups survived for 11 days after infection; no mice among the untreated controls survived beyond day 9. All the mice in the chloroquine group survived the course of the study, which was terminated after 13 days.

6.6.3.2 Compound 5.13

A:

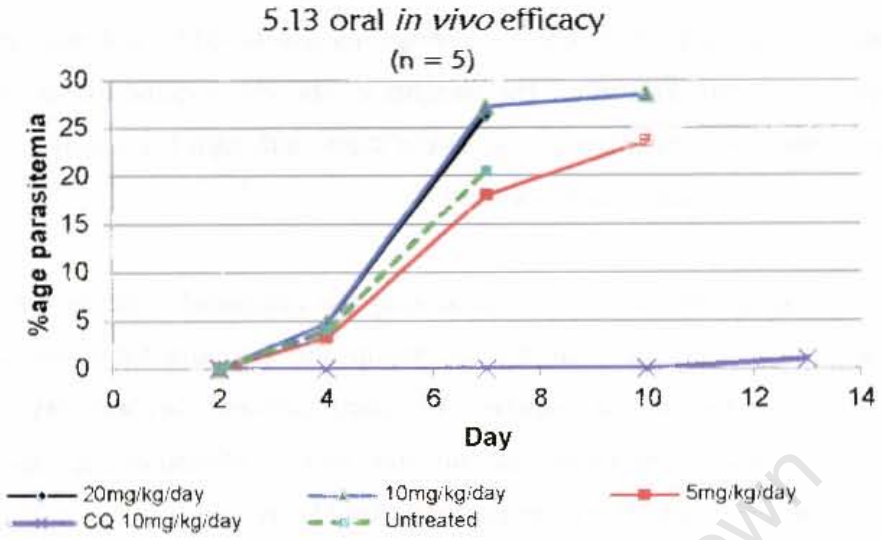

B:

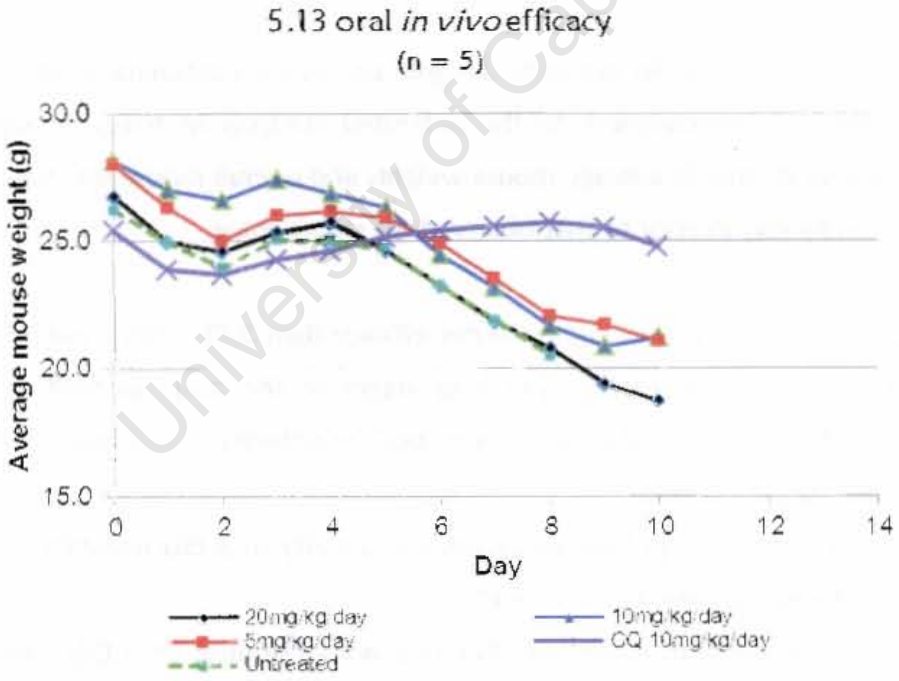

Figure 6.6: Graphs showing trends in %age parasitemia (A) and average mouse weights (B) after the oral administration of chloroquine and varying doses of 5.13

There was a similar trend among the three dosing levels of 5.13 with respect to suppression of parasitemia: interestingly, the rise in parasitemia is relatively higher in the 20 mg/kg/day and 10 mg/kg/day groups than in the 5 mg/kg/day groups. No improvement over the untreated controls was observed. The group of mice treated

with the non-curative dose of 10 mg/kg/day of chloroquine maintained parasitemias lower than 5% throughout the duration of the study.

The mice in the three groups treated with 5.13, as well as the untreated controls, showed similar rates of decline in average mouse weights, a trend similar to that observed for 3.15b. However, the weights of the chloroquine-treated mice did not change considerably over the course of the study, although there was a notable dip in mouse weights 1 – 3 days after infection.

In terms of mouse survival, no mice among the untreated controls survived beyond day 10; 2 mice from the 5 mg/kg/day group and 1 mouse from the 20 mg/kg/day group survived to day 12, whereas no mice survived beyond day 11 in the 10 mg/kg/day group. As expected, all the mice in the chloroquine group survived the course of the study, which was terminated after 13 days.

6.6.4 Discussion and conclusions

The two compounds did not exhibit significant *in vivo* antimalarial activity, showing only marginal improvement to the untreated controls in terms of suppression of parasitemia, decline in average mouse weights and overall mouse survival. This activity was considerably inferior to that observed for chloroquine.

Compound 3.15b showed slightly better efficacy than 5.13, with a notably slower rise in parasitemia in the middle and later stages of the study as well as more mice surviving for longer (relative to their respective untreated controls). This is probably explained by two facts:

- its relatively more potent antiplasmodial activity of 3.15b (exhibited during the *in vitro* tests, Chapters 3 and 5), and
- the better exposure achieved after oral administration of 3.15b relative to 5.13, both formulated in DMSO-water.

The fact that 5.13 did not show notably inferior *in vivo* efficacy to 3.15b despite its notably poorer antiplasmodial activity and oral bioavailability points to either a relatively higher susceptibility of the *P. yoelii* strain to 5.13, or perhaps a mechanism that enhances its antimalarial activity, such as accumulation into the acidic food vacuole of the parasite, the putative site of action of this compound. This could be

facilitated by its more basic characteristics conferred by the piperazine linker, which would allow for protonation and acid trapping within the acidic food vacuole.

In conclusion, though compound **5.13** offered the advantage of improved (pH dependent) solubility relative to **3.15b**, this compound had the poorer oral bioavailability of the two compounds, and did not offer any improvement on its antimalarial activity either *in vitro* or *in vivo*.

References

1. W Peters, S L Fleck, B L Robinson, L B Stewart, and C W Jefford. The chemotherapy of rodent malaria. LX. The importance of formulation in evaluating the blood schizonticidal activity of some peroxide antimalarials. *Ann. Trop. Med. Parasitol.* (2002) 96 (6) 559-573.

2. Y-C Lee, P D Zocharski, and B Samas. An intravenous formulation decision tree for discovery compound formulation development. *Int. J. Pharm.* (1993) 253 111-119.

3. E K Kerns and L Di. Drug-like Properties: Concepts, Structure, Design and Methods: from ADME to Toxicity Optimization. (2008) 1st Edition. Academic Press/Elselvier

4. A V Kamath, J Wang, F Y Lee, and P H Marathe. Preclinical pharmacokinetics and in vitro metabolism of dasatinib (BMS-354825): a potent oral multi-targeted kinase inhibitor against SRC and BCR-ABL. *Cancer Chemother. Pharmacol.* (2008) 61 365-376.

5. P P Constantinides. Lipid microemulsions for improving drug dissolution and oral absorption: physical and biopharmaceutical aspects. *Pharm. Res.* (1995) 12 1561-1572.

6. A R Patel and P R Vavia. Preparation and In Vivo Evaluation of SMEDDS (Self-Microemulsifying Drug Delivery System) Containing Fenofibrate. *AAPS J.* (2007) 9 (3) E344-E352.

7. M-J Huang. The transport of the Rooibos tea flavonoid aspalathin across the skin and the intestinal epithelium. *M.Pharm. Dissertation* (2006) (University of the Witwatersrand, South Africa)

8. E Holmes, J C Breytenbach, J du Plessis, and M Gerber. The synthesis of stavudine derivatives for transdermal delivery. *SA Pharm. J.* (2006) Nov/Dec 28.

9. W Wu, Y Wang, and L Que. Enhanced bioavailability of silymarin by self-microemulsifying drug delivery system. *Eur. J. Pharm. Biopharm.* (2006) 63 288-294.

10. C J H Porter, N L Trevaskis, and W N Charman. Lipids and lipid-based formulations: optimizing the oral delivery of lipophilic drugs. *Nature Rev. Drug Discov.* (2007) 6 (3) 231-248.

11. D A Smith, H van de Waterbeemd, and D K Walker. Pharmacokinetics and Metabolism in Drug Design. (2006) 2nd Revised Edition. WILEY-VCH Verlag GmbH & Co. KGaA, Weinheim

12. I L O Buxton. Pharmacokinetics and pharmacodynamics: the dynamics of drug absorption, distribution, action, and elimination. *In: Goodman and Gilman's The Pharmacological Basis of Therapeutics* (2006) 11th Edition. Edited by L L Brunton. McGraw-Hill: Medical Publishing Division. New York

13. D A Fidock, P J Rosenthal, S L Croft, R Brun, and S Nwaka. Antimalarial drug discovery: efficacy models for compound screening. *Nature Rev. Drug Discov.* (2004) 3 509-520.

14. C J Janse and A P Waters. *Plasmodium berghei*: The Application of Cultivation and Purification Techniques to Molecular Studies of Malaria Parasites. *Parasitol. Today* (1995) 11 (4) 138-143.

15. Impact Malaria website – Rodent malaria. *http://www.impact-malaria.com/iml/cx/en/layout.jsp?cnt* (2010)

16. I Angulo-Barturen, M B Jiménez-Díaz, T Mulet, J Rullas, E Herreros, S Ferrer, E Jimenez, A Mendoza, J Regadera, P J Rosenthal, I Bathurst, D L Pompliano, F G de las Heras, and D Gargallo-Viola. A Murine Model of *falciparum*-Malaria by *In Vivo* Selection of Competent Strains in Non-Myelodepleted Mice Engrafted with Human Erythrocytes. *PLoS ONE* (2008) 3 (5) e2252: 1-14.

17. M B Jiménez-Díaz, T Mulet, S Viera, V Gómez, H Garuti, J Ibánez, A Alvarez-Doval, L D Shultz, A Martínez, D Gargallo-Viola, and I Angulo-Barturen. Improved Murine Model of Malaria Using *Plasmodium falciparum* Competent Strains and Non-Myelodepleted NOD-*scid* IL2Rγ^{null} Mice Engrafted with Human Erythrocytes. *Antimicrob. Agents Chemother.* (2009) 53 (10) 4533-4536.

18. A Krishnan, K Viker, H Rietemer, M Telgenkamp, B Knusden, and M Charlton. Prolonged engraftment of human hepatocytes in mice transgenic for the deleted form of human hepatocyte growth factor. *Hepatol. Res.* (2007) 37 854-862.

19. W Peters. The chemotherapy of rodent malaria, XXII: The value of drug-resistant strains of *P. berghei* in screening for blood schizonticidal activity. *Ann. Trop. Med. Parasitol.* (1975) 69 (2) 155-171.

CHAPTER SEVEN

SUMMARY, CONCLUSIONS AND RECOMMENDATIONS FOR FUTURE WORK

7.1 Summary and conclusions

This study set out to identify novel hybrid compounds containing scaffolds that are structurally related to the natural product curcumin, and which possess *in vitro* and *in vivo* antimalarial potency.

The initial objective of the study was to design and synthesize novel hybrid compounds as potential antimalarial agents which contain scaffolds that are structurally related to the natural product curcumin. Targeted series of chalcone/AZT, chalcone/chloroquinoline, dienone/AZT and dienone/chloroquinoline hybrid compounds were therefore designed and synthesized, applying simple and robust click chemistry as the hybridization strategy.

The second objective of the study was to pharmacologically evaluate the synthesized compounds *in vitro* for antimalarial activity and possible mechanisms of action. The synthesized hybrid compounds, as well as selected intermediates, were therefore assayed for *in vitro* antimalarial activity. The acetylenic chalcones 3.9 and 3.10 exhibited moderate *in vitro* antimalarial activity consistent with published results for alkoxylated chalcones. The acetylenic dienones, as well as the acetylenic enone intermediate 3.11, exhibited comparable antimalarial activity to the acetylenic chalcones. The AZT hybrid compounds of both the chalcones and dienones did not exhibit notably higher *in vitro* antimalarial activity relative to their acetylenic precursors, though the retention of activity in most cases was still noteworthy. However, the chloroquinoline-hybridization strategy did lead to the identification of significantly active hybrid compounds, i.e. 3.15b, 3.15c and 3.17b, as well as the enone-chloroquinoline intermediate 3.19. Compound 3.15b was the most active of these, with sub-micromolar IC_{50} values for all three *P. falciparum* strains. No obvious trends were observed as far as the influence of the different substitution patterns of the chalcones or dienones on antimalarial activity was concerned. Results from mechanistic studies suggested that inhibition of hemozoin formation was likely to contribute substantially to the antimalarial activity of most of these compounds. This was particularly so for the hybrid compounds 3.15b, 3.15c and 3.15e, which were all comparably or more potent than chloroquine in inhibiting β-hematin formation. However, the lack of correlation between these proposed mechanisms of action and

the observed *in vitro* antimalarial activities of these compounds suggested the possibility of either the existence of additional mechanisms of action or of other factors that influence the *in vitro* antimalarial activities of these compounds such as varying degrees of lysosomal accumulation within the malaria parasite.

An additional objective of the study was to apply *in silico* (computational) techniques to guide the design of derivatives of the more active compounds with potentially superior physicochemical and/or ADMET properties for subsequent synthesis, *in vitro* antimalarial testing and mechanistic studies. **3.15b** and **3.19** were selected for structural modification with the aim of identifying analogs with improved solubility and which retained antimalarial potency. Eight analogs **5.8 – 5.15** were proposed, and these were characterized *in silico* for selected physicochemical and ADME parameters. These analogs were predicted to have improved solubilities relative to the parent compounds, particularly at low pH; they retained acceptable predicted Caco2 permeability, but were identified as possible substrates for N-dealkylation by hepatic cytochromes. The tentative conclusions that were drawn from the *in silico* solubility predictions and metabolism predictions were supported by experimental solubility determinations and *in vitro* metabolism studies. These proposed analogs were then synthesized and tested, and were found to exhibit notable *in vitro* antimalarial activity. **5.13** and **5.15** were the most active of the analogs. **5.7**, an intermediate in the synthesis (and a putative metabolite) of some of the analogs was also found to exhibit notable antimalarial activity *in vitro*. Results from mechanistic studies suggested that inhibition of hemozoin formation was likely to contribute substantially to the antiplasmodial activity of analogs **5.8 – 5.15**. These analogs were all more potent than chloroquine at inhibiting β-hematin formation.

The final objective of the study was to elucidate the pharmacokinetic profiles and evaluate the *in vivo* antimalarial activities of the most promising compounds using the mouse model. Compounds **3.15b** and **5.13** were therefore selected for preliminary PK profiling and *in vivo* antimalarial testing. The remarkably higher oral bioavailability of **3.15b** when administered as a DMSO-water formulation as opposed to the SMEDDS and Pheroid formulations indicated that these alternative formulations are not optimal for the oral delivery of this compound. Compound **3.15b** also exhibited a bi-phasic PK profile after oral administration as a DMSO-water formulation; this was most likely due to staggered absorption, i.e. absorption in two separate sections of the GI tract. The rapid decline in the circulating concentrations of **3.15b** after IV administration indicated an extremely efficient clearance of the compound, possibly arising from susceptibility to several routes of metabolism. The DMSO-water formulation also

yielded the better oral exposure than the buffer pH 4.0 formulation. Also noteworthy was that significantly higher exposure and circulating concentrations were observed for 3.15b compared to 5.13 after oral administration. The rapid decline in the circulating concentrations of 5.13 after IV administration also indicated an extremely efficient clearance of the compound. The circulating levels of the predicted *N*-dealkylation metabolite 5.7 after administration of 5.13 were very low, which suggested that either this was not the primary route of metabolism in mice, or that this particular metabolite was polar enough to be efficiently eliminated by the kidneys in urine before significantly accumulating in circulation.

The two compounds did not exhibit significant *in vivo* antimalarial activity, showing only marginal improvement to the untreated controls in terms of suppression of parasitemia, decline in average mouse weights and overall mouse survival. This activity was significantly inferior to that observed for chloroquine. Compound 3.15b showed slightly better efficacy than 5.13, with a notably slower rise in parasitemia in the middle and latter stages of the study as well as more mice surviving for longer (relative to their respective untreated controls).

Though compound 5.13 offered the advantage of improved (pH dependent) solubility relative to 3.15b, this compound had poorer oral bioavailability, and did not offer any improvement on its antimalarial activity either *in vitro* or *in vivo*.

7.2 Recommendations for future work

This study identified the existing potential in enone-chloroquinoline hybrid compounds. Guided by *in silico* ADME predictions, the design and synthesis of further analogs, such as those shown in Figure 5.15, presents a viable approach to investigating this potential.

Furthermore, structural modifications could be made in an attempt to address the metabolic instability observed with the first generation of analogs presented in this study. For example, new series of analogs could be designed by applying other hybridization strategies that yield linkers that are not very susceptible to N-dealkylation or other routes of metabolism. In addition, replacement of the methoxy groups with more metabolically stable substituents (e.g. trifluoromethyl groups) may afford more stable analogs.

PK studies on a somewhat larger scale could also be quite informative. For example, the investigation of other formulation strategies including, but not limited to, the

varying of the different components of the SMEDDS formulation could facilitate the identification of optimal formulations suitable for this type of compounds.

Also, pharmacokinetic and/or *in vivo* efficacy profiling of representative AZT-based hybrid compounds could also be useful as proof-of-principle, i.e. to test the hypothesis on the potential beneficial effects *in vivo* of hybridization to the hydrophilic nucleoside AZT.

CHAPTER EIGHT

EXPERIMENTAL

8.1 Chemistry

8.1.1 Reagents and Solvents

All commercially available chemicals and reagents were purchased from either Sigma-Aldrich or Merck, South Africa.

Anhydrous DMF, anhydrous 1,4-dioxane and anhydrous NMP were purchased as such from Sigma-Aldrich, South Africa. Other solvents were purchased from Kimix Chemicals or Protea Chemicals, South Africa. Chromatography solvents (EtOAc, CH_2Cl_2 and Hexane) were purchased as Chemically Pure (CP grade) solvents and distilled before use; the rest were purchased as Analytical Reagent (AR grade) solvents and used directly.

8.1.2 Chromatography

Reactions were monitored by thin layer chromatography (TLC) using Merck F_{254} aluminium-backed pre-coated silica gel plates, and were visualized under 254 nm ultraviolet light.

Product purification by silica gel column chromatography was performed using Merck kieselgel 60: 70-230 mesh by gravity column chromatography.

8.1.3 Physical and Spectroscopic characterization

Melting points were determined on a Reichert-Jung Thermovar hot-stage microscope, and are uncorrected.

Purity was determined by combustion analysis, and all compounds were confirmed to have >95% purity. This analysis was carried out on a Fisons EA 1108 CHNO-S microanalysis instrument.

All NMR spectra were recorded on a Varian Mercury (^{1}H - 300 MHz; ^{13}C - 75 MHz), Varian Unity (^{1}H - 400 MHz; ^{13}C – 100 MHz), or a Bruker Ultrashield-Plus Spectrometer (^{1}H - 400 MHz; ^{13}C – 100 MHz) Spectrometer. All spectra were recorded in deuterated

CHAPTER EIGHT

EXPERIMENTAL

8.1 Chemistry

8.1.1 Reagents and Solvents

All commercially available chemicals and reagents were purchased from either Sigma-Aldrich or Merck, South Africa.

Anhydrous DMF, anhydrous 1,4-dioxane and anhydrous NMP were purchased as such from Sigma-Aldrich, South Africa. Other solvents were purchased from Kimix Chemicals or Protea Chemicals, South Africa. Chromatography solvents (EtOAc, CH_2Cl_2 and Hexane) were purchased as Chemically Pure (CP grade) solvents and distilled before use; the rest were purchased as Analytical Reagent (AR grade) solvents and used directly.

8.1.2 Chromatography

Reactions were monitored by thin layer chromatography (TLC) using Merck F_{254} aluminium-backed pre-coated silica gel plates, and were visualized under 254 nm ultraviolet light.

Product purification by silica gel column chromatography was performed using Merck kieselgel 60: 70-230 mesh by gravity column chromatography.

8.1.3 Physical and Spectroscopic characterization

Melting points were determined on a Reichert-Jung Thermovar hot-stage microscope, and are uncorrected.

Purity was determined by combustion analysis, and all compounds were confirmed to have >95% purity. This analysis was carried out on a Fisons EA 1108 CHNO-S microanalysis instrument.

All NMR spectra were recorded on a Varian Mercury (^{1}H - 300 MHz; ^{13}C - 75 MHz), Varian Unity (^{1}H - 400 MHz; ^{13}C – 100 MHz), or a Bruker Ultrashield-Plus Spectrometer (^{1}H - 400 MHz; ^{13}C – 100 MHz) Spectrometer. All spectra were recorded in deuterated

chloroform ($CDCl_3$) or deuterated dimethylsulfoxide (DMSO-d_6) using tetramethylsilane (TMS) as an internal standard. All chemical shifts (δ) are recorded in ppm and are rounded off to two decimal places; coupling constants (J) are recorded in hertz (Hz) and rounded off to one decimal place. Abbreviations used in the assigning of ^{1}H-NMR signals are: br (broad), d (doublet), dd (doublet of doublets), m (multiplet), s (singlet) and t (triplet). ^{13}C-NMR chemical shift values are listed without assignment to specific carbon atoms, a format accepted by most international journals.

Infrared (IR) spectra were recorded on a Thermo Nicolete FTIR instrument in the 4000 – 1000 cm^{-1} range, with samples prepared either as chloroform solutions or as KBr discs.

Low resolution Mass spectra (LRMS) were recorded on an API 4000 Triple Quadropole from Applied Biosystems, fitted with a Turbo Ion Spray source, or on a JEOL GC Mate II single magnetic sector mass spectrometer.

8.1.4 Experimental

8.1.4.1 Curcumin

1,7-Bis-(4-hydroxy-3-methoxy-phenyl)-hepta-1,6-diene-3,5-dione; Curcumin.

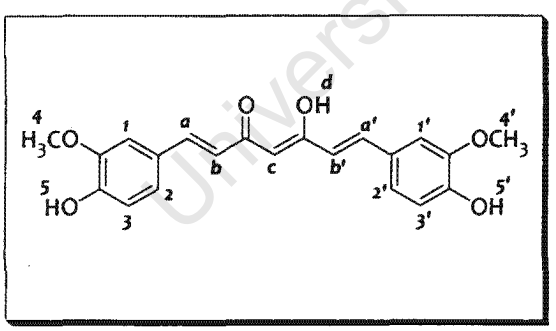

Technical grade curcumin, (Aldrich) was adsorbed onto silica and purified by conventional silica column chromatography (100% CH_2Cl_2). The residual solid after evacuation of the solvent was re-crystallized from a CH_2Cl_2/Hexane mixture to yield the pure target compound as a crystalline yellow solid; mp 174 - 176°C (from CH_2Cl_2/Hex); R_f (EtOAc:Hex 8:2) 0.69; IR ν_{max} (KBr)/cm^{-1} 3506 (Ar O-H), 3011 (Ar C-H), 1628 (C=O), 1600 (Ar C=C); δ_H (400 MHz, $CDCl_3$) 7.61 (2H, d, J 15.8, H-a, a'), 7.14 (2H, dd, J 1.9 and 8.2, H-2, 2'), 7.07 (2H, d, J 1.9, H-1, 1'), 6.95 (2H, d, J 8.2, H-3, 3'), 6.49 (2H, d, J 15.8, H-b, b'), 5.86 (1H, s, H-d), 5.82 (1H, s, H-c), 3.97 (6H, s, H-4, 4'); δ_C (100 MHz, $CDCl_3$) 168.6 (2C), 148.8 (2C), 147.9 (2C), 140.5 (2C), 127.8 (2C), 122.9 (2C), 121.9 (2C), 114.9 (2C), 109.7 (2C), 101.1, 56.0 (2C); LRMS (EI) m/z 366.9 (M + H) M^+ $C_{21}H_{20}O_6$ requires 368.1; Anal. Calcd. for $C_{21}H_{20}O_6$ - C 68.5%, H 5.5%; found C 68.5%, H 5.7%.

8.1.4.2:Experimental details pertaining to Chapter 3

General method I: synthesis of the acetylenic intermediates 3.7 and 3.8:

Vanillin (4-hydroxy-3-methoxybenzaldehyde) or acetovanillone (4-hydroxy-3-methoxyacetophenone) (13 mmol) was dissolved in 10 mL of anhydrous DMF. Anhydrous K_2CO_3 (2.7 g, 19.5 mmol) was then added to the solution, and the mixture stirred at 30°C for 30 minutes. Propargyl bromide (3-bromopropyne, 2.2 mL, 19.5 mmol) was then added slowly to the reaction mixture, which was subsequently stirred at 30°C for 6 hours upon which TLC indicated completion of the reaction.

The reaction mixture was then diluted with 50 ml water and extracted with EtOAc (3 x 50 mL). These extracts were then combined, washed with water (2 x 50 mL), dried over anhydrous Na_2SO_4 and evaporated *in vacuo* to yield the product residue that was then purified by crystallization from CH_2Cl_2/Hexane mixtures.

3-Methoxy-4-prop-2-ynyloxy-benzaldehyde, 3.7

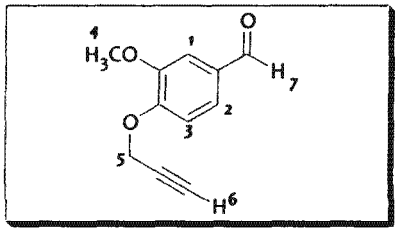

White crystalline solid (2.0 g, 82%); mp 86°C (from CH_2Cl_2/Hex); R_f (EtOAc: CH_2Cl_2:Hex) 0.43; IR ν_{max} ($CHCl_3$)/cm^{-1} 3307 (Alkynyl C-H), 3021 (Ar C-H), 2127 (C≡C), 1683 (C=O), 1590 (Ar C=C); δ_H (300 MHz, $CDCl_3$) 9.87 (1H, s, H-7), 7.45 (1H, dd, *J* 1.9 and 7.8, H-2), 7.43 (1H, d, *J* 1.9, H-1), 7.14 (1H, d, *J* 7.8, H-3), 4.85 (2H, d, *J* 2.4, H-5), 3.94 (3H, s, H-4), 2.55 (1H, t, *J* 2.4, H-6); δ_C (75 MHz, $CDCl_3$) 190.8, 152.1, 150.1, 131.0, 126.1, 112.7, 109.6, 77.4, 76.6, 56.6, 56.0; LRMS (EI) m/z 191.3 (M + H) M^+ $C_{11}H_{10}O_3$ requires 190.1; Anal. Calcd. for $C_{11}H_{10}O_3$ - C 69.5%, H 5.3%; found C 69.5%, H 5.2%.

1-(3-Methoxy-4-prop-2-ynyloxy-phenyl)-ethanone, 3.8

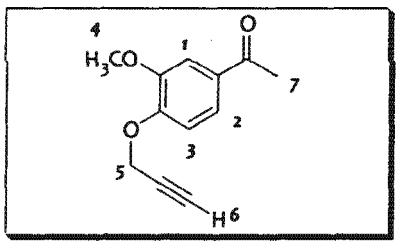

Off-white crystalline solid (2.2 g, 82%); mp 90 - 91°C (from CH_2Cl_2/Hex); R_f (EtOAc: CH_2Cl_2:Hex 1:4:5) 0.39; IR ν_{max} ($CHCl_3$)/cm^{-1} 3308 (Alkynyl C-H), 3017 (Ar C-H), 2127 (C≡C), 1675 (C=O), 1591 (Ar C=C); δ_H (400 MHz, $CDCl_3$) 7.56 (1H, dd, *J* 2.0 and 8.2, H-2), 7.54 (1H, d, *J* 2.0, H-1), 7.05 (1H, d, *J* 8.2, H-3), 4.83 (2H, d, *J* 2.4, H-5), 3.93 (3H, s, H-4) 2.56 (3H, s, H-7), 2.54 (1H, t, *J* 2.4, H-6); δ_C (100 MHz, $CDCl_3$) 196.8, 151.3, 149.6, 131.5, 122.8, 112.5, 110.7, 77.3, 76.4, 56.6, 56.0, 26.2; LRMS (EI) m/z 204.9 (M + H) M^+ $C_{12}H_{12}O_3$ requires 204.1; Anal. Calcd. for $C_{12}H_{12}O_3$ - C 70.6%, H 5.9%; found C 70.3%, H 6.0%.

General method II: synthesis of the acetylenic chalcones 3.9 – 3.10:

The appropriately substituted acetophenone (3 mmol) was dissolved in 10 mL methanol, after which 2.5M aqueous NaOH (4 mL) was added and the mixture stirred at 70°C for 15 minutes. The appropriately substituted benzaldehyde (3 mmol) was then added in one portion, and the mixture stirred at 70° C for a further 3 hours.

This series of products precipitated out of solution, and, after allowing the reaction mixture to cool to ambient temperature, the chalcone products were filtered, washed with water, air dried and purified by silica column chromatography (EtOAc/Hex).

1-(4-*Methoxy-phenyl*)-3-(3-*methoxy*-4-*prop*-2-*ynyloxy-phenyl*)-*propenone*, 3.9a

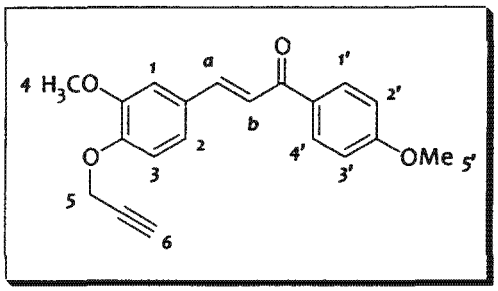

Yellow solid (980.4 mg, 76%); mp 128 - 130°C (from EtOAc/Hex); R_f (EtOAc: CH_2Cl_2:Hex) 0.30; IR ν_{max} ($CHCl_3$)/cm^{-1} 3301 (Alkynyl C-H), 3015 (Ar C-H), 1655 (C=O), 1601 (Ar C=C); δ_H (400 MHz, $CDCl_3$) 8.03 (2H, d, *J* 8.8, H-1',4'), 7.75 (1H, d, *J* 15.6, H-a), 7.41 (1H, d, *J* 15.6, H-b), 7.24 (1H, dd, *J* 2.0 and 8.4, H-2), 7.17 (1H, d, *J* 2.0, H-1), 7.06 (1H, d, *J* 8.2, H-3), 6.98 (2H, d, *J* 8.9, H-2',3'), 4.81 (2H, d, *J* 2.6, H-5), 3.95 (3H, s, H-5'), 3.89 (3H, s, H-4), 2.54 (1H, t, *J* 2.6, H-6); δ_C (100 MHZ, $CDCl_3$) 188.7, 163.3, 149.8, 148.9, 143.8, 131.3, 130.7, 129.3, 122.3, 120.4, 113.9, 113.8, 110.9, 78.0, 77.4, 76.6, 76.2, 56.7, 56.0, 55.5; LRMS (EI) m/z 323.4 (M + H) M^+ $C_{20}H_{16}O_4$ requires 322.1; Anal. Calcd. for $C_{20}H_{18}O_4.½H_2O$ - C 72.4%, H 5.4%; found C 72.5%, H 5.8%.

1-(2,4-*Dimethoxy-phenyl*)-3-(3-*methoxy*-4-*prop*-2-*ynyloxy-phenyl*)-*propenone*, 3.9b

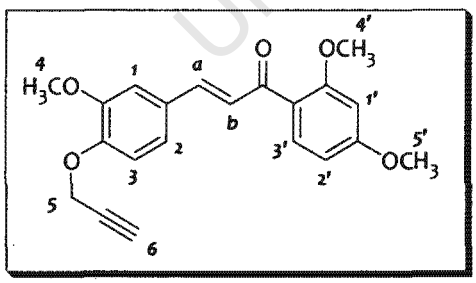

Yellow solid (948.9 mg, 90%); mp: 90° - 91°C (from EtOAc/Hex); R_f (EtOAc: CH_2Cl_2:Hex 1:4:5) 0.30; IR ν_{max} ($CHCl_3$)/cm^{-1} 3303 (Alkynyl C-H), 3015 (Ar C-H), 1651 (C=O), 1604 (Ar C=C); δ_H (400 MHz, $CDCl_3$) 7.72 (1H, d, *J* 8.6, H-3'), 7.60 (1H, d, *J* 15.7, H-a), 7.36 (1H, d, *J* 15.7, H-b), 7.18 (1H, dd, *J* 2.0 and 8.2, H-2), 7.12 (1H, d, *J* 2.0, H-1), 7.03 (1H, d, *J* 8.2, H-3), 6.56 (1H, dd, *J* 2.2 and 8.6, H-2'), 6.50 (1H, d, *J* 2.2, H-1'), 4.79 (2H, d, *J* 2.4, H-5), 3.91 (3H, s, H-4'), 3.89 (3H, s, H-5'), 3.87 (3H, s, H-4), 2.53 (1H, t, *J* 2.4, H-6); δ_C 100 (MHz, $CDCl_3$) 190.7, 163.9, 160.3, 149.8, 142.1, 132.7, 129.8, 125.9, 122.4, 122.0, 114.0, 111.1, 105.2, 98.9, 77.3, 76.7, 76.1, 56.7, 56.0, 55.5; LRMS (EI) m/z 353.3 (M + H) M^+

General method II: synthesis of the acetylenic chalcones 3.9 – 3.10:

The appropriately substituted acetophenone (3 mmol) was dissolved in 10 mL methanol, after which 2.5M aqueous NaOH (4 mL) was added and the mixture stirred at 70°C for 15 minutes. The appropriately substituted benzaldehyde (3 mmol) was then added in one portion, and the mixture stirred at 70° C for a further 3 hours.

This series of products precipitated out of solution, and, after allowing the reaction mixture to cool to ambient temperature, the chalcone products were filtered, washed with water, air dried and purified by silica column chromatography (EtOAc/Hex).

1-(4-*Methoxy-phenyl*)-3-(3-*methoxy*-4-*prop*-2-*ynyloxy-phenyl*)-*propenone*, 3.9a

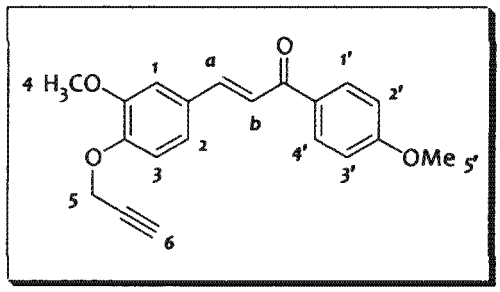

Yellow solid (980.4 mg, 76%); mp 128 - 130°C (from EtOAc/Hex); R_f (EtOAc: CH_2Cl_2:Hex) 0.30; IR ν_{max} ($CHCl_3$)/cm^{-1} 3301 (Alkynyl C-H), 3015 (Ar C-H), 1655 (C=O), 1601 (Ar C=C); δ_H (400 MHz, $CDCl_3$) 8.03 (2H, d, *J* 8.8, H-1',4'), 7.75 (1H, d, *J* 15.6, H-a), 7.41 (1H, d, *J* 15.6, H-b), 7.24 (1H, dd, *J* 2.0 and 8.4, H-2), 7.17 (1H, d, *J* 2.0, H-1), 7.06 (1H, d, *J* 8.2, H-3), 6.98 (2H, d, *J* 8.9, H-2',3'), 4.81 (2H, d, *J* 2.6, H-5), 3.95 (3H, s, H-5'), 3.89 (3H, s, H-4), 2.54 (1H, t, *J* 2.6, H-6); δ_C (100 MHZ, $CDCl_3$) 188.7, 163.3, 149.8, 148.9, 143.8, 131.3, 130.7, 129.3, 122.3, 120.4, 113.9, 113.8, 110.9, 78.0, 77.4, 76.6, 76.2, 56.7, 56.0, 55.5; LRMS (EI) m/z 323.4 (M + H) M^+ $C_{20}H_{16}O_4$ requires 322.1; Anal. Calcd. for $C_{20}H_{18}O_4.½H_2O$ - C 72.4%, H 5.4%; found C 72.5%, H 5.8%.

1-(2,4-*Dimethoxy-phenyl*)-3-(3-*methoxy*-4-*prop*-2-*ynyloxy-phenyl*)-*propenone*, 3.9b

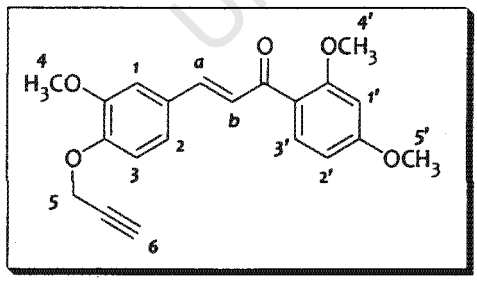

Yellow solid (948.9 mg, 90%); mp: 90° - 91°C (from EtOAc/Hex); R_f (EtOAc: CH_2Cl_2:Hex 1:4:5) 0.30; IR ν_{max} ($CHCl_3$)/cm^{-1} 3303 (Alkynyl C-H), 3015 (Ar C-H), 1651 (C=O), 1604 (Ar C=C); δ_H (400 MHz, $CDCl_3$) 7.72 (1H, d, *J* 8.6, H-3'), 7.60 (1H, d, *J* 15.7, H-a), 7.36 (1H, d, *J* 15.7, H-b), 7.18 (1H, dd, *J* 2.0 and 8.2, H-2), 7.12 (1H, d, *J* 2.0, H-1), 7.03 (1H, d, *J* 8.2, H-3), 6.56 (1H, dd, *J* 2.2 and 8.6, H-2'), 6.50 (1H, d, *J* 2.2, H-1'), 4.79 (2H, d, *J* 2.4, H-5), 3.91 (3H, s, H-4'), 3.89 (3H, s, H-5'), 3.87 (3H, s, H-4), 2.53 (1H, t, *J* 2.4, H-6); δ_C 100 (MHz, $CDCl_3$) 190.7, 163.9, 160.3, 149.8, 142.1, 132.7, 129.8, 125.9, 122.4, 122.0, 114.0, 111.1, 105.2, 98.9, 77.3, 76.7, 76.1, 56.7, 56.0, 55.5; LRMS (EI) m/z 353.3 (M + H) M^+

$C_{21}H_{20}O_5$ requires 352.1; Anal. Calcd. for $C_{21}H_{20}O_5$ - C 71.6%, H 5.7%; found C 71.2%, H 5.8%.

3-(3-*Methoxy-4-prop-2-ynyloxy-phenyl*)-1-(2,3,4-*trimethoxy-phenyl*)-*propenone*, 3.9c

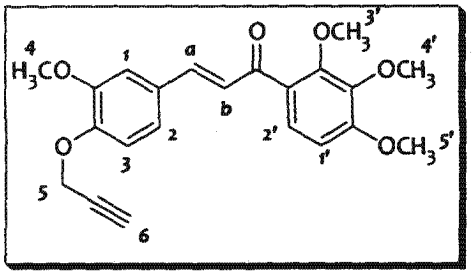

Yellow solid (1.1 g, 84%); mp: 85 - 86°C (from EtOAc/Hex); R_f (EtOAc:Hex 4:6) 0.30; IR ν_{max} ($CHCl_3$)/cm^{-1} 3308 (Alkynyl C-H), 3018 (Ar C-H), 1652 (C=O), 1594 (Ar C=C); δH (400 MHz, $CDCl_3$) 7.61 (1H, d, *J* 15.7, H-a), 7.45 (1H, d, *J* 8.6, H-2'), 7.34 (1H, d, *J* 15.7, H-b), 7.19 (1H, dd, *J* 2.0 and 8.4, H-2), 7.13 (1H, d, *J* 2.0, H-1), 7.03 (1H, d, *J* 8.4, H-3), 6.74 (1H, d, *J* 8.8, H-1'), 4.79 (2H, d, *J* 2.4, H-5), 3.92 – 3.91 (12H, m, H-3', 5', 4', 4), 2.53 (1H, t, *J* 2.4, H-6); δ_C (100 MHz, $CDCl_3$) 190.9, 156.9, 153.6, 149.7, 148.9, 143.0, 142.0, 129.4, 126.9, 125.7, 125.2, 122.3, 114.0, 110.0, 107.4, 77.3, 76.7, 76.1, 62.1, 61.1, 56.7, 56.1; LRMS (EI) m/z 383.4 (M + H) M^+ $C_{22}H_{22}O_6$ requires 382.1; Anal. Calcd. for $C_{22}H_{22}O_6$ C 69.1%, H 5.8%; found C 68.6%, H 5.8%.

3-(2,4-*Dimethoxy-phenyl*)-1-(3-*methoxy-4-prop-2-ynyloxy-phenyl*)-*propenone*, 3.10a

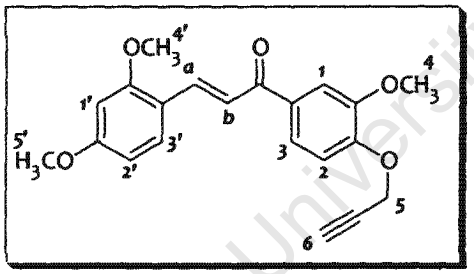

Yellow solid (946.1 mg, 89%); mp: 136 - 137°C (from EtOAc/Hex); R_f (EtOAc:Hex 3:7) 0.17; IR ν_{max} ($CHCl_3$)/cm^{-1} 3308 (Alkynyl C-H), 3019 (Ar C-H), 1651 (C=O), 1598 (Ar C=C); δ_H (300 MHz, $CDCl_3$) 8.04 (1H, d, *J* 15.6, H-a), 7.67 – 7.63 (2H, m, H-1, 3), 7.57 (1H, d, *J* 8.8, H-2), 7.55 (1H, d, *J* 15.6, H-b), 7.08 (1H, d, *J* 8.3, H-3'), 6.53 (1H, dd, *J* 2.4, 8.3, H-2'), 6.48 (1H, d, *J* 2.4, H-1'), 4.84 (2H, d, *J* 2.4, H-5), 3.96 (3H, s, H-4'), 3.85 (3H, s, H-5'), 3.85 (3H, s, H-4), 2.54 (1H, t, *J* 2.4, H-6); δ_C (75 MHz, $CDCl_3$) 189.4, 162.9, 160.4, 150,5, 149.6, 139.9, 133.0, 130.9, 122.3, 120.2, 117.3, 112.5, 111.5, 105.4, 98.5, 77.4, 76.6, 76.3, 56.6, 56.0, 55.5; LRMS (EI) m/z 353.0 (M + H) M^+ $C_{21}H_{20}O_5$ requires 352.1; Anal. Calcd. for $C_{21}H_{20}O_5.½H_2O$ - C 69.7%, H 5.5%; found C 69.6%*, H 5.7%.

1-(3-*Methoxy*-4-*prop*-2-*ynyloxy*-*phenyl*)-3-(2,3,4-*trimethoxy*-*phenyl*)-*propenone*, 3.10b

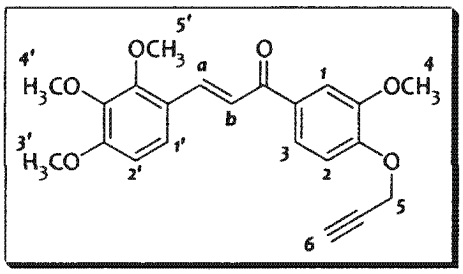

Yellow solid (1.5 g, 78%); mp 134 - 135°C (from EtOAc/Hex); R_f (EtOAc:Hex 3:7) 0.21; IR ν_{max} ($CHCl_3$)/cm^{-1} 3308 (Alkynyl C-H), 3017 (Ar C-H), 1654 (C=O), 1594 (Ar C=C); δ_H (400 MHz, $CDCl_3$) 7.97 (1H, d, *J* 15.7, H-a), 7.65 (1H, dd, *J* 2.0 and 8.2, H-3), 7.64 (1H, d, *J* 2.0, H-1), 7.56 (1H, d, *J* 15.7, H-b), 7.36 (1H, d, *J* 8.8, H-1'), 7.09 (1H, d, *J* 8.2, H-2), 6.72 (1H, d, *J* 8.8, H-2'), 4.85 (2H, d, *J* 2.4, H-5), 3.96 (3H, s, H-5'), 3.95 (3H, s, H-3'), 3.90 (3H, s, H-4), 3.89 (3H, s, H-4'), 2.55 (1H, t, *J* 2.4, H-6); ; δ_C (100 MHz, $CDCl_3$) 189.1, 155.7, 153.8, 150.7, 149.7, 142.6, 139.6, 132.8, 123.9, 122.4, 121.1, 112.6, 111.5, 107.7, 77.3, 76.7, 76.3, 61.4, 60.9, 56.6, 56.1; LRMS (EI) m/z 383.4 (M + H) M^+ $C_{22}H_{22}O_6$ requires 382.1; Anal. Calcd. for $C_{22}H_{22}O_6$ - C 69.1%, H 5.8%; found C 68.7%, H 5.2%.

3-(2,4-*Dichloro*-*phenyl*)-1-(3-*methoxy*-4-*prop*-2-*ynyloxy*-*phenyl*)-*propenone*, 3.10c

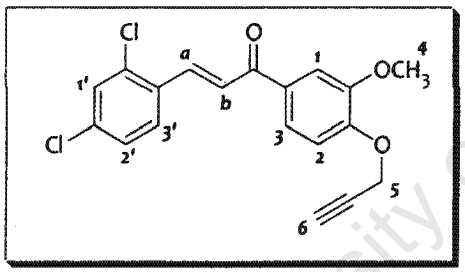

Yellow solid (1.4 g, 79%); mp: 115 - 117°C (from EtOAc/Hex); R_f (EtOAc:Hex 4:6) 0.52; IR ν_{max} ($CHCl_3$)/cm^{-1} 3308 (Alkynyl C-H), 3017 (Ar C-H), 1661 (C=O), 1584 (Ar C=C); δ_H (300 MHz, $CDCl_3$) 8.08 (1H, d, *J* 15.6, H-a), 7.67 (1H, d, *J* 8.2, H-3'), 7.64 (1H, dd, *J* 1.9 and 8.3, H-3), 7.63 ((1H, d, *J* 1.9, H-1), 7.47 (1H, d, *J* 15.6, H-b), 7.46 (1H, d, *J* 1.9, H-1'), 7.29 (1H, dd, *J* 1.9 and 8.3, H-2'), 7.09 (1H, d, *J* 8.3, H-2), 4.86 (2H, d, *J* 2.4, H-5), 3.96 (3H, s, H-4), 2.55 (1H, t, *J* 2.4, H-6); δ_C (75 MHz, $CDCl_3$) 188.3, 151.2, 149.8, 138.7, 136.3, 135.9, 132.1, 131.9, 130.1, 128.5, 127.5, 124.9, 122.7, 112.5, 111.4, 77.4, 76.6, 56.6, 56.1; LRMS (EI) m/z 362.4 (M + H) M^+ $C_{19}H_{14}Cl_2O_3$ requires 361.2; Anal. Calcd. for $C_{19}H_{14}Cl_2O_3$ - C 63.2%, H 3.9%; found C 63.4%, H 3.8%.

3-(4-*Fluoro*-*phenyl*)-1-(3-*methoxy*-4-*prop*-2-*ynyloxy*-*phenyl*)-*propenone*, 3.10d

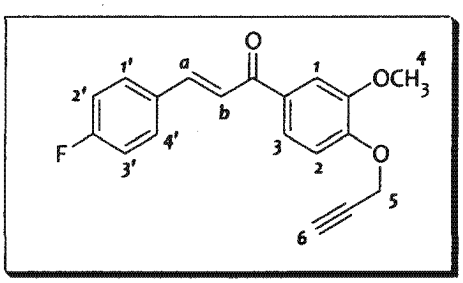

Yellow solid (1.4 g, 88%); mp 151 - 152°C (from EtOAc/Hex); R_f (EtOAc: CH_2Cl_2:Hex 1:4:5) 0.43; IR ν_{max} ($CHCl_3$)/cm^{-1} 3304 (Alkynyl C-H), 3018 (Ar C-H), 1656 (C=O), 1597 (Ar C=C); δ_H (400 MHz, $CDCl_3$) 7.78 (1H, d, *J* 15.6, H-a), 7.65 (1H, dd, *J*

2.0 and 8.2, H-3), 7.63 (1H, d, *J* 2.0, H-1), 7.59 (2H, d, *J* 8.8, H-1', 4'), 7.42 (1H, d, *J* 15.6, H-b), 7.09 (1H, d, *J* 8.2, H-2), 6.94 (2H, d, *J* 8.8, H-2', 3'), 4.85 (2H, d, *J* 2.4, H-5), 3.86 (3H, s, H-4), 2.55 (1H, t, *J* 2.4, H-6); δ_C (100 MHz, $CDCl_3$) 188.7, 150.6, 149.7, 144.0, 142.8, 132.7, 130.1, 127.8, 122.3, 121.4, 119.4, 116.2, 114.4, 112.5, 111.4, 77.3, 76.6, 56.7, 56.1; LRMS (EI) m/z 311.3 (M + H) M^+ $C_{19}H_{15}FO_3$ requires 310.0; Anal. Calcd. for $C_{19}H_{15}FO_3$ - C 73.5%, H 4.9%; found C 73.4%, H 5.4%.

3-(2,4-*Difluoro-phenyl*)-1-(3-*methoxy-4-prop-2-ynyloxy-phenyl*)-*propenone*, 3.10e

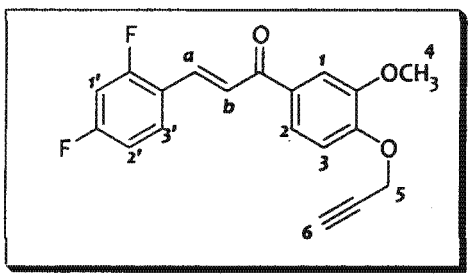

Yellow solid (1.4 g, 85%); mp 98 - 99°C (from EtOAc/Hex); R_f (EtOAc:Hex 3:7) 0.19; IR ν_{max} ($CHCl_3$)/cm^{-1} 3295 (Alkynyl C-H), 2954 (Ar C-H), 1654 (C=O), 1595 (Ar C=C); δ_H (300 MHz, $CDCl_3$) 7.85 (1H, d, *J* 15.6, H-a), 7.66 (1H, dd, *J* 1.9 and 8.3, H-2), 7.63 (1H, d, *J* 1.9, H-1), 7.57 (1H, d, *J* 8.8, H-3'), 7.54 (1H, d, *J* 15.6, H-b), 7.09 (1H, d, *J* 8.3, H-3), 6.73 (1H, dd, *J* 2.4 and 8.8, H-2'), 6.69 (1H, d, *J* 2.4, H-1'), 4.85 (2H, d, *J* 2.4, H-5), 3.96 (3H, s, H-4), 2.55 (1H, t, *J* 2.4, H-6); δ_C (75 MHz, $CDCl_3$) 188.8, 150.9, 149.7, 139.9, 137.1, 132.5, 130.9, 122.5, 120.2, 117.3, 112.5, 111.4, 105.4, 101.9, 98.5, 77.4, 76.6, 56.6, 56.1; LRMS (EI) m/z 329.2 (M + H) M^+ $C_{19}H_{14}F_2O_3$ requires 328.1; Anal. Calcd. for $C_{19}H_{14}F_2O_3$ - C 69.5%, H 4.3% found C 69.1%, H 4.2%

4-(3-Methoxy-4-prop-2-ynyloxy-phenyl)-but-3-en-2-one, 3.11

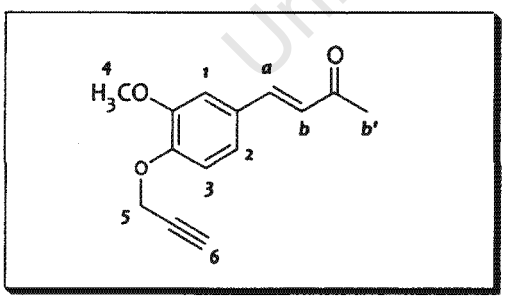

6.2 g (32 mmol) of the O-alkylated benzaldehyde (3.7) was dissolved in 30 mL acetone, after which 2.5M aqueous NaOH (19 mL, 48 mmol) was added. The mixture was then stirred at room temperature for 6 hours, after which TLC showed complete consumption of the benzaldehyde starting material.

The reaction mixture was then gradually neutralized with 2.5M HCl, during which the crude product precipitated out as an amorphous yellow solid. This crude product was then filtered, washed with water, air dried and purified by silica column chromatography (EtOAc/Hex) to yield a pale yellow, crystalline solid (5.3 g, 71%); mp 103 - 105°C (from EtOAc/Hex); R_f (EtOAc:Hex 4:6) 0.33; IR ν_{max} (KBr)/cm^{-1} 3253 (Alkynyl C-H), 2985 (Ar C-H), 1671 (C=O), 1595 (Ar C=C); δ_H (400 MHz, $CDCl_3$) 7.49 (1H, d, *J* 16.2, H-a), 7.14

(1H, dd, *J* 2.0 and 8.3, H-2), 7.10 (1H, d, *J* 2.0, H-1), 7.05 (1H, d, *J* 8.3, H-3), 6.63 (1H, d, *J* 16.2, H-b), 4.81 (2H, d, *J* 2.4, H-5), 3.93 (3H, s, H-4), 2.43 (1H, t, *J* 2.4, H-6), 2.38 (3H, s, H-b'); δ_C (100 MHZ, $CDCl_3$) 198.1, 149.9, 143.2, 128.6, 125.8, 122.4 (2C), 113.9, 110.4, 77.9, 76.2, 56.6, 55.9, 27.4; LRMS (EI) m/z 231.3 (M + H) M^+ $C_{14}H_{14}O_3$ requires 230.1; Anal. Calcd. for $C_{14}H_{14}O_3$ - C 73.0%, H 6.1%; found C 72.8%, H 6.2 %;

General method IV: synthesis of the acetylenic dienones (3.12a – 3.12f):

A mixture of 230 mg (1 mmol) of the acetylenic enone (**3.11**) and the appropriately substituted benzaldehyde (1.1 mmol) were dissolved in 10 mL anhydrous 1,4-dioxane under a nitrogen atmosphere. To the stirring mixture, BF_3-Et_2O (0.2mL, 1.5 mmol) was added, and the mixture stirred overnight at 50°C.

The reaction mixture was then allowed to cool to ambient temperature, diluted with CH_2Cl_2 and washed twice with water. The organic layer was then collected, dried over anhydrous Na_2SO_4, concentrated *in vacuo* and the product residue purified by silica column chromatography (EtOAc/Hex).

1-(4-Methoxy-phenyl)-5-(3-methoxy-4-prop-2-ynyloxy-phenyl)-penta-1,4-dien-3-one, 3.12a

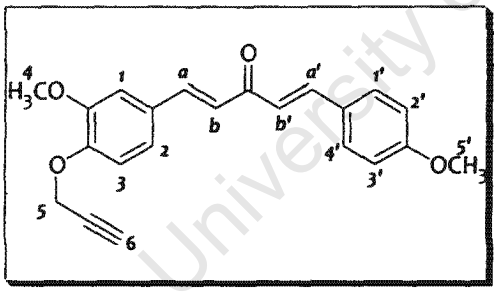

Yellow solid (135 mg, 39%); mp 124 - 125°C (from EtOAc/Hex); R_f (EtOAc:Hex 4:6) 0.30; IR ν_{max} (KBr)/cm^{-1} 3289 (Alkynyl C-H), 3035 (Ar C-H), 1643 (C=O), 1599 (Ar C=C); δ_H (300 MHz, $CDCl_3$) 7.70 (1H, d, *J* 16.0, H-a), 7.68 (1H, d, *J* 16.0, H-a'), 7.56 (2H, d, *J* 8.8, H-1', 4'), 7.19 (1H, dd, *J* 2.0 and 8.3, H-2), 7.15 (1H, d, *J* 2.0, H-1), 7.05 (1H, d, *J* 8.3, H-3), 6.97 (1H, d, *J* 16.0, H-b), 6.94 (1H, d, *J* 16.0, H-b'), 6.92 (2H, d, *J* 8.8, H-2', 3'), 4.81 (2H, d, *J* 2.4, H-5), 3.94 (3H, s, H-4), 3.85 (3H, s, H-4'), 2.54 (1H, t, *J* 2.4, H-6); δ_C (75 MHZ, $CDCl_3$) 188.7, 161.6, 149.9, 148.9, 142.8, 142.6, 130.1 (2C), 129.1, 127.6, 124.4, 123.3, 122.4, 114.4 (2C), 113.9, 110.7, 78.0, 76.2, 56.7, 55.9, 55.4; LRMS (EI) m/z 348.9 (M + H) M^+ $C_{22}H_{20}O_4$ requires 348.1; Anal. Calcd. for $C_{22}H_{20}O_4$ - C 75.8%, H 5.8%; found C 75.7%, H 5.7%.

1-(2,4-Dimethoxy-phenyl)-5-(3-methoxy-4-prop-2-ynyloxy-phenyl)-penta-1,4-dien-3-one, 3.12b

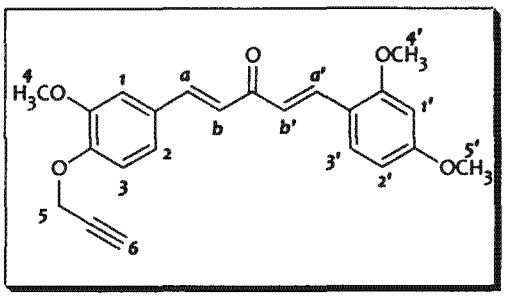

Yellow solid (185 mg, 49%); mp 57 - 59°C (from EtOAc/Hex); R_f (EtOAc:Hex 4:6) 0.30; IR ν_{max} (KBr)/cm^{-1} 3260 (Alkynyl C-H), 2927 (Ar C-H), 1642 (C=O), 1595 (Ar C=C); δ_H (300 MHz, $CDCl_3$) 8.01 (1H, d, *J* 16.1, H-a'), 7.67 (1H, d, *J* 15.9, H-a), 7.55 (1H, d, *J* 8.6, H-3'), 7.19 (1H, dd, *J* 1.9 and 8.3, H-2), 7.15 (1H, d, *J* 1.9, H-1), 7.07 (1H, d, *J* 16.0, H-b'), 7.05 (1H, d, *J* 8.3, H-3), 6.98 (1H, d, *J* 15.8, H-b), 6.53 (1H, dd, *J* 2.3 and 8.6, H-2'), 6.46 (1H, d, *J* 2.2, H-1'), 4.81 (2H, d, *J* 2.4 H-5), 3.94 (3H, s, H-4'), 3.90 (3H, s, H-5'), 3.85 (3H, s, H-4), 2.54 (1H, t, *J* 2.4, H-6); δ_C (75 MHZ, $CDCl_3$) 189.3, 163.0, 160.1, 149.8, 142.2, 138.5, 137.8, 130.4, 130.2, 129.4, 124.0, 122.2, 117.1, 113.9, 110.8, 105.5, 98.5, 77.4, 76.2, 56.7, 55.9, 55.5, 55.4; LRMS (EI) m/z 378.9 (M + H) M^+ $C_{23}H_{22}O_5$ requires 378.2; Anal. Calcd. for $C_{23}H_{22}O_5$.½H_2O- C 71.2%, H 5.9%; found C 71.5%, H 5.9%.

1-(3-Methoxy-4-prop-2-ynyloxy-phenyl)-5-(2,3,4-trimethoxy-phenyl)-penta-1,4-dien-3-one, 3.12c

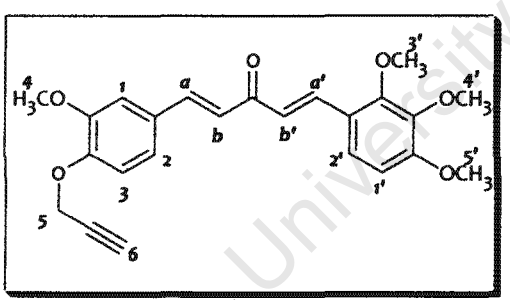

Yellow solid (191 mg, 47%); mp 67 - 69°C (from EtOAc/Hex); R_f (EtOAc:Hex 4:6) 0.33; IR ν_{max} (KBr)/cm^{-1} 3260 (Alkynyl C-H), 2934 (Ar C-H), 1645 (C=O), 1588 (Ar C=C); δ_H (300 MHz, $CDCl_3$) 7.94 (1H, d, *J* 16.1, H-a'), 7.67 (1H, d, *J* 15.9, H-a), 7.36 (1H, d, *J* 8.8, H-2'), 7.20 (1H, dd, *J* 1.9 and 8.4, H-2), 7.15 (1H, d, *J* 1.9, H-1), 7.06 (1H, d, *J* 16.1, H-b'), 7.04 (1H, d, *J* 8.3, H-3), 6.97 (1H, d, *J* 15.8, H-b), 6.71 (1H, d, *J* 8.8, H-1'), 4.81 (2H, d, *J* 2.4 H-5), 3.95 (3H, s, H-3'), 3.94 (3H, s, H-5'), 3.91 (3H, s, H-4'), 3.89 (3H, s, H-4), 2.54 (1H, t, *J* 2.4, H-6); δ_C (100 MHZ, $CDCl_3$) 189.1, 155.7, 149.8, 148.9, 142.6, 138.1 (2C), 129.2, 124.9, 124.3, 123.5, 122.3, 121.9, 113.9, 110.7 (2C), 107.7, 78.0, 76.2, 61.5, 60.9, 56.7, 56.1, 55.9; LRMS (EI) m/z 409.4 (M + H) M^+ $C_{24}H_{24}O_6$ requires 408.2; Anal. Calcd. for $C_{24}H_{24}O_6$.½H_2O- C 69.0%, H 6.0%; found C 69.5%, H 6.1%.

1-(2,4-Dichloro-phenyl)-5-(3-methoxy-4-prop-2-ynyloxy-phenyl)-penta-1,4-dien-3-one, 3.12d

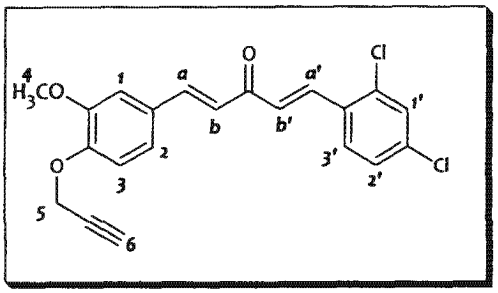

Yellow solid (251 mg, 65%); mp 74 - 76°C (from EtOAc/Hex); R_f (EtOAc:Hex 4:6) 0.59; IR ν_{max} (KBr)/cm^{-1} 3239 (Alkynyl C-H), 2949 (Ar C-H), 1653 (C=O), 1588 (Ar C=C); δ_H (300 MHz, $CDCl_3$) 8.03 (1H, d, *J* 16.0, H-a'), 7.67 (1H, d, *J* 15.9, H-a), 7.64 (1H, d, *J* 8.5, H-3'), 7.46 (1H, d, *J* 2.1, H-1'), 7.29 (1H, dd, *J* 2.1 and 8.5, H-2'), 7.21 (1H, dd, *J* 2.0 and 8.4, , H-2), 7.14 (1H, d, *J* 2.0, H-1), 7.06 (1H, d, *J* 8.3, H-3), 7.04 (1H, d, *J* 16.0, H-b'), 6.96 (1H, d, *J* 15.9, H-b), 4.82 (2H, d, *J* 2.4 H-5), 3.94 (3H, s, H-4), 2.54 (1H, t, *J* 2.4, H-6); δ_C (75 MHZ, $CDCl_3$) 188.5, 150.2, 149.2, 143.8, 137.4, 136.3, 135.9, 131.9, 130.1, 128.8, 128.4, 128.2, 127.6, 123.7, 122.6, 113.9, 110.8, 77.9, 76.3, 56.7, 56.0; LRMS (EI) m/z 387.2 (M + H) M^+ $C_{21}H_{16}Cl_2O_3$ requires 386.1; Anal. Calcd. for $C_{21}H_{16}Cl_2O_3$ - C 65.1%, H 4.2%; found C 64.8%, H 4.2%.

1-(4-Fluoro-phenyl)-5-(3-methoxy-4-prop-2-ynyloxy-phenyl)-penta-1,4-dien-3-one, 3.12e

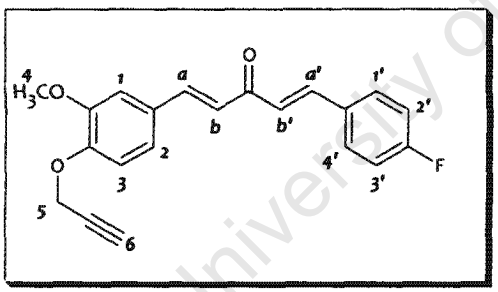

Yellow solid (151 mg, 45%); mp 106 - 108°C (from EtOAc/Hex); R_f (EtOAc:Hex 4:6) 0.50; IR ν_{max} (KBr)/cm^{-1} 3231 (Alkynyl C-H), 2920 (Ar C-H), 1667 (C=O), 1591 (Ar C=C); δ_H (300 MHz, $CDCl_3$) 7.69 (1H, d, *J* 15.9, H-a'), 7.67 (1H, d, *J* 15.9, H-a), 7.61 (1H, d, *J* 8.7, H-4'), 7.60 (1H, d, *J* 8.7, H-1'), 7.20 (1H, dd, *J* 1.9 ad 8.3, H-2), 7.15 (1H, d, *J* 2.0, H-1), 7.13-7.04 (3H, m, H-2', 3', 3), 7.01 (1H, d, *J* 16.3, H-b'), 6.93 (1H, d, *J* 15.9, H-b), 4.81 (2H, d, *J* 2.4 H-5), 3.93 (3H, s, H-4), 2.54 (1H, t, *J* 2.4, H-6); δ_C (75 MHZ, $CDCl_3$) 188.5, 165.7, 149.9, 149.1, 143.2, 141.7, 130.3, 130.1, 128.9, 125.0, 124.2, 122.6 (2C), 116.2, 115.9, 113.9, 110.7, 77.9, 76.2, 56.7, 55.9; LRMS (EI) m/z 336.9 (M + H) M^+ $C_{21}H_{17}FO_3$ requires 336.1; Anal. Calcd. for $C_{21}H_{17}FO_3$ - C 74.9%, H 5.1%; found C 74.5%, H 5.1%.

1-(2,4-Difluoro-phenyl)-5-(3-methoxy-4-prop-2-ynyloxy-phenyl)-penta-1,4-dien-3-one, 3.12f

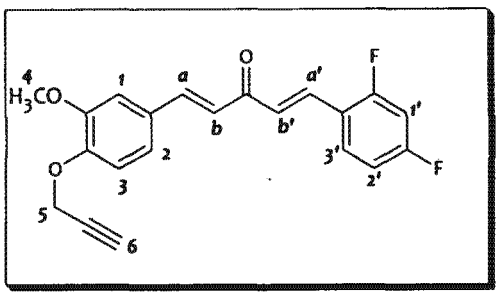

Yellow solid (153 mg, 43%); mp 99 - 101°C (from EtOAc/Hex); R_f (EtOAc:Hex 4:6) 0.55; IR ν_{max} (KBr)/cm^{-1} 3224 (Alkynyl C-H), 2992 (Ar C-H), 1645 (C=O), 1584 (Ar C=C); δ_H (300 MHz, $CDCl_3$) 7.78 (1H, d, *J* 16.1, H-a'), 7.70 (1H, d, *J* 15.9, H-a), 7.62 (1H, d, *J* 8.5, H-3'), 7.21 (1H, dd, *J* 2.0 ad 8.3, H-2), 7.16-7.12 (2H, m, H-b', 1), 7.07 (1H, d, *J* 8.3, H-3), 6.95 (1H, d, *J* 15.9, H-b), 6.90 (1H, dd, *J* 2.4 and 8.6, H-2'), 6.87 (1H, d, *J* 2.4, H-1'), 4.83 (2H, d, *J* 2.4 H-5), 3.94 (3H, s, H-4), 2.55 (1H, t, *J* 2.4, H-6); δ_C (75 MHZ, $CDCl_3$) 188.5, 165.3, 160.7, 149.9, 149.0, 143.5, 134.5, 130.6, 128.9, 127.3, 124.1, 122.7, 113.9, 112.3, 112.0, 110.7, 104.9, 78.0, 76.3, 56.7, 56.0; LRMS (EI) m/z 355.0 (M + H) M^+ $C_{21}H_{16}F_2O_3$ requires 354.1; Anal. Calcd. for $C_{21}H_{16}F_2O_3$ - C 71.2%, H 4.6%; found C 70.8%, H 5.0%.

4-Azido-7-chloro-quinoline, 3.13

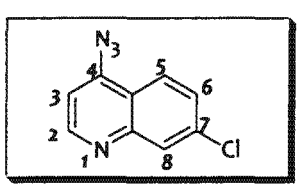

4,7-dichloroquinoline (2.0 g, 10 mmol) was dissolved in 5 mL anhydrous DMF. NaN_3 (1.3 g, 20 mmol) was then added in one portion, and the resulting mixture stirred at 65° C for 6 hours, whereupon TLC indicated reaction completion.

The reaction mixture was then allowed to cool to ambient temperature, after which it was diluted with 100 mL CH_2Cl_2, washed with water (3 x 30 mL), dried over anhydrous Na_2SO_4, and evaporated to dryness. The resulting product residue was crystallised from a CH_2Cl_2/Hexane mixture to yield the final pure product as colourless, needle-like crystals (1.7 g, 86%); mp 115°C (from CH_2Cl_2/Hex); R_f (EtOAc:Hex 3:7) 0.29; IR ν_{max} ($CHCl_3$)/cm^{-1} 3021 (Ar C-H), 2123 (azide), 1609 (Ar C=C); δ_H (300 MHz, $CDCl_3$) 8.83 (1H, d, *J* 4.9, H-2), 8.09 (1H, d, *J* 2.4, H-8), 8.01 (1H, d, *J* 9.3, H-5), 7.49 (1H, dd, *J* 2.4 and 9.3, H-6) 7.13 (1H, d, *J* 4.9, H-3); δ_C (100 MHz, $CDCl_3$) 150.9, 149.1, 146.8, 136.9, 127.9, 123.8, 119.9, 108.7; LRMS (EI) m/z 204.9 (M + H) M^+ $C_9H_5ClN_4$ requires 204.0; Anal. Calcd. for $C_9H_5ClN_4$ C 52.8%, H 2.5%, N 27.4%; found C 52.8%, H 2.4%, N 27.5%.

General method III: synthesis of the chalcone-triazole derivatives 3.14 – 3.17:

The appropriate acetylenic chalcone (1 mmol) and the appropriate azide (AZT or 10, 1 mmol) were dissolved in 5 mL DMF and, while stirring at 65° C, 1 M sodium ascorbate (0.4 mL, 0.4 mmol) and 1 M $CuSO_4$ (0.2 mL, 20 mol%) were added sequentially, in that order. The reaction mixture was then stirred at 65° C for 24 hrs.

The crude product was then precipitated out by slowly adding cold water to the reaction mixture, after which it was filtered, washed with water, air dried and purified by silica column chromatography (eluents ranging in polarity from EtOAc:Hex 3:7 to 5%MeOH in EtOAc).

1-[5-*Hydroxymethyl*-4-(4-{2-*methoxy*-4-[3-(4-*methoxy-phenyl*)-3-*oxo-propenyl*]-*phenoxymethyl*}-[1,2,3]*triazol*-1-*yl*)-*tetrahydro-furan*-2-*yl*]-5-*methyl*-1H-*pyrimidine*-2,4-*dione*, 3.14a

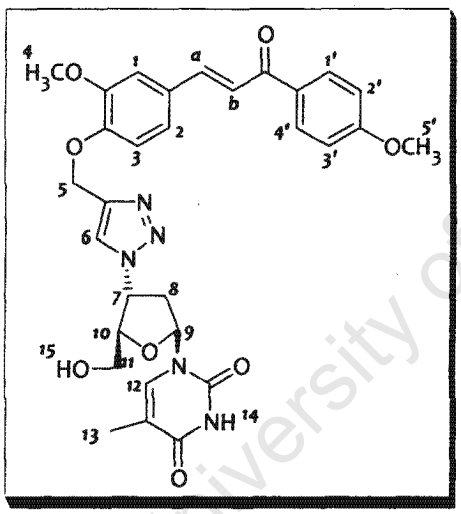

Yellow solid (294.4 mg, 50%); mp 121 - 122°C (from MeOH/EtOAc); R_f (EtOAc:Hex 9:1) 0.11; IR ν_{max} ($CHCl_3$)/cm^{-1} 3385 (O-H), 3015 (Ar C-H), 1691 (C=O), 1599 (Ar C=C); δ_H (300 MHz, DMSO-d_6) 11.30 (1H, s, H-14), 8.41 (1H, s, H-6), 8.14 (2H, d, *J* 8.8, H-1', 4'), 7.81 (1H, d, *J* 15.6, H-a), 7.80 (1H, s, H-12), 7.65 (1H, d, *J* 15.6, H-b), 7.52 (1H, d, *J* 1.7, H-1), 7.38 (1H, dd, *J* 1.7 and 8.3, H-2), 7.22 (1H, d, *J* 8.3, H-3), 7.07 (2H, d, *J* 8.9, H-2', 3'), 6.42 (1H, t, *J* 6.6, H-9), 5.42 - 5.37 (1H, m, H-7), 5.20 (2H, s, H-5), 4.25 – 4.22 (1H, m, H-10), 3.86 (3H, s, H-5'), 3.84 (3H, s, H-4), 3.72 – 3.60 (2H, m, H-11), 2.78 – 2.62 (2H, m, H-8), 1.8(3H, s, H-13); δ_C (100 MHz, DMSO-d_6) 187.9, 164.4, 163.8, 151.1, 150.5, 149.9, 144.2, 143.3, 136.9, 131.5, 130.9, 128.9, 125.2, 124.1, 120.6, 114.6, 113.9, 111.8, 110.3, 85.1, 84.6, 62.4, 61.5, 60.0, 56.4, 56.2, 37.9, 12.9; LRMS (EI) m/z 590.5 (M + H) M^+ $C_{30}H_{31}N_5O_8$ requires 589.2; Anal.Calcd. for $C_{30}H_{31}N_5O_8.H_2O$ - C 59.2%, H 5.4%, N 11.5%; found C 59.3%, H 5.4%, N 11.6%.

1-[4-(4-{4-[3-(2,4-*Dimethoxy-phenyl*)-3-*oxo-propenyl*]-2-*methoxy-phenoxymethyl*}-[1,2,3]*triazol*-1-*yl*)-5-*hydroxymethyl*-*tetrahydro-furan*-2-*yl*]-5-*methyl*-1H-*pyrimidine*-2,4-*dione*, 3.14b

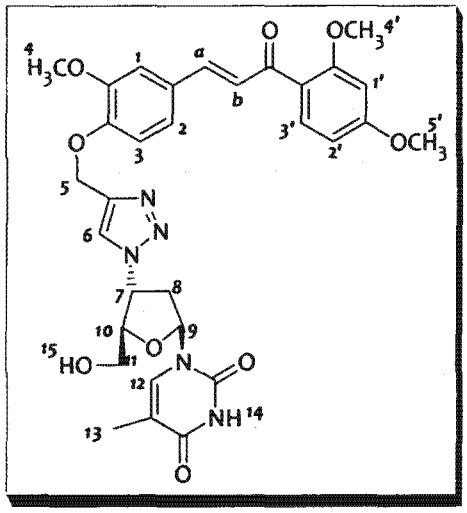

Yellow solid (289.6 mg, 47%); mp: 133 - 134°C (from MeOH/EtOAc); R_f (EtOAc:Hex 9:1) 0.11; IR ν_{max} ($CHCl_3$)/cm^{-1} 3385 (O-H), 3015 (Ar C-H), 1694 (C=O), 1602(Ar C=C); δ_H (400 MHz, DMSO-d_6) 11.30 (1H, s, H-14), 8.41 (1H, s, H-6), 7.79 (1H, s, H-12), 7.56 (1H, d, *J* .5, H-3'), 7.47 (1H, d, *J* 15.8, H-a), 7.39 (1H, d, *J* 15.8, H-b), 7.31 (1H, d, *J* 1.9, H-1), 7.26 (1H, dd, *J* 1.9 and 8.3, H-2), 7.20 (1H, d, *J* 8.3 H-3), 6.66 (1H, d, *J* 2.4, H-1'), 6.62 (1H, dd, *J* 2.4 and 8.4, H-2'), 6.42 (1H, t, *J* 6.6, H-9), 5.41 – 5.36 (1H, m, H-7), 5.25 (1H, s, H-15), 5.19 (2H, s, H-5), 4.24 – 4.21 (1H, m, H-10), 3.87 (3H, s, H-4'), 3.83 (3H, s, H-5'), 3.79 (3H, s, H-4), 3.71 – 3.60 (2H, m, H-11), 2.77 – 2.61 (2H, m, H-8), 1.80 (3H, s, H-13); δ_C (100 MHz, DMSO-d_6) 190.3, 164.3, 160.6, 151.1, 150.2, 149.9, 143.3, 142.5, 136.9, 132.4, 128.9, 126.0, 125.2, 123.0, 122.4, 114.1, 111.8, 110.3, 106.6, 99.4, 92.2, 85.0, 84.6, 65.5, 62.4, 61.5, 60.0, 56.6, 56.1, 37.9, 12.9; LRMS (EI) m/z 620.5 (M + H) M^+ $C_{31}H_{33}N_5O_9$ requires 619.2; Anal. Calcd. for $C_{31}H_{33}N_5O_9.½H_2O$ C 59.2%, H 5.4%, N 11.1%; found C 59.0%, H 5.1%, N 10.6%.

1-[5-*Hydroxymethyl*-4-(4-{2-*methoxy*-4-[3-*oxo*-3-(2,3,4-*trimethoxy-phenyl*)-*propenyl*]-*phenoxymethyl*}-[1,2,3]*triazol*-1-*yl*)-*tetrahydro-furan*-2-*yl*]-5-*methyl*-1H-*pyrimidine*-2,4-*dione*, 3.14c

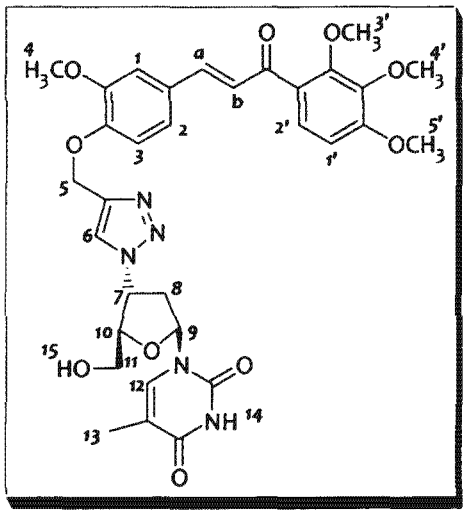

Yellow solid (299.1 mg, 46%); mp 103 - 105°C (from MeOH/EtOAc); R_f (EtOAc:Hex 9:1) 0.10; IR ν_{max} ($CHCl_3$)/cm^{-1} 3385 (O-H), 3015 (Ar C-H), 1694 (C=O), 1593 (Ar C=C); δ_H (400 MHz, DMSO-d_6) 11.29 (1H, s, H-14), 8.42 (1H, s, H-6), 7.80 (1H, s, H-12), 7.48 (1H, d, *J* 16.1, H-a), 7.32 (1H, d, *J* 16.1, H-b), 7.36 – 7.28 (3H, m, H-2', 1, 2), 7.22 (1H, d, *J* 8.3, H-3), 6.93 (1H, d, *J* 8.8, H-1'), 6.43 (1H, t, *J* 6.3, H-9), 5.43 – 5.37 (1H, m,

H-7), 5.24 (1H, s, H-15), 5.21 (2H, s, H-5), 4.27 – 4.23 (1H, m, H-10), 3.88 (3H, s, H-3'), 3.84 (3H, s, H-5'), 3.81 (3H, s, H-4'), 3.80 (3H, s, H-4), 3.75 – 3.63 (2H, m, H-11), 2.81 – 2.62 (2H, m, H-8), 1.82 (3H, s, H-13); δ_C (100 MHz, DMSO-d_6) 191.3, 164.4, 157.0, 153.3, 151.1, 150.4, 149.9, 143.8, 143.3, 142.4, 136.9, 128.6, 127.3, 125.5, 125.2, 123.3, 114.1, 111.8, 110.2, 108.5, 92.1, 85.1, 84.6, 62.3, 61.5, 61.2, 60.4, 60.0, 56.8, 56.3, 37.9, 12.9; LRMS (EI) m/z 650.7 (M + H) M^+ $C_{32}H_{35}N_5O_{10}$ requires 649.2; Anal. Calcd. for $C_{32}H_{35}N_5O_{10}.½H_2O$ - C 58.3%, H 5.3%, N 10.6%; found C 58.2%, H 5.4%, N 10.8%.

3-{4-[1-(7-*Chloro-quinolin-4-yl*)-1H-[1,2,3]*triazol-4-ylmethoxy*]-3-*methoxy-phenyl*}-1-(4-*methoxy-phenyl*)-*propenone*, 3.15a

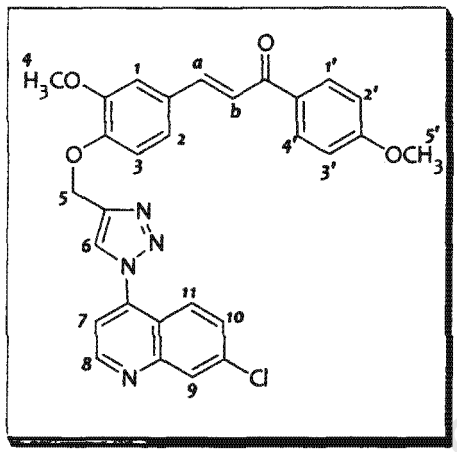

Yellow solid (303.4 mg, 58%); mp 178 - 180°C (from EtOAc); R_f (EtOAc:Hex 6:4) 0.25; IR ν_{max} ($CHCl_3$)/cm^{-1} 3021 (Ar C-H), 1657 (C=O), 1599 (Ar C=C); δ_H (400 MHz, $CDCl_3$) 9.06 (1H, d, *J* 4.8, H-8), 8.27 (1H, d, *J* 2.0, H-9), 8.15 (1H, s, H-6), 8.01 (2H, d, *J* 9.0, H-1', 4'), 7.98 (1H, d, *J* 9.0, H-11), 7.74 (1H, d, *J* 15.6, H-a), 7.59 (1H, dd, *J* 2.0 and 8.9, H-10), 7.51 (1H, d, *J* 4.8, H-7), 7.42 (1H, d, *J* 15.6, H-b), 7.23 (1H, d, *J* 1.8, H-1), 7.18 – 7.14 (2H, m, H-2, 3), 6.97 (2H, d, *J* 9.0, H-2', 3'), 5.43 (2H, s, H-5), 3.94 (3H, s, H-5'), 3.88 (3H, s, H-4); δ_C (100 MHz, $CDCl_3$) 188.7, 163.3, 151.1, 149.8, 149.5, 144.8, 143.7, 141.1, 137.2, 131.2, 130.7, 129.6, 129.4, 128.8, 124.8, 124.5, 122.5, 120.6, 116.0, 114.1, 113.9, 111.1, 62.9, 56.1, 55.5; LRMS (EI) m/z 527.6 (M + H) M^+ $C_{29}H_{23}ClN_4O_4$ requires 526.1; Anal. Calcd. for $C_{29}H_{23}ClN_4O_4.½H_2O$ C 64.9%, H 4.5%, N 10.4%; found C 65.1%, H 4.5%, N 10.7.

3-{4-[1-(7-*Chloro-quinolin*-4-*yl*)-1H-[1,2,3]*triazol*-4-*ylmethoxy*]-3-*methoxy-phenyl*}-1-(2,4-*dimethoxy-phenyl*)-*propenone*, 3.15b

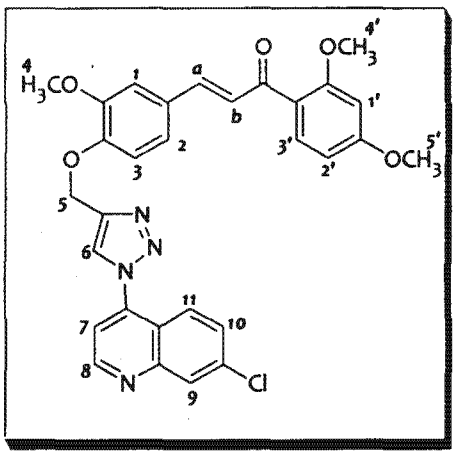

Yellow solid (282.7 mg, 51%); mp: 122 - 124°C (from EtOAc); R_f (EtOAc:Hex 6:4) 0.12; IR ν_{max} ($CHCl_3$)/cm^{-1} 3020 (Ar C-H), 1653 (C=O), 1604 (Ar C=C); δ_H (400 MHz, $CDCl_3$) 9.05 (1H, d, *J* 4.8, H-8), 8.26 (1H, d, *J* 2.0, H-9), 8.13 (1H, s, H-6), 7.96 (1H, d, *J* 9.2, H-11), 7.74 (1H, d, *J* 8.6, H-3'), 7.60 (1H, d, *J* 15.6, H-a), 7.58 (1H, dd, *J* 2.0 and 9.2, H-10), 7.49 (1H, d, *J* 4.6, H-7), 7.38 (1H, d, *J* 15.6, H-b), 7.20 (1H, dd, *J* 2.0 and 8.4, H-2), 7.14 – 7.12 (2H, m, H-1, 3), 6.57 (1H, dd, *J* 2.2 and 8.6, H-2'), 6.50 (1H, d, *J* 2.2, H-1'), 5.48 (2H, s, H-5), 3.92 (3H, s, H-4'), 3.90 (3H, s, H-5'), 3.87 (3H, s, H-4); δ_C (100 MHz, $CDCl_3$) 190.5, 164.1, 160.2, 151.3, 150.2, 149.8, 149.2, 144.9, 141.9, 140.9, 137.0, 132.7, 129.8, 129.5, 129.0, 126.0, 124.8, 124.5, 122.4, 122.1, 120.6, 116.0, 114.2, 111.3, 105.2, 98.7, 63.0, 55.9, 55.9, 55.5; LRMS (EI) m/z 557.5 (M + H) M^+ $C_{30}H_{25}ClN_4O_5$ requires 556.2; Anal. Calcd. for $C_{30}H_{25}ClN_4O_5$ C 64.7%, H 4.5%, N 10.1%; found C 64.9%, H 4.4%, N 10.0%.

3-{4-[1-(7-*Chloro-quinolin*-4-*yl*)-1H-[1,2,3]*triazol*-4-*ylmethoxy*]-3-*methoxy-phenyl*}-1-(2,3,4-*trimethoxy-phenyl*)-*propenone*, 3.15c

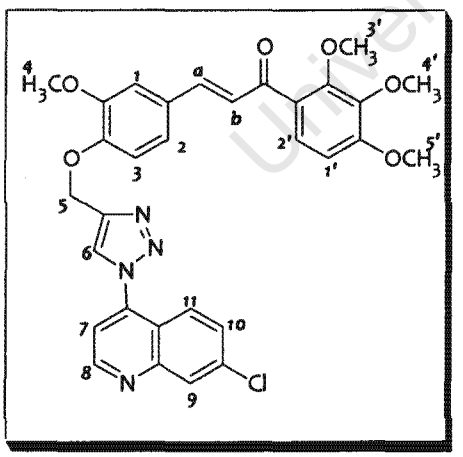

Yellow solid (318.3 mg, 54%); mp: 124°C (from EtOAc); R_f (EtOAc:Hex 6:4) 0.20; IR ν_{max} ($CHCl_3$)/cm^{-1} 3015 (Ar C-H), 1649 (C=O), 1593 (Ar C=C); δ_H (300 MHz, $CDCl_3$) 9.05 (1H, d, *J* 4.4, H-8), 8.27 (1H, d, *J* 1.9, H-9), 8.14 (1H, s, H-6), 7.99 (1H, d, *J* 9.3, H-11), 7.61 (1H, d, *J* 16.1, H-a), 7.59 (1H, dd, *J* 1.9 and 9.3, H-10), 7.50 (1H, d, *J* 4.4, H-7), 7.45 (1H, d, *J* 8.8, H-2'), 7.37 (1H, d, *J* 16.1, H-b), 7.21 (1H, dd, *J* 1.9, 8.3, H-2), 7.16 – 7.12 (2H, m, H-1, 3), 6.75 (1H, d, *J* 8.8, H-1'), 5.48 (2H, s, H-5), 3.92 – 3.90 (12H, m, H-3', 5', 4', 4);δ_C (75 MHz, $CDCl_3$) 190.8, 156.9, 151.1, 149.8, 149.4, 144.9, 142.9, 142.2, 137.2, 129.6, 129.5, 128.8, 126.9, 125.6, 125.3, 124.8, 124.6, 122.5, 116.0, 114.0, 111.0, 107.4, 62.9, 62.1, 61.1, 56.1, 56.0; LRMS (EI) m/z 587.4 (M +

H) M+ $C_{31}H_{27}ClN_4O_6$ requires 586.2; Anal. Calcd. for $C_{31}H_{27}ClN_4O_6$ C 63.4%, H 4.6%, N 9.6%; found C 63.2%, H 4.5%, N 9.5%.

1-[4-(4-{4-[3-(2,4-*Dimethoxy-phenyl*)-*acryloyl*]-2-*methoxy-phenoxymethyl*}-[1,2,3]*triazol*-1-*yl*)-5-*hydroxymethyl*-*tetrahydro-furan*-2-*yl*]-5-*methyl*-1H-*pyrimidine*-2,4-*dione*, 3.16a

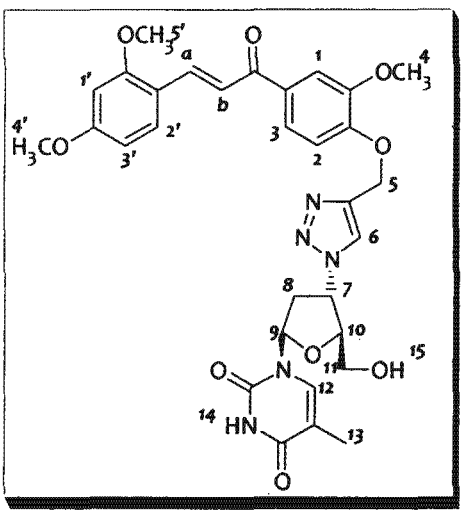

Yellow solid (272.6 mg, 44%); mp 135 - 136°C (from MeOH/EtOAc); R_f (EtOAc:Hex 9:1) 0.15; IR ν_{max} ($CHCl_3$)/cm^{-1} 3021 (Ar C-H), 1691 (C=O), 1599 (Ar C=C); δ_H (400 MHz, DMSO-d_6) 8.43 (1H, s, H-6), 7.95 (1H, d, *J* 15.7, H-a), 7.90 (1H, d, *J* 8.6, H-2'), 7.81 (1H, dd, *J* 1.8 and 8.6, H-3), 7.78 (2H, m, H-1, 12), 7.74 (1H, d, *J* 15.6, H-b), 7.57 (1H, d, *J* 2.0, H-1'), 7.31 (1H, d, *J* 8.6, H-2), 6.61 (1H, dd, *J* 2.0 and 8.6, H-3'), 6.61 (1H, t, *J* 6.6, H-9), 5.42 – 5.37 (1H, m, H-7), 5.26 (2H, s, H-5), 4.24 – 4.21 (1H, m, H-10), 3.89 (3H, s, H-5'), 3.83 (6H, s, H-4, 4'), 3.74 – 3.63 (2H, m, H-11), 2.77 – 2.61 (2H, m, H-8), 1.79 (3H, s, H-13); δ_C (75 MHz, DMSO-d_6) 187.4, 163.6, 162.9, 159.8, 151.5, 150.3, 148.9, 142.4, 137.8, 136.1, 131.3, 129.9, 124.5, 122.6, 119.0, 116.0, 112.4, 110.9, 109.5, 106.3, 98.2, 84.4, 83.9, 61.7, 60.7, 59.3, 55.8, 55.5, 55.4, 37.1, 12.1; LRMS (EI) m/z 620.6 (M + H) M+ $C_{31}H_{33}N_5O_9$ requires 619.2; Anal. Calcd. for $C_{31}H_{33}N_5O_9.\frac{1}{2}H_2O$ C 59.2%, H 5.3%, N 11.1%; found C 59.0%, H 5.5%, N 11.0%.

1-[5-*Hydroxymethyl*-4-(4-{2-*methoxy*-4-[3-(2,3,4-*trimethoxy*-*phenyl*)-*acryloyl*]-*phenoxymethyl*}-[1,2,3]*triazol*-1-*yl*)-*tetrahydro*-*furan*-2-*yl*]-5-*methyl*-1H-*pyrimidine*-2,4-*dione*, 3.16b

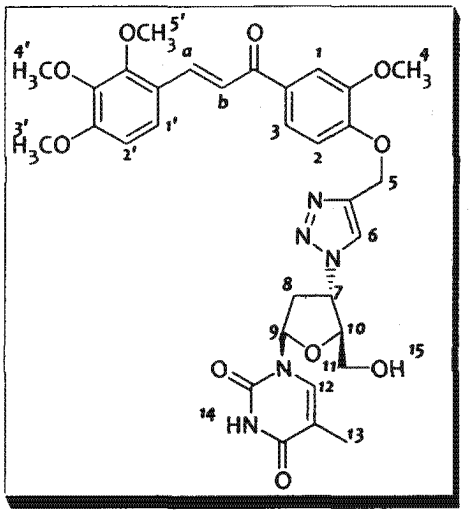

Yellow solid (332.4 mg, 51%); mp 121 - 122°C (from MeOH/EtOAc); R_f (EtOAc:Hex 9:1) 0.21; IR ν_{max} ($CHCl_3$)/cm^{-1} 3391 (O-H), 3015 (Ar C-H), 1694 (C=O), 1593 (Ar C=C); δ_H (400 MHz, DMSO-d_6) 11.28 (1H, s, H-14), 8.43 (1H, s, H-6), 7.87 (1H, d, *J* 15.6, H-a), 7.83 (1H, dd, *J* 2.0 and 8.6, H-3), 7.82 (1H, d, *J* 15.6, H-b), 7.79 (1H, s, H-12), 7.76 (1H, d, *J* 8.9, H-1'), 7.58 (1H, d, *J* 2.0, H-1), 7.32 (1H, d, *J* 8.6, H-2), 6.91 (1H, d, *J* 8.9, H-2'), 6.42 (1H, t, *J* 6.6, H-9), 5.42 – 5.37 (1H, m, H-7), 5.27 (2H, s, H-5), 5.24 (1H, s, H-15), 4.25 – 4.22 (1H, m, H-10), 3.86 (3H, s, H-5'), 3.85 (3H, s, H-3'), 3.83 (3H, s, H-4), 3.77 (3H, s, H-4'), 3.76 – 3.63 (2H, m, H-11), 2.77 – 2.62 (2H, m, H-8), 1.80 (3H, s, H-13); δ_C (75 MHz, DMSO-d_6) 187.4, 163.6, 155.5, 152.9, 151.6, 150.3, 148.9, 142.4, 141.8, 137.5, 136.1, 131.2, 124.5, 123.3, 122.7, 121.1, 120.4, 112.4, 111.0, 109.5, 108.4, 84.4, 83.9, 61.7, 61.4, 60.7, 60.4, 59.3, 56.0, 55.5, 37.1, 12.1; LRMS (EI) m/z 650.8 (M + H) M^+ $C_{32}H_{35}N_5O_{10}$ requires 649.2; Anal. Calcd. for $C_{32}H_{35}N_5O_{10}.1H_2O$ C 57.5%, H 5.5%, N 10.5%; found C 57.3%, H 5.4%, N 10.4%.

1-[4-(4-{4-[3-(2,4-*Dichloro*-*phenyl*)-*acryloyl*]-2-*methoxy*-*phenoxymethyl*}-[1,2,3]*triazol*-1-yl)-5-*hydroxymethyl*-*tetrahydro*-*furan*-2-*yl*]-5-*methyl*-1H-*pyrimidine*-2,4-*dione*, 3.16c

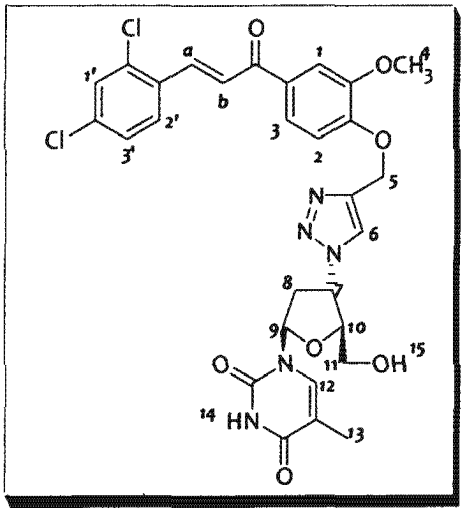

Yellow solid (279.3 mg, 45%); mp 112 - 114°C (from MeOH/EtOAc); R_f (EtOAc:Hex 8:2) 0.10; IR ν_{max} ($CHCl_3$)/cm^{-1} 3391 (O-H), 3018 (Ar C-H), 1692 (C=O), 1582 (Ar C=C); δ_H (400 MHz, DMSO-d_6) 11.30 (1H, s, H-14), 8.43 (1H, s, H-6), 8.23 (1H, d, *J* 8.6, H-2'), 8.02 (1H, d, *J* 15.6, H-a), 7.94 – 7.91 (2H, m, H-b, 3), 7.79 (1H, s, H-12), 7.73 (1H, d, *J* 2.0, H-1), 7.61 (1H, d, *J* 2.0, H-1'), 7.54 (1H, dd, *J* 2.0 and 8.6, H-3'), 7.33 (1H, d, *J* 8.6, H-2), 6.42 (1H, t, *J* 6.6, H-9), 5.42 –

5.37 (1H, m, H-7), 5.28 (2H, s, H-5), 4.25 – 4.22 (1H, m, H-10), 3.83 (3H, s, H-4), 3.73 – 3.60 (2H, m, H-11), 2.77 – 2.61 (2H, m, H-8), 1.80 (3H, s, H-13); δ_C (75 MHz, DMSO) 187.0, 163.6, 152.2, 150.4, 149.0, 142.3, 136.5, 136.1, 135.3, 134.9, 131.5, 130.5, 129.8, 129.4, 127.8, 125.3, 124.5, 123.4, 112.4, 111.1, 109.6, 84.4, 83.9, 61.7, 60.7, 59.3, 55.6, 37.1, 12.1; LRMS (EI) m/z 628.6 (M + H) M^+ $C_{29}H_{27}Cl_2N_5O_7$ requires 627.1; Anal. Calcd. for $C_{29}H_{27}Cl_2N_5O_7.½H_2O$ - C 54.7%, H 4.2%, N 11.0%; found C 54.4%, H 4.8%, N 10.8%.

1-[4-(4-{4-[3-(4-*Fluoro-phenyl*)-*acryloyl*]-2-*methoxy-phenoxymethyl*}-[1,2,3]*triazol*-1-*yl*)-5-*hydroxymethyl*-*tetrahydro-furan*-2-*yl*]-5-*methyl*-1H-*pyrimidine*-2,4-*dione*, 3.16d

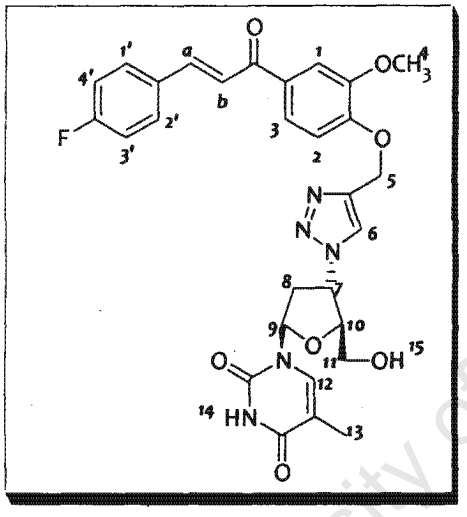

Yellow solid (278.1 mg, 48%); mp 130 - 132°C (from MeOH/EtOAc); R_f (EtOAc:Hex 9:1) 0.18; IR ν_{max} ($CHCl_3$)/cm^{-1} 3386 (O-H), 3018 (Ar C-H), 1689 (C=O), 1597 (Ar C=C); δ_H (300 MHz, DMSO-d_6) 11.28 (1H, s, H-14), 8.43 (1H, s, H-6), 7.85 (1H, d, *J* 15.6, H-a), 7.81 (1H, dd, *J* 1.9 and 8.8, H-3), 7.79 (1H, s, H-12), 7.78 (1H, d, *J* 15.6, H-b), 7.76 (2H, d, *J* 8.8, H-1', 4'), 7.58 (1H, d, *J* 1.9, H-1), 7.31 (2H, d, *J* 8.8, H-2', 3'), 6.89 (1H, d, *J* 8.8, H-2), 6.42 (1H, t, *J* 6.8, H-9), 5.43 – 5.36 (1H, m, H-7), 5.27 (2H, s, H-5), 4.26 – 4.22 (1H, m, H-10), 3.85 (3H, s, H-4), 3.70 – 3.59 (2H, m, H-11), 2.80 – 2.61 (2H, m, H-8), 1.80 (3H, s, H-13); δ_C (75 MHz, DMSO-d_6) 187.4, 163.6, 155.5, 152.9, 151.6, 150.3, 148.9, 142.4, 137.5, 136.1, 131.2, 124.5, 123.3, 122.8, 121.1, 120.4, 112.4, 111.0, 109.5, 108.4, 84.4, 83.9, 61.7, 60.7, 59.3, 55.5, 37.1, 12.1; LRMS (EI) m/z 578.6 (M + H) M^+ $C_{29}H_{28}FN_5O_7$ requires 577.2; Anal. Calcd. for $C_{29}H_{28}FN_5O_7$ C 60.3%, H 4.9%, N 12.1%; found C 60.1%, H 5.5%, N 11.9%.

1-[4-(4-{4-[3-(2,4-*Difluoro-phenyl*)-*acryloyl*]-2-*methoxy-phenoxymethyl*}-[1,2,3]*triazol*-1-*yl*)-5-*hydroxymethyl-tetrahydro-furan*-2-*yl*]-5-*methyl*-1H-*pyrimidine*-2,4-*dione*, 3.16e

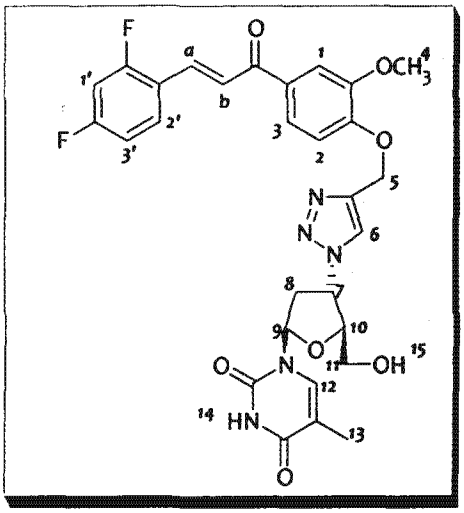

Yellow solid (248.9 mg, 44%); mp 128 - 130°C (from MeOH/EtOAc); R_f (EtOAc:Hex 9:1) 0.18; IR ν_{max} ($CHCl_3$)/cm^{-1} 3386 (O-H), 3018 (Ar C-H), 1692 (C=O), 1600 (Ar C=C); δ_H (300 MHz, DMSO-d_6) 11.30 (1H, s, H-14), 8.44 (1H, s, H-6), 7.97 (1H, d, *J* 15.6, H-a), 7.90 (1H, d, *J* 8.3, H-2'), 7.83 – 7.79 (2H, m, H-1, 3), 7.76 (1H, d, *J* 15.6, H-b), 7.59 (1H, d, *J* 1.9, H-1'), 7.34 (1H, dd, *J* 1.9 and 8.3, H-3'), 6.64 (1H, d, *J* 8.8, H-2), 6.44 (1H, t, *J* 6.3, H-9), 5.44 – 5.38 (1H, m, H-7), 5.28 (2H, s, H-5), 5.25 (1H, *bs*, H-15), 4.28 – 4.24 (1H, m, H-10), 3.85 (3H, s, H-4), 3.76 – 3.63 (2H, m, H-11), 2.81 – 2.62 (2H, m, H-8), 1.82 (3H, s, H-13); δ_C (75 MHz, DMSO-d_6) 187.4, 163.6, 162.9, 159.8, 151.5, 150.3, 148.9, 142.4, 137.8, 136.1, 131.4, 129.9, 124.5, 122.6, 119.0, 116.0, 112.4, 110.9, 109.5, 106.3, 84.4, 83.9, 61.7, 60.7, 59.3, 55.4, 37.1, 12.1; LRMS (EI) m/z 596.4 (M + H) M^+ $C_{29}H_{27}F_2N_5O_7$ requires 595.2; Anal. Calcd. for $C_{29}H_{27}F_2N_5O_7.½H_2O$. C 57.6%, H 4.6%, N 11.5%; found C 57.8%, H 4.6%, N 10.9%.

1-{4-[1-(7-*Chloro-quinolin*-4-*yl*)-1H-[1,2,3]*triazol*-4-*ylmethoxy*]-3-*methoxy-phenyl*}-3-(2,4-*dimethoxy-phenyl*)-*propenone*, 3.17a

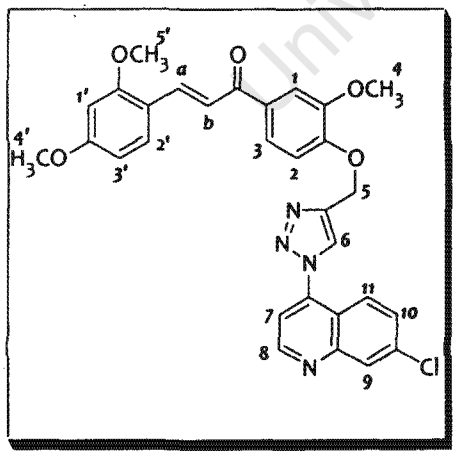

Yellow solid (228.3 mg, 41%); mp 157 - 158°C (from EtOAc); R_f (EtOAc:Hex 7:3) 0.25; IR ν_{max} ($CHCl_3$)/cm^{-1} 3020 (Ar C-H), 1649 (C=O), 1599 (Ar C=C); δ_H (400 MHz, $CDCl_3$) 9.09 (1H, *bs*, H-8), 8.26 (1H, s, H-9), 8.15 (1H, s, H-6), 8.04 (1H, d, *J* 15.7, H-a), 7.98 (1H, d, *J* 9.2, H-11), 7.68 – 7.65 (2H, m, H-1, 3), 7.59 (1H, d, *J* 9.2, H-10), 7.57 (1H, d, *J* 8.4, H-2'), 7.55 (1H, d, *J* 15.7, H-b), 7.51 (1H, *bs*, H-7), 7.18 (1H, d, *J* 8.6, H-2), 6,53 (1H, dd, *J* 2.2 and 8.4, H-3'), 6.48 (1H, d, *J* 2.2, H-1'), 5.53 (2H, s, H-5), 3.96 (3H, s, H-5'), 3.91 (3H, s, H-4'), 3.86 (3H, s, H-4); δ_C (75 MHz, $CDCl_3$) 189.3, 163.0, 160.4, 151.1, 149.6, 140.1, 137.2, 133.0, 131.0, 129.7, 124.6, 122.5, 119.9, 117.2, 112.6, 111.5, 105.4, 98.5, 62.8, 56.1, 55.6, 55.5; LRMS (EI) m/z 557.5

(M + H) M^+ $C_{30}H_{25}ClN_4O_5$ requires 556.2; Anal. Calcd. for $C_{30}H_{25}ClN_4O_5.H_2O$ C 62.6%, H 4.4%, N 9.7%; found C 62.7%, H 4.3%, N 9.4%.

1-{4-[1-(7-*Chloro-quinolin-4-yl*)-1H-[1,2,3]*triazol-4-ylmethoxy*]-3-*methoxy-phenyl*}-3-(2,3,4-*trimethoxy-phenyl*)-*propenone*, 3.17b

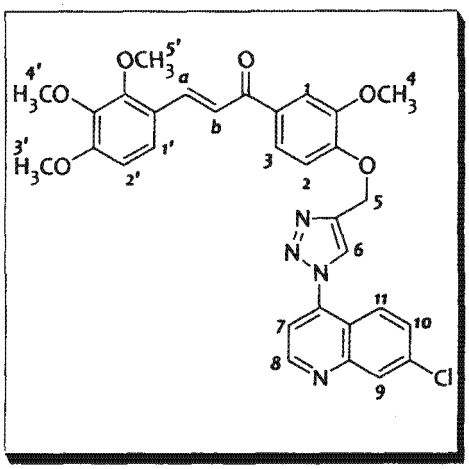

Yellow solid (318.9 mg, 54%); mp 82 - 83°C (from EtOAc); R_f (EtOAc:Hex 6:4) 0.33; IR ν_{max} ($CHCl_3$)/cm^{-1} 3015 (Ar C-H), 1670 (C=O), 1596 (Ar C=C); δ_H (400 MHz, $CDCl_3$) 9.07 (1H, d, *J* 4.8, H-8), 8.27 (1H, d, *J* 2.0, H-9), 8.16 (1H, s, H-6), 7.98 (1H, d, *J* 9.2, H-11), 7.98 (1H, d, *J* 15.7, H-a), 7.68 – 7.66 (2H, m, H-1, 3), 7.60 (1H, dd, *J* 2.0 and 9.2, H-10), 7.57 (1H, d, *J* 15.7, H-b), 7.51 (1H, d, *J* 4.8, H-7), 7.36 (1H, d, *J* 8.8, H-1'), 7.20 (1H, d, *J* 8.6, H-2), 6.72 (1H, d, *J* 8.8, H-2'), 5.53 (2H, s, H-5), 3.96 (3H, s, H-5'), 3.95 (3H, s, H-3'), 3.91 (3H, s, H-4), 3.89 (3H, s, H-4'); δ_C (100 MHz, $CDCl_3$) 189.1, 155.8, 153.7, 151.1, 149.7, 144.7, 142.6, 141.1, 139.7, 137.3, 132.8, 129.7, 128.8, 124.9, 124.6, 123.9, 122.6, 122.1, 121.0, 116.0, 112.6, 111.5, 107.5, 62.9, 61.4, 60.9, 56.1; LRMS (EI) m/z 587.5 (M + H) M^+ $C_{31}H_{27}ClN_4O_6$ requires 586.2; Anal. Calcd. for $C_{31}H_{27}ClN_4O_6.½H_2O$ - C 62.5%, H 4.5%, N 9.4%; found C 62.1%, H 4.5%, N 9.2%.

1-{4-[1-(7-*Chloro-quinolin-4-yl*)-1H-[1,2,3]*triazol-4-ylmethoxy*]-3-*methoxy-phenyl*}-3-(2,4-*dichloro-phenyl*)-*propenone*, 3.17c

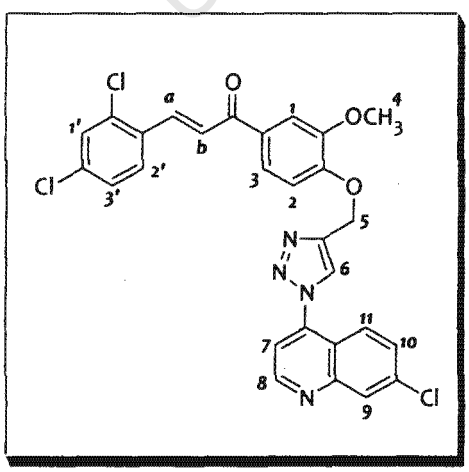

Yellow solid (295.7 mg, 52%); mp 85 - 87°C (from EtOAc); R_f (EtOAc:Hex 1:1) 0.2; IR ν_{max} ($CHCl_3$)/cm^{-1} 3018 (Ar C-H), 1651 (C=O), 1595 (Ar C=C); δ_H (400 MHz, $CDCl_3$) 9.05 (1H, d, *J* 4.8, H-8), 8.27 (1H, d, *J* 2.2, H-9), 8.16 (1H, s, H-6), 8.01 (1H, d, *J* 15.6, H-a), 7.96 (1H, d, *J* 9.2, H-11), 7.67 – 7.65 (2H, m, H-1, 3), 7.59 (1H, dd, *J* 2.2 and 9.2, H-10), 7.56 (1H, d, *J* 8.4, H-2'), 7.55 (1H, d, *J* 15.7, H-b), 7.51 (1H, d, *J* 4.8, H-7), 7.19 (1H, d, *J* 8.6, H-2), 6.53 (1H, dd, *J* 2.4 and 8.4, H-3'), 6.48 (1H, d, *J* 2.4, H-1'), 5.53 (2H, s, H-5), 3.96 (3H, s, H-4); δ_C (100 MHz, $CDCl_3$)

189.3, 163.0, 160.3, 151.0, 149.6, 144.5, 141.0, 140.1, 137.1, 133.0, 131.1, 129.6, 128.8, 125.0, 124.5, 122.5, 120.1, 117.2, 115.9, 112.8, 111.6, 105.5, 98.6, 62.8, 55.5; LRMS (EI) m/z 565.3 (M + H) M^+ $C_{28}H_{19}Cl_3N_4O_3$ requires 564.1); Anal. Calcd. for $C_{28}H_{19}Cl_3N_4O_3$ C 59.4%, H 3.4%, N 9.9%; found C 59.7%, H 3.1%, N 9.5%.

1-{4-[1-(7-*Chloro-quinolin-4-yl*)-1H-[1,2,3]*triazol-4-ylmethoxy*]-3-*methoxy-phenyl*}-3-(4-*fluoro-phenyl*)-*propenone*, 3.17d

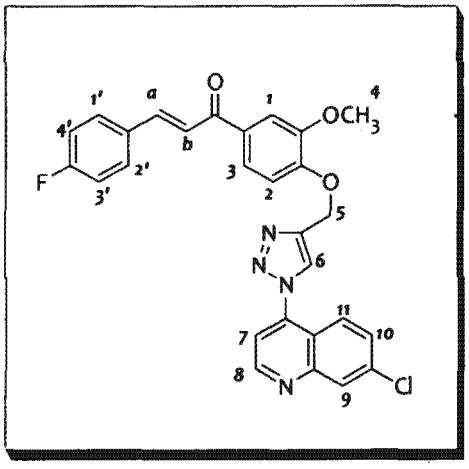

Yellow solid (266.9 mg, 52%); mp 164 - 166°C (from EtOAc); R_f (EtOAc:Hex 6:4) 0.3; IR ν_{max} ($CHCl_3$)/cm^{-1} 3018 (Ar C-H), 1656 (C=O), 1595 (Ar C=C); δ_H (400 MHz, $CDCl_3$) 9.05 (1H, d, 4.6, H-8), 8.25 (1H, d, *J* 2.2, H-9), 8.16 (1H, s, H-6), 7.96 (1H, d, *J* 9.2, H-11), 7.80 (1H, d, *J* 15.6, H-a), 7.67 (1H, dd, *J* 1.8 and 8.4, H-3), 7.65 (1H, d, *J* 1.8, H-1), 7.61 – 7.58 (3H, m, H-1', 2', 10), 7.49 (1H, d, *J* 4.6, H-7), 7.42 (1H, d, *J* 15.6, H-b), 7.21 (1H, d, *H* 8.4, H-2), 6.94 (2H, d, *J* 8.9, H-3', 4'), 5.53 (2H, s, H-5), 3.97 (3H, s, H-4); δ_C (100 MHz, $CDCl_3$) 188.6, 161.7, 151.3, 150.2, 149.8, 144.6, 144.2, 142.9, 140.9, 137.0, 132.7, 130.2, 129.6, 129.0, 127.7, 124.8, 124.5, 122.6, 119.3, 116.0, 114.5, 112.6, 111.5, 62.9, 56.1; LRMS (EI) m/z 515.4 (M + H) M^+ $C_{28}H_{20}ClFN_4O_3$ requires 514.2; Anal. Calcd. for $C_{28}H_{20}ClFN_4O_3$ C 65.3%, H 3.9%, N 10.9%; found C 64.9%, H 4.1%, N 10.6%.

1-{4-[1-(7-*Chloro-quinolin*-4-yl)-1H-[1,2,3]*triazol*-4-*ylmethoxy*]-3-*methoxy-phenyl*}-3-(2,4-*difluoro-phenyl*)-*propenone*, 3.17e

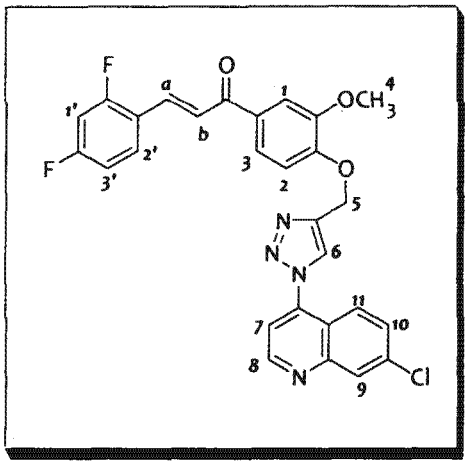

Yellow solid (202.5 mg, 38%); mp 106 - 108°C (from EtOAc); R_f (EtOAc:Hex 6:4) 0.3; IR ν_{max} ($CHCl_3$)/cm^{-1} 3000 (Ar C-H), 1657 (C=O), 1595 (Ar C=C); δ_H (300 MHz, $CDCl_3$) 9.06 (1H, d, *J* 4.4, H-8), 8.27 (1H, d, *J* 1.9, H-9), 8.16 (1H, s, H-6), 7.96 (1H, d, *J* 9.3, H-11), 7.85 (1H, d, *J* 15.6, H-a), 7.69 – 7.65 (2H, m, H-1, 3), 7.59 (1H, dd, *J* 1.9 and 9.3, H-10), 7.55 (1H, d, *J* 8.3, H-2'), 7.52 (1H, d, *J* 15.6, H-b), 7.51 (1H, d, *J* 4.4, H-7), 7.19 (1H, d, *J* 8.8, H-2), 6.73 (1H, dd, *J* 2.4 and 8.3, H-3'), 6.64 (1H, d, *J* 2.4, H-1'), 5.53 (2H, s, H-5), 3.96 (3H, s, H-4); δ_C (75 MHz, $CDCl_3$) 151.0, 149.8, 144.6, 137.2, 132.5, 130.9, 129.7, 128.8, 124.8, 124.6, 122.9, 122.7, 121.7, 116.0, 112.6, 111.4, 110.8, 102.2, 101.9, 98.5, 62.8, 56.1; LRMS (EI) m/z 533.4 (M + H) M^+ $C_{28}H_{19}ClF_2N_4O_3$ requires 532.1; Anal. Calcd. for $C_{28}H_{19}ClF_2N_4O_3$ C 63.1%, H 3.6%, N 10.5%; found C 63.4 %, H 4.0%, N 10.2%.

Synthesis of the vanillin-triazole enone- derivatives 3.18 and 3.19:

These were synthesized as described under General method III, applying the alkylated vanillin-acetone enone **3.11** (2.3 g, 10 mmol), the appropriate azide (AZT or **3.13**, 15 mmol), 1 M Na ascorbate (4 mL, 4 mmol) and 1 M $CuSO_4$ (2 mL, 20 mol%).

1-(5-Hydroxymethyl-4-[4-[2-methoxy-4-(3-oxo-but-1-enyl)-phenoxymethyl]-[1,2,3]triazol-1-yl]-tetrahydro-furan-2-yl)-5-methyl-1H-pyrimidine-2,4-dione, 3.18

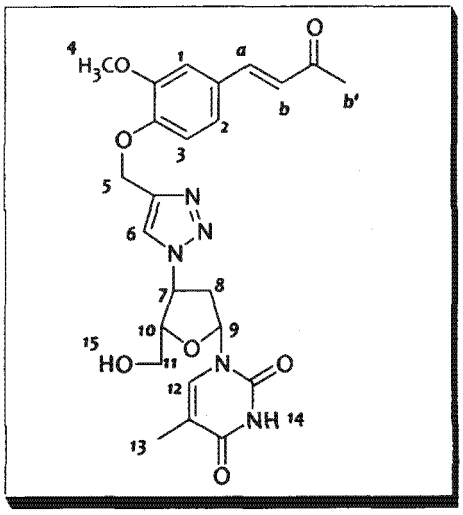

Fluffy white solid (3.9 g, 80%); mp 177 - 179°C (from MeOH/EtOAc); R_f (MeOH: CH_2Cl_2 5:95) 0.42; IR ν_{max} (KBr)/cm^{-1} 3072 (Ar C-H), 1627 (C=O), 1595(Ar C=C); δ_H (400 MHz, DMSO-d_6) 11.30 (1H, s, H-14), 8.41 (1H, s, H-6), 7.80 (1H, s, H-12), 7.56 (1H, d, *J* 16.3, H-a), 7.33 (1H, d, *J* 1.6, H-1), 7.25 (1H, dd, *J* 1.8 and 8.3, H-2), 7.21 (1H, d, *J* 8.4, H-3), 6.74 (1H, d, *J* 16.3, H-b), 6.42 (1H, t, *J* 6.5, H-9), 5.42 - 5.37 (1H, m, H-7), 5.19 (2H, s, H-5), 4.25 – 4.22 (1H, m, H-10), 3.80 (3H, s, H-4), 3.75 – 3.61 (2H, m, H-11), 2.78 – 2.62 (2H, m, H-8), 2.30 (3H, s, H-b'), 1.8 (3H, s, H-13); δ_C (100 MHz, DMSO-d_6) 197.8, 163.6, 150.4, 149.6, 149.1, 143.3, 142.5, 136.1, 127.6, 125.4, 124.4, 122.7, 113.2, 110.7, 109.5, 84.4, 83.9, 61.6, 60.7, 59.2, 55.5, 37.1, 27.1, 12.1; LRMS (EI) m/z 498.5 (M + H) M$^+$ $C_{24}H_{27}N_5O_7$ requires 497.2; Anal.Calcd. for $C_{24}H_{27}N_5O_7.1H_2O$ - C 55.9%, H 5.6%, N 13.6%; found C 55.6%, H 5.4%, N 14.0%.

4-[4-[1-(7-Chloro-quinolin-4-yl)-1H-[1,2,3]triazol-4-ylmethoxy]-3-methoxy-phenyl]-but-3-en-2-one, 3.19

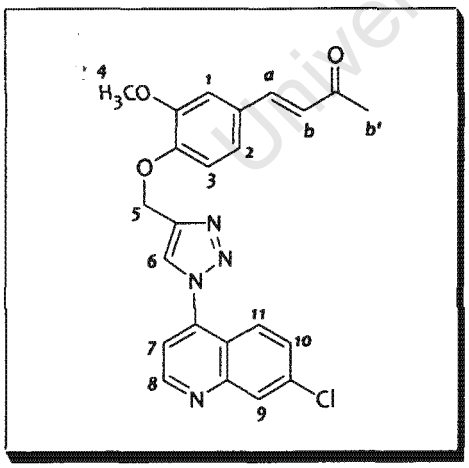

Off-white to pale brown solid (2.7 g, 62%); mp 82 - 84°C (from EtOAc); R_f (EtOAc:Hex 8:2) 0.20; IR ν_{max} (KBr)/cm^{-1} 2927 (Ar C-H), 1663 (C=O), 1595 (Ar C=C); δ_H (300 MHz, $CDCl_3$) 9.05 (1H, d, 4.9, H-8), 8.24 (1H, d, *J* 2.0, H-9), 8.14 (1H, s, H-6), 7.94 (1H, d, *J* 9.3, H-11), 7.58 (1H, dd, *J* 2.0 and 9.3, H-10), 7.48 (1H, d, *J* 4.9, H-7), 7.46 (1H, d, *J* 15.6, H-a), 7.15 – 7.10 (3H, m, H-1, 2, 3), 6.62 (1H, d, *J* 15.6, H-b), 5.48 (2H, s, H-5), 3.91 (3H, s, H-4), 2.37 (3H, s, H-b'); δ_C (75 MHz, $CDCl_3$) 198.2, 151.4, 149.9, 149.7, 144.7, 143.0, 140.8, 137.0, 129.5, 129.1, 128.6, 125.9, 124.8, 124.5, 122.7, 120.5, 116.0 (2C), 113.9, 110.4, 62.9, 55.9, 27.4; LRMS (EI) m/z 435.2 (M + H) M$^+$ $C_{23}H_{19}ClN_4O_3$ requires 434.1; Anal. Calcd. for $C_{23}H_{19}ClN_4O_3.2H_2O$ C 58.6%, H 4.9%, N 11.9%; found C 58.4%, H 4.6%, N 11.6%.

Synthesis of the dienone-triazole derivatives 3.20 – 3.21:

These were synthesized as described under **General method IV**, applying of the triazole enone **3.18** or **3.19** (1 mmol), the appropriately substituted benzaldehyde (1 mmol) and BF_3-Et_2O (0.2mL, 1.5 mmol).

1-[5-Hydroxymethyl-4-(4-[2-methoxy-4-[5-(4-methoxy-phenyl)-3-oxo-penta-1,4-dienyl]-phenoxy methyl]-[1,2,3]triazol-1-yl)-tetrahydro-furan-2-yl]-5-methyl-1H-pyrimidine-2,4-dione, **3.10a**

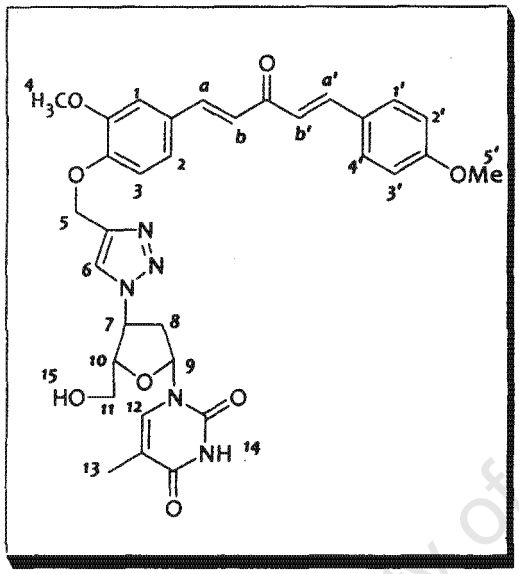

Yellow solid (258 mg, 42%); mp: 192 - 194°C (from MeOH/EtOAc); R_f (MeOH:EtOAc 5:95) 0.30; IR ν_{max} (KBr)/cm^{-1} 3340 (O-H), 3057 (Ar C-H), 1689 (C=O), 1584(Ar C=C); δ_H (400 MHz, DMSO-d_6) 11.31 (1H, s, H-14), 8.43 (1H, s, H-6), 7.81 (1H, s, H-12), 7.75 (4H, m, H-a, a', 1', 4'), 7.41 (1H, d, *J* 1.7, H-1), 7.33 (1H, dd, *J* 1.8 and 8.3, H-2), 7.22 (1H, d, *J* 15.8, H-b'), 7.19 (1H, d, *J* 15.9, H-b), 7.02 (2H, d, *J* 8.7, H-2', 3'), 6.43 (1H, t, *J* 6.4, H-9), 5.43 – 5.38 (1H, m, H-7), 5.21 (2H, s, H-5), 4.26 – 4.23 (1H, m, H-10), 3.83 (3H, s, H-5'), 3.82 (3H, s, H-4, 3.74 – 3.62 (2H, m, H-11), 2.79 – 2.63 (2H, m, H-8), 1.81 (3H, s, H-13); δ_C (100 MHz, DMSO-d_6) 188.0, 163.6, 161.1, 150.8, 150.4, 149.6, 149.2, 142.5, 142.4, 142.0, 136.1, 130.2, 128.1, 127.3, 124.4, 124.1, 123.4, 122.8, 114.4, 113.9, 113.2, 110.9, 109.5, 84.4, 83.9, 61.6, 60.7, 59.3, 55.6, 55.3, 37.1, 12.1; LRMS (EI) m/z 616.2 (M + H) M^+ $C_{32}H_{33}N_5O_8$ requires 615.2; Anal. Calcd. for $C_{32}H_{33}N_5O_8.1½H_2O$ C 59.8%, H 5.6%, N 10.9%; found C 59.7%, H 5.6%, N 10.5%.

1-[4-(4-[4-[5-(2,4-Dimethoxy-phenyl)-3-oxo-penta-1,4-dienyl]-2-methoxy-phenoxymethyl]-[1,2,3]-triazol-1-yl)-5-hydroxymethyl-tetrahydro-furan-2-yl]-5-methyl-1H-pyrimidine-2,4-dione, **3.20b**

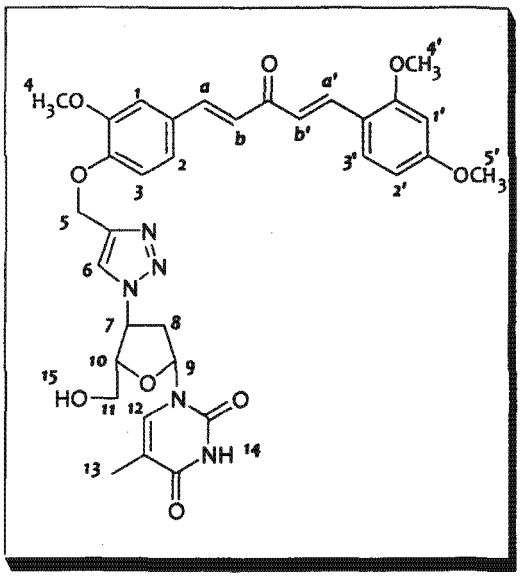

Yellow solid (337 mg, 52%); mp 129 - 131°C (from MeOH/EtOAc); R_f (MeOH:EtOAc 5:95) 0.30; IR ν_{max} (KBr)/cm^{-1} 3384 (O-H), 3057 (Ar C-H), 1692 (C=O), 1595 (Ar C=C); δ_H (300 MHz, DMSO-d_6) 11.20 (1H, s, H-14), 8.39 (1H, s, H-6), 7.87 (1H, d, *J* 16.0, H-a'), 7.78 (1H, s, H-12), 7.72 (1H, d, *J* 8.3, H-3'), 7.66 (1H, d, *J* 16.0, H-a), 7.56 (1H, dd, *J* 1.9 and 8.3, H-2), 7.43 (1H, d, *J* 1.9, H-1), 7.39 (1H, d, *J* 1.9, H-1'), 7.30 (1H, dd, *J* 1.9 and 8.4, H-2'), 7.23 (1H, d, *J* 8.4, H-3), 7.21 (1H, d, *J* 16.0, H-b'), 7.11 (1H, d, *J* 16.0, H-b), 6.42 (1H, t, *J* 6.5, H-9), 5.43 - 5.36 (1H, m, H-7), 5.22 (2H, s, H-5), 4.28 – 4.24 (1H, m, H-10), 3.90 (3H, s, H-4'), 3.84 (3H, s, H-5'), 3.82 (3H, s, H-4), 3.81 – 3.57 (2H, m, H-11), 2.82 – 2.62 (2H, m, H-8), 1.82 (3H, s, H-13); δ_C (75 MHz, DMSO-d_6) 191.0, 187.9, 163.4, 162.7, 159.7, 150.2, 149.5, 142.5, 141.9, 136.8, 135.9, 129.7, 128.1, 125.3, 124.7, 124.3, 124.1, 123.1, 122.5, 113.6, 111.1, 109.4, 106.2, 98.3, 84.3, 83.9, 61.7, 60.6, 59.2, 55.6, 55.3, 36.9, 11.9; LRMS (EI) m/z 646.2 (M + H) M$^+$ $C_{33}H_{35}N_5O_9$ requires 645.2; Anal.Calcd. for $C_{33}H_{35}N_5O_9$ - C 61.4%, H 5.5%, N 10.9%; found C 61.7%, H 5.6%, N 10.6%.

1-[5-Hydroxymethyl-4-(4-[2-methoxy-4-[3-oxo-5-(2,3,4-trimethoxy-phenyl)-penta-1,4-dienyl]-phenoxymethyl]-[1,2,3]triazol-1-yl)-tetrahydro-furan-2-yl]-5-methyl-1H-pyrimidine-2,4-dione, **3.20c**

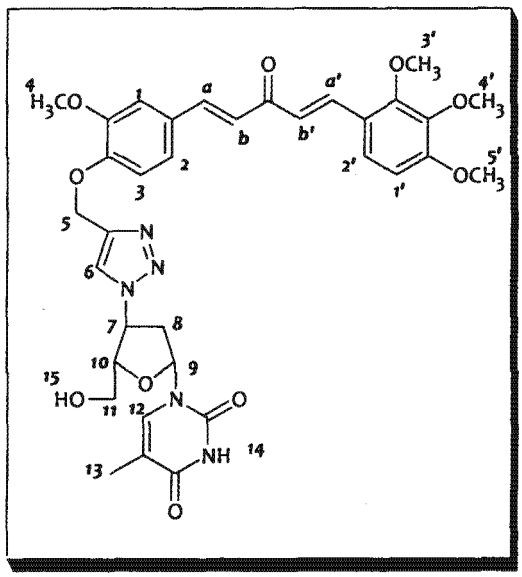

Yellow solid (263 mg, 40%); mp 144 - 146°C (from MeOH/EtOAc); R_f (MeOH:EtOAc 5:95) 0.33; IR ν_{max} (KBr)/cm^{-1} 3391 (O-H), 2934 (Ar C-H), 1689 (C=O), 1584 (Ar C=C); δ_H (300 MHz, DMSO-d_6) 11.21 (1H, s, H-14), 8.38 (1H, s, H-6), 7.79 (1H, d, *J* 16.0, H-a'), 7.78 (1H, s, H-12), 7.69 (1H, d, *J* 16.0, H-a), 7.56 (1H, d, *J* 8.8, H-2'), 7.40 (1H, d, *J* 1.8 H-1), 7.32 (1H, dd, *J* 1.8 and 8.4, H-2), 7.24 (1H, d, *J* 16.0, H-b'), 7.23 (1H, d, *J* 8.4, H-3), 7.14 (1H, d, *J* 16.1, H-b), 6.91 (1H, d, *J* 8.9, H-1'), 6.42 (1H, t, *J* 6.6, H-9), 5.43 - 5.37 (1H, m, H-7), 5.22 (2H, s, H-5), 4.28 – 4.24 (1H, m, H-10), 3.87 (6H, s, H-3', 5'), 3.84 (3H, s, H-4'), 3.79 (3H, s, H-4), 3.76 – 3.64 (2H, m, H-11), 2.82 – 2.63 (2H, m, H-8), 1.82 (3H, s, H-13); δ_C (75 MHz, DMSO-d_6) 187.9, 163.4, 155.3, 152.7, 150.2, 149.6, 149.2, 142.5, 142.3, 141.8, 136.5, 135.9, 128.1, 124.7, 124.2, 124.1, 122.9, 122.6, 120.9, 113.6, 111.2, 109.4, 108.4, 84.3, 83.9, 61.7, 61.1, 60.6, 60.2, 59.2, 55.9, 55.5, 36.9, 11.9; LRMS (EI) m/z 676.5 (M + H) M^+ $C_{34}H_{37}N_5O_{10}$ requires 675.3; Anal.Calcd. for $C_{34}H_{37}N_5O_{10}.1½H_2O$ - C 58.0%, H 5.7%, N 9.9%; found C 57.5%, H 5.7%, N 9.5%.

1-[4-(4-{4-[5-(2,4-Dichloro-phenyl)-3-oxo-penta-1,4-dienyl]-2-methoxy-phenoxymethyl}-[1,2,3] triazol-1-yl)-5-hydroxymethyl-tetrahydro-furan-2-yl]-5-methyl-1H-pyrimidine-2,4-dione, 3.20d

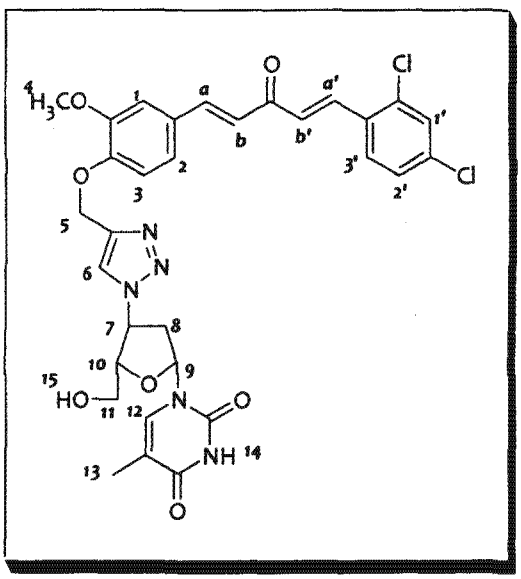

Yellow solid (379 mg, 58%); mp 239 - 241°C (from MeOH/EtOAc); R_f (MeOH:EtOAc 5:95) 0.50; IR ν_{max} (KBr)/cm^{-1} 3442(O-H), 3057(Ar C-H), 1692 (C=O), 1580 (Ar C=C); δ_H (400 MHz, DMSO-d_6) 11.31 (1H, s, H-14), 8.43 (1H, s, H-6), 8.07 (1H, d, *J* 8.6, H-3'), 7.86 (1H, d, *J* 15.8, H-a'), 7.84 (1H, d, *J* 16.1, H-a), 7.81 (1H, s, H-12), 7.74 (1H, d, *J* 2.1, H-1), 7.55 (1H, d, *J* 15.5, H-b'), 7.54 (1H, dd, *J* 2.1 and 8.5, H-2), 7.41 (1H, d, *J* 1.7, H-1'), 7.33 (1H, dd, *J* 1.7 and 8.5, H-2'), 7.26 (1H, d, *J* 8.4, H-3), 7.13 (1H, d, *J* 16.1, H-b), 6.43 (1H, t, *J* 6.6, H-9), 5.43 - 5.38 (1H, m, H-7), 5.22 (2H, s, H-5), 4.26 – 4.23 (1H, m, H-10), 3.82 (3H, s, H-4), 3.78 – 3.61 (2H, m, H-11), 2.79 – 2.63 (2H, m, H-8), 1.81 (3H, s, H-13); δ_C (100 MHz, DMSO-d_6) 187.9, 164.6, 163.6, 150.4, 149.9, 149.2, 145.4, 144.1, 142.5, 140.9, 136.1, 134.8, 131.8, 131.6, 129.5, 128.0, 126.9, 124.5, 123.1, 114.7, 110.9, 109.5, 100.8, 84.4, 83.9, 61.6, 60.7, 59.3, 55.5, 37.1, 12.1; LRMS (EI) m/z 654.6 (M + H) M$^+$ $C_{31}H_{29}Cl_2N_5O_7$ requires 653.1; Anal.Calcd. for $C_{31}H_{29}Cl_2N_5O_7.½H_2O$ - C 56.1%, H 4.5%, N 10.6%; found C 56.0%, H 4.6%, N 10.7%.

1-[4-(4-[4-[5-(4-Fluoro-phenyl)-3-oxo-penta-1,4-dienyl]-2-methoxy-phenoxymethyl]-[1,2,3]-triazol-1-yl)-5-hydroxymethyl-tetrahydro-furan-2-yl]-5-methyl-1H-pyrimidine-2,4-dione, 3.20e

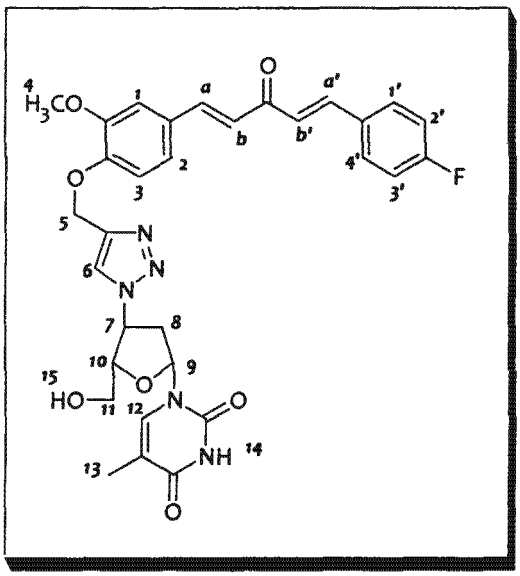

Yellow solid (193 mg, 32%); mp °C (from MeOH/EtOAc); R_f (MeOH:EtOAc 5:95) 0.50; IR ν_{max} (KBr)/cm^{-1} 3387 (O-H), 3010 (Ar C-H), 1688 (C=O), 1602 (Ar C=C); δ_H (400 MHz, DMSO-d_6) 11.30 (1H, s, H-14), 8.43 (1H, s, H-6), 7.86 (1H, d, *J* 8.9, H-1'), 7.85 (1H, d, *J* 8.8, H-4'), 7.81 (1H, s, H-12), 7.75 (1H, d, *J* 16.0, H-a'), 7.72 (1H, d, *J* 16.0, H-a), 7.41 (1H, d, *J* 1.9, H-1), 7.34 (1H, dd, *J* 1.9 and 8.5, H-2), 7.32 (1H, d, *J* 16.1, H-b'), 7.30 (1H, d, *J* 8.9, H-2'), 7.29 (1H, d, *J* 8.9, H-3'), 7.25 (1H, d, *J* 8.4, H-3), 7,20 (1H, d, *J* 16.0, H-b), 6.43 (1H, t, *J* 6.5, H-9), 5.42 - 5.38 (1H, m, H-7), 5.21 (2H, s, H-5), 4.26 – 4.22 (1H, m, H-10), 3.83 (3H, s, H-4), 3.77 – 3.61 (2H, m, H-11), 2.78 – 2.63 (2H, m, H-8), 1.81 (3H, s, H-13); δ_C (100 MHz, DMSO-d_6 188.2, 163.6, 150.4, 149.8, 149.2, 145.4, 144.1, 143.1, 142.5, 137.6, 136.1, 131.4, 130.6, 127.9, 125.4, 124.4, 124.0, 122.9, 116.0, 113.2, 110.9, 109.5, 84.4, 83.9, 67.8, 61.6, 60.7, 59.3, 55.5, 37.1, 12.1; LRMS (EI) m/z 604.4 (M + H) M$^+$ $C_{31}H_{30}FN_5O_7$ requires 603.2; Anal.Calcd. for $C_{31}H_{30}FN_5O_7$ - C 61.7%, H 5.0%, N 11.6%; found C 61.4%, H 5.2%, N 11.5%.

1-[4-(4-[4-[5-(2,4-Difluoro-phenyl)-3-oxo-penta-1,4-dienyl]-2-methoxy-phenoxymethyl]-[1,2,3]-triazol-1-yl)-5-hydroxymethyl-tetrahydro-furan-2-yl]-5-methyl-1H-pyrimidine-2,4-dione, 3.20f

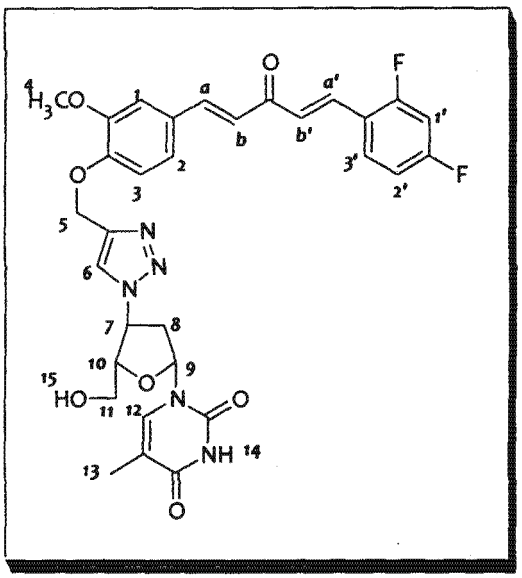

Yellow solid (191 mg, 31%); mp 197 - 199°C (from MeOH/EtOAc); R_f (MeOH:EtOAc 5:95) 0.50; IR ν_{max} (KBr)/cm^{-1} 3434 (O-H), 3065 (Ar C-H), 1696 (C=O), 1609 (Ar C=C); δ_H (400 MHz, DMSO-d_6) 11.31 (1H, s, H-14), 8.43 (1H, s, H-6), 8.02 (1H, d, *J* 8.7, H-3'), 7.81 (1H, s, H-12), 7.77 (1H, d, *J* 16.0, H-a'), 7.70 (1H, d, *J* 16.1, H-a), 7.43 (1H, d, *J* 1.9, H-1), 7.42 (1H, d, *J* 16.1, H-b'), 7.37 (1H, d, *J* 2.1, H-1'), 7.35 (1H, dd, *J* 1.9 and 8.4, H-2), 7.25 (1H, d, *J* 8.5, H-3), 7.21 (1H, dd, *J* 2.1 and 8.5, H-2'), 7.19 (1H, d, *J* 16.1, H-b), 6.43 (1H, t, *J* 6.6, H-9), 5.42 - 5.38 (1H, m, H-7), 5.21 (2H, s, H-5), 4.26 – 4.22 (1H, m, H-10), 3.82 (3H, s, H-4), 3.77 – 3.61 (2H, m, H-11), 2.78 – 2.63 (2H, m, H-8), 1.81 (3H, s, H-13); δ_C (100 MHz, DMSO-d_6) 188.1, 163.6, 153.2, 150.4, 149.9, 149.2, 143.6, 140.9, 139.7, 136.1, 132.7, 130.8, 127.9, 127.4, 124.5, 124.2, 123.1, 113.2, 112.6, 112.4, 110.9, 109.5, 104.6, 84.4, 83.9, 61.6, 60.7, 59.3, 55.5, 37.1, 12.1; LRMS (EI) m/z 622.3 (M + H) M$^+$ $C_{31}H_{29}F_2N_5O_7$ requires 621.2; Anal.Calcd. for $C_{31}H_{29}F_2N_5O_7.½H_2O$ - C 59.0%, H 4.8%, N 11.1%; found C 59.2%, H 5.0%, N 11.3%.

1-[4-[1-(7-Chloro-quinolin-4-yl)-1H-[1,2,3]triazol-4-ylmethoxy]-3-methoxy-phenyl]-5-(4-methoxy-phenyl)-penta-1,4-dien-3-one, 3.21a

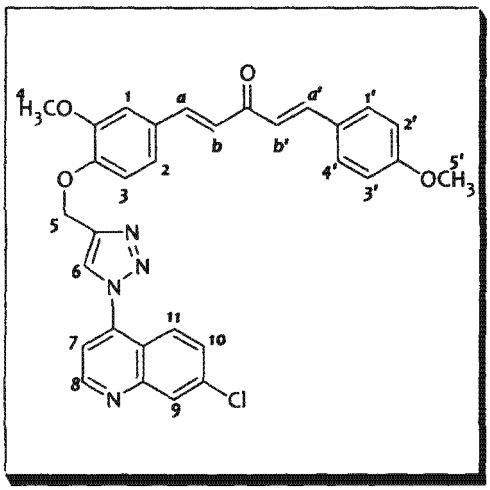

Yellow solid (199 mg, 36%); mp: 173 - 175°C (from EtOAc); R_f (EtOAc:Hex 7.3) 0.50; IR ν_{max} (KBr)/cm^{-1} 3036 (Ar C-H), 1642 (C=O), 1580 (Ar C=C); δ_H (400 MHz, $CDCl_3$) 9.08 (1H, d, *J* 4.6, H-8), 8.27 (1H, d, *J* 2.0, H-9), 8.13 (1H, s, H-6), 7.96 (1H, d, *J* 9.1, H-11), 7.71 (1H, d, *J* 15.6, H-a'), 7.68 (1H, d, *J* 15.8, H-a), 7.60 (1H, dd, *J* 2.0 and 9.1, H-10), 7.58 (2H, d, *J* 8.8, H-1', 4'), 7.51 (1H, d, *J* 4.6, H-7), 7.23 (1H, dd, *J*

1.8 and 8.3, H-2), 7.19 (1H, d, *J* 1.7, H-1), 7.16 (1H, d, *J* 8.1, H-3), 6.97 (1H, d, *J* 15.8 H-b'), 6.96 (1H, d, *J* 15.8, H-b), 6.95 (2H, dd, *J* 2.1 and 8.8, H-2', 3'), 5.50 (2H, s, H-5), 3.96 (3H, s, H-5'), 3.87 (3H, s, H-4); δ_C (100 MHz, $CDCl_3$) 161.7, 151.4, 150.3, 147.3, 144.8, 142.9, 142.5, 137.0, 136.8, 130.1, 129.5, 129.1, 128.6, 124.8, 124.5 (2C), 124.2, 123.2, 122.8, 122.6, 120.6, 116.1, 114.5, 114.0, 113.6, 111.3, 110.8, 110.4, 62.9, 56.0, 55.4; LRMS (EI) m/z 553.2 (M + H) M^+ $C_{31}H_{25}ClN_4O_4$ requires 552.1; Anal. Calcd. for $C_{31}H_{25}ClN_4O_4.1H_2O$ - C 65.1%, H 4.7%, N 9.8%; found C 64.9%, H 4.7%, N 9.4%.

1-[4-[1-(7-Chloro-quinolin-4-yl)-1H-[1,2,3]triazol-4-ylmethoxy]-3-methoxy-phenyl]-5-(2,4-dimethoxy-phenyl)-penta-1,4-dien-3-one, 3.21b

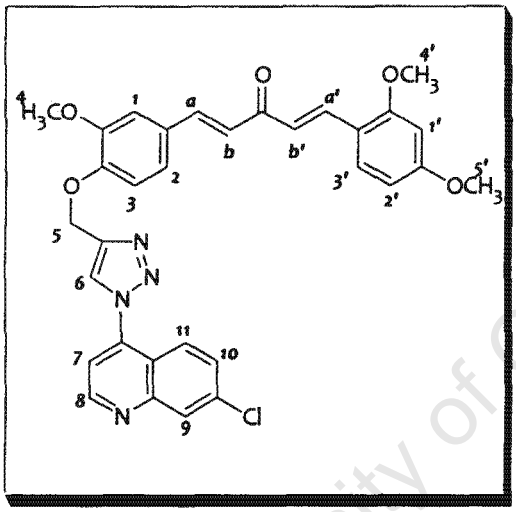

Yellow solid (192 mg, 33%); mp: 103 - 105°C (from EtOAc); R_f (EtOAc:Hex 8:2) 0.30; IR ν_{max} (KBr)/cm^{-1} 3079(Ar C-H), 1656(C=O), 1602 (Ar C=C); δ_H (300 MHz, $CDCl_3$) 9.07 (1H, d, *J* 4.6, H-8), 8.24 (1H, d, *J* 1.9, H-9), 8.14 (1H, s, H-6), 7.99 (1H, d, *J* 16.0, H-a'), 7.96 (1H, d, *J* 8.9, H-11), 7.65 (1H, d, *J* 15.8, H-a), 7.60 (1H, dd, *J* 2.1 and 9.1, H-10), 7.55 (1H, d, *J* 8.6, H-3'), 7.49 (1H, d, *J* 4.6, H-7), 7.21 (1H, dd, *J* 1.9 and 8.3, H-2), 7.16 (1H, d, *J* 1.9, H-1), 7.14 (1H, d, *J* 8.3, H-3), 7.05 (1H, d, *J* 16.0 H-b'), 6.98 (1H, d, *J* 15.8, H-b), 6.52 (1H, dd, *J* 2.3 and 8.6, H-2'), 6.47 (1H, d, *J* 2.3, H-1'), 5.49 (2H, s, H-5), 3.94 (3H, s, H-4'), 3.89 (3H, s, H-5'), 3.85 (3H, s, H-4); δ_C (75 MHz, $CDCl_3$) 183.9, 151.4, 142.0, 138.7, 137.1, 134.2, 132.6, 131.1, 130.4, 129.5, 129.1, 127.3, 124.8, 124.6, 123.9, 122.4, 120.6, 117.1, 116.5, 116.1, 114.8, 114.0, 112.8, 110.9, 109.6, 105.6, 103.6, 98.5, 63.0, 56.0, 55.6, 55.5; LRMS (EI) m/z 583.4 (M + H) M^+ $C_{32}H_{27}ClN_4O_5$ requires 582.2; Anal. Calcd. for $C_{32}H_{27}ClN_4O_5.1½H_2O$ - C 63.0%, H 4.9%, N 9.2%; found C 62.9%, H 4.9%, N 9.8%.

1-[4-[1-(7-Chloro-quinolin-4-yl)-1H-[1,2,3]triazol-4-ylmethoxy]-3-methoxy-phenyl]-5-(2,3,4-trimethoxy-phenyl)-penta-1,4-dien-3-one, 3.21c

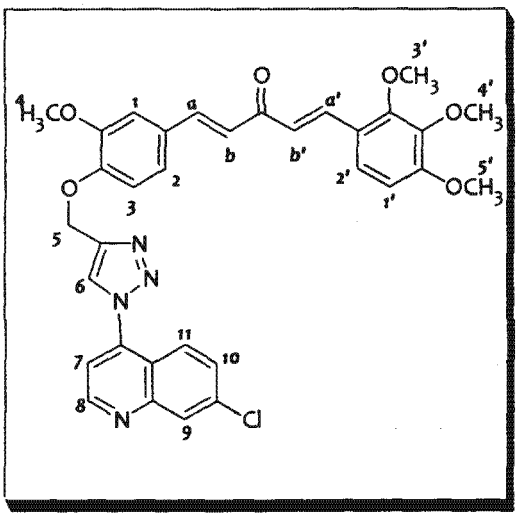

Yellow solid (202 mg, 33%); mp: 96 - 98°C (from EtOAc); R_f (EtOAc:Hex 8:2) 0.30; IR ν_{max} (KBr)/cm^{-1} 3086(Ar C-H), 1660 (C=O), 1588 (Ar C=C); δ_H (400 MHz, $CDCl_3$) 9.08 (1H, d, *J* 4.6, H-8), 8.27 (1H, d, *J* 1.9, H-9), 8.16 (1H, s, H-6), 7.99-7.93 (2H, m, H-11, a'), 7.66 (1H, d, *J* 15.8, H-a), 7.62 (1H, dd, *J* 2.0 and 9.1, H-10), 7.51 (1H, d, *J* 4.6, H-7), 7.38 (1H, d, *J* 8.8, H-2'), 7.23 (1H, dd, *J* 1.7 and 8.3, H-2), 7.18-7.16 (2H, m, H-1, 3), 7.09 (1H, d, *J* 16.0, H-b'), 6.97 (1H, d, *J* 15.9 H-b), 6.72 (1H, d, *J* 8.8, H-1'), 5.51 (2H, s, H-5), 3.97 (3H, s, H-3'), 3.96 (3H, s, H-5'), 3.92 (3H, s, H-4'), 3.90 (3H, s, H-4); δ_C (100 MHz, $CDCl_3$) 189.1, 151.4, 150.3, 149.9, 149.5, 144.8, 142.4, 140.9, 138.3, 129.5, 129.3, 129.1, 125.9, 124.9, 124.8, 124.5, 124.4, 123.5, 122.5, 121.9, 120.9, 116.1, 114.1, 111.6, 110.9, 110.5, 109.4, 107.7, 62.9, 61.5, 60.9, 56.1, 56.0; LRMS (EI) m/z 613.3 (M + H) M^+ $C_{33}H_{29}ClN_4O_6$ requires 612.2; Anal. Calcd. for $C_{33}H_{29}ClN_4O_6.1H_2O$ - C 62.7%, H 4.9%, N 8.9%; found C 62.5%, H 4.9%, N 9.4%.

1-[4-[1-(7-Chloro-quinolin-4-yl)-1H-[1,2,3]triazol-4-ylmethoxy]-3-methoxy-phenyl]-5-(2,4-dichloro-phenyl)-penta-1,4-dien-3-one, 3.21d

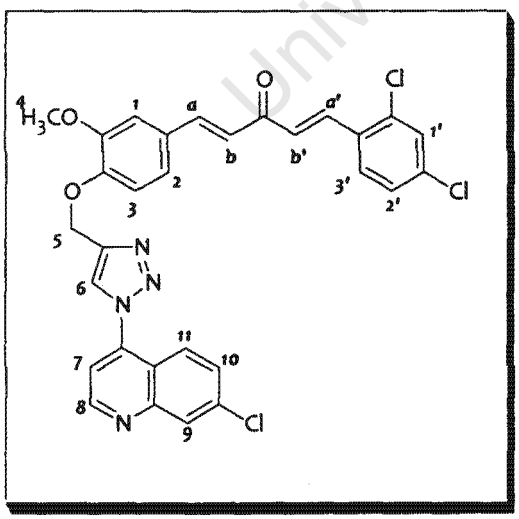

Yellow solid (248 mg, 42%); mp: 159 - 161°C (from EtOAc); R_f (EtOAc:Hex 8:2) 0.33; IR ν_{max} (KBr)/cm^{-1} 3050 (Ar C-H), 1653 (C=O), 1584 (Ar C=C); δ_H (400 MHz, $CDCl_3$) 9.08 (1H, d, *J* 4.6, H-8), 8.26 (1H, d, *J* 2.1, H-9), 8.16 (1H, s, H-6), 8.04 (1H, d, *J* 16.0, H-a'), 7.98 (1H, d, *J* 9.1, H-11), 7.71 (1H, d, *J* 15.9, H-a), 7.66 (1H, d, *J* 8.5, H-3'), 7.61 (1H, dd, *J* 2.1 and 9.1, H-10), 7.51 (1H, d, *J* 4.6, H-7), 7.48 (1H, d, *J* 2.0, H-1), 7.30 (1H, dd, *J* 2.1 and 8.5, H-2), 7.25 (1H, dd, *J* 1.9 and 8.4, H-2'), 7.20-7.18 (2H, m, H-1', 3), 7.04 (1H, d, *J* 15.9, H-b'), 6.98 (1H, d, *J* 15.9, H-b), 5.51 (2H, s, H-5), 3.96 (3H, s, H-4); δ_C (100 MHz, $CDCl_3$) 188.3, 154.9, 153.2, 151.4, 150.3,

149.9, 144.7, 143.6, 140.9, 138.6, 137.5, 137.0, 136.4, 135.9, 131.8, 130.1, 129.5, 129.1, 128.4, 128.2 127.6, 124.8, 124.4, 123.8, 122.8, 120.6, 116.1, 110.9, 62.9, 56.1; LRMS (EI) m/z 591.1 (M + H) M^+ $C_{30}H_{21}Cl_3N_4O_3$ requires 590.1; Anal. Calcd. for $C_{30}H_{21}Cl_3N_4O_3$. - C 60.9%, H 3.6%, N 9.5%; found C 60.4%, H 3.7%, N 9.5%.

1-{4-[1-(7-Chloro-quinolin-4-yl)-1H-[1,2,3]triazol-4-ylmethoxy]-3-methoxy-phenyl}-5-(4-fluoro-phenyl)-penta-1,4-dien-3-one, 3.21e

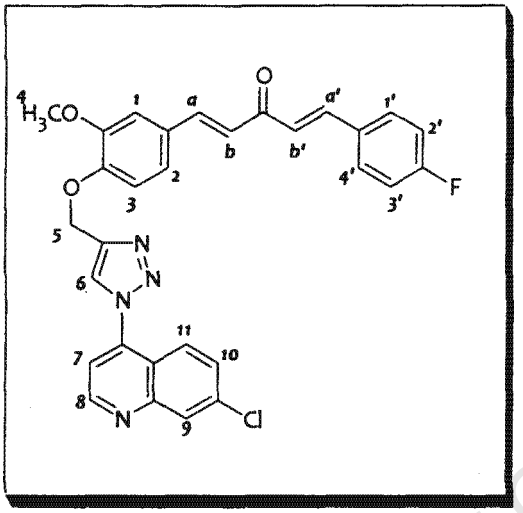

Yellow solid (206 mg, 38%); mp: 107 - 109°C (from EtOAc); R_f (EtOAc:Hex 7.3) 0.30; IR ν_{max} (KBr)/cm^{-1} 3036 (Ar C-H), 1653 (C=O), 1588 (Ar C=C); δ_H (400 MHz, $CDCl_3$) 9.08 (1H, d, *J* 4.6, H-8), 8.26 (1H, d, *J* 2.1, H-9), 8.16 (1H, s, H-6), 7.97 (1H, d, *J* 9.1, H-11), 7.78 (1H, d, *J* 16.1, H-a'), 7.70 (1H, d, *J* 15.9, H-a), 7.64 (1H, d, *J* 8.5, H-1'), 7.62 (1H, d, *J* 8.5, H-4'), 7.60 (1H, dd, *J* 2.2 and 9.1, H-10), 7.50 (1H, d, *J* 4.6, H-7), 7.24 (1H, dd, *J* 1.8 and 8.5, H-2), 7.18-7.16 (2H, m, H-1, 3), 7.14 (1H, d, *J* 16.1 H-b'), 6.95 (1H, d, *J* 15.9, H-b), 6.91 (1H, dd, *J* 2.1 and 8.6, H-2'), 6.88 (1H, dd, *J* 2.5 and 8.5, H-3'), 5.50 (2H, s, H-5), 3.95 (3H, s, H-4); δ_C (100 MHz, $CDCl_3$) 188.5, 151.4, 150.3, 149.9, 144.7, 143.4, 140.9, 138.5, 137.0, 135.3, 134.7, 130.7, 129.5, 129.1, 127.2, 124.8, 124.5, 124.2, 122.9, 120.6, 116.0, 113.9, 112.3, 112.1, 110.8, 104.9, 104.7, 104.5, 62.9, 56.0 ; LRMS (EI) m/z 541.4 (M + H) M^+ $C_{30}H_{22}ClFN_4O_3$ requires 540.1; Anal. Calcd. for $C_{30}H_{22}ClFN_4O_3.½H_2O$ - C 65.5%, H 4.2%, N 10.2%; found C 65.9%, H 4.2%, N 10.0%.

1-[4-[1-(7-Chloro-quinolin-4-yl)-1H-[1,2,3]triazol-4-ylmethoxy]-3-methoxy-phenyl]-5-(2,4-difluoro-phenyl)-penta-1,4-dien-3-one, 3.21f

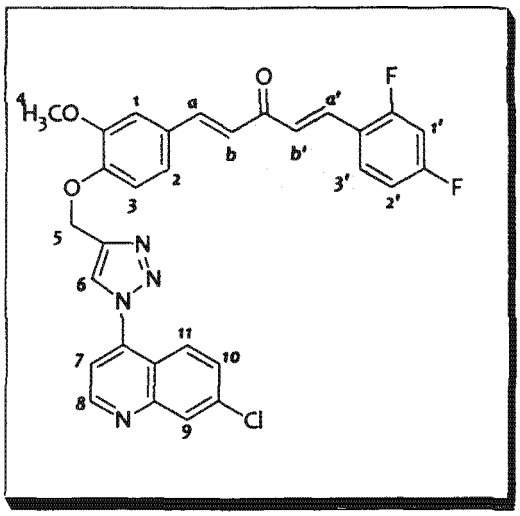

Yellow solid (173 mg, 31%); mp: 124 - 126°C (from EtOAc); R_f (EtOAc:Hex 8:2) 0.30; IR ν_{max} (KBr)/cm^{-1} 3043 (Ar C-H), 1653 (C=O), 1580 (Ar C=C); δ_H (400 MHz, $CDCl_3$) 9.08 (1H, d, *J* 4.6, H-8), 8.26 (1H, d, *J* 2.1, H-9), 8.16 (1H, s, H-6), 7.97 (1H, d, *J* 9.1, H-11), 7.71 (1H, d, *J* 15.9, H-a'), 7.69 (1H, d, *J* 15.9, H-a), 7.62 (1H, d, *J* 8.5, H-3'), 7.60 (1H, dd, *J* 2.1 and 9.1, H-10), 7.50 (1H, d, *J* 4.6, H-7), 7.24 (1H, dd, *J* 1.9 and 8.3, H-2), 7.18 (1H, d, *J* 1.9, H-1), 7.17 (1H, d, *J* 8.3, H-3), 7.13 (1H, d, *J* 1.9, H-1'), 7.11 (1H, dd, *J* 1.8 and 8.5, H-2'), 7.03 (1H, d, *J* 15.9, H-b'), 6.95 (1H, d, *J* 15.9, H-b), 5.51 (2H, s, H-5), 3.95 (3H, s, H-4); δ_C (100 MHz, $CDCl_3$) 188.5, 151.4, 150.3, 149.9, 149.8, 146.5, 144.7, 143.7, 140.9, 137.0, 132.2, 131.1, 130.3, 129.5, 129.1, 125.0, 124.8, 124.5, 124.3, 122.8, 120.6, 118.6, 116.2, 116.0, 115.2, 114.0, 110.8, 105.9, 62.9, 56.0; LRMS (EI) m/z 559.3 (M + H) M^+ $C_{30}H_{21}ClF_2N_4O_3$ requires 558.1; Anal. Calcd. for $C_{30}H_{21}ClF_2N_4O_3$ - C 64.5%, H 3.5%, N 10.0%; found C 64.6%, H 3.7%, N 10.2%.

8.1.4.3:Experimental details pertaining to Chapter 5

General method V: synthesis of hydroxylated enones 5.1 and 5.3:

Vanillin or 4-hydroxybenzaldehyde (20 mmol) was dissolved in 30 mL acetone, and 5 mL of 5 M HCl was then added gradually to the stirring mixture. The reaction mixture was then stirred at room temperature for 24 hours.

The reaction mixture was then neutralized with 2.5 M NaOH, after which the acetone in the mixture was removed at reduced pressure. The remaining compound mixture was then taken up in 100 mL EtOAc, washed three times with water, dried over anhydrous Na_2SO_4, concentrated *in vacuo* and purified by column chromatography (EtOAc/Hex) to yield the pure target compound.

4-(4-Hydroxy-3-methoxy-phenyl)-but-3-en-2-one, 5.1

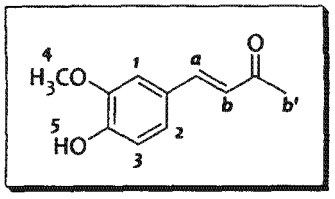

Pale yellow solid (3.2 g, 84%); mp 124 - 125°C (from EtOAc/Hex); R_f (EtOAc:Hex 4:6) 0.30; IR ν_{max} (KBr)/cm^{-1} 3261 (Ar O-H), 3000 (Ar C-H), 1668 (C=O), 1581 (Ar C=C); δ_H (400 MHz, $CDCl_3$) 7.46 (1H, d, *J* 16.2, H-a), 7.09 (1H, dd, *J* 1.9 and 8.2, H-2), 7.07 (1H, d, *J* 1.9, H-1), 6.94(1H, d, *J* 8.1, H-3), 6.60 (1H, d, *J* 16.2, H-b), 5.98 (1H, s, H-5), 3.95 (3H, s, H-4), 2.37 (3H, s, H-b'); δ_C (100 MHz, $CDCl_3$) 198.3, 150.4, 146.9, 143.5, 126.5, 125.0, 123.8, 114.9, 109.4, 55.8, 24.5; LRMS (EI) m/z 193.1 (M + H) M^+ $C_{11}H_{12}O_3$ requires 192.1; Anal. Calcd. for $C_{11}H_{12}O_3$ - C 68.7%, H 6.3%; found C 68.3%, H 6.1%.

4-(4-Hydroxy-phenyl)-but-3-en-2-one, 5.3

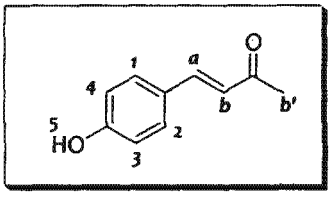

Dark yellow solid (2.4 g, 76%); mp 81 - 82°C (from EtOAc/Hex); R_f (EtOAc:Hex 4:6) 0.40; IR ν_{max} (KBr)/cm^{-1} 3150 (Ar C-H), 1666 (C=O), 1590 (Ar C=C); δ_H (400 MHz, $CDCl_3$) 7.50 (1H, d, *J* 16.2, H-a), 7.42 (2H, d, *J* 8.7, H-1, 2), 6.88 (2H, d, *J* 8.7, H-3, 4), 6.58 (1H, d, *J* 16.2, H-b), 2.35 (3H, s, H-b'); δ_C (100 MHz, $CDCl_3$) 200.0, 159.1, 144.8, 130.4 (2C), 126.5, 124.3 (2C), 116.2, 27.2; LRMS (EI) m/z 163.3 (M + H) M^+ $C_{10}H_{10}O_2$ requires 162.1; Anal. Calcd. for $C_{10}H_{10}O_2$ - C 74.1%, H 6.2%; found C 74.6%, H 6.0%.

General method VI: synthesis of hydroxylated chalcones 5.2 and 5.4:

Vanillin or 4-hydroxybenzaldehyde (20 mmol) and 2,4-dimethoxyacetophenone (4.0 g, 22 mmol) were dissolved in 20 mL MeOH. 5 mL of 5 M HCl was then added gradually to the stirring mixture. The reaction mixture was then stirred at 50°C for 24 hours.

The reaction mixture was then allowed to cool to ambient temperature and neutralized with 2.5 M NaOH, after which the MeOH in the mixture was removed under reduced pressure. The remaining compound mixture was then taken up in 100 mL EtOAc, washed three times with water, dried over anhydrous Na_2SO_4, concentrated *in vacuo* and purified by column chromatography (EtOAc/Hex) to yield the pure target compound.

1-(2,4-Dimethoxy-phenyl)-3-(4-hydroxy-3-methoxy-phenyl)-propenone, 5.2

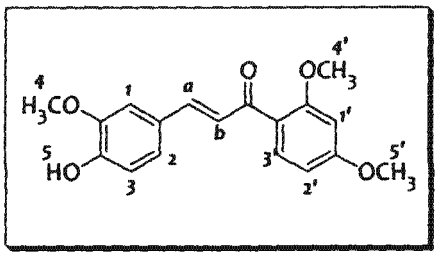

Yellow solid (4.3 g, 68%); mp 92 - 94°C (from EtOAc/Hex); R_f (EtOAc:Hex 4:6) 0.30; IR ν_{max} (KBr)/cm^{-1} 3506 (Ar O-H), 3113 (Ar C-H), 1640 (C=O), 1598 (Ar C=C); δ_H (400 MHz, $CDCl_3$) 7.74 (1H, d, *J* 8.6, H-3'), 7.61 (1H, d, *J* 15.7, H-a), 7.35 (1H, d, *J* 15.7, H-b), 7.17 (1H, dd, *J* 1.9 and 8.3, H-2), 7.10 (1H, d, *J* 1.9, H-1), 6.94 (1H, d, *J* 8.3, H-3), 6.58 (1H, dd, *J* 2.3 and 8.6, H-2'), 6.51 (1H, d, *J* 2.3, H-1'), 5.93 (1H, s, H-5), 3.94 (3H, s, H-4'), 3.91 (3H, s, H-5'), 3.88 (3H, s, H-4); δ_C (100 MHz, $CDCl_3$) 190.8, 163.9, 160.2, 147.8, 146.7, 142.6, 132.6, 128.0, 125.1, 122.8, 122.5, 114.8, 110.2, 105.1, 98.8, 55.9, 55.8, 55.5; LRMS (EI) m/z 314.0 M^+ $C_{18}H_{18}O_5$ requires 314.1; Anal. Calcd. for $C_{18}H_{18}O_5$. - C 68.8%, H 5.8%; found C 68.7%, H 5.9%.

1-(2,4-Dimethoxy-phenyl)-3-(4-hydroxy-phenyl)-propenone, 5.4

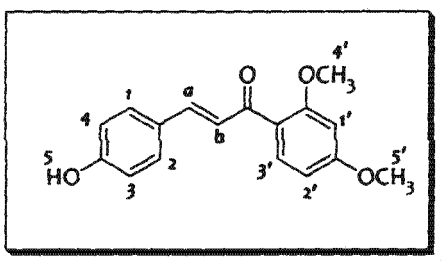

Yellow solid (3.2 g, 59%); mp 135 - 137°C (from EtOAc/Hex); R_f (EtOAc:Hex 4:6) 0.27; IR ν_{max} (KBr)/cm^{-1} 3204 (Ar O-H), 1635 (C=O), 1600(Ar C=C); δ_H (400 MHz, $CDCl_3$) 7.53 (2H, d, *J* 8.7, H-1, 2), 7.51 (1H, d, *J* 8.7, H-3'), 7.43 (1H, d, *J* 15.8, H-a), 7.28 (1H, d, *J* 15.7, H-b), 6.78 (2H, d, *J* 8.5, H-3, 4), 6.62 (1H, d, *J* 2.1, H-1'), 6.58 (1H, dd, *J* 2.0 and 8.6, H-2'), 3.83 (3H, s, H-4'), 3.79 (3H, s, H-5'); δ_C (100 MHz, $CDCl_3$) 189.9, 164.1, 160.4, 160.3, 142.4, 132.3, 130.8, 126.3, 124.3, 122.3, 116.4, 106.4, 99.2, 56.4, 56.0; LRMS (EI) m/z 284.0 M^+ $C_{17}H_{16}O_4$ requires 284.1; Anal. Calcd. for $C_{17}H_{16}O_4$ - C 71.8%, H 5.7%; found C 72.1%, H 5.9%.

2-(7-Chloro-quinolin-4-ylamino)-ethanol, 5.5

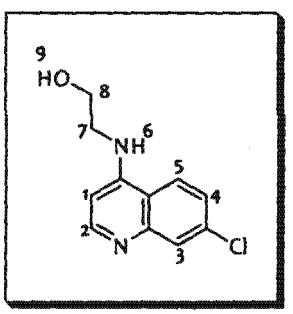

4,7-dichloroquinoline (2 g, 10mmol) was heated with stirring in neat ethanolamine (10 mL) at 130 °C for 5 hours. The mixture was then allowed to cool to room temperature, during which the product precipitated. This crude mixture was then suspended in water, filtered and crystallized from hot MeOH to yield pure 5.5 as a white solid (1.97 g, 89%). Mp 215-216°C (from MeOH) (lit. 214 °C) [1]. R*f* (MeOH/EtOAc, 1:9) 0.20; δ_H (400 MHz; DMSO-d_6) 8.41 (1H, d, *J* 5.4, H2), 8.30 (1H, d, *J* 9.0, H5), 7.81 (1H, d, *J* 2.2, H3), 7.46

(1H, dd, *J* 2.2 and 8.9, H4), 7.26 (1H, t, *J* 5.2, H-6), 6.52 (1H, d, *J* 5.5, H1), 4.85 (1H, s, H-9), 3.70 (2H, t, *J* 5.9, H8), 3.38 (2H, q, *J* 5.8, H7).

2-[4-(7-Chloro-quinolin-4-yl)-piperazin-1-yl]-ethanol, 5.6

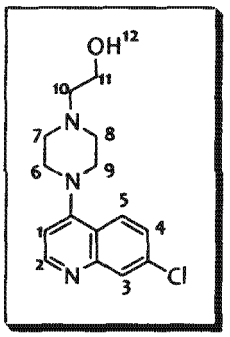

4,7-dichloroquinoline (2 g, 10mmol) was dissolved in 10 mL anhydrous DMF, after which K_2CO_3 (2.1 g, 15 mmol) and 1-(2-hydroxyethyl)piperazine (1.3 g, 10 mmol) were added. This reaction mixture was then stirred at 80 °C for 24 hrs, upon which TLC indicated completion of the reaction. The mixture was then diluted in 100 mL EtOAc, washed with water (2 x 30 mL), dried over anhydrous Na_2SO_4 and concentrated under reduced pressure. The resultant oily product crystallized on standing, and these crystals were washed with hexane and dried to yield 5.6 as pale yellow crystals (1.83 g, 63%). M.p. 111-112 °C (from EtOAc); R_f (MeOH/EtOAc, 1:9) 0.24; IR ν_{max} ($CHCl_3$)/cm^{-1} 3222 (O-H), 2903 (C-H), 1677 (C=O), 1569 (Ar C=C); δ_H (400 MHz, DMSO-*d*$_6$) 8.66 (1H, d, *J* 5.0, H-2), 7.99 (1H, d, *J* 9.0, H-5), 7.95 (1H, d, *J* 2.2, H-3), 7.51 (1H, dd, *J* 2.2 and 9.0, H-4), 6.96 (1H, d, *J* 5.1, H-1), 4.33 (1H, t, *J* 5.3, H-12), 3.55 (2H, q, *J* 6.0, H-11), 3.17 (4H, t, *J* 4.8, H-6, 9), 2.70 (4H, t, *J* 4.8, H-7, 8), 2.51 (2H, t, *J* 6.2, H-10); δ_C (100 MHz, $CDCl_3$) 156.2, 151.9, 149.6, 133.4, 127.9, 125.9, 125.5, 121.3, 109.1, 60.0, 58.5 (2C), 52.8 (2C), 51.7; LRMS (EI) m/z 290.5 (M - H) M^+ $C_{15}H_{18}ClN_3O$ requires 291.1; Anal. Calcd. for $C_{15}H_{18}ClN_3O$ - C 61.8%, H 6.2%, N 14.4%; found C 61.7%, H 6.1%, N 14.5%.

7-Chloro-4-piperazin-1-yl-quinoline, 5.7

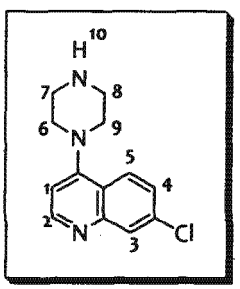

4,7-dichloroquinoline (2 g, 10mmol) was dissolved in 15 mL anhydrous NMP, after which K_2CO_3 (2.8 g, 20 mmol) and piperazine (5.2 g, 60 mmol) were added. This reaction mixture was then stirred at 135 °C for 4 hrs, upon which TLC indicated completion of the reaction. The mixture was then diluted in 100 mL EtOAc, washed with water (2 x 30 mL), dried over anhydrous Na_2SO_4, concentrated under reduced pressure and purified by column chromatography (NH_4OH/MeOH/EtOAC, 1:9:90) to yield 5.7 as an off-white solid (1.9 g, 78%). M.p. 111-113 °C (lit. 113 - 115 °C) [2]; δ_H (400 MHz, DMSO-*d*$_6$) 8.68 (1H, d, *J* 5.0, H-2), 8.01 (1H, d, *J* 9.0, H-3), 7.89 (1H, d, *J* 2.0, H-5), 7.52 (1H, dd, *J* 2.1 and 9.0, H-4), 6.95 (1H, d, *J*

5.0, H-1), 3.05 - 3.11 (4H, m, H-6, 9), 2.92 – 2.97 (4H, m, H-7, 8), 3.19 (1H, br s, H-10); δ_C (100 MHz, DMSO-d_6) 157.4, 152.6, 150.2, 133.9, 128.5, 126.6, 121.9, 109.7, 53.7 (2C), 45.9 (2C).

General method VII: synthesis of analogues 5.8 - 5.11:

Hydroxylated chloroquinoline intermediate 5.5 or 5.6 (1 eq.), enone 5.1 or chalcone 5.2 (1 eq.) and triphenylphosphine (1.2 eq.) were dissolved in anhydrous CH_2Cl_2 under a N_2 atmosphere. The solution was cooled to 0°C, and di-isopropyl azodicarboxylate (DIAD, 1.2 eq.) was added slowly over 5 min. The stirred reaction mixture was then allowed to warm to ambient temperature, and was further stirred for 6 hrs. The mixture was then concentrated under reduced pressure, and the target compound purified by silica column chromatography (5% MeOH in EtOAc).

4-[4-[2-(7-Chloro-quinolin-4-ylamino)-ethoxy]-3-methoxy-phenyl]-but-3-en-2-one, 5.8

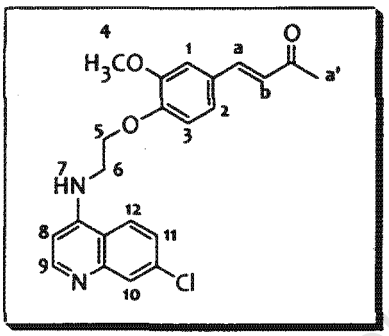

Yellow solid (289 mg, 73%); mp 143 - 144°C (from MeOH/EtOAc); R_f (MeOH/EtOAc 1:9) 0.23; IR ν_{max} (KBr)/cm^{-1} 3420 (N-H), 2972 (Ar C-H), 1686 (C=O), 1584 (Ar C=C); δ_H (400 MHz, $CDCl_3$) 8.57 (1H, d, *J* 5.3, H-9), 7.99 (1H, d, *J* 1.8, H-10), 7.76 (1H, d, *J* 8.9, H-12), 7.46 (1H, d, *J* 16.2, H-a), 7.39 (1H, dd, *J* 1.9 and 8.9, H-11), 7.13-7.11 (2H, m, H-1, 2), 6.98 (1H, d, *J* 8.0, H-3), 6.63 (1H, d, *J* 16.2, H-b), 6.49 (1H, d, *J* 5.3, H-8), 5.70 (1H, s, H-7), 4.39 (2H, t, H-5.0, H-5), 3.92 (3H, s, H-4), 3.73 (2H, q, *J* 5.0, H-6), 2.37 (3H, s, H-a'); δ_C (100 MHZ, $CDCl_3$) 198.2, 151.7, 150.1, 149.8, 148.9, 142.9, 135.1, 128.9, 125.9, 125.5, 122.6, 121.2, 117.4, 114.7, 110.5, 99.3, 67.7, 55.8, 42.3, 27.4, 21.9; LRMS (EI) m/z 395.3 (M - H) M$^+$ $C_{22}H_{21}ClN_2O_3$ requires 396.1; Anal. Calcd. for $C_{22}H_{21}ClN_2O_3$ - C 66.6%, H 5.3%, N 7.1%; found C 66.5%, H 5.6%, N 7.3%.

3-{4-[2-(7-Chloro-quinolin-4-ylamino)-ethoxy]-3-methoxy-phenyl}-1-(2,4-dimethoxy-phenyl)-propenone, 5.9

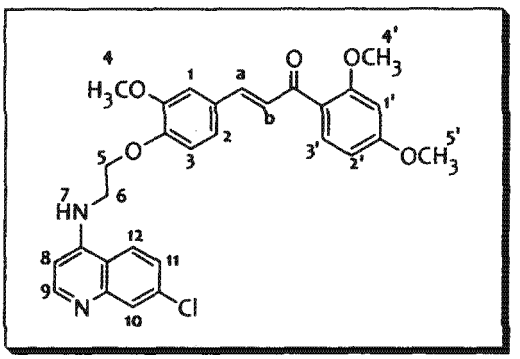

Pale yellow solid (310 mg, 60%); mp 164 - 166°C (from MeOH/EtOAc); R_f (MeOH: EtOAc 1:9) 0.27; IR ν_{max} (KBr)/cm^{-1} 3406 (N-H), 2942 (Ar C-H), 1646 (C=O), 1584 (Ar C=C); δ_H (400 MHz, $CDCl_3$) 8.57 (1H, d, *J* 5.3, H-9), 7.98 (1H, d, *J* 2.1, H-10), 7.78-7.74 (2H, m, H-3', 12), 7.61 (1H, d, *J* 15.7, H-a), 7.39 (1H, d, *J* 15.7, H-b), 7.38 (1H, dd, *J* 2.1 and 8.9, H-11), 7.17 (1H, dd, *J* 1.7 and 8.2, H-2), 7.14 (1H, d, *J* 1.7, H-1), 6.96 (1H, d, *J* 8.2, H-3), 6.57 (1H, dd, 2.2 and 8.6, H-2'), 6.52 (1H, d, *J* 2.2, H-1'), 6.48 (1H, d, *J* 5.3, H-8), 5.78 (1H, t, *J* 5.5, H-7), 4.39 (2H, t, *J* 5.2, H-5), 3.92 (3H, s, H-4'), 3.90 (3H, s, H-5'), 3.88 (3H, s, H-4), 3.72 (2H, q, *J* 5.2, H-6); δ_C (100 MHZ, $CDCl_3$) 190.5, 164.1, 160.3, 152.0, 150.1, 149.6, 149.4, 149.2, 141.8, 134.9, 132.7, 130.2, 128.9, 126.1, 125.4, 122.3, 122.2, 121.2, 117.5, 115.0, 111.2, 105.2, 99.3, 98.8, 67.8, 55.9, 55.7, 55.5, 42.3; LRMS (EI) m/z 517.1(M - H) M$^+$ $C_{29}H_{27}ClN_2O_5$ requires 518.2; Anal. Calcd. for $C_{29}H_{27}ClN_2O_5$ - C 67.1%, H 5.2%, N 5.4%; found C 66.8%, H 5.6%, N 5.3%.

4-(4-{2-[4-(7-Chloro-quinolin-4-yl)-piperazin-1-yl]-ethoxy}-3-methoxy-phenyl)-but-3-en-2-one, 5.10

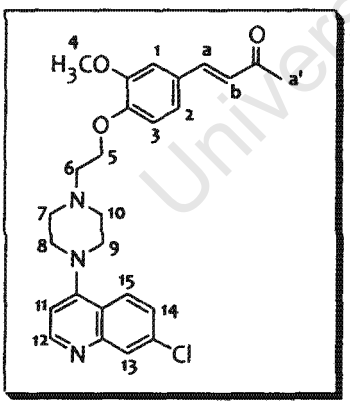

Pale yellow (316 mg, 68%); mp 61 - 62°C (from MeOH/EtOAc); R_f (MeOH/EtOAc 1:9) 0.26; IR ν_{max} (KBr)/cm$^-$ 2977 (Ar C-H), 1714 (C=O), 1594 (Ar C=C); δ_H (300 MHz, $CDCl_3$) 8.72 (1H, d, *J* 5.0, H-12), 8.04 (1H, d, *J* 2.0, H-13), 7.93 (1H, d, *J* 8.9, H-15), 7.46 (1H, d, *J* 16.1, H-a), 7.41 (1H, dd, *J* 2.2 and 9.0, H-14), 7.12 (1H, dd, *J* 1.9 and 8.3, H-2), 7.09 (1H, d, *J* 1.9, H-1), 6.92 (1H, d, *J* 8.2, H-3), 6.83 (1H, d, *J* 5.0, H-11), 6.61 (1H, d, *J* 16.1, H-b), 4.25 (2H, t, *J* 5.9, H-5), 3.90 (3H, s, H-4), 3.28-3.25 (4H, m, H-8, 9), 2.99 (2H, t, *J* 5.9, H-6), 2.91-2.88 (4H, m, H-7, 10), 2.36 (3H, s, H-a'); δ_C (75 MHZ, $CDCl_3$) 198.0, 156.9, 151.9, 150.5, 150.1, 149.7, 143.2, 134.8, 128.8, 127.8, 126.1, 125.4, 125.1, 122.7, 113.0, 110.3, 108.9, 67.0, 56.8, 55.9, 53.4, 52.9, 52.1, 27.3, 21.9; LRMS (EI) m/z 464.2 (M - H) M$^+$ $C_{26}H_{28}ClN_3O_3$ requires 465.2; Anal. Calcd. for $C_{26}H_{28}ClN_3O_3$ - C 67.0%, H 6.1%, N 9.0%; found C 66.7%, H 5.8%, N 9.3%.

3-(4-{2-[4-(7-Chloro-quinolin-4-yl)-piperazin-1-yl]-ethoxy}-3-methoxy-phenyl)-1-(2,4-dimethoxy-phenyl)-propenone, 5.11

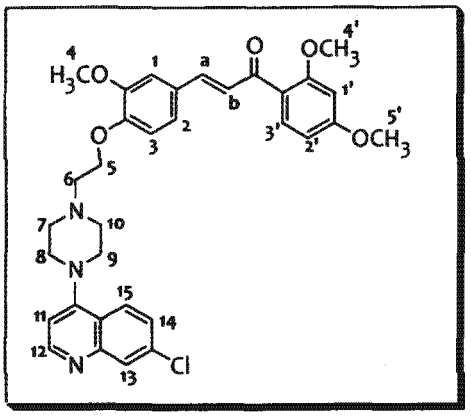

Yellow solid (435 mg, 74%); mp 62 - 63°C (from MeOH/EtOAc); R_f (MeOH/EtOAc 1:9) 0.30; IR ν_{max} (KBr)/cm^{-1} 2938 (C-H), 1648 (C=O), 1600 (Ar C=C); δ_H (300 MHz, $CDCl_3$) 8.66 (1H, d, *J* 5.0, H-12), 8.01 (1H, d, *J* 9.0, H-15), 7.95 (1H, d, *J* 2.1, H-13), 7.56 (1H, d, *J* 8.5, H-3'), 7.53 (1H, dd, *J* 2.3 and 9.0, H-14), 7.46 (1H, d, *J* 15.8, H-a), 7.37 (1H, d, *J* 15.8, H-b), 7.30 (1H, d, *J* 1.9, H-1), 7.23 (1H, dd, *J* 1.9 and 8.4, H-2), 7.05 (1H, d, *J* 8.4, H-3), 6.99 (1H, d, *J* 5.1, H-11), 6.67 (1H, d, *J* 2.2, H-1'), 6.62 (1H, dd, *J* 2.2 and 8.6, H-2'), 4.19 (2H, t, *J* 5.8 H-5), 3.87 (3H, s, H-4'), 3.84 (3H, s, H-5'), 3.83 (3H, s, H-4), 3.19 (4H, t, *J* 4.8, H-8, 9), 2.85 (2H, t, *J* 5.8, H-6), 2.79 (4H, t, *J* 4.8, H-7, 10); δ_C (75 MHZ, $CDCl_3$) 189.7, 163.5, 159.9, 156.2, 151.9, 150.1, 149.6, 149.2, 141.6, 133.4, 131.5, 127.9, 125.8, 125.5, 125.1, 122.3, 121.7, 121.2, 113.3, 111.4, 109.2, 105.8, 98.7, 65.6, 56.3, 55.8 (2C), 52.8 (2C), 51.7 (2C); LRMS (EI) m/z 586.0 (M - H) M^+ $C_{33}H_{34}ClN_3O_5$ requires 587.2; Anal. Calcd. for $C_{33}H_{34}ClN_3O_5$ - C 67.4%, H 5.8%, N 5.2%; found C 67.3%, H 5.9%, N 5.3%.

General method VIII: synthesis of analogues 5.12 – 5.15:

The appropriate hydroxylated chalcone or enone (5.1 – 5.4) (1 eq.) and the piperazinylquinoline intermediate, 5.7 (1 eq) were dissolved in EtOH. Formaldehyde (37% solution in water, 10 eq.) was then added to the stirring solution, which was then refluxed at 110°C for 12 hrs.

The reaction mixture was then allowed to cool to ambient temperature, after which it was concentrated under reduced pressure and purified by column chromatography (EtOAc) to yield the pure target compounds.

4-[3-[4-(7-Chloro-quinolin-4-yl)-piperazin-1-ylmethyl]-4-hydroxy-5-methoxy-phenyl]-but-3-en-2-one, 5.12

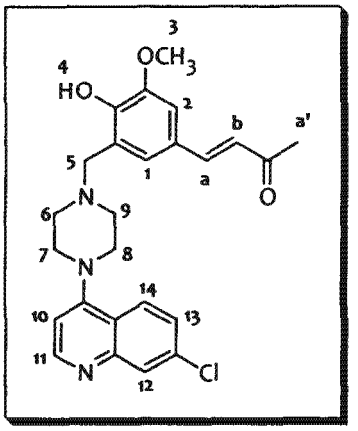

Yellow solid (58%); mp 91 - 92 °C (from EtOAc); R_f (EtOAc) 0.15; IR ν_{max} (KBr)/cm^{-1} 2943 (C-H), 1662 (C=O), 1575 (Ar C=C); δ_H (300 MHz, $CDCl_3$) 8.73 (1H, d, *J* 5.0, H-11), 8.06 (1H, d, *J* 2.1, H-12), 7.89 (1H, d, *J* 9.0, H-14), 7.43 (1H, d, *J* 16.1, H-a), 7.40 (1H, dd, *J* 2.1 and 9.0, H-13), 7.03 (1H, d, *J* 1.5, H-2), 6.91 (1H, d, *J* 1.5, H-1), 6.82 (1H, d, *J* 5.0, H-10), 6.58 (1H, d, *J* 16.1, H-b), 3.91 (3H, s, H-3), 3.89 (2H, s, H-5), 3.28 – 3.34 (4H, m, H-7, 8), 2.90 – 2.96 (4H, m, H-6, 9), 2.35 (3H, s, H-a'); δ_C (75 MHz, $CDCl_3$) 198.1, 156.4, 151.6, 149.9, 149.6, 148.4, 143.5, 135.2, 128.8, 126.5, 125.8, 124.9, 124.8, 122.5, 121.7, 120.9, 110.1, 109.1, 60.7, 55.9, 52.4 (2C), 51.9 (2C), 27.4; LRMS (EI) m/z 450.7 (M - H) M^+ $C_{25}H_{26}ClN_3O_3$ requires 451.9; Anal. Calcd. for $C_{25}H_{26}ClN_3O_3.H_2O$ - C 63.8%, H 6.0%, N 8.9%; found C 64.0%, H 6.2%, N 8.7%.

3-[3-[4-(7-Chloro-quinolin-4-yl)-piperazin-1-ylmethyl]-4-hydroxy-5-methoxy-phenyl]-1-(2,4-dimethoxy-phenyl)-propenone, 5.13

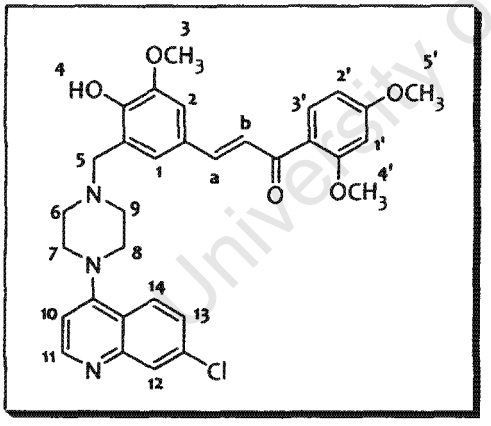

Deep yellow solid (66%); mp 95 - 97°C (from EtOAc); R_f (EtOAc) 0.20; IR ν_{max} (KBr)/cm^{-1} 2938 (C-H), 1648 (C=O), 1597 (Ar C=C); δ_H (400 MHz, $CDCl_3$) 8.71 (1H, d, *J* 5.1, H-11), 8.10 (1H, d, *J* 1.9, H-12), 7.89 (1H, d, *J* 9.0, H-14), 7.72 (1H, d, *J* 8.6, H-3'), 7.58 (1H, d, *J* 15.8, H-a), 7.44 (1H, dd, *J* 1.9 and 8.9, H-13), 7.33 (1H, d, *J* 15.7, H-b), 7.09 (1H, d, *J* 1.8, H-2), 6.97 (1H, d, *J* 1.8, H-1), 6.84 (1H, d, *J* 5.1, H-10), 6.57 (1H, dd, *J* 1.7 and 8.6, H-2'), 6.51 (1H, d, *J* 1.8, H-1'), 3.92 (3H, s, H-4'), 3.91 (5H, s, H-5, 5'), 3.87 (3H, s, H-3), 3.32 – 3.55 (4H, m, H-7, 8), 2.90 – 2.96 (4H, m, H-6, 9); δ_C (100 MHz, $CDCl_3$) 190.9, 163.9, 160.3, 156.7, 151.2, 149.4, 149.2, 148.3, 142.5, 135.5, 132.6, 128.4, 126.6, 124.9, 124.8, 122.7, 122.6, 121.6, 120.7, 110.8, 110.5, 109.0, 105.2, 98.8, 60.6, 56.0, 55.8, 55.5, 52.3 (2C), 51.8 (2C); LRMS (EI) m/z 572.7 (M - H) M^+ $C_{32}H_{32}ClN_3O_5$ requires 573.2; Anal. Calcd. for $C_{32}H_{32}ClN_3O_5.H_2O$ - C 64.8%, H 5.7%, N 7.1%; found C 64.4%, H 6.0%, N 6.7%.

4-[3-[4-(7-Chloro-quinolin-4-yl)-piperazin-1-ylmethyl]-4-hydroxy-phenyl]-but-3-en-2-one, 5.14

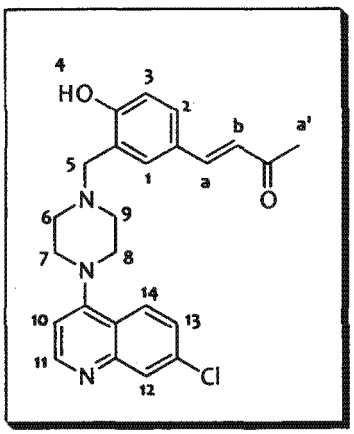

Pale yellow solid (45%); mp 83 - 85 °C (from EtOAc); R_f (EtOAc) 0.35; IR ν_{max} (KBr)/cm^{-1} 2823 (C-H), 1663 (C=O), 1578 (Ar C=C); δ_H (300 MHz, $CDCl_3$) 8.71 (1H, d, *J* 5.1, H-11), 8.07 (1H, d, *J* 2.1, H-12), 7.89 (1H, d, *J* 9.0, H-14), 7.44 (1H, d, *J* 16.4, H-a), 7.43 (1H, dd, *J* 2.1 and 9.0, H-13), 7.41 (1H, dd, *J* 2.3 and 8.4, H-2), 7.30 (1H, d, *J* 2.3, H-1), 6.86 (1H, d, *J* 8.4, H-3), 6.85 (1H, d, *J* 5.1, H-10), 6.58 (1H, d, *J* 16.3, H-b), 3.88 (2H, s, H-5), 3.28 – 3.35 (4H, m, H-7, 8), 2.85 – 2.93 (4H, m, H-6, 9), 2.34 (3H, s, H-a'); δ_C (75 MHz, $CDCl_3$) 198.2, 160.1, 156.5, 151.5, 149.7, 143.2, 135.3, 129.8, 129.1, 128.7, 126.5, 126.0, 124.8, 124.6, 121.7, 121.1, 116.9, 109.1, 61.2, 52.4 (2C), 51.9 (2C), 27.4; LRMS (EI) m/z 420.7 (M - H) M^+ $C_{24}H_{24}ClN_3O_2$ requires 421.9; Anal. Calcd. for $C_{24}H_{24}ClN_3O_2.H_2O$ - C 65.5%, H 5.9%, N 9.5%; found C 65.7%, H 6.0%, N 9.4%.

3-[3-[4-(7-Chloro-quinolin-4-yl)-piperazin-1-ylmethyl]-4-hydroxy-phenyl]-1-(2,4-dimethoxy-phenyl)-propenone, 5.15

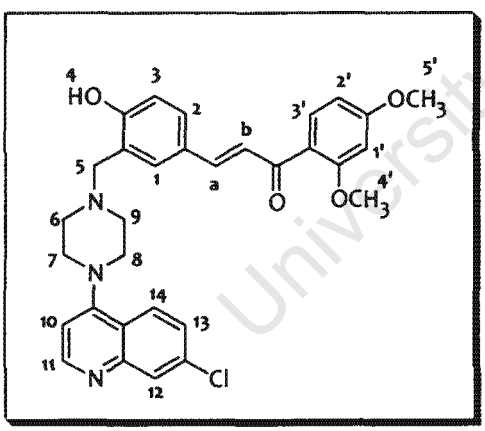

Yellow solid (49%); mp 85 - 87 °C (from EtOAc); R_f (EtOAc) 0.40; IR ν_{max} (KBr)/cm^{-1} 2935 (C-H), 1649 (C=O), 1598 (Ar C=C); δ_H (400 MHz, $CDCl_3$) 8.68 (1H, d, *J* 5.0, H-11), 8.07 (1H, d, *J* 1.8, H-12), 7.89 (1H, d, *J* 9.0, H-14), 7.69 (1H, d, *J* 8.6, H-3'), 7.57 (1H, d, *J* 15.7, H-a), 7.46 (1H, dd, *J* 1.9 and 8.5, H-2), 7.41 (1H, dd, *J* 1.8 and 8.9, H-13), 7.32 (1H, d, *J* 15.7, H-b), 7.24 (1H, d, *J* 1.9, H-1), 6.83 (1H, d, *J* 8.3, H-3), 6.82 (1H, d, *J* 4.9, H-10), 6.52 (1H, dd, *J* 2.0 and 8.6, H-2'), 6.47 (1H, d, *J* 2.0, H-1'), 3.87 (3H, s, H-4'), 3.85 (2H, s, H-5), 3.83 (3H, s, H-5'), 3.28 – 3.34 (4H, m, H-7, 8), 2.84 – 2.90 (4H, m, H-6, 9); δ_C (100 MHz, $CDCl_3$) 190.6, 163.9, 160.2, 159.6, 156.7, 151.1, 149.3, 142.1, 135.5, 132.6, 129.6, 129.3, 128.4, 127.1, 126.6, 124.8, 124.6, 122.5, 121.5, 120.8, 116.9, 108.9, 105.1, 98.7, 61.55, 55.7, 55.4, 52.4 (2C), 51.8 (2C); LRMS (EI) m/z 542.8 M^+ $C_{31}H_{30}ClN_3O_4$ requires 543.2; Anal. Calcd. for $C_{31}H_{30}ClN_3O_4.H_2O$ - C 66.2%, H 5.7%, N 7.5%; found C 66.4%, H 5.6%, N 7.2%.

8.2 Biological evaluation

The biological evaluation procedures not described in the main text are outlined below.

8.2.1 β-hematin inhibition assay

This assay was carried out as described by Kanyile and Egan, 2004 [3], and is based on the pyridine-hemochrome method of quantifying heme. Briefly, serial dilutions of the drug solutions were carried out in triplicate across a 96-well plate such that each well contained 10.12 μL of drug solution. Concentrations of drug solution corresponded to 0–10 equivalents relative to hematin in the final mixture. 101.2 μL of hematin stock solution (1.680 mM in 0.1 M NaOH) was then added to each well, and the solutions mixed. Subsequently, 58.7 μL of sodium acetate solution (12.9 M, pH 5.0) preincubated at 60 °C was added and the plates incubated at 60 °C for 60 min. Thereafter, 80 μL of 30% (v/v) pyridine solution in 20 mM HEPES buffer pH 7.5 was added at ambient temperature. Solids were resuspended and then allowed to settle for 15 minutes, after which 38 μL of supernatant was transferred to another plate and diluted to 250 μL with 30% (v/v) pyridine solution (pH 7.5,20 mM HEPES buffer). The plates were then read on a microplate reader, and the resulting data was plotted and analyzed.

8.2.2 Falcipain 2 inhibition assay

This assay was carried out as described by Rosenthal *et al.* 1996 [4], with modifications described by Greenbaum *et al.* 2004 [5]. This assay is based on the quantifiable fluorescence caused by the cleavage of benzyloxycarbonyl-Phe-Arg-7-amino-4-methyl-coumarin (Z-Phe-Arg-AMC) by Falcipain 2. The assays were carried out in 96-well plates. Briefly, different concentrations of each test compound (prepared from stock solutions in DMSO by dilution with 0.1M sodium acetate) were incubated in duplicate or triplicate with equal amounts of recombinant Falcipain 2 (in 0.1 M sodium acetate and 10 mM dithiothreitol [pH 5.5]) for 30 min at room temperature. Positive controls were incubated with E-64 (10 mM). The substrate (Z-Phe-Arg-AMC) was then added in the same buffer to give a final concentration of 15 μM, and the fluorescence caused by the cleavage of Z-Phe-Arg-AMC was monitored continuously over 15 min at room temperature. IC_{50} values were determined from plots of percentage activity versus compound concentrations.

References

1. R C Elderfield, W J Gensler, O Birstein, F J Kreysa, J T Maynard, and J Galbreath. Synthesis of Certain Simple 4-Aminoquinoline Derivatives. *J. Am. Chem. Soc.* (1946) 68 1250-1251.

2. T Singh, R G Stein, J F Hoops, J H Biel, W K Hoya, and D R Cruz. Antimalarials. 7-Chloro-4-(substituted amino)quinolines. *J. Med. Chem.* (1971) 14 (4) 283-286.

3. K Ncokazi and T Egan. A colorimetric high-throughput β-hematin inhibition screening assay for use in the search for antimalarial compounds. *Anal. Biochem.* (2004) 338 306-319.

4. P J Rosenthal, J E Olson, G K Lee, J T Palmer, J L Klaus, and D Rasnick. Antimalarial Effects of Vinyl Sulfone Cysteine Proteinase Inhibitors. *Antimicrob. Agents Chemother.* (1996) 40 (7) 1600-1603.

5. D C Greenbaum, Z Mackey, E Hansell, P Doyle, J Gut, C R Caffrey, J Lehrman, P J Rosenthal, J H McKerrow, and K Chibale. Synthesis and Structure-Activity Relationships of Parasiticidal Thiosemicarbazone Cysteine Protease Inhibitors against *Plasmodium falciparum*, *Trypanosoma brucei*, and *Trypanosoma cruzi*. *J. Med. Chem.* (2004) 47 3212-3219.

APPENDICES

APPENDIX A: TABLES OF RESULTS FROM PHARMACOKINETIC STUDIES

Table A1: Table of the determined concentrations (ng/mL) of compound 3.15b in the mouse samples

	Time (hours)	Mouse 1	Mouse 2	Mouse 3	Mouse 4	Mouse 5	Ave	Std Dev
3.15b DMSO/Water oral 20mg/kg	0	0	0	0	0	0	0	0
	0.5	251	390	384	674	116	424.75	207.03
	1	401	429	514	739	89	520.75	234.29
	2	421	202	426	497	91.6	386.5	172.17
	5	84.7	22.2	39.9	191	37.1	84.45	68.93
	8	164	434	350	26.6	67	243.65	177.46
	24	137	BLQ	BLQ	65.4	39.7	101.2	50.42
3.15b Pheroid A oral 20mg/kg	0	0	0	0	0	0	0	0
	0.5	9.85	28.3	32.3	13.3	22	21.15	9.56
	1	0	9.19	9.12	8.75	18.3	9.077	4.64
	2	BLQ	BLQ	BLQ	BLQ	BLQ	-	-
	5	BLQ	BLQ	BLQ	BLQ	BLQ	-	-
	8	BLQ	BLQ	BLQ	BLQ	BLQ	-	-
	24	BLQ	BLQ	BLQ	BLQ	BLQ	-	-
3.15b SMEDDS oral 10mg/kg	0	0	0	0	0	0	0	0
	0.5	0	17.7	BLQ	29.1	47.4	18.84	14.98
	1	34.6	BLQ	75.9	16	83.1	41.92	32.33
	2	41	BLQ	65.6	BLQ	86.7	38.66	22.87
	5	BLQ	BLQ	BLQ	BLQ	BLQ	-	-
	8	BLQ	BLQ	BLQ	BLQ	BLQ	-	-
	24	BLQ	BLQ	BLQ	BLQ	BLQ	-	-
3.15b DMSO/water IV 2mg/kg	0.083	2530	3400	114			2965	615.18
	0.5	878	1310	18.9			1094	305.47
	1	415	428	34.5			421.5	9.19
	2	297	252	8.11			274.5	31.82
	5	52.2	21.5	BLQ			36.85	21.71
	8	BLQ	BLQ	BLQ			-	-
	24	BLQ	BLQ	BLQ			-	-

NB; *BLQ: below limit of quantitation

Table A2: Table of the determined concentrations (ng/mL) of compound 5.13 in the mouse samples

	Time (hours)	Mouse 1	Mouse 2	Mouse 3	Mouse 4	Mouse 5	Ave	Std Dev
5.13 DMSO/Water oral 20mg/kg	0	0	0	0	0	0	0	0
	0.5	839	164	152	111	58.2	121.3	47.80
	1	219	48.4	27.2	7.31	6.77	27.64	19.76
	2	98.4	49.1	17	0	0	33.05	22.70
	5	BLQ	BLQ	BLQ	BLQ	BLQ	-	-
	8	BLQ	BLQ	BLQ	BLQ	BLQ	-	-
	24	BLQ	BLQ	BLQ	BLQ	BLQ	-	-
5.13 pH4 oral 20mg/kg	0	0	0	0	0	0	0	0
	0.5	16.3	24.8	161	24.1	47.8	54.8	60.52
	1	20.2	9.15	80.5	13.6	30.7	30.83	28.93
	2	BLQ	5.45	18.5	4.25	16.4	8.92	8.08
	5	BLQ	BLQ	4.75	BLQ	5.57	2.06	2.84
	8	BLQ	BLQ	BLQ	BLQ	BLQ	-	-
	24	BLQ	BLQ	BLQ	BLQ	BLQ	-	-
5.13 DMSO/water IV 2mg/kg	0.083	1430	1280	710			1140	379.87
	0.5	119	166	83.6			122.87	41.34
	1	65.1	77.6	32.1			58.27	23.51
	2	23.4	42.2	8.62			24.74	16.83
	5	BLQ	BLQ	BLQ			-	-
	8	BLQ	BLQ	BLQ			-	-
	24	BLQ	BLQ	BLQ			-	-

NB: *BLQ: below limit of quantitation

Table A3: Table of the determined concentrations (ng/mL) of compound 5.7 in the mouse samples

	Time (hours)	Mouse 1	Mouse 2	Mouse 3	Mouse 4	Mouse 5	Ave	Std Dev
5.13 DMSO/Water oral 20mg/kg	0	0	0	0	BLQ	BLQ	0.00	-
	0.5	3.93	14.9	4.8	BLQ	BLQ	7.88	6.10
	1	BLQ	4.99	BLQ	BLQ	BLQ	4.99	-
	2	BLQ	6.64	BLQ	BLQ	BLQ	6.64	-
	5	BLQ	4.87	BLQ	BLQ	BLQ	4.87	-
	8	BLQ	BLQ	BLQ	BLQ	BLQ	-	-
	24	BLQ	BLQ	BLQ	BLQ	BLQ	-	-
5.13 pH4 oral 20mg/kg	0	BLQ	BLQ	BLQ	BLQ	BLQ		
	0.5	BLQ	BLQ	BLQ	BLQ	BLQ		
	1	BLQ	BLQ	BLQ	BLQ	BLQ		
	2	BLQ	BLQ	BLQ	BLQ	BLQ		
	5	BLQ	BLQ	BLQ	BLQ	BLQ		
	8	BLQ	BLQ	BLQ	BLQ	BLQ		
	24	BLQ	BLQ	BLQ	BLQ	BLQ		
5.13 DMSO/water IV 2mg/kg	0.083	4.12	13	29.6			15.57	12.93
	0.5	BLQ	BLQ	BLQ			-	-
	1	BLQ	BLQ	BLQ			-	-
	2	BLQ	BLQ	BLQ			-	-
	5	BLQ	BLQ	BLQ			-	-
	8	BLQ	BLQ	BLQ			-	-
	24	BLQ	BLQ	BLQ			-	-

NB: 'BLQ: below limit of quantitation